Ph.D. Thesis

Analyzes of selected methods of limiting the spread of air pollutants in the occupied ventilated rooms

Author:

Seyedkeivan Nateghi

Supervisor:

dr hab. inż. Jan Kaczmarczyk, prof. PŚ

Silesian University of Technology

Faculty of Energy and Environmental Engineering

Department of Heating, Ventilation and Dust Removal Technology

Gliwice, 2025

Acknowledgements

This thesis would not have been possible without the dedication and expertise of numerous collaborators and institutions. I would like to express my sincere gratitude to my supervisor, Professor Jan Kaczmarczyk, whose insightful guidance and unwavering support have been invaluable throughout this journey. I also extend my heartfelt thanks to all my colleagues in the Department of Heating, Ventilation and Dust Removal Technology, whose expertise and camaraderie have greatly enriched this work. Finally, I am deeply grateful to my family and friends for their continuous encouragement, understanding, and support during the challenges.

Abstract

Maintaining high indoor environmental quality, including air quality, is a major challenge in densely occupied spaces such as classrooms—a challenge that gained particular importance during the COVID-19 pandemic. This dissertation presents a comprehensive study of advanced ventilation and airborne infection control strategies. The research encompasses a range of approaches, from smart natural ventilation to hybrid systems, as well as localized and integrated personal ventilation systems combined with physical barriers.

In the initial phase, an automated window-opening controller was developed and simulated to manage natural ventilation in a classroom. This strategy significantly improved indoor air quality and thermal comfort; however, without additional measures—such as air purifiers or face masks—the infection risk remained high. In the next phase, a multi-objective optimization approach was proposed to simultaneously regulate window openings and thermostat settings. The model aimed to minimize energy use, average indoor CO_2 concentration, and occupant discomfort. This solution was analyzed under two distinct climate conditions. Subsequently, a novel hybrid ventilation strategy was developed to synchronize the use of natural and mechanical ventilation based on outdoor air pollution levels and the risk of pollutant infiltration. Optimization of this strategy ensured compliance with indoor environmental quality standards while minimizing energy consumption in three cities characterized by varying outdoor air quality and climate conditions.

Experimental studies began with evaluating the role of physical barriers in aerosol transmission under mechanical ventilation. Tests were carried out in a laboratory test chamber equipped with two types of mixing ventilation systems. Nebulized aerosols and bioaerosols were used to simulate airborne infection transmission. The results indicated that physical barriers with a height of 65 cm reduced aerosol transmission when effective air mixing was present. However, in cases of insufficient airflow, the use of barriers could lead to local accumulation of contaminants. In the following stage, physical barriers were combined with a local exhaust system providing 9 L/s per person. This configuration resulted in a significant local reduction of pollutant concentration across all tested air distribution systems. Moreover, numerical studies using Computational Fluid Dynamics (CFD) showed that reducing the barrier height to 45 cm and the exhaust airflow to 6 L/s per person resulted in only a ~5% decrease in aerosol removal efficiency, while significantly reducing energy and material demand.

The final part of the dissertation provides a comparative analysis of various infection control strategies, combining infection risk assessment with Life Cycle Assessment (LCA). The results

demonstrated that although some hybrid strategies—such as masks and air purifiers—offered the lowest infection risk, they also imposed substantial environmental burdens. The most balanced solution, considering both infection control effectiveness and environmental impact, was the integrated system of physical barriers and localized exhaust ventilation.

Keywords: indoor air pollution reduction; spread of air pollutants; ventilation strategies; physical barriers; life cycle assessment.

Streszczenie

Utrzymanie wysokiej jakości środowiska wewnętrznego, w tym jakości powietrza, jest istotnym wyzwaniem w gęsto zaludnionych przestrzeniach, takich jak sale lekcyjne, co stało się szczególnie ważne w czasie pandemii COVID-19. Niniejsza rozprawa przedstawia badania nad zaawansowanymi strategiami wentylacji i kontroli przenoszenia się infekcji drogą powietrzną. Badania obejęły analizy szeregu rozwiązań, od inteligentnej wentylacji naturalnej, przez systemy hybrydowe, aż po lokalne i zintegrowane systemy wentylacji osobistej z zastosowaniem fizycznych barier.

W pierwszym etapie opracowano automatyczny sterownik otwierania okien, który został zasymulowany do kontroli naturalnej wentylacji pomieszczenia klasowego. Podejście to znacząco poprawiło jakość powietrza wewnętrznego i komfort cieplny, choć bez dodatkowych środków, takich jak oczyszczacze powietrza czy maseczki, ryzyko zakażenia pozostawało wysokie. W kolejnym etapie opracowano wielokryterialne podejście optymalizacyjne, które zakładało jednoczesną regulację otwiercia okien oraz ustawień termostatu. Model ten minimalizował zużycie energii, średnie stężenie CO_2 w pomieszczeniu oraz poziom niezadowolenia użytkowników. Rozwiązanie to przeanalizowano dla dwóch różnych klimatów. Następnie opracowano nowatorską strategię wentylacji hybrydowej, synchronizującą współpracę wentylacji naturalnej i mechanicznej w zależności od poziomu zanieczyszczenia pwietrza na zewnątrz i ryzyka ich przenoszenia do wnętrza budynku. Przeprowadzono optymalizację tej strategii w celu spełnienia norm środowiska wewnętrznego przy jednoczesnym ograniczeniu zużycia energii dla trzech miast o zróżnicowanej jakości powietrza zewnętrznego i znajdujących się w różnych klimatach.

Badania eksperymentalne rozpoczęto od oceny roli barier fizycznych w rozprzestrzenianiu aerozoli w pomieszczeniach wyposażonych w wentylację mechaniczną. Eksperymenty przeprowadzono w komorze testowej wyposażonej w dwa różne systemy wentylacji mieszającej. Do symulacji transmisji zakażeń drogą powietrzną użyto rozpylonych aerozoli oraz bioaerozoli. Wyniki wskazały, że bariery fizyczne o wysokości 65 cm redukują transmisję aerozoli, w przypadku sprawnie działającej wentylacji mieszającej. jednak gdy mieszanie powietrza jest niewystarczające stosowanie barier fizycznych może prowadzić do lokalnej akumulacji zanieczyszczeń. W kolejnym etapie bariery fizyczne wyposażono w lokalny systemem wyciągu powietrza w ilości 9 l/s na osobę, co pozwoliło zaobserwować znaczący lokalny spadek stężenia zanieczyszczeń dla wszystkich analizowanych systemów dystrybucji powietrza. Ponadto, badania numeryczne z wykorzystanem obliczeniowej mechaniki płynów

(CFD) wykazały, że redukcja wysokości barier do 0.45 cm i przepływu powietrza w systemie wyciągowym do 6 l/s na osobę spowoduje spadek efektywności usuwania aerozoli jedynie o ~5%, a jednoczesśnie pozwoli ograniczyć zużycie energii i materiałów.

Ostatnia część pracy zawiera analizy porównawcze kilku strategii kontroli zakażeń łączące ocenę ryzyka zakażenia z analizą cyklu życia (LCA) . Wykazano, że choć niektóre strategie hybrydowe (maseczki i oczyszczacze) charakteryzują się najniższym ryzykiem zakażenia, to generują one znaczne obciążenia środowiskowe. Najbardziej zrównoważonym rozwiązaniem, uwzględniającym zarówno skuteczność redukcji ryzyka zakażenia, jak i wpływ na środowisko, okazał się zintegrowany system fizycznych barier i lokalnej wentylacji wyciągowej.

Słowa kluczowe: redukcja zanieczyszczeń powietrza wewnętrznego; rozprzestrzenianie zanieczyszczeń powietrza; strategie wentylacyjne; bariery fizyczne; analiza cyklu życia.

Table of contents

List of appended papers

The thesis consists of 6 scientific articles listed below, categorized into chapters 2 and 3. The full texts of these papers can be found in the appendices.

Chapter 2: Ventilation strategies and smart control

Paper 1: Grygierek, Krzysztof, **Seyedkeivan Nateghi**, Joanna Ferdyn-Grygierek, and Jan Kaczmarczyk. "Controlling and limiting infection risk, thermal discomfort, and low indoor air quality in a classroom through natural ventilation controlled by smart windows." Energies 16, no. 2 (2023): 592. IF: 3, DOI: 10.3390/en16020592

Paper 2: **Nateghi, Seyedkeivan**, and Jan Kaczmarczyk. "Multi-objective optimization of window opening and thermostat control for enhanced indoor environment quality and energy efficiency in contrasting climates." Journal of Building Engineering 78 (2023): 107617. IF: 6.7, DOI: 10.1016/j.jobe.2023.107617

Paper 3: **Nateghi, Seyedkeivan**, Amirmohammad Behzadi, Jan Kaczmarczyk, Pawel Wargocki, and Sasan Sadrizadeh. "Optimal control strategy for a cutting-edge hybrid ventilation system in classrooms: Comparative analysis based on air pollution levels across cities." Building and Environment 267 (2025): 112295. IF: 7.1, DOI: 10.1016/j.buildenv.2024.112295

Chapter 3: Local strategies for infection control

Paper 4: **Nateghi, Seyedkeivan**, Jan Kaczmarczyk, Ewa Zabłocka-Godlewska, and Wioletta Przystaś. "Investigating the Impact of Physical Barriers on Air Change Effectiveness and Aerosol Transmission Under Mixing Air Distribution." Building and Environment (2025): 112676. IF: 7.1, DOI: 10.1016/j.buildenv.2025.112676

Paper 5: **Nateghi, Seyedkeivan**, and Jan Kaczmarczyk. "Compatibility of integrated physical barriers and personal exhaust ventilation with air distribution systems to mitigate airborne infection risk." Sustainable Cities and Society 103 (2024): 105282. IF: 10.5, DOI: 10.1016/j.scs.2024.105282

Paper 6: **Nateghi, Seyedkeivan**, Shahrzad Marashian, Jan Kaczmarczyk, and Sasan Sadrizadeh. "Resource-efficient design of integrated personal exhaust ventilation and physical barriers for airborne transmission mitigation: A numerical and experimental evaluation." Building and Environment 268 (2025): 112336. IF: 7.1, DOI: 10.1016/j.buildenv.2024.112336

CRediT authorship contribution statement

The author and co-authors contribution to each paper was provided in the section of "CRediT authorship contribution statement" in each corresponding paper in the Appendices. The author's contribution is as follows:

Paper 1: Seyedkeivan Nateghi: Formal analysis, Writing – original draft, Conceptualization, Methodology. (Seyedkeivan Nateghi's contribution was equal to 35%.).

Paper 2: Seyedkeivan Nateghi: Formal analysis, Writing – original draft, Investigation, Software, Methodology, Formal analysis. (Seyedkeivan Nateghi's contribution was equal to 80%.).

Paper 3: Seyedkeivan Nateghi: Writing – original draft, Visualization, Validation, Methodology, Formal analysis. (Seyedkeivan Nateghi's contribution was equal to 70%.).

Paper 4: Seyedkeivan Nateghi: Formal analysis, Writing – original draft, Investigation, Funding acquisition, Formal analysis. (Seyedkeivan Nateghi's contribution was equal to 35%.).

Paper 5: Seyedkeivan Nateghi: Writing – original draft, Investigation, Funding acquisition, Formal analysis, Data curation. (Seyedkeivan Nateghi's contribution was equal to 50%.).

Paper 6: Seyedkeivan Nateghi: Writing – original draft, Software, Investigation, Funding acquisition, Formal analysis. (Seyedkeivan Nateghi's contribution was equal to 35%.).

Nomenclature

$QC_{(t)}$	quanta concentration (quanta/m³)
V	volume (m^3)
I	number of infected individuals (-)
t	time (s, min, h)
k_f	filtration by portable air cleaner (1/h)
k	virus decay (1/h)
R(t)	average quantum concentration (quanta/m³)
n	number of susceptible people in the room (-)
F_B	Brownian force (N)
F_D	drag force (N)
g	gravitational acceleration (m/s^2)
F_e	thermophoretic force (N)
$D_{i,m}$	mass diffusion coefficient (m²/s)
$D_{T,i}$	thermal diffusion coefficient (m²/s)
Sc_t	turbulent Schmidt number (-)
Y_i	local mass fraction (-)
U_∞	free-stream air velocity (m/s)
d_c	characteristic dimension of the obstacle (m)
d	diameter (m)

Abbreviations

CFD	Computational Fluid Dynamics
IAQ	Indoor Air quality
Covid-19	Corona Virus Disease 2019
VOC	Volatile organic compounds
ETS	Environmental Tobacco Smoke
HEPA	High-Efficiency Particulate Air
UV	Ultraviolet
PM	Particulate Matter
PV	Personalized Ventilation
DOAS	Dedicated Outdoor Air Systems
DCV	Demand-Controlled Ventilation
ACH	Air Change Rate

MV	Mixing Ventilation
DV	Displacement Ventilation
PPE	Personal Protective Equipment
MERV	Minimum Efficiency Reporting Value
HVAC	Heating, Ventilation, and Air Conditioning
AI	Artificial Intelligence
PMV	Predicted Mean Vote
PPD	Predicted Percentage of Dissatisfied
HRV	Heat Recovery Ventilators
LCA	Life Cycle Assessment
FMI	Functional Mock-up Interface
API	Application programming interface
FCM	Fast Concentration Meters
NDIR	Non-dispersive Infrared
GSD	Geometric Standard Deviation
GMD	Geometric Mean Diameter
TSA	Trypticase Soy Agar
EMS	Energy Management System
NSGA	Non-dominated Sorting Genetic Algorithm
WHO	World Health Organization
LCE	Localized-Chair Exhaust
DPV	Downward Piston Ventilation
PE	Personal Exhaust
PB	Physical Barrier
FCM	Fast Concentration Meters
NDIR	Non-Dispersive Infrared
DRW	Discrete Random Walk
RNG	Re-Normalization Group
EPT	Eulerian Particle Tracking
LPT	Lagrangian Particle Tracking
STK	Stokes number

Greek letters

η_i	facial mask efficiency for infected person (-)
λ	first-order loss rate coefficient (1/h)

λ_{dep}	deposition onto surfaces (1/h)
λv	outdoor air change rate (1/h)
η_s	facial mask efficiency for susceptible person (-)
ρ_p	Particle density (kg/m^3)
μ_g	Molecular dynamic viscosity (kg/m.s)
ρ	Fluid density (kg/m^3)
υ	Velocity (m/s)
ϕ	Solving variables (i.e., velocity, temperature, and concentration)
S_ϕ	Term contributing to sources
μ_t	Turbulent viscosity (kg/m.s)
Γ_ϕ	Effective diffusion coefficient (m²/s)

Note on Thesis Format

This doctoral dissertation is presented in a paper-based format, consisting of six peer-reviewed publications. The appended papers are referenced in the respective chapters 1, 2 and 3. The structure of the thesis follows the order in which the studies were conducted and thematically developed, building a comprehensive understanding of indoor air quality (IAQ) and airborne infection control in buildings.

During the implementation of the doctoral thesis, additional LCA analyses were conducted to assess selected methods of reducing the risk of infection in terms of their impact on the environment. This work is included in Chapter 4, which is an addition to the monothematic series of publications presented in the previous chapters. A shortened scope of the chapters is summarized below:

- Chapter 1 provides the introduction, including the motivation for the work, background on indoor pollutants and infection mitigation strategies, and the formulation of research objectives and hypotheses.
- Chapter 2 includes the results of three simulation-based studies (Papers 1–3), focusing on natural, mechanical, and hybrid ventilation strategies with smart control to enhance IAQ and energy efficiency.
- Chapter 3 presents experimental and numerical studies (Papers 4–6) addressing local infection control strategies, such as physical barriers and personal exhaust ventilation.
- Chapter 4 is based on an additional study that combines infection risk modelling and life cycle assessment (LCA) to evaluate the environmental sustainability of different infection mitigation strategies. This was conducted to address a critical research gap not covered in the published papers.
- Chapter 5 concludes the research by synthesizing the findings, evaluating the research hypotheses, and suggesting directions for future work.

Chapter 1: Introduction

1.1. Motivation of the work

The high occupational density of indoor environments, particularly in classrooms, offices, and shared public spaces, has made indoor air quality a critical public health concern. As people now spend the majority of their time indoors, buildings' ability to manage air quality directly affects respiratory health, productivity, and the transmission of infectious diseases. Many indoor environments continue to suffer from inadequate air management, either due to insufficient ventilation—often resulting from inappropriate system operation—or because existing systems were originally designed without accounting for recent changes in occupancy patterns, pollutant sources, or evolving health risks. These shortcomings became especially evident during the COVID-19 pandemic, which exposed the inability of conventional systems to mitigate airborne transmission of pathogens in densely occupied indoor spaces. This crisis also accelerated global awareness of the need for more adaptive and effective strategies to limit airborne pollutant spread, particularly in educational spaces where students and teachers remain in close proximity for extended durations.

Furthermore, most studies examine indoor air quality, thermal comfort, energy consumption, and environmental impacts separately rather than through an integrated perspective. Buildings are among the largest consumers of energy worldwide. According to the IEA, operational energy use in buildings represents about 30% of global final energy consumption. In terms of environmental impacts, the building sector is responsible for approximately 21% of global greenhouse gas emissions. However, integrated solutions that consider both indoor pollutants mitigation and broader indoor environmental quality objectives are limited. There is a clear need for innovative, comprehensive strategies that target the pathways of pollutant spread, while also accounting for energy use, comfort, and environmental impact. This thesis is motivated by the need to develop and evaluate targeted, scalable methods to limit the spread of airborne pollutants in occupied rooms.

1.2. Background

Given that individuals spend approximately 90% of their time indoors [1], the quality of indoor air has become a critical determinant of health, well-being, and productivity—particularly in

settings where people gather for extended periods, such as classrooms, offices, and healthcare facilities. High concentrations of indoor pollutants—such as $PM_{2.5}$, PM_{10}, VOCs, and biological agents—are frequently reported to exceed outdoor levels by two to five times [2]. In school environments, the World Health Organization (WHO) has highlighted poor IAQ as a major contributor to absenteeism, respiratory illnesses, and diminished academic performance [3]. While specific estimates vary, studies indicate that exposure to elevated levels of fine particulate matter ($PM_{2.5}$) in classrooms is associated with a reduction in students' academic performance. Research suggests that improving indoor air quality can lead to positive effects on cognitive development and learning [4]. The COVID-19 pandemic further amplified awareness regarding the importance of managing indoor air. Research confirmed that SARS-CoV-2 can be transmitted through aerosols that linger in the air for extended periods, particularly in poorly ventilated spaces [5]. In one notable study, poorly ventilated indoor environments were associated with 19 times higher odds of transmission compared to outdoor settings [6]. As a result, ensuring adequate ventilation and air quality became critical not only for infection control but also for supporting mental health and maintaining productivity. However, improving IAQ presents complex trade-offs. Increasing ventilation rates, for instance, often leads to higher energy consumption, particularly in climates with extreme temperatures, where additional heating or cooling is required [7]. Furthermore, building systems designed for energy efficiency sometimes inadvertently compromise ventilation effectiveness, creating environments where pollutant concentrations can accumulate despite compliance with energy codes [8]. In addition to energy and comfort concerns, there is an emerging recognition of the environmental footprint associated with air quality interventions. For example, the use of portable air cleaners, personal protective equipment, and increased filtration measures—while effective for short-term health protection—can also contribute to higher greenhouse gas emissions and material waste if not properly managed [9].

Taken together, these findings highlight the urgent need for integrated strategies that can enhance IAQ, mitigate infection risks, maintain thermal comfort, optimize energy efficiency, and minimize environmental impacts. Achieving this balance is particularly critical in educational settings, where children's health, cognitive development, and learning outcomes are at stake. This study aims to address these interconnected challenges by systematically evaluating and comparing various indoor air management and infection mitigation strategies, considering not only their health benefits but also their broader environmental and operational implications.

1.3. Indoor pollutants

Indoor pollutants may originate from indoor sources or infiltrate from the outdoors and have varying effects on human health and comfort. Their presence and behavior indoors depend on building design, ventilation, occupant activities, and surrounding environmental conditions. Indoor pollutants can be broadly categorized into three primary groups: chemical, particulate, and biological.

- Chemical pollutants include volatile organic compounds (VOCs), carbon monoxide (CO), nitrogen dioxide (NO_2), ozone (O_3), formaldehyde and many other compounds and their mixtures [10]. VOCs are emitted from a variety of indoor sources such as paints, adhesives, cleaning agents, and furnishings, and exposure has been associated with symptoms including headaches, respiratory irritation, and neurological effects [11]. Carbon monoxide, produced primarily by incomplete combustion, binds to hemoglobin more effectively than oxygen, reducing oxygen delivery to tissues and causing dizziness, confusion, and at high concentrations, fatality [12]. Nitrogen dioxide, typically originating from gas appliances and outdoor infiltration, exacerbates asthma and reduces lung function [13]. Ozone, sometimes generated indoors by air purifiers, can provoke respiratory inflammation and exacerbate chronic respiratory diseases [9]. Formaldehyde, emitted from composite wood products and certain insulation materials, is a known respiratory irritant and classified as a human carcinogen [14].
- Particulate pollutants, notably fine particulate matter ($PM_{2.5}$) and coarse particles (PM_{10}), arise from combustion activities, resuspension of dust, indoor activities, and infiltration of outdoor air pollution. Exposure to particulate matter is linked to a wide range of adverse outcomes, including respiratory and cardiovascular diseases, lung cancer, and premature mortality [15].
- Biological pollutants include bacteria, viruses, fungi (including mold spores), and allergens originating from pets, dust mites, and pests such as insects. Microorganisms like molds thrive in moist indoor environments and release spores that can cause or exacerbate respiratory illnesses, allergic reactions, and asthma, particularly in environments with poor ventilation and high occupant density. The COVID-19 pandemic placed particular emphasis on airborne biological contaminants, especially respiratory viruses such as SARS-CoV-2, which are transmitted via respiratory droplets and aerosols. This allows for both short-range (droplet) and long-range (aerosol) airborne transmission, with the risk significantly heightened in confined and poorly ventilated spaces. Evidence from pandemic

studies showed that inadequate air exchange was strongly associated with higher infection rates in indoor settings, highlighting the urgent need for well-designed ventilation and control measures [16]

- Carbon dioxide (CO_2), although not typically classified within the above categories, serves as a crucial IAQ indicator and can indirectly influence occupant health and cognitive performance. Elevated CO_2 concentrations are associated with symptoms such as drowsiness, headaches, and measurable declines in cognitive performance and decision-making abilities [17]. Thus, while CO_2 is not itself a health-threatening pollutant at ordinary indoor levels, it is an important parameter in assessing indoor environmental quality and the adequacy of ventilation. Classification systems such as those proposed by the Federation of European Heating, Ventilation and Air Conditioning Associations (REHVA) categorize indoor environments based on pollutant levels and ventilation adequacy. These classifications (ranging from Category I, indicating high IAQ, to Category IV, indicating poor IAQ) provide benchmarks for designing and evaluating indoor environments according to health and comfort standards [18].

1.4. Methods to mitigate spread of indoor pollutants

Maintaining healthy indoor environments often requires well-thought-out strategies to limit the accumulation and spread of indoor pollutants. Ventilation plays a fundamental role in this process by ensuring sufficient airflow to dilute and remove airborne contaminants such as particulate matter (PM), volatile organic compounds (VOCs), bioaerosols, and excess carbon dioxide (CO_2). According to standards [19–21], specific ventilation rates are prescribed based on building type, occupancy levels, and activity to ensure acceptable indoor air quality. However, while ventilation is a critical and often mandatory component of indoor environmental control, it may not be sufficient on its own—particularly in densely occupied spaces, poorly ventilated areas, or during infectious disease outbreaks. In such cases, a combination of complementary interventions, including personal protective equipment (PPE), physical barriers, air purifiers, and other emerging technologies, is increasingly utilized to promote healthier indoor environments. The following subsections outline the principal strategies implemented to reduce exposure to indoor airborne contaminants.

1.4.1. Ventilation-based strategies

In high-occupancy spaces like classrooms, effective ventilation strategies are critical. Ventilation-based approaches aim to reduce the concentration of infectious aerosols through

dilution, removal, or localized containment. Indoor spaces typically employ three primary ventilation approaches: natural ventilation, mechanical ventilation, and hybrid systems.

- Natural ventilation relies on passive airflow through openings such as windows, vents, and doors, driven by wind pressure and thermal buoyancy. It is a cost-effective and commonly implemented approach, often found in residential, educational, and office buildings, particularly in regions where outdoor air quality is acceptable. When well-designed, natural ventilation can support acceptable indoor air quality (IAQ) with minimal mechanical intervention. Studies indicate that it can achieve adequate air exchange rates in moderate climates, particularly when architectural features are optimized to support cross-ventilation and airflow paths [22]. Historical examples, such as post-1918 influenza pandemic hospital designs, demonstrate how large windows and intentional cross-ventilation were employed to reduce airborne infection risks [23]. However, despite these advantages, natural ventilation is inherently variable and may become unreliable in extreme climatic conditions. Cold outdoor temperatures, high humidity, and urban pollution can restrict its usability, especially during winter when open windows lead to thermal discomfort and increased heating demand [24]. Additionally, cross-ventilation can be ineffective when openings are poorly positioned, resulting in air stagnation and inadequate pollutant removal. In settings like classrooms or offices, relying solely on natural ventilation may fall short of providing sufficient contaminant control, often necessitating hybrid strategies that combine passive airflow with mechanical ventilation systems [25].
- Mechanical ventilation systems utilize fans, ducts, and filtration to actively control indoor air exchange, ensuring consistent IAQ regardless of external environmental fluctuations. These systems are essential in environments where natural ventilation is insufficient or unreliable, such as densely populated urban areas or buildings with complex architectural designs. Mechanical ventilation offers precise control over airflow rates, filtration efficiency, and air distribution, which are crucial for maintaining optimal IAQ and mitigating airborne contaminant transmission. Mechanical ventilation systems can be configured in various ways to achieve specific IAQ objectives. For instance, Dedicated Outdoor Air Systems (DOAS) provide 100% outdoor air to the space, independently controlling ventilation and thermal comfort [26]. This approach is particularly effective, as it eliminates the recirculation of contaminated air. Furthermore, integrating HEPA filters within mechanical systems significantly enhances their ability to remove airborne particles, including pathogens, contributing to a healthier indoor environment [27], but due to high

air pressure resistance they are not commonly used in typical indoor settings. Demand-Controlled Ventilation (DCV), another mechanical strategy, modulates ventilation rates based on real-time occupancy or pollutant levels, optimizing energy consumption while maintaining adequate IAQ [28]. The implementation of advanced control systems and sensors enables these systems to dynamically adapt to changing indoor conditions, ensuring continuous and efficient air quality management.

- Hybrid ventilation, also known as mixed-mode ventilation, combines natural and mechanical ventilation to optimize air exchange rates, energy efficiency, and IAQ. By dynamically switching between natural and mechanical modes based on indoor air conditions, occupancy levels, and outdoor climate, hybrid systems offer a flexible approach to maintaining adequate ventilation while reducing energy consumption. A key advantage of hybrid ventilation is its ability to maximize passive airflow when outdoor conditions permit while activating mechanical ventilation when necessary [29]. For instance, in moderate climates, windows can be automatically controlled to introduce fresh air, with mechanical fans supplementing airflow when required. This approach can significantly reduce CO_2 accumulation, enhance thermal comfort, and lower energy demand compared to fully mechanical systems. However, hybrid ventilation requires advanced control strategies to function effectively. Smart ventilation algorithms, CO_2 and pollutant sensors, and occupancy-based controls are commonly used to adjust airflow rates dynamically [30]. These systems are particularly beneficial in buildings with variable occupancy patterns, such as schools and office spaces, where ventilation needs fluctuate throughout the day. Despite its advantages, hybrid ventilation systems may not be suitable in areas with high outdoor pollution or extreme climates, where reliance on natural airflow could introduce contaminants or cause discomfort [31]. Proper design, sensor calibration, and integration with filtration systems are essential to ensure consistent IAQ under varying environmental conditions.

While increasing air change rate (ACH) is a widely recognized method for lowering airborne infection risk, several additional factors influence the overall effectiveness of ventilation systems [32]. These include airflow patterns, distribution mechanisms, and the configuration of air inlets and exhausts, all of which determine whether contaminants are efficiently extracted or recirculated within the space [33]. Moreover, particle size significantly affects the behavior and removal efficiency of airborne contaminants. Studies have shown that smaller particles ($< 20\ \mu m$) are more readily removed by ventilation systems, whereas larger particles ($> 40\ \mu m$)

tend to settle on surfaces rather than being extracted from the air [34]. This emphasizes the need for carefully designed airflow strategies that target particle transport and deposition, particularly in occupied zones [35]. The type and placement of air diffusers also play a critical role in shaping airflow, influencing how pathogens disperse and whether they accumulate or are effectively removed.

- Mixing ventilation (MV) is one of the most commonly implemented ventilation strategies in indoor environments such as classrooms, offices, and healthcare facilities. In this approach, air is typically introduced at high velocity through ceiling diffusers or wall-mounted inlets, aiming to dilute indoor air pollutants and maintain uniform environmental conditions. However, in the context of infection control, MV presents significant limitations. Due to its principle of creating a well-mixed environment, infectious aerosols released from an infected individual are rapidly dispersed and distributed throughout the entire space. This uniform mixing increases the risk of exposure for all occupants, regardless of their distance from the source. Both experimental studies and numerical simulations have demonstrated that MV does not effectively confine or remove exhaled contaminants, leading to higher overall infection risk compared to more localized ventilation approaches [32]. Despite these limitations, MV remains widely used due to its simplicity, ease of design, and ability to meet thermal comfort and regulatory ventilation requirements in various building types.
- Displacement ventilation (DV) is an alternative to mixing ventilation that supplies cooler air at low velocity near the floor level and relies on thermal stratification to transport heat and airborne contaminants upward toward ceiling-mounted exhaust outlets. This stratified airflow pattern reduces mixing between the clean air zone in the occupied region and the warmer, contaminated air rising toward the ceiling. As a result, DV can significantly reduce occupants' exposure to exhaled aerosols and is considered a more effective strategy for airborne infection control in comparison to mixing systems. Experimental results and CFD analyses have shown that DV can maintain lower contaminant concentrations in the breathing zone by confining exhaled particles to thermal plumes that are rapidly carried away from occupants [36]. DV has been successfully implemented in environments such as office buildings, lecture halls, and patient rooms, especially where thermal plumes from occupants and equipment can support vertical air movement. However, its performance is sensitive to internal heat loads and space layout, which can influence stratification and pollutant removal efficiency [37].

- Personalized ventilation (PV) is emerging as a solution for localized air supply, reducing exposure to shared pollutants. PV refers to a localized airflow approach that delivers or removes air directly within the breathing zone of occupants, offering individualized control over their immediate thermal and air quality conditions [38]. Unlike general ventilation systems—whether natural, mechanical, or hybrid—which treat the entire room uniformly, PV systems focus on optimizing the occupant's microenvironment without altering the background ventilation. PV systems can supply clean and conditioned air using devices such as adjustable nozzles, desktop diffusers, or chair-mounted outlets [39]. Alternatively, they may function as personalized exhaust systems by extracting exhaled air near the source to improve surrounding air quality [40]. By addressing diverse comfort preferences in shared environments like offices, classrooms, and transport vehicles, PV offers a flexible and user-centric solution. Additionally, it can contribute to energy savings by reducing the need for high-volume room-wide ventilation. However, its design and performance depend on careful consideration of airflow patterns, noise levels, positioning relative to occupants, and potential interactions with background systems [41]. Moreover, there is lack of clear design guidelines for this type of ventilation.

1.4.2. Personal Protective Equipment

Personal protective equipment (PPE), including face masks, face shields, and gowns, has been extensively studied as an effective strategy to reduce the transmission of airborne pathogens, especially in indoor environments with limited ventilation. Face masks are among the most widely used PPE, with research showing that surgical masks and respirators such as N95/FFP2 can significantly reduce the emission and inhalation of infectious aerosols by filtering fine particles at various efficiency levels [42]. Cloth masks offer limited protection but can still contribute to source control when combined with other interventions [43]. Face shields and protective eyewear provide additional protection against droplet transmission, particularly in environments with high exposure risk, though their efficacy against aerosols is limited due to open gaps [44]. While PPE is considered an essential layer of protection, especially in densely occupied or poorly ventilated spaces, studies emphasize that its effectiveness is highly dependent on correct usage, fit, and compliance [45]. Moreover, PPE should be considered a complementary measure rather than a standalone solution, ideally used in combination with environmental and engineering controls for enhanced infection mitigation.

1.4.3. Physical barriers and spatial separation

Physical barriers, such as transparent partitions, curtains, and air curtains, have been explored as cost-effective measures to reduce direct person-to-person transmission in shared indoor environments. These barriers function by disrupting airflow patterns and limiting the direct spread of respiratory droplets between occupants [46]. However, their effectiveness largely depends on their size, placement, and integration with the ventilation system [47]. Improper design may lead to airflow stagnation or localized accumulation of aerosols, particularly if ventilation is insufficient [48]. In parallel, spatial distancing has also been shown to reduce exposure to infectious particles [49]. Studies have demonstrated that increasing the distance between occupants—typically to at least 1–2 meters—can significantly lower the probability of inhaling pathogen-laden aerosols or droplets [50]. However, distancing alone may not be sufficient in poorly ventilated spaces where aerosolized particles can accumulate and disperse beyond short-range. Research suggests that combining physical barriers with adequate ventilation and distancing measures can create layered protection that enhances indoor air safety [51]. Optimizing barrier height, material, and placement, while ensuring proper airflow, is crucial to maintaining both effectiveness and comfort in occupied spaces.

1.4.4. Filtration and air cleaning technologies

Filtration and air cleaning technologies have been widely studied for their ability to remove airborne pathogens from recirculated air. HEPA filters and filters rated Minimum Efficiency Reporting Value (MERV) 13–16 are among the most effective at capturing fine aerosols, including viral particles, and are increasingly used in heating, ventilation, and air conditioning (HVAC) systems and portable air cleaners [52]. Several studies report significant reductions in aerosol concentrations when these filters are properly integrated into mechanical ventilation systems [53]. However, higher filtration efficiencies typically lead to increased pressure drop and energy demand, which may affect system performance and operational costs [54]. To balance indoor air quality and energy efficiency, some research suggests combining medium-efficiency filters with optimized airflow rates or supplementing existing systems with portable air cleaners [55]. The effectiveness of filtration strategies also depends on maintenance practices, filter replacement intervals, and system compatibility, making long-term planning and operational management crucial for sustained infection control.

1.4.5. Emerging technologies for infection control

Recent studies have explored the application of advanced technologies to enhance infection control in indoor environments. These include smart sensors, automated systems, and data-driven control strategies. For example, real-time environmental monitoring tools—capable of tracking parameters such as CO_2 concentration, temperature, and particulate matter—have been used to inform ventilation management and assess indoor air quality in occupied spaces [56]. Artificial Intelligence (AI) and machine learning techniques have also emerged as promising tools in this area. Some studies have used AI models to optimize ventilation strategies, predict pollutant dispersion, or control disinfection processes, demonstrating potential for reducing occupant exposure to airborne pathogens [57]. Additionally, technologies such as UV-C disinfection robots and smart control systems for air cleaners or HVAC settings have been tested in healthcare and educational settings to support infection prevention efforts [58]. While these approaches offer potential for improving infection risk management, current research highlights the importance of proper system integration, data quality, and ongoing evaluation to ensure reliability and effectiveness in real-world applications.

1.5. Implications of IAQ management and infection control

Approaches aimed at limiting the spread of airborne pollutants—including IAQ management and infection control measures—often introduce complex trade-offs that extend beyond occupant health. According to existing literature, such strategies can lead to significant consequences. A well-balanced design must therefore consider these interrelated aspects to ensure effective, acceptable, and sustainable solutions for indoor environments.

1.5.1. Thermal comfort implications

Strategies such as increased ventilation, designed to reduce airborne contaminant concentrations and infection risk, frequently affect thermal comfort. Numerous studies have reported that higher outdoor air exchange rates can lead to thermal discomfort, particularly in climates with seasonal extremes. For instance, excessive fresh air intake during winter can reduce indoor temperatures below comfort thresholds, increasing heating demand and occupant dissatisfaction [59]. Conversely, during summer, enhanced airflow may cause overcooling or raise indoor humidity levels, again leading to discomfort [60]. These effects are often quantified using thermal comfort models such as the Predicted Mean Vote (PMV) and Predicted Percentage of Dissatisfied (PPD). To reconcile thermal comfort with air quality targets, recent studies have proposed adaptive ventilation control, where ventilation rates dynamically

respond to indoor CO_2 levels or contaminant concentration while maintaining thermal setpoints. These integrated strategies can help optimize comfort without compromising IAQ or infection control goals [61].

1.5.2. Energy efficiency considerations

Ventilation, filtration, and air purification technologies used for managing IAQ and infection risk often require considerable energy input. Studies have shown that mechanical systems operating at high ventilation rates significantly increase energy consumption, especially when paired with heating or cooling demands [62]. This raises concerns about long-term operational costs and energy efficiency in buildings. To address this, the literature supports several energy-efficient alternatives. DCV systems, which adjust airflow based on occupancy and IAQ indicators, and heat recovery ventilators (HRVs), which capture thermal energy from exhaust air, have demonstrated energy savings without compromising pollutant control. Hybrid ventilation approaches that switch between natural and mechanical ventilation based on environmental conditions have also shown energy reductions of up to 40% in comparative studies [29]. Moreover, simulation-based optimization using algorithms such as multi-objective genetic algorithms has been employed to find the optimal trade-offs between IAQ, infection risk, and energy performance [63].

1.5.3. Environmental impact and sustainability

Infection control and IAQ management strategies carry environmental implications across their life cycles, including manufacturing, operation, and disposal stages. For example, several studies have drawn attention to the environmental footprint of single-use PPE [64], HEPA filters, and portable air cleaners. The disposal of large quantities of used filters and masks contributes to solid waste and resource depletion concerns [65]. To assess these impacts, Life Cycle Assessment (LCA) has been increasingly applied. Findings suggest that integrated and localized solutions—such as combining partial natural ventilation, physical barriers, and low-energy filtration—can lead to lower greenhouse gas emissions compared to systems relying solely on high-volume mechanical ventilation. Additionally, studies recommend exploring biodegradable PPE, long-life filtration materials, and renewable energy sources such as photovoltaic panels to reduce the environmental burden of IAQ technologies [66,67].

1.6. Objectives and scope

This thesis aims to advance the understanding and development of effective and sustainable strategies to improve IAQ and mitigate airborne infection risks, particularly in educational environments. The study seeks to balance health protection, occupant comfort, energy efficiency, and environmental sustainability within classroom environments. The primary objectives of this research are:

- Evaluating different ventilation strategies in maintaining IAQ and reducing airborne infection risks in densely occupied spaces.
- Investigating localized mitigation measures such as physical barriers, personal ventilation, mask and portable air cleaners in controlling aerosol transmission in densely occupied space.
- Analysing energy and comfort impacts with various IAQ improvement and infection control strategies.

Based on these objectives, the following questions were formulated at the outset of this work:

1) Can natural ventilation through smart windows provide sufficient indoor air quality and infection control in classroom settings?
2) What are the energy use and thermal comfort implications of natural ventilation, and how can they be optimized?
3) How can hybrid ventilation systems be designed to adapt to varying indoor and outdoor air quality conditions effectively?
4) What are the possible impacts of introducing physical barriers on ventilation effectiveness and airborne contaminant transmission in ventilated rooms?
5) Can combining local exhaust ventilation with physical barriers enhance infection control?

To address these questions, several hypotheses are formulated:

- Natural ventilation through smart windows may control infection risk when there is not access to mechanical ventilation.
- Conducting multi objective optimization on defined parameters of ventilation system may lead to control IAQ, thermal comfort and energy demand simultaneously.
- Controlled integration of natural and mechanical ventilation (hybrid ventilation) can improve indoor environmental quality and reduce energy use.

- Physical barriers can reduce airborne transmission risk between occupants.
- Local control strategies such as personal exhaust ventilation combined with physical barriers can significantly reduce exposure to airborne contaminants.

In pursuit of these objectives and hypotheses, this thesis is structured around a series of six peer-reviewed publications and one additional study that collectively form the foundation of the research. Each publication addresses a specific aspect of the overarching research problem, with insights from earlier studies informing the design and scope of subsequent investigations. The works are presented in a logical sequence, beginning with advanced natural ventilation control, followed by the integration of hybrid and mechanical systems, and continuing with experimental and numerical assessments of local infection mitigation strategies such as physical barriers and personal exhaust ventilation. In addition to the main part of the thesis, a life cycle assessment (LCA) study was conducted to evaluate the environmental impact of various infection control strategies. Each part of the research builds upon the last, progressively addressing new dimensions of the core challenge: how to maintain a healthy, comfortable, and environmentally responsible indoor environment in classrooms during airborne infectious disease outbreaks. A graphical summary of the full sequence of investigations is presented in Figure 1.

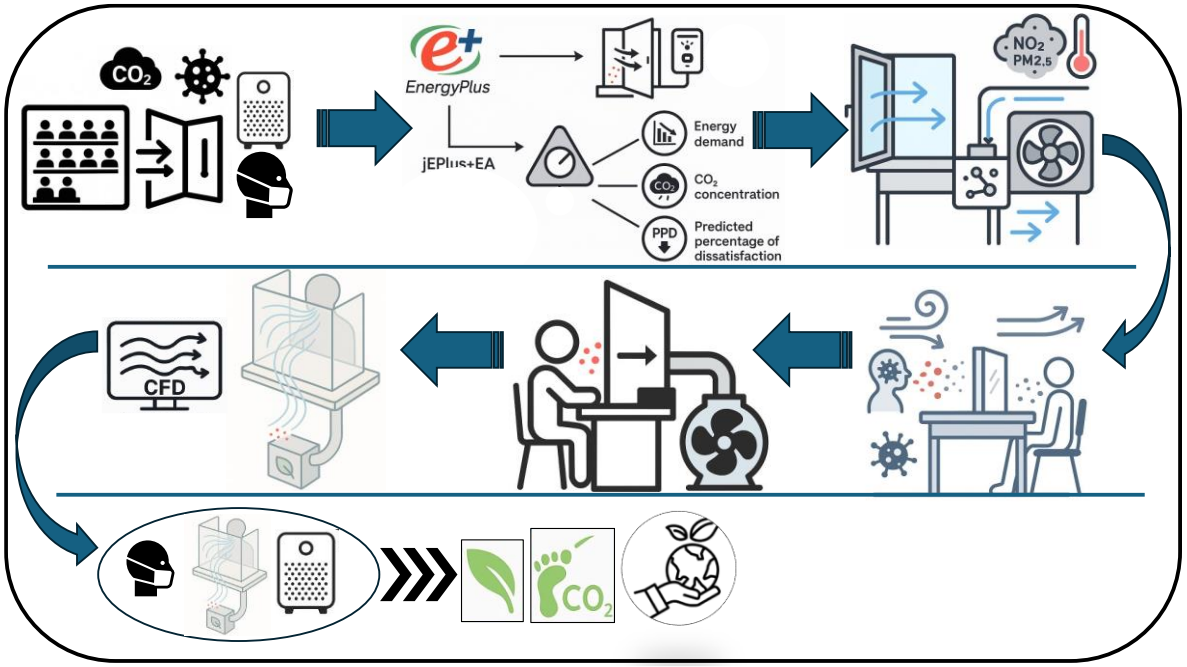

Fig.1. Graphical commentary of the series of investigations.

To ensure comparability and internal consistency across all studies included in this thesis, both experimental and numerical investigations were conducted using a standardized indoor environment—a room with dimensions of 9 m (L) × 6 m (W) × 3.3 m (H), representative of a typical classroom. This consistent framework allowed for reliable cross-comparison of results and supported a cohesive evaluation of multiple ventilation and mitigation strategies. The standardized setup served as the basis for numerical simulations, experimental testing, and environmental assessments, thereby reinforcing the integrated nature of the research.

Chapter 2: Ventilation strategies and smart control

2.1. Scope of study

This chapter summarizes a sequence of studies— (Papers 1-3), which focused on the development and optimization of smart and hybrid ventilation strategies for improving indoor environmental conditions in classrooms. The overarching goal is to enhance indoor air quality (IAQ), thermal comfort, and energy efficiency, while also addressing airborne infection risk.

- Paper 1 introduced a novel control algorithm for regulating natural ventilation using smart windows, guided by indoor environmental parameters such as CO_2 concentration and temperature. The study demonstrated that while smart natural ventilation can significantly improve IAQ and thermal comfort, it alone is insufficient to control infection risk in densely occupied spaces. This paper laid the foundation by showing the potential and limitations of relying solely on natural ventilation, indicating a need for additional measures such as air cleaners and face masks.
- Paper 2 was built directly upon the findings of Paper 1 by employing a multi-objective genetic algorithm to optimize both window opening and thermostat setpoints. This approach enabled a more comprehensive control strategy that accounts for climate variability, user comfort, and energy use, in addition to indoor air quality. The study addressed a key methodological gap by showing how simultaneous optimization of parameters for smart window and thermostat setpoints can yield substantial improvements in indoor environmental quality and operational efficiency across different climatic conditions.
- Paper 3 responded to the shortcomings of natural ventilation by proposing a hybrid ventilation system that integrates window control with mechanical ventilation, driven by both indoor and outdoor air quality data, including real-time $PM_{2.5}$ and NO_2 levels. This

hybrid approach enhances system responsiveness and robustness, particularly in urban settings with fluctuating pollution levels. The strategy was tested through simulation in three diverse cities—Delhi, Warsaw, and Stockholm—illustrating its adaptability to different climates and pollution levels.

Together, these three papers provide a comprehensive exploration of smart ventilation control strategies, transitioning from passive natural ventilation to advanced hybrid systems that dynamically adapt to changing environmental conditions. The findings contribute to the broader goal of creating classroom environments that are not only healthy and comfortable but also energy-efficient and resilient to outdoor pollution variability.

2.2. Methods

This chapter applies a set of numerical methods to evaluate and optimize ventilation strategies aimed at improving indoor environmental quality in classrooms. The methods include dynamic building performance simulations, multi-objective optimization techniques, and infection risk modelling. These methods were used systematically to analyze natural ventilation control, thermostat setpoint optimization, and hybrid ventilation systems across different climatic and pollution contexts.

2.2.1. Building performance simulation

In Papers 1, 2, and 3, the architectural and thermal layout of the classroom was first developed using a SketchUp plugin. The classroom is described in section 3. This model was then imported into EnergyPlus to define the building's thermal properties, including aspects such as lighting and ventilation, in order to calculate heating and cooling demands [68]. EnergyPlus, which operates based on a thermal balance model, was chosen for its reliability in estimating a building's thermal performance [69]. In Paper 3, a Unitary Packaged Terminal Heat Pump model was utilized to simulate the integrated heating and cooling system [70].

- To capture air and contaminant exchange between zones, Paper 1 incorporated CONTAM software for detailed inter-zone airflow calculations. CONTAM was coupled with EnergyPlus via co-simulation using the Functional Mock-up Interface (FMI), enabled through CONTAM's inter-process communication application programming interface (API). This setup allowed real-time data transfer between the two programs at each simulation step, enhancing the accuracy of airflow and contaminant transport modelling. To simulate contaminant behaviour and predict indoor concentration levels, a time-

dependent, perfectly mixed mass balance model was used in all three papers, governed by the following principles [68]:

$$V\frac{dC_f^t}{dt} = \sum_{i=1}^{N_{sink}} R_{f,i}C_f + \dot{m}\left(C_{f,z,i} - C_{f,z}^t\right) + \dot{m}\left(C_{f,\infty} - C_f^t\right) + \dot{m}\left(C_{f,sup} - C_f^t\right) + S_f\left(C_f^{t-\delta t}\right) \quad (1)$$

In the equation, $V\frac{dC_f^t}{dt}$ represents the storage of a general contaminant within the zone air (ppm.kg/s). The term $\sum_{i=1}^{N_{sink}} R_{f,i}C_f$ signifies the total removal of contaminants by sinks located on both the zone and interior surfaces (ppm.kg/s). The expression $\dot{m}\left(C_{f,z,i} - C_{f,z}^t\right)$ illustrates the movement of contaminants due to air mixing between different zones (ppm.kg/s). The term $\dot{m}\left(C_{f,\infty} - C_f^t\right)$ indicates the movement of contaminants resulting from outdoor air infiltration and ventilation (ppm.kg/s). The expression $\dot{m}\left(C_{f,sup} - C_f^t\right)$ quantifies the transfer of contaminants due to the system's air supply (ppm.kg/s), and $S_f\left(C_f^{t-\delta t}\right)$ denotes the rate of contaminant generation or removal based on the contaminant level in the zone air from the previous time step.

- Paper 3 leveraged the Energy Management System (EMS) in EnergyPlus to implement dynamic control strategies, particularly for operable windows and their integration with the ventilation system [71]. EMS offers a robust scripting environment that empowers users to design high-level supervisory control routines, enabling the override of standard EnergyPlus logic [72]. This allowed for the simulation of advanced, demand-driven ventilation strategies that responded dynamically to indoor conditions [71]. Together, these tools—EnergyPlus, CONTAM, and EMS—provided a comprehensive platform for modelling thermal behaviour, contaminant dynamics, and responsive control systems within the classroom environment.

2.2.2. Multi-objective optimization

In papers 2 and 3, the JEPlus + EA program, an online optimization tool, uses the Non-dominated Sorting Genetic Algorithm (NSGA-II) for optimization [73]. This software is built using the Java programming language. JEPlus, working in conjunction with EnergyPlus, was used to define the design parameters (decision variables) and desired outcomes (objective functions). In the context of optimizing indoor environments, a genetic algorithm approach is used to manage competing objectives. This powerful technique effectively balances factors like energy consumption, air quality, and thermal comfort. The genetic algorithm operates within the solution space, generating a Pareto front diagram to display optimal trade-offs [74]. The

NSGA-II algorithm, chosen for its adaptability to various variables, processes EnergyPlus outputs in "rvx" format. The configuration of the NSGA-II algorithm, including population size, maximum generations, crossover rate, and mutation rate, was carefully determined based on previous research and the specific characteristics of this study [73]. In multi-objective optimizations, the algorithm produces a set of optimal solutions along a Pareto front, where no single solution is superior to the others [75]. The best compromise is then selected using statistical methods, with the total weighted average method being a common choice in this study [76]. This method is calculated according to the following equation:

$$f_{ws}(x) = \sum_{i=1}^{n} a_i \frac{f_i(x) - f_i(x)^{min}}{f_i(x)^{max} - f_i(x)^{min}} \quad (2)$$

where $f_i(x)$ are the objective functions and $f_i(x)^{max}$ and $f_i(x)^{min}$ are the minimum and maximum of each objective function, respectively. a_i is also the weight coefficient of each objective function.

2.2.3. Infection risk calculation

In paper 1, the Wells-Riley model [77] was used to determine the likelihood of infection for students in the classroom, considering their different activities. The model relies on the quantum emission rate (E), which represents the amount of virus released. In this study, E was assumed to vary based on whether students were sitting, lightly moving, or speaking during lectures. The initial quanta concentration (QC_0) was assumed to be zero at the start of the first class and increased over time until the students left the classroom. The change in average quanta concentration, $QC_{(t)}$ (quanta/m3), over time was calculated using Equation (3).

$$QC_{(t)} = \frac{E \cdot I \cdot (1 - \eta_i)}{V \cdot \lambda} + \left(QC_0 - \frac{E \cdot I}{V \cdot \lambda}\right) \cdot e^{-t \cdot \lambda} \quad (3)$$

where V, I, η_i, and λ represent the volume of the room (m^3), number of infected individuals, facial mask efficiency for the infected person, and first-order loss rate coefficient, respectively. The quanta are reduced not only by facial mask efficiency, but also due to ventilation (λv), filtration (k_f), deposition (λ_{dep}), and airborne virus decay (k). Hence, λ is defined as summed effects of these values (Equation (4)).

$$\lambda = \lambda v + \lambda_{dep} + k + k_f \quad (4)$$

The likelihood of infection, R(t), represents the probability that susceptible individuals in a closed space will become infected at a given time (t). This probability can be determined using Equation (5), which is derived from the Wells-Riley model [78] and refined by Gammaitoni-Nucci [79]. Infection risk depends on the inhalation rate (Q_i) of susceptible persons. If all

susceptible students wear masks, the facial mask efficiency (η_s) reduces the quanta inhaled. A perfect mixing of indoor air with a constant source was assumed to use the calculated average, $QC_{(t)}$, which increases with time.

$$R(t_1) = n(1 - e^{-Q_i(1-\eta_s)\int_0^{t_1} QC_{(t)}dt}) \quad (5)$$

To establish a reasonable infection risk level for the classroom, the basic reproduction number (R_0) can be used. R_0 is determined by the ratio of new infections to the initially infected individuals. Public health recommendations suggest keeping R_0 below 1 ($R_0 < 1$) to effectively control the spread of an epidemic.

2.3. Study design

All numerical simulations presented in this thesis were conducted using a consistent indoor environment model to ensure methodological coherence and facilitate meaningful comparisons. The simulated domain represents a classroom located on the top floor of a three-story school building constructed with energy-efficient materials—polystyrene insulation in the walls and floors (U-values of 0.23 and 0.17 W/(m²·K), respectively), and double-glazed windows with a U-value of 1.1 W/(m²·K). Depending on the study, the ventilation setup included natural ventilation via cracks and stack-effect chimneys, or mechanical ventilation systems, in line with the strategy under investigation. Occupancy was modelled based on a typical school schedule with 30 students attending 45-minute lessons followed by 15-minute breaks. Internal heat and CO_2 generation per occupant were assumed to be 95 W and 0.238 L/min, respectively, with a baseline indoor CO_2 level of 400 ppm. Clothing insulation levels were tailored to local climate conditions: 0.5 clo for Bangkok and Delhi, and 1.0–1.2 clo for Warsaw and Stockholm. Artificial lighting was activated when daylight illumination dropped below 250 lux.

2.3.1. Paper 1 – Smart window control for natural ventilation

Paper 1 focused on developing a smart window controller governed by indoor CO_2 levels, temperature, and infection risk considering Warsaw climate. The windows could operate in three modes— tilt, open, and closed—based on thresholds for CO_2 concentration and indoor/outdoor temperature. The optimization minimized hours exceeding thresholds for comfort (PMV < −0.7 or > 0.7), indoor air quality (CO_2 > 1200 ppm), and infection risk (R_0> 1). The controller had separate branches for CO_2 response and overheating mitigation and was limited to daytime operation for safety. It supported three modes of window operation—one tilt (O1), one open (O2), and one tilt and one open (O3)—selected based on indoor/outdoor

temperature and CO_2 concentration. The optimization was based on indoor environmental parameters including CO_2 concentration, temperature, and the probability of airborne infection transmission. The resulting optimal setpoints determined the operation of each window mode. As outlined in Table 1, seven different cases were investigated to assess the performance of the proposed controller under various intervention scenarios.

Table 1. Test cases conducted in the study.

Case	Controller Basis	Number of People	Mask	Clean Air Delivery Rate by Air Cleaner (CADR, m^3/h)
1	Opening window during breaks	30	No	–
2	Objective function: (1) Thermal comfort (2) CO_2 concentration.	30	No	–
3	Objective function: (1) Thermal comfort (2) CO_2 concentration (3) Infection risk.	30	No	–
4		30	Yes	–
5		30	Yes	330
6		30	Yes	2 × 330
7		15	Yes	-

2.3.2. Paper 2 – Optimization of window and thermostat settings

Paper 2 extended the work by applying a multi-objective optimization through five decision parameters: minimum and maximum temperatures for window opening, heating and cooling setpoints, and window opening area. Three conflicting objectives are included: annual energy demand, average indoor CO_2 concentration, and thermal comfort, quantified via the Predicted Percentage of Dissatisfied (PPD) index. This study included two contrasting climates—Warsaw (continental) and Bangkok (tropical)—highlighting the trade-offs between indoor air quality, thermal comfort, and energy consumption. Warsaw required seasonal heating, while Bangkok required continuous cooling. A time-dependent controller was used as the base case to compare with the optimal cases. The temperature-dependent controller includes two parameters: the maximum and minimum indoor temperatures at which the window can be opened. Outside the set interval, the controller automatically closes the window. This study uses the temperature-dependent controller to perform optimization of all objective functions. The full list of decision variables and their ranges is provided in Table 2, including the minimum and maximum allowable indoor temperature for window operation (P1 and P2), heating and cooling setpoints (P3 and P4), and the window open area (P5).

Table 2. Properties of the decision parameters.

Parameter	Object Controller	Description parameter	Unit	Range[1]	Base value
P1	Window	Minimum indoor temperature for keeping the window open	(°C)	(17-23)	21
P2	Window	Maximum indoor temperature for keeping the window open	(°C)	(23-28)	25
P3	Thermostat	Heating setpoint	(°C)	(17-23)	21
P4	Thermostat	Cooling setpoint	(°C)	(23-28)	25
P5	Window	Open area	m^2	[0,16)	1

[1]All defined ranges are Continues.

To capture diverse optimization priorities, five cases were defined, including two base cases and three optimized scenarios with varying weight coefficient of objective functions. Table 3 outlines these cases and their weighting schemes for each objective function. Notably, Case 3 assigns equal importance to energy demand (a_1), average CO_2 concentration (a_2), and thermal comfort (a_3), Case 4 prioritizes energy demand, and Case 5 prioritizes average CO_2 concentration or indoor air quality improvement.

Table 3. Selected cases based on WSM coefficient.

	Case	Controller type	Coefficient a_1	Coefficient a_2	Coefficient a_3
Base cases	1	Time	-	-	-
	2	Indoor Temperature	-	-	-
Optimized cases	3	Indoor Temperature	$\frac{1}{3}$	$\frac{1}{3}$	$\frac{1}{3}$
	4	Indoor Temperature	$\frac{1}{2}$	$\frac{1}{4}$	$\frac{1}{4}$
	5	Indoor Temperature	$\frac{1}{4}$	$\frac{1}{2}$	$\frac{1}{4}$

2.3.3. Paper 3 – Hybrid ventilation with outdoor pollution constraints

Paper 3 built upon the optimization work by integrating outdoor air pollution infiltration constraints through an EMS for hybrid ventilation control. Airflow was driven by natural and mechanical forces depending on the case. When mechanical ventilation was off and windows were open, a 300 CFM exhaust fan was modelled to assist ventilation. Mechanical ventilation used a packaged terminal heat pump (PTHP) with heating/cooling coils and filters to remove PM2.5 and NO_2 (initial efficiency 90%, declining to 50% over 6 months). It has been scheduled to replace the filter after six months. Simulations were conducted in three cities—Delhi,

Warsaw, and Stockholm—selected for their varied pollution profiles. The EMS used three external parameters: PM2.5, NO_2 concentrations, and outdoor temperature. When all three parameters met defined thresholds (city-specific air quality standards), the system activated natural ventilation and disabled mechanical ventilation. If any exceeded their threshold, mechanical systems were enabled to ensure indoor air quality. Delhi's PM2.5 threshold was 60 μg/m³, compared to 40 μg/m³ in Warsaw and 15 μg/m³ in Stockholm. As for NO_2, standard values are 80 μg/m³ for Delhi, 40 μg/m³ for Warsaw, and 25 μg/m³ for Stockholm. EMS logic, illustrated in Figure 2, ensured that the system dynamically adjusted based on real-time outdoor conditions.

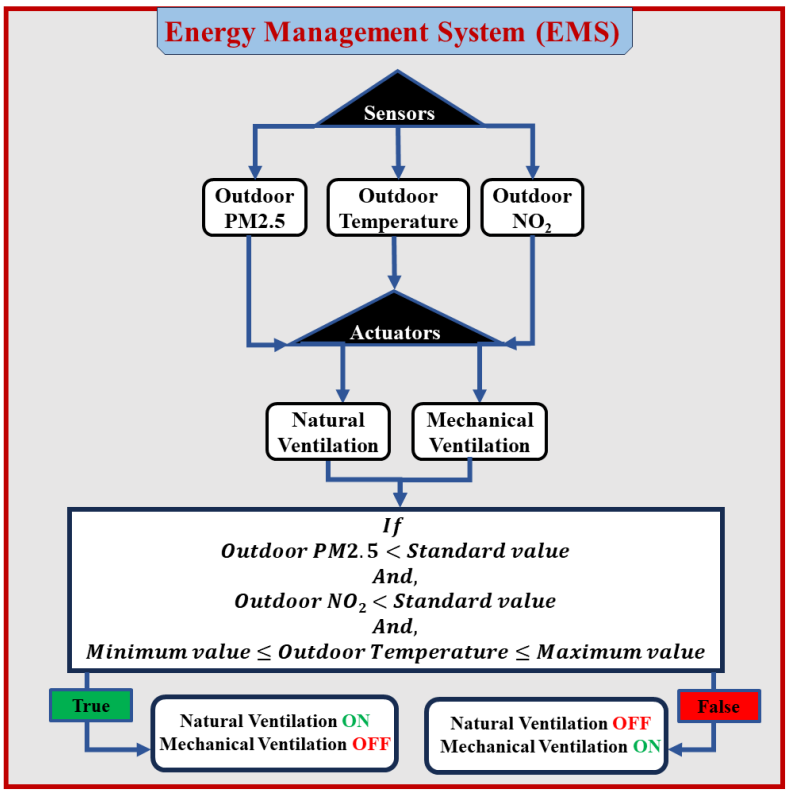

Fig. 2. Schematic of the developed energy management system

The optimization task involved four continuous parameters: P1 and P2, which determined the minimum and maximum outdoor temperature thresholds for activating natural ventilation (window opening) and deactivating the ventilation system, respectively, through the EMS control strategy. The heating and cooling set point thermostat related to the ventilation system (P3&P4) are also defined as the third and fourth parameters. Table 4 shows the decision variables and their respective ranges.

Table 4. The domain of decision variables for the optimization

Parameter	Object	Description parameter	Unit	Range
P1	EMS	Minimum outdoor temperature for keeping the window open	(°C)	(0–21)
P2	EMS	Maximum outdoor temperature for keeping the window open	(°C)	(21–35)
P3	Ventilation system	Heating setpoint	(°C)	(16–21)
P4	Ventilation system	Cooling setpoint	(°C)	(21–27)

2.4. Result and discussion

2.4.1. Natural ventilation optimization via smart window control

This section presents the outcomes of Paper 1, which introduces an optimized smart window control strategy for a naturally ventilated classroom. The window controller significantly influenced the air change rate (ACH) and indoor CO_2 levels. Case 1, representing conventional manual opening during breaks, showed severe IAQ degradation, with CO_2 concentrations exceeding 2500 ppm by the end of each class. In contrast, Case 2—where windows operated dynamically based on CO_2 and thermal comfort—reduced CO_2 levels to within 600–1200 ppm, thus maintaining air quality within acceptable categories for 80% of occupied hours. However, increased ACH also introduced energy penalties. Case 2 increased heating demand by approximately 190% compared to the base case. This reflects the trade-off between improved ventilation and thermal energy loss during colder months. When infection risk was included in the controller logic (Case 3), only marginal improvement was observed: the fraction of time with a basic reproduction number (R_0) below 1 rose from 14% in Case 1 to 20.2% in Case 3. Thus, optimization of window operation alone was insufficient for infection control. Further interventions were evaluated. Wearing 50% efficient masks (Case 4) reduced $R_0 > 1$ occurrences to 23% of lecture time. Adding one and two air cleaners (Cases 5 and 6) further dropped this to 7% and 1.6%, respectively. Case 7, with only 15 students present, also achieved a desirable infection risk profile with 4% of hours exceeding $R_0 = 1$. Therefore, while natural ventilation optimization improved IAQ and thermal comfort, significant infection risk mitigation required combined strategies. The comprehensive overview in Figure 3 illustrates the trade-offs between thermal discomfort, elevated CO_2 concentration, infection probability,

and heating energy demand across all seven cases. It highlights the need for hybrid strategies to balance occupant health and energy sustainability.

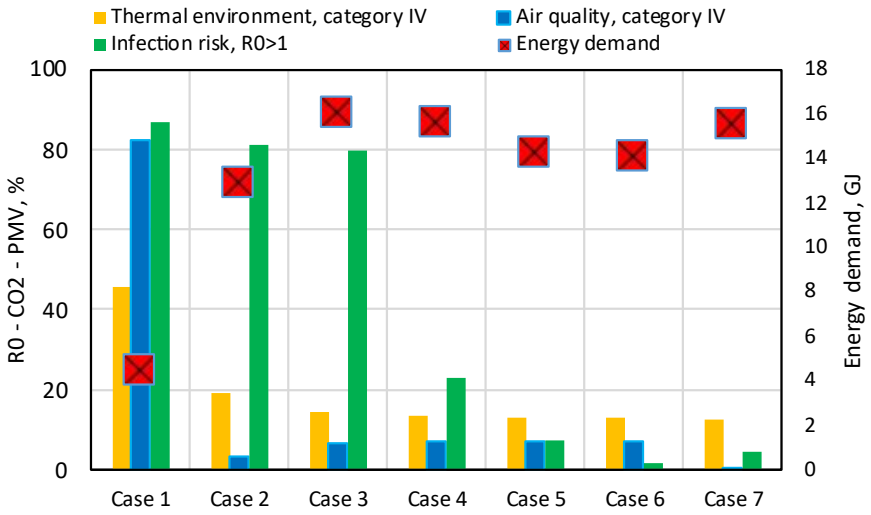

Fig. 3. Summary of all objective functions performed in the cases: the percentage of hours that each function is out of acceptable range (left axis) and annual energy demand (right axis).

2.4.2. Multi-objective optimization of window and thermostat control

In continuation of the natural ventilation control strategy, Paper 2 extended the investigation by optimizing not only window opening but also thermostat setpoints through a multi-objective approach. The results revealed that no single solution could simultaneously minimize all three objectives due to inherent trade-offs. This was visualized using Pareto fronts, which illustrated how minimizing CO_2 often increases energy demand, especially in Warsaw where heating demand is substantial. In contrast, Bangkok's climate, lacking heating needs, allowed a smoother compromise between thermal comfort and CO_2 concentration. The clustering of Pareto points in Warsaw along a vertical trajectory indicated stronger opposition between air quality and thermal comfort under colder conditions, while in Bangkok, the objectives were more synergistic. After max-min normalization, final optimum answers were determined based on the weighted coefficient of each case. For example, in Warsaw, Case 5—where indoor air quality was prioritized—resulted in the lowest minimum indoor temperature (P1), allowing for more aggressive natural ventilation. Conversely, Case 4, which emphasized energy reduction, maintained higher thresholds to reduce unnecessary window opening. The overall impact of these control strategies was evaluated using a comprehensive objective function index. Figure 4 presents this evaluation based on a weighted normalization scheme. It shows that Case 3 consistently balanced all performance indicators across both cities, while Case 4 was the most

energy-efficient, and Case 5 delivered the best air quality outcomes. This highlights the necessity of context-sensitive optimization when designing window and thermostat controllers in classrooms.

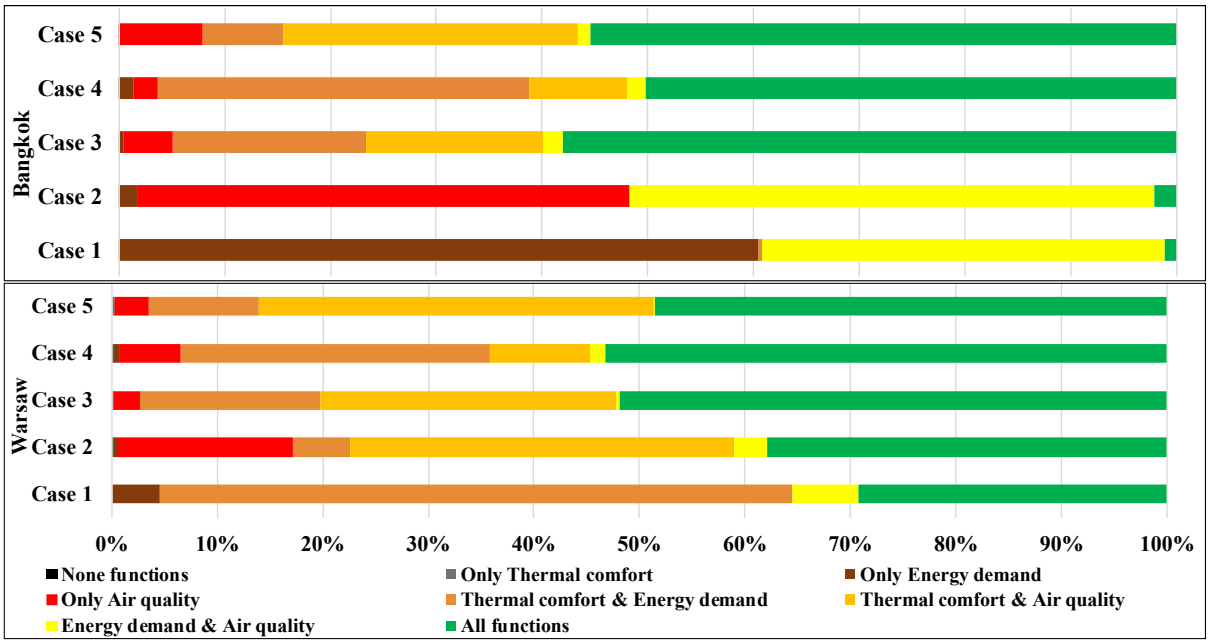

Fig. 4. Summary of results of objective functions: The percentage of hours that each function remains within an acceptable range based on standards.

2.4.3. Hybrid ventilation under outdoor air pollution constraints

The third study investigated the performance of a smart hybrid ventilation system that synchronized the operation of natural ventilation (via automatic windows) with mechanical ventilation, adapting its behaviour to both indoor conditions and outdoor air pollution levels. The system was evaluated in three cities—Delhi, Warsaw, and Stockholm—representing various climates with significantly different pollution characteristics. A multi-objective optimization approach was applied to minimize energy use, CO_2 concentration, and thermal discomfort while considering the constraints imposed by PM2.5 and NO_2 thresholds. The optimization results revealed a clear trade-off among the objective functions, especially in cities with high pollution levels. In Delhi, maintaining low CO_2 concentrations often conflicted with energy savings and thermal comfort due to the limited availability of clean outdoor air. In contrast, Warsaw, with cleaner air and a temperate climate, achieved better balance across all objectives. Stockholm, despite its clean air, faced limitations due to cold outdoor temperatures, which constrained window opening. The Pareto frontier diagrams demonstrated that simultaneous minimization of all three objective functions was not feasible, highlighting the

need for compromise solutions based on local conditions. The controller's effectiveness in enabling natural ventilation was directly influenced by outdoor air quality. As illustrated in Figure 5, the percentage of time when the outdoor environment allowed natural ventilation (based on PM2.5 and NO_2 thresholds) was only 11% in Delhi, compared to 44% in Warsaw and 31% in Stockholm. Interestingly, even though Stockholm has cleaner air than Warsaw, the less restrictive standards in Warsaw allowed windows to remain open for a longer period throughout the year.

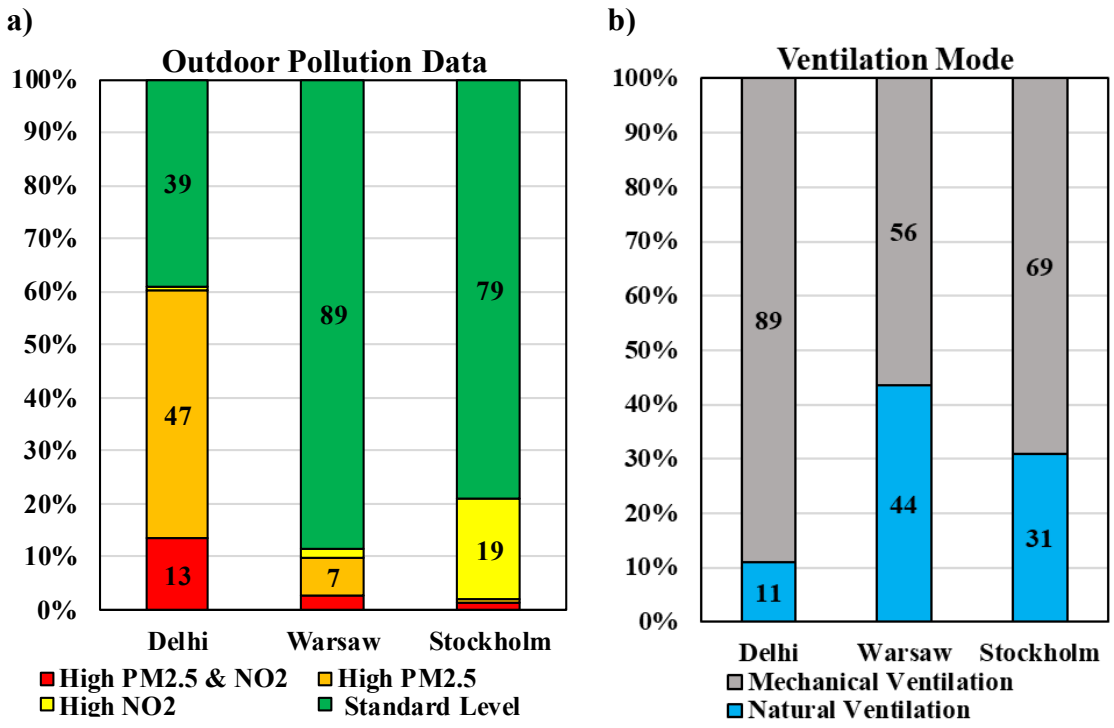

Fig. 5. The percentage bar of hour-average pollution data and ventilation mode in examined cities.

From an energy performance perspective, the optimized hybrid model outperformed both the base case (mechanical ventilation only) and the optimized non-hybrid model (window control without mechanical integration). Compared to the base case, the optimized hybrid controller reduced energy use by 65% in Warsaw, 57% in Stockholm, and 13% in Delhi. The indoor CO_2 concentration, one of the primary indicators of ventilation effectiveness, also improved under the optimized model. All base cases were classified under Category III (worst air quality level according to European standards). After optimization, Warsaw achieved 43% of the year in Category I, Stockholm reached 30%, and Delhi improved to 8%. In terms of thermal comfort, measured using the Predicted Percentage of Dissatisfied (PPD) index, the hybrid model maintained acceptable levels. Thermal comfort was acceptable for 99% of the year in Delhi,

and for over 80% of the year in Warsaw and Stockholm. This performance was slightly lower than in the base cases but still within the acceptable threshold defined by comfort standards.

Chapter 3: Local strategies for infection control

3.1. Scope of study

This chapter focuses on localized strategies for airborne infection risk reduction in ventilated indoor environments. It presents the findings from Paper 4, Paper 5 and Paper 6, which collectively explore the use of physical barriers and personal exhaust systems as source-control interventions. The goal is to assess their compatibility with different ventilation systems, quantify their effectiveness in limiting aerosol transmission, and evaluate their sustainability trade-offs.

- Paper 4 examines the role of physical barriers—specifically desk partitions—in modifying airflow patterns and influencing aerosol dispersion under mixing ventilation conditions. The study addresses a critical gap in understanding how these barriers affect air change effectiveness and contaminant transport in mechanically ventilated spaces. By conducting full-scale tracer gas and aerosol experiments in a classroom-sized test chamber, the paper provides empirical data on the spatial impact of partitions in real-world settings.
- Paper 5 expands on these findings by introducing a novel strategy that combines physical barriers and personal exhaust ventilation systems. The study investigates how this integrated setup performs across different types of air distribution, including mixing and displacement ventilation. The study provided empirical evidence on how proposed strategies must be tailored to specific air distribution methods.
- Paper 6 advances the previous research by introducing a sustainability dimension. It employs CFD simulations supported by experimental validation to optimize the design of integrated personal exhaust ventilation and physical barriers. This study quantifies the trade-offs between infection control performance and resource efficiency, focusing on variables such as barrier height and exhaust flow rate. This paper supports the development of a design recommendation that balances efficiency and sustainability.

Taken together, these three studies evaluate and design efficient and sustainable local infection control strategies in indoor environments, focusing on physical barriers and personal exhaust ventilation.

3.2. Methods

This chapter employs a combination of experimental and numerical methods to assess the performance of local infection control strategies, including physical barriers and personal exhaust ventilation. The methods used include tracer gas decay to evaluate air change effectiveness, aerosol and bioaerosol measurements to quantify particle dispersion and exposure, and computational fluid dynamics (CFD) simulations to analyze airflow patterns and contaminant transport. These techniques were applied consistently across the studies to enable detailed, quantitative evaluation under varying ventilation scenarios.

3.2.1. Tracer gas

To evaluate ventilation performance and airborne contaminant dispersion, two different tracer gases were employed in separate studies: carbon dioxide (CO_2) and nitrous oxide (N_2O). The selection of these tracer gases was driven by their specific physical and chemical properties, making them well-suited for distinct experimental objectives [80]. CO_2, being an inert gas commonly exhaled by humans, is widely recognized as a proxy for assessing ventilation effectiveness and indoor air quality [81]. In contrast, N_2O was chosen to model airborne virus-laden aerosols due to its ability to replicate the transport behaviour of small respiratory particles (<5 μm) [82]. In Paper 4, CO_2 was used to assess the ability of a mechanical ventilation system to deliver clean air to occupant locations. The decay method (step-down technique) was applied, wherein CO_2 was injected into the test environment and allowed to mix thoroughly with the ambient air to establish a uniform distribution. Once dosing ceased, CO_2 concentration decay was monitored over time to determine air exchange effectiveness. Measurements were conducted using Testo 160 sensors, which recorded CO_2 levels at 1-minute intervals within a 0–5000 ppm range with an uncertainty of ±50 ppm. In Paper 5, N_2O was introduced to simulate exhaled contaminants from an infected individual. A constant flow of 0.532 L/min was regulated by a Bürkert mass flow controller, ensuring precise and stable dosing conditions. The tracer gas was mixed with air and released through an 8 mm opening tube at a fixed airflow rate of 14 L/min, positioned at the edge of a cylinder representing an infected occupant. Fast Concentration Meters (FCMs) utilizing non-dispersive infrared (NDIR) absorption technology were employed to quantify N_2O concentration in real time. These instruments featured a sampling rate of 4 Hz, a time constant of 0.8 s, and an uncertainty of ±20 ppm (95% confidence level) [83]. To enhance accuracy, pre- and post-experiment intercalibration was conducted.

3.2.2. Aerosol

To simulate human exhaled droplets and assess their dispersion in indoor environments, a 3-jet Collison nebulizer [84] was used in both Paper 4 and Paper 6. This method has been widely applied in virus transmission studies due to its ability to generate polydisperse aerosols with a size distribution representative of respiratory emissions [85]. Sodium chloride (NaCl) solution was selected as the aerosolizing medium because it closely mimics the evaporation behaviour and chemical composition of human saliva [38], ensuring the accuracy of the experimental representation [86]. The NaCl solution consisted of 1 gram of NaCl dissolved in 250 cm^3 of a 50:50 mixture of distilled water and isopropyl alcohol. This formulation was chosen based on its well-documented similarity to respiratory secretions, allowing for reliable simulation of airborne droplet dynamics. The addition of isopropyl alcohol enhances the evaporation characteristics of the generated droplets, replicating real-world exhaled particle behaviour. The nebulizer operated at a pressure of 20 psi, producing aerosolized droplets with a geometric mean diameter (GMD) of 0.7 µm and a geometric standard deviation (GSD) ranging from 1.22 to 1.35. The resulting log-normal droplet size distribution (0.05 μm to 20 μm) aligns well with the full spectrum of human respiratory emissions, which include both larger droplets that settle quickly and finer particles that remain airborne for prolonged periods [84]. The 0.7 µm mean diameter specifically represents the finer fraction of exhaled aerosols, which are of critical concern in airborne disease transmission as they can stay suspended in indoor air for extended durations and travel significant distances. The ejection velocity of the aerosolized droplets was approximately 2 m/s, which closely simulates natural breathing conditions. The nebulizer was placed at the mouth level of a thermal dummy, accurately modelling the release of respiratory particles in a realistic seated exhalation scenario. To capture the dispersion characteristics, five measurement locations were designated at the mouth positions of surrounding mannequins, representing potential exposure points for nearby individuals. To quantify airborne particle concentrations and their size distribution, an Aerodynamic Particle Sizer (PCE-MPC 20 Particle Counter) was used. This instrument is capable of measuring particles within the 0.3–10 µm range, with measurements recorded at 1-minute intervals. The PM2.5 fraction was specifically analysed, as fine particulate matter plays a crucial role in indoor air quality assessments and health impact evaluations.

3.2.3. Bioaerosol

The method used for bioaerosol generation and sampling in this study was applied in Paper 4. To evaluate airborne biological contamination and its removal efficiency, bioaerosols were generated using Micrococcus luteus, a commonly used bacterial model for airborne microbial studies. The Collison nebulizer, previously applied in aerosol generation, was employed to ensure consistency with bioaerosol generation methods. The bacterial concentration was standardized at 150 × 10^6 CFU/ml, determined using McFarland standards and spectrophotometric measurements at 600 nm. This concentration provided a representative microbial load for evaluating ventilation efficiency. Bioaerosols were continuously released for 4 minutes at a 6 L/min airflow rate, simulating exhaled pathogen-laden droplets in an indoor environment. Sampling was conducted using an AirIdeal 3P impactor sampler, a widely used device for bioaerosol collection. Two measurement time points were selected. First, immediately after the 4-minute nebulization – capturing the initial bacterial concentration in the air. Second, 45 minutes post-nebulization – evaluating bacterial survival and decay under experimental conditions. Prior to each experiment, the room was sterilized with UV light (250–270 nm) for 60 minutes to eliminate background contamination. Trypticase Soy Agar (TSA) plates were used as the culture medium, and samples were incubated at 37°C for 48 hours to allow bacterial growth. Colony-forming units per cubic meter (CFU/m^3) were quantified to assess bioaerosol concentrations and determine the ventilation system's effectiveness in reducing microbial loads under different conditions.

3.2.4. Computational Fluid Dynamics

Numerical part of Paper 6 used CFD method to validate and improve the experimental design. The fundamental equations for mass, momentum, and energy conservation in incompressible steady airflow are expressed as follows:

$$\frac{\partial(\rho\phi)}{\partial t} + \nabla.\left(\rho\phi\vec{V}\right) = \nabla.\left(\Gamma_\phi \nabla_\phi\right) + S_\phi \quad (6)$$

The RNG k-ε model, recognized for its reliability in turbulence simulation, is commonly used to model air movement within confined spaces, and its effectiveness has been validated in numerous research projects [87]. To improve the accuracy of the numerical calculations, a second-order upwind method was used to discretize all relevant variables. Furthermore, a coupled algorithm was implemented to effectively link pressure and velocity in the steady-state calculations, ensuring both accuracy and stability in the results.

Two common methods for simulating how particles move within indoor spaces are Eulerian Particle Tracking (EPT) and Lagrangian Particle Tracking (LPT). EPT focuses on particle concentration within a stationary grid, whereas LPT follows the path of each individual particle [88]. Recent studies [89] suggest that LPT might provide more accurate predictions of pollutant spread and concentration compared to EPT. However, LPT typically demands significant computer resources and processing time to produce reliable results. Even with these requirements, the Lagrangian method is favoured when a detailed understanding of particle movement is needed, as it calculates each particle's trajectory by analysing the forces acting on it. This enables a more accurate portrayal of particle behaviour in intricate indoor settings. In this study, particle movement was simulated in Fluent using the Discrete Phase Model (DPM), which implements LPT with an automatically adjusted time step.

$$\frac{dv_p}{d_t} = F_D\left(u - u_p\right) + \frac{g(\rho_p - \rho)}{\rho_p} + F_B + F_e \tag{7}$$

In this context, terms without subscripts denote air properties. The terms $\frac{dv_p}{d_t}$ and $F_D\left(u - u_p\right)$ represent the particle's acceleration and the drag force exerted on the particle, respectively, both normalized by the particle's mass. Other forces, such as the Basset history force, pressure gradient force, and virtual mass force, are deemed negligible in comparison to the drag force [90]. To model the random velocity changes within the air, which are assumed to follow a normal distribution, the Discrete Random Walk (DRW) model is employed. To reduce computational burden, particles are introduced into the simulation only after the air flow pattern has stabilized, rather than being continuously injected. The impact of the particle movements on the air flow is not accounted for. In typical indoor air simulations, the interaction between particles and air is treated as a one-way coupling [91]. The motion of each particle was calculated until it either left the simulation through an escape boundary, was captured at a designated surface, or reached a predetermined maximum number of calculation steps. To accurately represent the behavior of very small particles, Brownian diffusion was included in the simulation [91]. Particle dispersion is typically influenced by the Stokes number (Stk), which compares a particle's response time to air flow changes with a characteristic time scale. Particles with a Stk below 0.1 tend to follow the air flow patterns closely [92]. The Stokes number is defined as:

$$STK = \frac{\rho_p d_p U_\infty}{18\mu_g d_c} \tag{8}$$

Using a maximum particle diameter of 20 μm and the simulated air speeds, the highest possible Stokes number was determined to be 10−3. Particles smaller than this would have an even lower Stokes number. This low value indicates that the particles react very quickly to the air's movement. Therefore, changes in particle size between 5 and 20 μm have almost no effect on their paths, with only very small differences caused by slight variations in drag and gravity. Consequently, these tiny droplets and their remaining nuclei stay fully airborne, moving almost exactly with the airflow. Because the Stokes number is much less than 1.0, the particles have very little inertia compared to the air, meaning their movement is primarily controlled by how the air flows.

To measure airborne particle concentrations, active air sampling was used in the experiments. This technique gathers data on the amount of living particles present in the air. To mirror this process, sensors were positioned close to the mouths of mannequins to capture airborne particles. In the computer simulations, the active air sampling method was replicated to analyse how particles spread and settle. Particles were considered removed from the simulation if they reached the main air exhaust or personal exhaust, and they were considered captured if they contacted a solid surface, with no bounce considered [88]. The sensor's particle collection flow rate was adjusted to match the experimental active sampling rates, allowing the simulation to accurately reproduce the active air sampling environment.

3.3. Study design

The experimental setup was developed within the climate chamber laboratory at the Department of Heating, Ventilation and Dust Removal Technology. It was designed to replicate a realistic classroom environment and included modular desk layouts, thermally active cylindrical dummies, controlled ventilation systems, and aerosol and tracer gas measurement instrumentation. As shown in Figure 6, the test room incorporated thermal dummies and desks arranged to reflect classroom use. Each dummy—intended to simulate the thermal profile of a seated high school student—was constructed from a cylindrical steel shell (1.10 m in height, 0.40 m in diameter) with a total surface area of 1.63 m² and an internal electric heating element delivering a constant 60 W of heat. While anatomically simplified, this design has been validated by Zukowska et al. [93] for its ability to reproduce realistic enthalpy and buoyancy fluxes, both essential for capturing accurate airflow behaviour and contaminant dispersion.

Fig. 6. Photo of the test room with desks and heated dummies.

The indoor environmental conditions were kept consistent across all tests:

- Ventilation rate: 148 L/s of fresh air (±10 L/s), resulting in 3 h^{-1} air change rate.
- Supply air temperature: 20 ± 1 °C
- Room air temperature: 22 ± 1 °C
- Relative humidity: 40 ± 10%

3.3.1. Ventilation designs

Different air distribution strategies were implemented depending on the experimental case. Their arrangements are shown in Figure 7 and are described below:

- **MV1** – Mixing Ventilation 1: A fabric duct with small nozzles supplied air from above the desks. Exhaust grilles were installed at floor level on the opposite side, generating horizontal airflow across the breathing zone.
- **MV2** – Mixing Ventilation 2: Four ceiling terminal devices were symmetrically positioned on both sides of the room. Air was supplied downward via square diffusers, and exhaust air was collected above these outlets through adjacent grilles on the ceiling.

- **MV3** – Mixing Ventilation 3: Air was introduced through ceiling swirl diffusers that directed flow in a spiralling downward motion. Exhaust air was removed via grilles near the floor on the opposite side, promoting turbulent mixing across the space.
- **DV** – Displacement Ventilation: Low-velocity, cooler air was supplied from floor-level diffusers placed at the front corners of the room. Polluted air was removed via ceiling-level grilles located at the back of the room. This configuration leverages buoyant plumes generated by the dummies to lift heat and contaminants upwards, creating a stratified airflow pattern that minimizes horizontal mixing in the breathing zone.

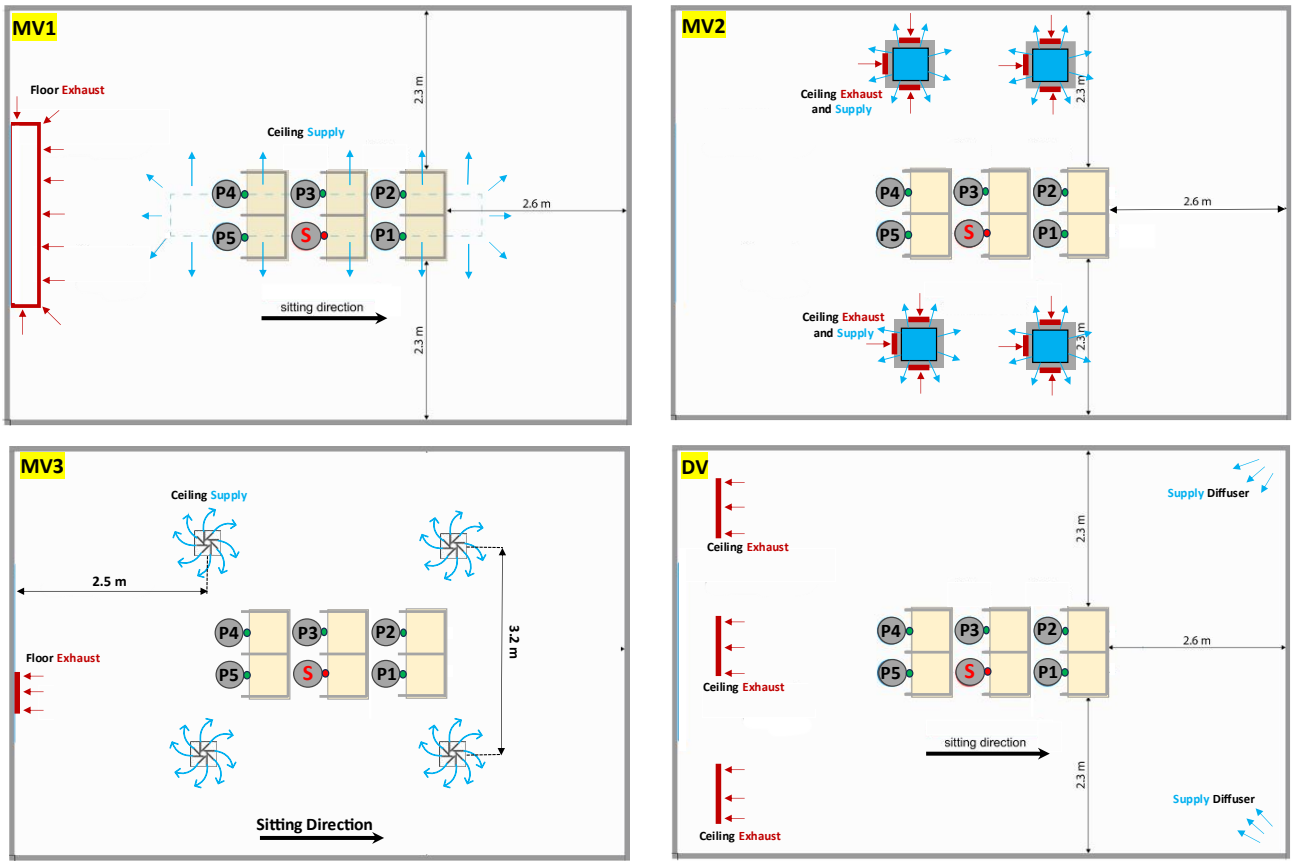

Fig. 7. Test room arrangement with four different air distributions[1]: MV1, MV2, MV3, and DV

Each setup includes six thermal manikins, represented by grey circles, simulating seated occupants. Measurement points P1 to P5, shown as small green circles, are positioned at the mouth level of the manikins to represent typical breathing zones. A red circle placed at the middle row desk indicates the location of the simulated infection source.

[1] The naming convention for ventilation systems in this thesis differs from that used in the corresponding publications.

3.3.2. Integrated personal exhaust ventilation and physical barriers

To explore local source control strategies, personal exhaust (PE) ventilation and physical barriers (PB) were integrated. The physical barriers were transparent acrylic partitions mounted on two-person desks. Each installation featured:

- One front panel (65 × 138 cm) and three side panels to separate adjacent seats
- An integrated plenum box located at the front panel
- 1 cm high horizontal slit outlet, spanning the desk width, which directed air toward the infectious source

Each plenum was connected to a dedicated exhaust duct equipped with a flow meter and an adjustable exhaust fan to control the extraction rate. To maintain mass balance, the total room exhaust flow was divided between the central exhaust system and the PE units, with the main system adjusted accordingly. Figure 8 shows both the real experimental setup and a schematic diagram of the PE+PB system, capturing the integration of airflow capture with physical separation at the source.

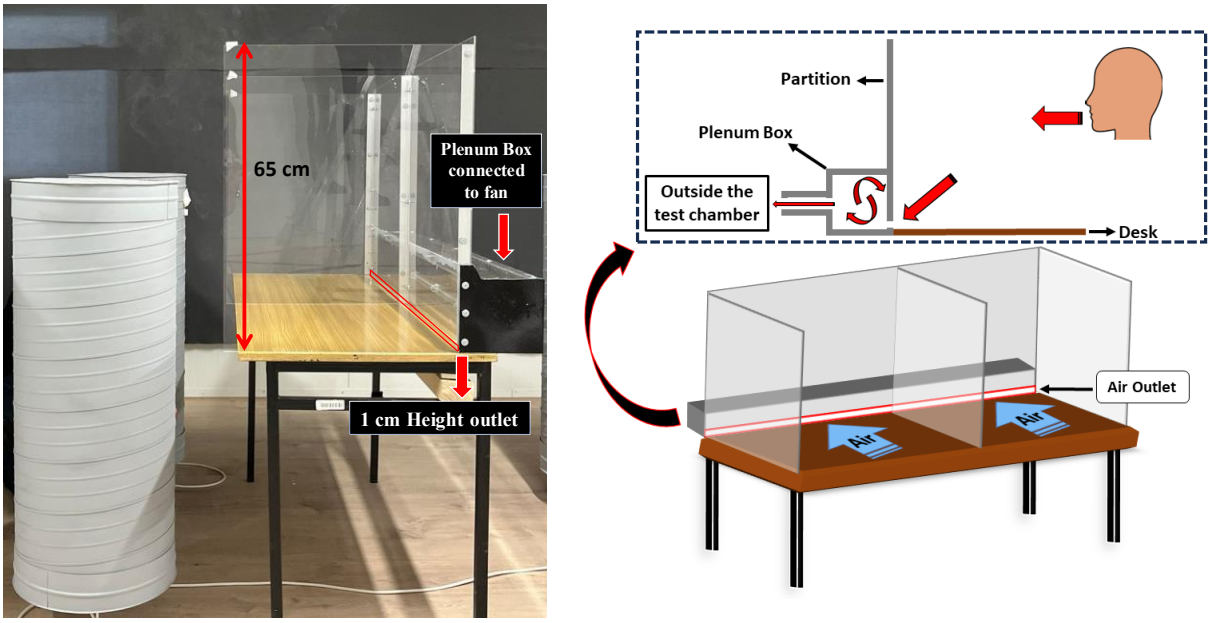

Fig. 8. Real setup picture (left) and diagram (right) depicting a two-person desk with integrated physical barriers and a personal exhaust system.

3.3.3. Definition of selected cases in papers 4-6

Each of the experimental studies employed specific ventilation configurations aligned with their respective research aims. While the physical dimensions and test conditions remained

consistent, the variation in air distribution systems and test scenarios served to isolate and compare ventilation effectiveness and infection mitigation strategies.

- Paper 4 assessed the influence of physical barriers on airflow and aerosol transmission under two mixing ventilation strategies: MV2 and MV3. Both setups were tested with and without the presence of physical desk partitions. The setup consisted of a single pollutant source, simulating an infected person, and five measurement points (P1-P5) representing susceptible individuals.
- Paper 5 expanded the analysis by integrating personal exhaust (PE) systems with physical barriers (PB) and evaluating their performance under three distinct ventilation strategies: MV1, MV2 and DV. For each ventilation type, several scenarios were tested: no barrier or PE system, PB alone, and PB+PE. Table 5 presents the full list of experimental scenarios tested under each ventilation system.

Table 5. Overview of measurement scenarios.

Ventilation principle	Physical barrier (PB)	PE flow rate (L/s per person)
MV_1	×	×
	✓	0, 9
MV_2	×	×
	✓	0, 4, 9, 12
DV	×	×
	✓	0, 9

Tracer gas measurements were taken at three susceptible occupant locations—in front of, next to, and behind the source (P1, P3, P5)—to represent various exposure scenarios.

- Paper 6 focused on optimizing the geometry and efficiency of integrated PB and PE systems under a single ventilation scheme of MV3. A detailed parametric study was carried out to determine the optimal height and placement of physical barriers, along with adjustments to the PE slot design. CFD and experimental results were used to quantify airflow interference and aerosol removal efficiency of system.

3.4. Result and discussion

3.4.1. Effects of physical barriers on air change effectiveness and aerosol transmission

Following the simulation-driven investigations presented in the previous sections, this part of the thesis shifts the focus to experimental studies exploring localized infection control strategies. Specifically, Paper 4 investigates how physical barriers (PB), commonly used in indoor environments during the pandemic, interact with different air distribution systems in reducing aerosol and bioaerosol concentrations. The main objective was to assess whether such barriers compromise the air change effectiveness (ACE) and particle dilution in a mechanically ventilated classroom setup. To evaluate the impact of barriers on ventilation efficiency, local air change effectiveness (ACE) was calculated using the CO_2 decay method [94]. It was calculated as the ratio of the age of air in the exhaust duct (τ_e) to the local mean age of air at a measured location (τ_m):

$$ACE = \frac{\tau_e}{\tau_m} \quad (9)$$

The higher the ACE values, the more effective the ventilation system is in that area. In this study, the CO_2 concentrations were obtained during a decay test, where the decay of tracer gas concentration over time was measured at different points. As depicted in Figure 9, measurements were conducted under two air distribution systems (MV2 and MV3) and two conditions (with physical barriers and without physical barriers). Under both systems, ACE was generally higher in the absence of partitions, confirming that PBs can disrupt airflow uniformity. For MV2, the ACE values dropped noticeably at P4 and P5 with partitions in place, suggesting airflow stagnation and poor contaminant removal. In contrast, MV3 maintained relatively consistent ACE values even with barriers, indicating its superior capacity to preserve ventilation efficiency despite the added obstruction.

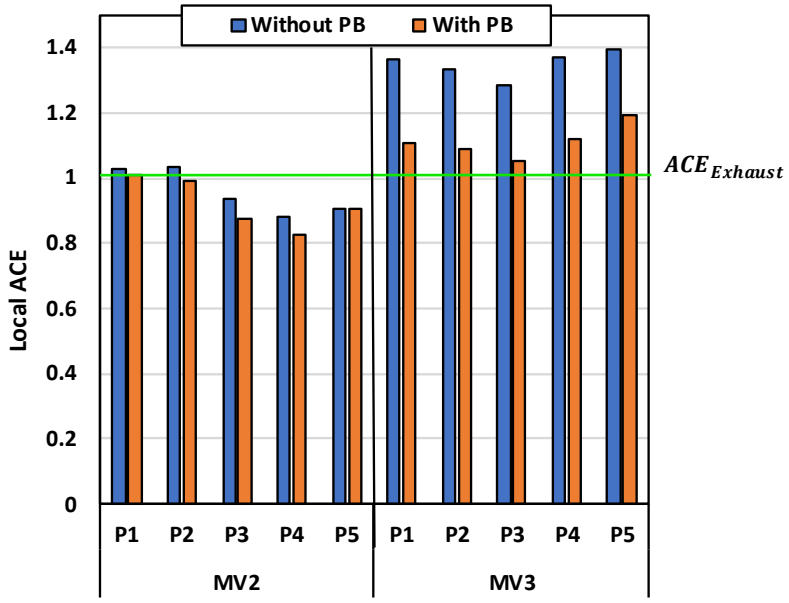

Fig. 9. Local air change effectiveness (ACE) at points P1-P5 comparison across air distribution systems and physical barriers (PB).

Complementing ACE, the aerosol concentration reduction rate (CR) was calculated by comparing particle concentrations. Figure 10 illustrates CR of aerosol particles under two different air distribution systems, MV2 and MV3, at five points (P1 to P5) near the infection source where exposed individuals were situated. The C_R was determined by comparing the particle concentration with and without the use of partitions, following the equation:

$$C_R = \frac{C_{Without\ PB} - C_{With\ PB}}{C_{Without\ PB}} \quad (10)$$

Under MV3, CR values remained strongly positive at all points, averaging around 0.8 at P1–P3 and around 0.6–0.7 at P4 and P5. This suggests a robust capacity of MV3 to reduce particle levels near and behind the source, even when partitions altered the airflow path. In contrast, MV2 exhibited mixed results. At P1 and P2, moderate CR values (~0.4) were observed, while P4 and P5 experienced negative CRs, indicating higher particle levels behind the source when partitions were used. These findings imply that under MV2, PBs may inadvertently obstruct airflow and cause pollutant accumulation in downwind regions. The study also included bioaerosol experiments using Micrococcus luteus as a surrogate for pathogen-laden droplets. Under MV2, partitions substantially reduced concentrations at P1 (from 1089 CFU/m³ to 423 CFU/m³) but increased them at P3 and P5 (to 1569 and 1363 CFU/m³, respectively), indicating unintended redirection of bioaerosols. Under MV3, PBs effectively reduced concentrations at both P1 and P5, and only a minor increase was seen at P3. Although standard deviations were

higher for bioaerosols due to complex deposition behaviour, MV3 consistently demonstrated more stable performance and lower concentrations overall. These results collectively highlight the critical interaction between room airflow design and infection mitigation measures like PBs. While partitions can support localized containment near the source, their efficacy is strongly tied to the underlying air distribution system. MV3's swirling pattern and higher inlet velocity proved more capable of offsetting the barrier-induced disruption, maintaining a well-mixed environment, and preventing pollutant accumulation. MV2, lacking such features, performed less reliably in partitioned scenarios and showed reduced ventilation effectiveness.

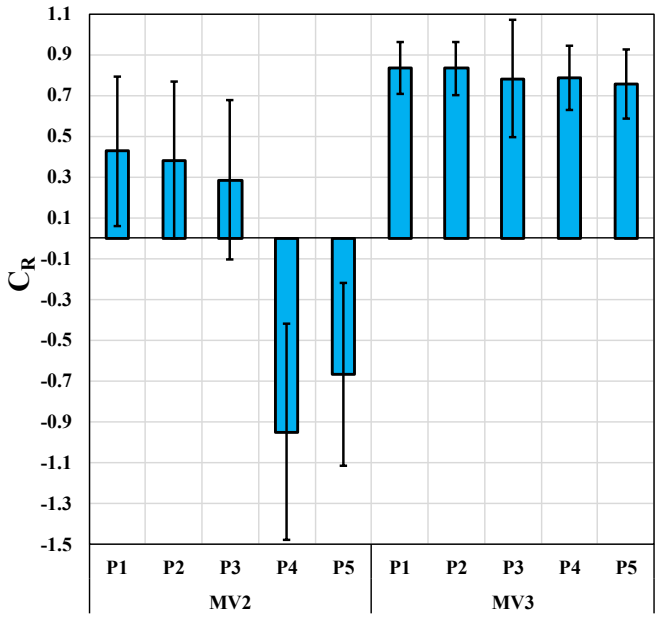

Figure 10. Comparison of aerosol concentration reduction rates (C_R) across air distribution systems and prevention measures.

3.4.2. Compatibility of integrated personal exhaust ventilation and physical barriers with air distribution systems

Building on the previous experimental investigation focused solely on physical barriers, paper 5 evaluates a more advanced local mitigation strategy that integrates physical barriers (PB) with personal exhaust (PE) ventilation. The study investigates how this combination performs across three different air distribution systems: two mixing ventilation configurations (MV1 and MV2), and displacement ventilation (DV). Figure 11 presents the average N_2O concentration values at equilibrium obtained at three points under various scenarios. In the baseline condition without any preventive measures, DV outperformed both MV1 and MV2 by maintaining the lowest N_2O concentrations at all measurement points. Notably, MV1 yielded the highest risk

in front of the source (P1), whereas MV2 had the highest concentration next to the source (P2), highlighting how airflow directionality affects risk zones. With physical barriers alone (PE = 0), the performance varied considerably between systems. The barriers were most effective under DV and MV2, reducing concentrations by up to 63% depending on the location. However, in MV1, PB's presence increased N_2O concentration—especially at the desk shared with the infected person (P2)—where N_2O levels nearly doubled compared to the baseline. This confirmed that physical barriers can obstruct airflow and trap contaminants, leading to unintended accumulation in poorly designed systems. The introduction of personal exhaust (PE = 9 L/s/person) in combination with partitions resulted in consistent and significant reductions in N_2O concentrations across all ventilation systems and measurement points. In MV1, where partitions alone worsened conditions, the integration of PE reversed this effect. For example, N_2O concentrations at P2 dropped by a factor of 2.5, bringing MV1's performance in line with MV2 and DV.

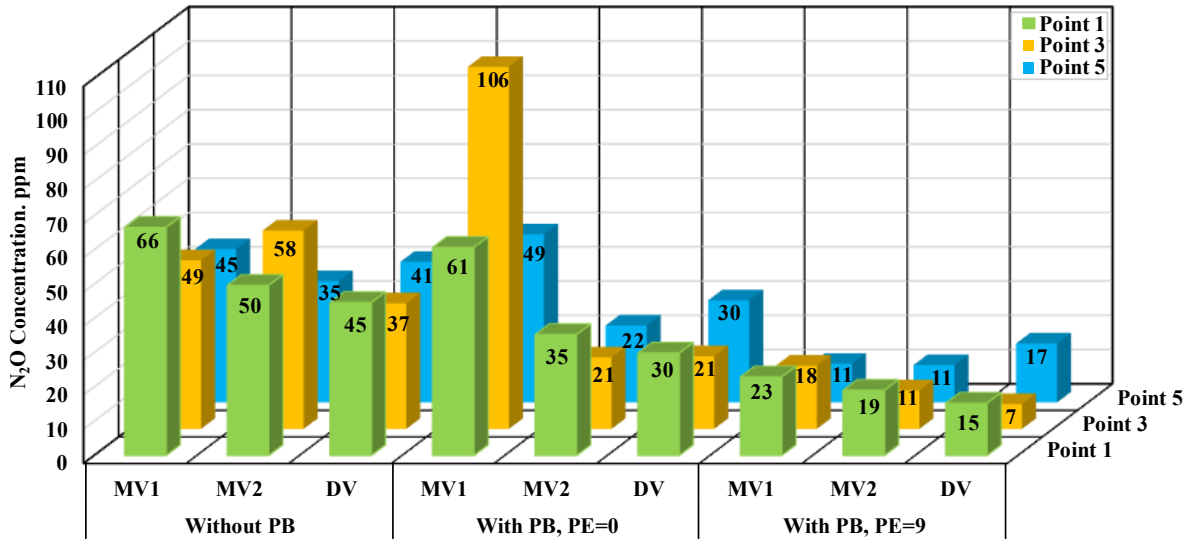

Fig. 11. N_2O concentrations measured at three points in three examined scenarios.

To further optimize the system, three different airflow rates (4, 9, and 12 L/s per person) were tested for MV2. Results showed that increasing the PE flow rate enhanced contaminant removal efficiency at all points. From 4 to 9 L/s, concentrations fell by up to 35%, and increasing to 12 L/s provided an additional 30–50% reduction. However, this improvement comes with a trade-off in system complexity and potential energy use. The results underscore a clear synergy between physical barriers and localized personal exhaust systems. While partitions alone offer only modest and inconsistent protection, especially under turbulent mixing conditions, the addition of PE transforms the setup into a robust localized mitigation

strategy. The consistent performance across ventilation types also suggests this integrated approach is compatible for classrooms and offices alike.

3.4.3. Resource efficient design of local exhaust ventilation with physical barriers

Building upon the findings of Paper 5, which demonstrated the effectiveness of combining physical barriers and personal exhaust systems, Paper 6 advances the analysis by integrating experimental validation and CFD simulations to optimize the design for resource efficiency. Validation of CFD results was performed by comparing simulated airflow and temperature profiles with experimental measurements at three height levels along three vertical measurement lines. The results showed good agreement, with deviations of ~16% in air velocity and 5% in temperature, confirming the reliability of the CFD model. According to Figure 12, the velocity distribution shows a distinct pattern influenced by the air distribution system, physical barriers, and heated dummies. On the top of the dummies, a pronounced thermal plume is observed. This thermal plume is characterized by a vertical column of increased velocity extending upwards, a result of the heat emitted by the dummy that causes the surrounding air to rise due to buoyancy effects. The air distribution system, with supply air descending from the ceiling diffusers and spreading out across the room, contributes to an even distribution of air velocities, effectively maintaining a gentle airflow around the occupants and minimizing drafts. However, the presence of physical barriers also influences the airflow patterns, causing deviations and creating recirculation areas. The middle dummy, which acts as an infection source, generates particles along with the airflow.

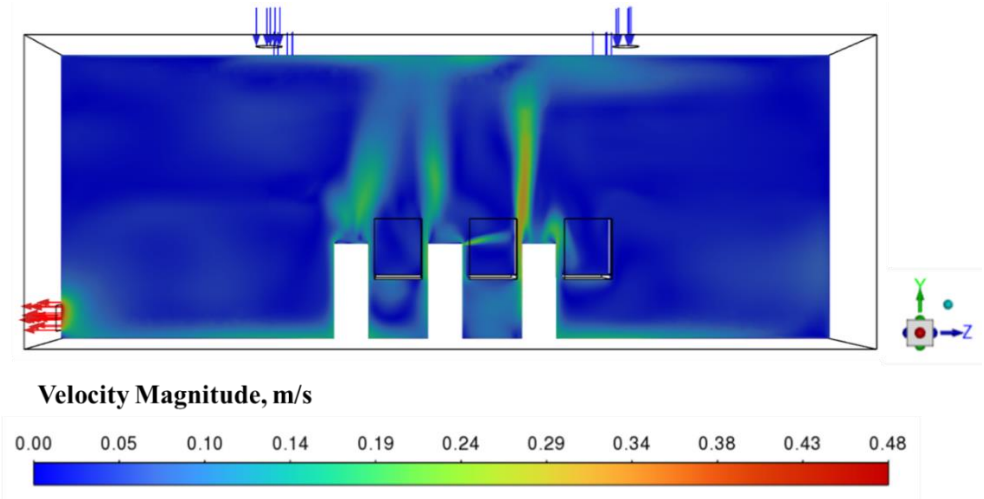

Fig. 12. Velocity magnitude contour at the YZ-plane through the centreline of dummies−With PB

Aerosol concentrations were measured at five breathing zone locations for each scenario and normalized for comparison. The baseline case without mitigation showed high concentrations at all locations. When physical barriers were introduced, concentrations dropped by ~50%, indicating their capacity to limit lateral aerosol spread. The combined use of physical barriers and personal exhaust achieved the most notable improvement. Concentrations dropped to nearly zero at four out of five points, with only a modest value at the source location (P3), reflecting high capture efficiency. The CFD results mirrored experimental trends, providing robust evidence for system effectiveness. To refine the system design, CFD simulations assessed the influence of barrier height and exhaust flow rate on aerosol removal efficiency, quantified by the Relative Aerosol Removal (RAR) metric. RAR is defined as:

$$RAR = \frac{N_{removed}(h)}{N_{removed}(65cm)} \tag{11}$$

Reducing barrier height from 65 cm to 45 cm retained 95% of the baseline removal efficiency, while a further reduction to 25 cm led to a more noticeable drop (RAR ≈ 0.83). This finding suggests that shorter barrier heights up to 45 cm can achieve effective protection while improving visibility and reducing material use. Similarly, lowering the exhaust flow rate to 6 L/s per person retained 94% of the removal efficiency seen at the baseline 9 L/s. Further reductions, however, significantly compromised performance, highlighting 6 L/s as the practical lower limit for maintaining efficacy with energy savings. These findings are illustrated in Figure 13.

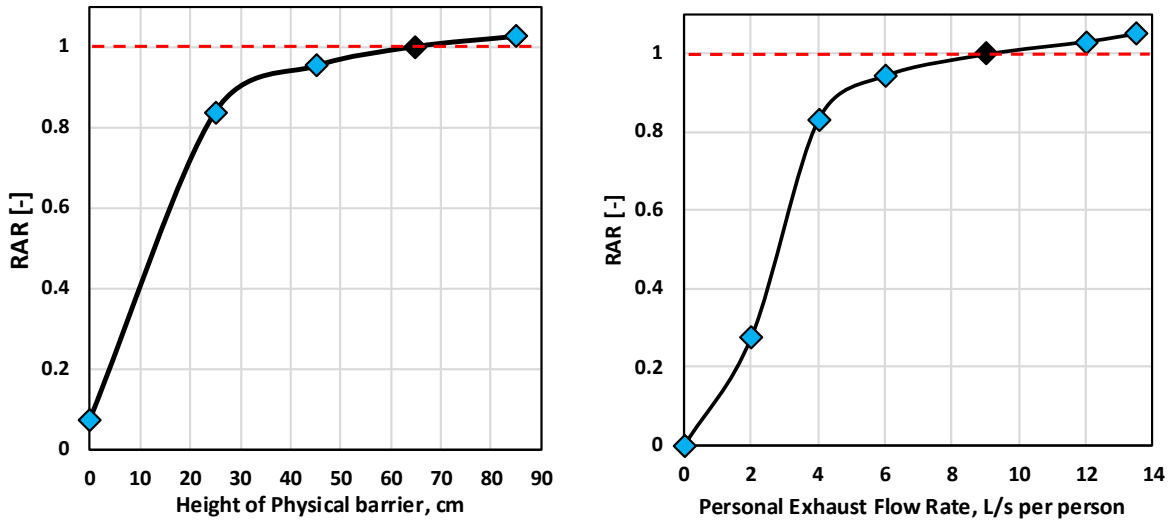

Fig. 13. Relative Aerosol Removal (RAR) for various heights and flow rates of PE+PE

Chapter 4: Life cycle assessment of infection control strategies

4.1. Scope of study

This chapter explores the trade-off between airborne infection control and environmental sustainability within educational indoor environments. The primary aim is to assess the broader implications of commonly used mitigation strategies by examining not only their effectiveness in reducing infection risk but also their long-term environmental consequences. The scope is limited to strategies applicable in classroom settings, where high occupant density and prolonged exposure make infection risk and resource efficiency especially critical. The strategies considered represent a range of interventions—from mechanical and natural ventilation to local source-control measures such as air cleaners, physical barriers, and personal exhaust systems. This study was conducted as an extension to the main body of research and is not based on a separate peer-reviewed publication. While the core contributions of the thesis are fully addressed through the six published papers, this chapter adds value by responding to a recognized research gap: infection control strategies are often evaluated solely on their health performance without regard for material consumption, energy demand, or carbon emissions. By adopting a dual-perspective approach, the chapter provides a broader context for decision-making that integrates both public health and environmental objectives. The analysis emphasizes the importance of identifying solutions that are not only effective in mitigating transmission but also feasible and sustainable in the long term. In doing so, it supports the development of balanced indoor environmental strategies that align with the goals of energy efficiency, carbon reduction, and occupant well-being.

4.2. Methods

To assess the environmental consequences, a life cycle assessment (LCA) was conducted, using OpenLCA (version 2.3.1). The inventory data was tailored and modelled using the Environmental Footprint v.3.0 database. Environmental impacts were quantified using the adapted EF 3.0 method, incorporating normalization and weighting to comprehensively analyze various impact categories. The study systematically defines the production, usage, and disposal stages, providing a foundation for the LCA results and multi-faceted evaluation. While LCI quantifies the input and output flows (e.g. materials, energy, emissions) associated with each strategy, LCIA evaluates the environmental consequences of these flows by applying characterization factors to impact categories such as climate change, resource depletion, and

human toxicity. A key output of this method is the environmental burden expressed in normalized and weighted units known as “Points” (Pt). Pt values are derived through a two-step process:

1. **Normalization**: The characterized impact results for each environmental category is divided by a reference value representing the annual average impact per person in the EU. This expresses the impact in terms of its relevance to an average European citizen's environmental footprint.
2. **Weighting**: The normalized results are then multiplied by weighting factors reflecting the relative importance of each category, as determined through expert consensus and policy priorities within the EF methodology. This process converts multi-category results into a single aggregated score (Pt) that simplifies comparison across strategies.

The total environmental impact of each strategy, represented as $LCIA_{total}$, was calculated using the following equation 12:

$$LCIA_{total} = LCIA_{production} + \sum_{i=1}^{10} LCIA_{use} + LCIA_{disposal} \quad (12)$$

In this formula, $LCIA_{production}$ reflects the environmental impacts associated with obtaining raw materials, their processing, and the manufacturing of equipment, supplies, filters, and packaging. The sum $\sum_{i=1}^{n} LCIA_{use}$ represents the combined impacts during the operational phase, including energy usage and periodic replacements like filter changes, throughout the 10-year period. Finally, $LCIA_{disposal}$ covers the impacts from the end-of-life stage, such as recycling, burning, or landfilling the products. This comprehensive approach allows for a complete evaluation of each strategy's environmental performance across its entire lifespan. By combining these three stages, the methodology accounts for the initial production impacts, the ongoing operational impacts, and the final disposal impacts.

4.3. Study design

This section outlines the setup and assumptions employed for evaluating the environmental impact of airborne infection control strategies. Three types of infection mitigation strategies were considered, each with distinct material requirements and operational features:

- **Air Cleaners**: Two portable units equipped with HEPA filters (330 m^3/h CADR each). The operation phase includes electricity consumption and periodic HEPA filter replacement.

- **Disposable Masks**: Daily use of disposable medical masks by all students.
- **Integrated PE+PB System**: The physical barrier and personal exhaust system were modelled based on the laboratory-tested setup described in section 3.2.

A comprehensive list of input materials per strategy is shown in table 6.

Table 6. Life cycle inventory of selected strategies [95,96].

Strategy	Inventory	Amount (kg/FU)
Air cleaner	PP (polypropylene)	0.906
	PET (polyethylene terephthalate)	0.002
	PE (polyethylene)	0.566
	Paper	0.426
	Mix plastics	8.096
	Metals (steel)	4.152
	Metals (non-ferrous)	0.266
	Electronics	1.246
	Cardboard	4.130
	Carbon pellet	0.652
	Aluminium	0.030
	Adhesive	0.230
Disposable masks	Polypropylene spun-bonded non-woven fabric	137.700
	Polypropylene melt-blown non-woven fabric	82.620
	Aluminium strip	25.920
	Polyester/nylon blends	35.640
	Polyethylene film	5.022
	Ivory board	80.028
	Corrugating medium	38.880
PE+PB	PMMA (polymethyl methacrylate)	110.000
	3D-printed PLA	2.000
	Aluminium sheet	6.100
	Flexible ducting	10.100
	Stainless steel	8.900

The functional unit (FU) was defined as the implementation of a given infection control strategy in a classroom with 30 students, operating for six hours per day, five days per week, across a 9-month school year. All strategies were evaluated over a 10-year period, corresponding to the assumed lifespan of air cleaners which is designated by the manufacturer. The system boundary adopted a cradle-to-grave approach, incorporating raw material extraction, manufacturing, use, and disposal (see Figure 14). Transportation impacts were excluded due to their marginal contribution, as supported by previous studies.

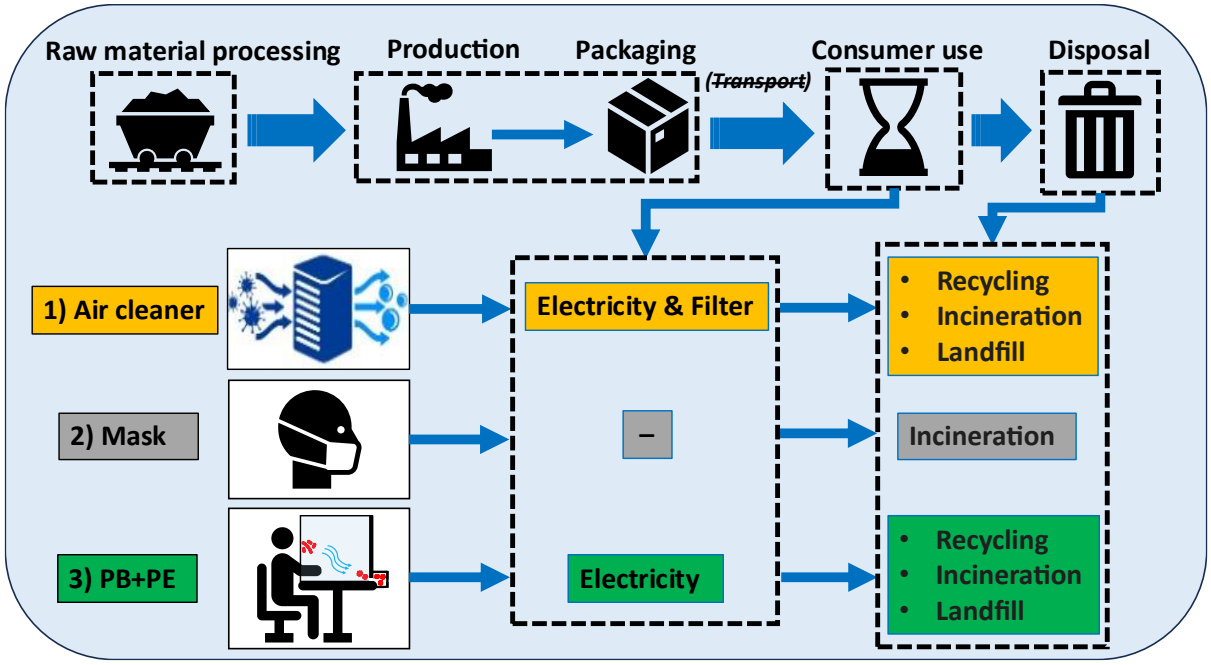

Fig. 14. Cradle-to-Grave stages of airborne infection control strategies.

To assess the environmental performance of each strategy, five scenarios were defined, all assuming a mechanical mixing ventilation system delivering 148 L/s of outdoor air (3 ACH). The strategy configurations are summarized in table 7.

Table 7. Selected cases conducted in the study.

Case	Ventilation	Air cleaner	Mask	PE+PB
1	✓	-	-	-
2	✓	✓	-	-
3	✓	-	✓	-
4	✓	✓	✓	-
5	✓	-	-	✓

4.4. Result and discussion

4.4.1. Probability of infection risk

The probability of infection risk was quantified using the Wells-Riley model, focusing on the reproduction number, R_0, as the key outcome. Figure 15 presents the variation in R_0 over time for each selected case, illustrating how different strategies influence infection risk over the duration of a single lesson (45 minutes). Case 1 (ventilation only) showed the highest infection

risk with R₀ exceeding 1.25, well above the recommended epidemic control threshold ($R_0 < 1$). The addition of air cleaners (Case 2) lowered R_0 to ~0.75. The use of masks (Case 3) further reduced it to ~0.45. The best result was achieved in Case 4, where the hybrid strategy-maintained R_0 at ~0.27. Notably, Case 5 also demonstrated a substantial reduction with R_0 at ~0.36, indicating the strength of source control and local exhaust. This analysis reinforced that combining control strategies offers synergistic benefits, and that localized interventions like PE+PB provide comparable infection control to multi-layered personal protection approaches.

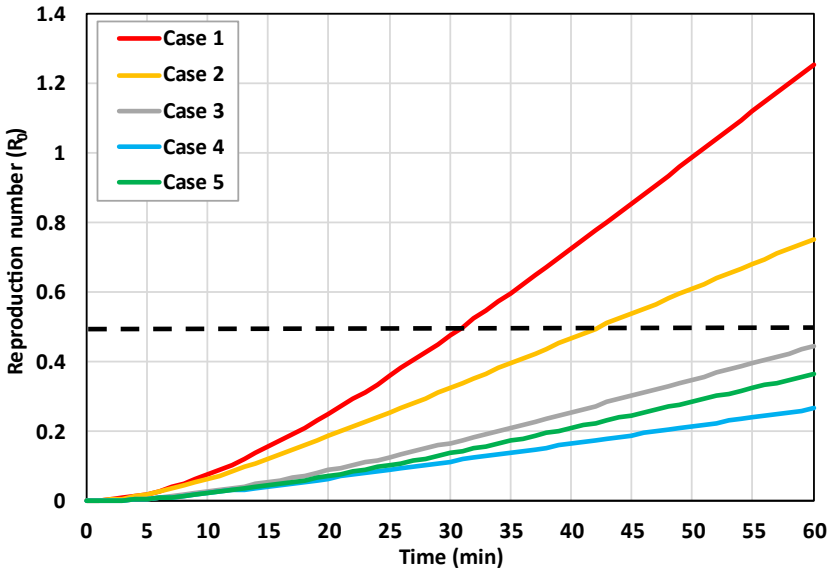

Fig. 15. Temporal variation of event reproduction number for different infection control strategies in a classroom setting - Dashed line exhibits the recommended threshold.

4.4.2. Hotspot analysis of input inventory flows

A hotspot analysis was carried out to pinpoint the major contributors to the environmental footprint of three mitigation strategies: air cleaners, disposable masks, and the integrated physical barrier plus personal exhaust (PB+PE) system. The analysis focused on the proportional impact of input materials across various environmental categories, with results visualized in Figures 16 (a–c). This evaluation highlights which material flows are responsible for the highest environmental burdens, serving as a foundation for identifying opportunities for impact reduction. In the case of disposable masks, the analysis reveals a strong reliance on fossil-derived materials, contributing notably to indicators such as water consumption and global warming potential. For air cleaners, electronic components emerge as the most impactful, especially in categories related to human toxicity and resource depletion. The

PB+PE system, on the other hand, demonstrates a concentrated environmental load due to its heavy use of polymethyl methacrylate (PMMA), commonly used in transparent barriers. The findings underscore the importance of material selection in the design and development of infection control technologies. For instance, optimizing electronics in air cleaners and substituting or reducing PMMA in partition-based systems could lead to significant environmental benefits. This hotspot analysis also informs the sensitivity analysis by identifying the most influential material inputs for further exploration of potential improvements in environmental performance.

a)Air cleaner

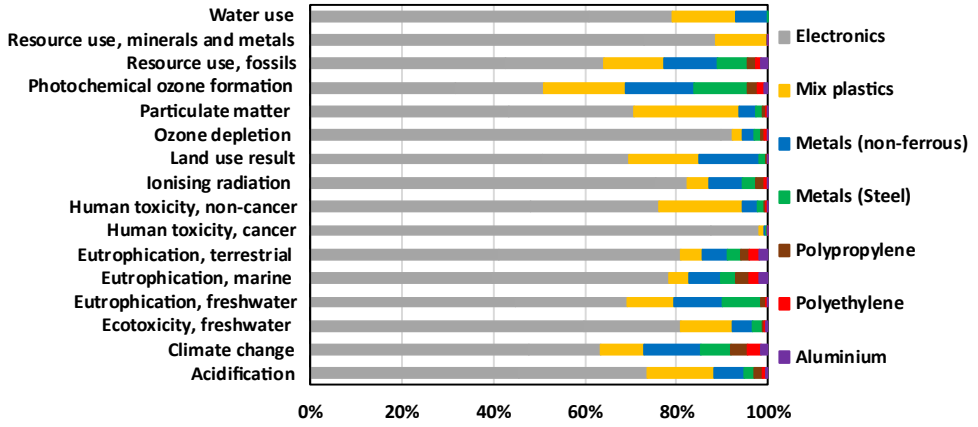

b) Mask

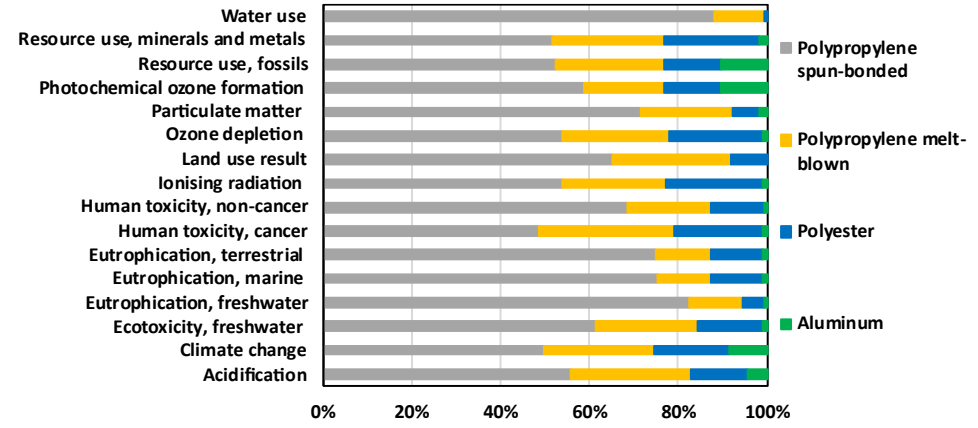

c) PB+PE

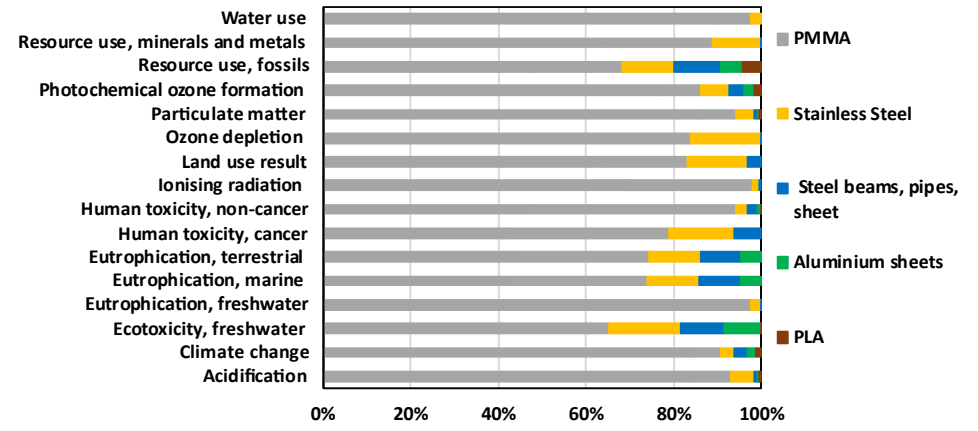

Fig. 16. Hot-spot analysis. Contribution of input inventory flows on the total Environmental Footprint impact indicators: a) Air cleaner, b) Mask, and c) PB+PE.

4.4.3. Environmental impact of use phase

To determine the operational environmental burdens associated with each infection mitigation approach, the use-phase impacts were evaluated over a defined 10-year functional lifespan. This phase focused on electricity consumption as the main contributor, with filter replacements and disposable masks excluded to isolate the effects of energy use alone. As shown in Table 8, the energy required to operate the air cleaners (680.4 kWh) contributed significantly to impact categories such as climate change, particulate matter formation, and photochemical smog. The PB+PE system, with a higher operational demand of 1900 kWh, exhibited even greater impacts across all assessed categories, indicating that electricity usage is a critical factor in the system's overall environmental profile. This analysis identifies the use phase as a major driver of environmental burden—particularly for electricity-intensive systems. The results highlight the need for energy-efficient designs and technologies to mitigate long-term impacts, with climate-related emissions, resource depletion, and fine particulate emissions emerging as key areas for improvement.

Table 8. Calculated impact categories for using phase of infection control strategies.

Process	Unit	Air cleaner	PB+PE
Required amount	kwh	680.4	1900
Acidification	mol H+ eq	1.65	4.61
Climate change	kg CO_2 eq	570.31	1592.5
Ecotoxicity, freshwater	CTUe	14.21	32.18
Eutrophication, freshwater	kg P eq	1.87E-04	1.67E-04
Eutrophication, marine	kg N eq	0.28	0.8
Eutrophication, terrestrial	mol N eq	3.14	8.78
Human toxicity, cancer	CTUh	4.56E-08	6.39E-09
Human toxicity, non-cancer	CTUh	1.81E-07	5.27E-07
Ionising radiation	kBq U-235 eq	0.06	0.112
Land use result	Pt	1.7	43.63
Ozone depletion	kg CFC11 eq	4.95E-08	2.81E-07
Particulate matter	disease inc.	1.51E-05	4.22E-05
Photochemical ozone formation	kg NMVOC eq	0.84	2.36
Resource use, fossils	MJ	3884	10845.98
Resource use, minerals and metals	kg Sb eq	0.01	2.24E-06
Water use	m^3 depriv.	0.001	2.69

4.4.4. Sensitivity analysis on LCIA results

To assess the influence of key input variables on the environmental outcomes of the evaluated mitigation strategies, a sensitivity analysis was performed. Selected parameters were adjusted by ±2%, a standard practice in life cycle assessment studies aimed at gauging result stability without introducing excessive computational complexity [97]. The analysis examined how these variations affect multiple Environmental Footprint (EF) impact categories. The outcomes, summarized in Table 9, reveal material- and process-specific sensitivities. A color-coded gradient is employed for visualization purposes, with red indicating the highest sensitivity within each impact category and dark green representing the lowest. Intermediate shades (e.g., yellow and orange) denote proportional differences relative to these extremes. The analysis identifies several critical environmental hotspots. Energy consumption, the use of PMMA in barrier systems, and electronic components in air purifiers emerge as particularly influential in driving overall environmental impacts. These findings suggest that targeted improvements—such as enhancing energy efficiency, sourcing sustainable alternatives to PMMA, reducing water demand in polypropylene-based mask production, and redesigning electronics for lower toxicity and resource intensity—could significantly improve the environmental profile of infection mitigation strategies.

Table 9. Sensitivity analysis of impact indicators with a variation of the main input flows of the strategies.

Impact categories	Unit	Electronics	Polypropylene	PMMA	Electricity
Acidification	mol H+ eq	0.119	0.132	0.102	0.624
Climate change	kg CO_2 eq	0.011	0.102	0.063	0.728
Ecotoxicity, freshwater	CTUe	0.033	0.015	0.186	0.018
Eutrophication, freshwater	kg P eq	0.00	0.018	0.00	0.00
Eutrophication, marine	kg N eq	0.00	0.012	0.006	0.94
Eutrophication, terrestrial	mol N eq	0.001	0.015	0.007	0.939
Human toxicity, cancer	CTUh	0.532	0.047	0.023	0.00
Human toxicity, non-cancer	CTUh	0.180	0.03	0.109	0.02
Ionising radiation	kBq U-235 eq	0.016	0.005	0.171	0.00
Land use	Pt	0.000	0.676	0.155	0.00
Ozone depletion	kg CFC11 eq	0.045	0.001	0.02	0.00
Particulate matter	disease inc.	0.256	0.385	0.086	0.688
Photochemical ozone formation	kg NMVOC eq	0.021	0.049	0.039	0.829
Resource use, fossils	MJ	0.019	0.051	0.033	1.055
Resource use, minerals and metals	kg Sb eq	0.433	0	0.064	0
Water use	m^3 depriv.	0	0.714	0.005	0

4.4.5. Total life cycle environmental footprint

This section presents a comprehensive evaluation of the total environmental impact associated with each infection control strategy, accounting for all stages of the life cycle—from raw material extraction and manufacturing to usage and end-of-life disposal. To enable a unified comparison across strategies, a single score weighting method (expressed in Pt) was applied, aggregating all environmental impact categories into a single performance indicator. The analysis follows a Cradle-to-Grave perspective, encompassing raw material sourcing, production processes, packaging, user-phase emissions, and final waste treatment. The results, illustrated in Figure 17, reveal a distinct ranking of the strategies based on their overall environmental footprint. The combination of mask and air cleaners (Case 4) demonstrate the highest total impact (~0.33 Pt), indicating the significant environmental cost of employing multiple layers of protection simultaneously. Case 3, which relies solely on disposable masks, shows a similarly high burden (~0.27 Pt), reinforcing the long-term environmental drawbacks of single-use personal protective equipment. In comparison, Case 5—incorporating local ventilation and physical barriers—shows a considerably lower footprint (~0.14 Pt), suggesting a more sustainable pathway for reducing exposure. Case 2, involving air purifiers, results in an even lower environmental impact (~0.12 Pt), supporting the notion that filtration-based strategies may provide a favourable balance between efficacy and sustainability. Unsurprisingly, the baseline scenario without additional mitigation (Case 1) produces the lowest impact (~0.06 Pt), serving as a minimal reference point. These findings emphasize the critical importance of evaluating infection control measures not only for their health effectiveness but also for their long-term environmental implications. In particular, the substantial environmental load associated with disposable masks suggests a need to explore and promote reusable or locally targeted mitigation options. Shifting toward ventilation-based strategies and integrated physical barriers offers an opportunity to align public health goals with environmental responsibility.

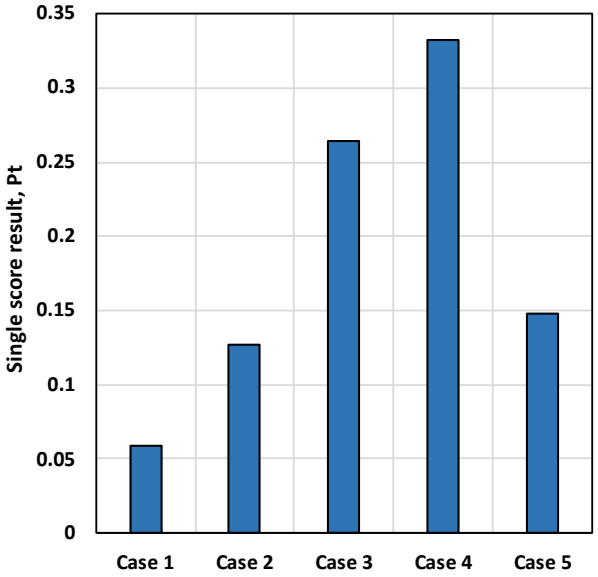

Fig. 17. Weighted single-score of environmental burden for infection control strategies over a 10-year period.

4.4.6. Weighted trade-off analysis

The results of the sensitivity analysis highlighted key contributors to environmental burden across infection mitigation strategies, particularly components associated with energy use, electronics, and high-impact polymers. These findings reinforce the need to prioritize sustainability in infection control interventions by exploring options such as renewable energy sources, efficient designs, and environmentally preferable materials. However, the analysis also revealed a core challenge: the strategies that most effectively minimize infection risk often entail considerable environmental costs, while more sustainable methods may fall short in curbing transmission effectively. This tension presents a complex design problem, requiring careful consideration of trade-offs. To systematically investigate this balance, a dual-criteria evaluation was carried out, integrating both infection risk and life cycle environmental impact into a unified framework. This approach allows for flexible weighting between the two objectives—health protection and sustainability—depending on the context or decision-making priorities. A normalized composite function, F_{ws}, was used to evaluate each strategy. Weighting coefficients a_1 allows prioritization of infection risk (R_0) and a_2 allows prioritization of total environmental impact (pt), constrained by $a_1 + a_2 = 1$. When environmental impact is prioritized, (a_1 is low and a_2 is high), strategies with minimal technological complexity—such as the basic ventilation-only approach—emerge as optimal

due to their low environmental footprint, even though they offer limited infection risk control. On the other end of the spectrum, when infection risk is prioritized, (a_1 is high and a_2 is low) strategies like combining air cleaners with disposable masks is known as the optimal strategy. As illustrated in Figure 18, the ranking of strategies shifts considerably as the weight assigned to infection risk increases. When infection control and sustainability are valued equally, the configuration involving personal exhaust ventilation and physical barriers provides the best compromise. This approach effectively reduces airborne transmission while maintaining a moderate environmental profile. Notably, this strategy becomes the most favourable when moderate-to-high emphasis is placed on infection risk (e.g., when a_1 is between 0.5 and 0.9). In contrast, although the basic ventilation strategy consistently demonstrates environmental efficiency, its limited infection control capacity renders it less suitable as the priority shifts toward health protection. Likewise, the hybrid approach integrating masks and air cleaners, despite its superior infection control performance, remains penalized due to its significant energy and material demands, leading to consistently high F_{ws} values. An important observation is the robustness of the strategy based on portable air cleaners alone, which maintains a relatively stable position across different priority settings. This is attributed to its balanced performance: it reduces infection risk effectively and produces less environmental damage compared to more intensive approaches. The technology used—HEPA filtration—offers reliable pollutant removal with manageable operational costs and material requirements. It is also worth considering that alternative purification methods such as ionization, UVGI, or electrostatic precipitation may influence the environmental profiles of air-cleaning solutions. While these technologies were not directly assessed in this study, their inclusion in future evaluations could further clarify the trade-offs involved in infection control. In summary, the analysis reveals that no single strategy is universally superior across all objectives. The most suitable option depends on the specific weighting assigned to infection risk versus sustainability. If sustainability is the dominant concern, minimalist approaches prevail. If health protection is the priority, more targeted ventilation or hybrid strategies offer superior outcomes. For balanced decision-making, personal exhaust ventilation combined with physical barriers provides a compelling option that aligns well with both objectives. These insights emphasize the importance of context-specific decision-making and the need for adaptable design frameworks that can respond to changing public health risks and environmental goals.

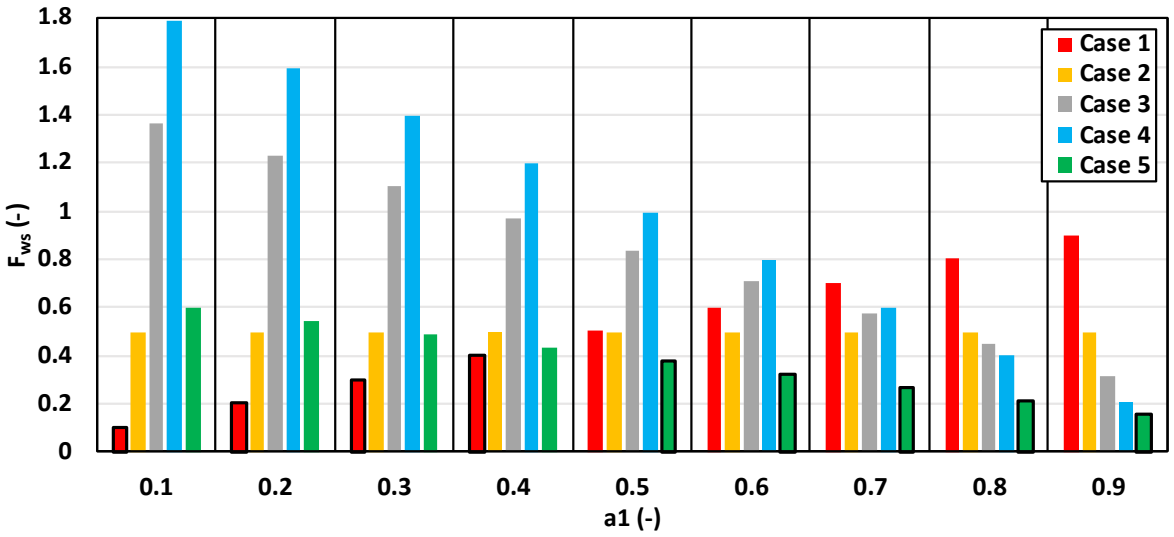

Fig. 6. Weighted multi-criteria evaluation of infection risk and environmental impact across different cases- best choices highlighted for each weighting coefficient.

Chapter 5: Conclusions

The research work carried out presents a comprehensive investigation into strategies for improving indoor environmental quality and mitigating airborne infection risks, with a particular focus on classrooms. In the first step, the development of a smart window controller marked improved air quality and thermal comfort through natural ventilation. However, results showed that natural ventilation alone, even when intelligently controlled, was insufficient to reduce infection risk to safe levels under high occupancy. This finding indicates that the first hypothesis—suggesting that natural ventilation through smart windows may control infection risk when there is no access to mechanical ventilation—was only partially confirmed. Supplementary measures such as air cleaners, personal protective equipment, and mechanical ventilation were required to effectively mitigate infection risks. Multi-objective optimization approaches further refined smart window operation by balancing annual energy demand, CO_2 levels, and predicted percentage of dissatisfaction. Simultaneously adjusting window operation and thermostat setpoints enabled substantial improvements in energy efficiency, indoor air quality, and thermal comfort across climates. However, these solutions required careful balancing of trade-offs between objective functions. This supports the hypothesis that multi-objective optimization can lead to simultaneous control of IAQ, thermal comfort, and energy demand. Recognizing the limitations of natural ventilation, the next study explored hybrid ventilation systems that integrate smart windows and mechanical ventilation based on outdoor

pollution levels and temperature. Simulations and optimizations conducted for diverse climatic and urban conditions confirmed the efficiency of this approach in limiting pollution penetration, reducing energy use, and keeping acceptable thermal comfort. These findings confirm the hypothesis that hybrid systems can effectively adapt to indoor and outdoor air quality variations.

The second phase of the research focused on experimental investigations of local control strategies. Physical barriers were shown to be effective in reducing short-range aerosol transmission under well-mixed ventilation conditions, but their performance was dependent on the operation of air distribution systems. In poorly ventilated rooms, barriers could lead to localized particle build-up. Thus, the hypothesis that physical barriers reduce airborne transmission was validated, but with the caveat that their effectiveness is conditional on ventilation type and layout. The integration of personal exhaust ventilation with physical barriers proved to be a highly effective solution, enabling the removal of contaminants directly at the source and reducing cross-infection risk across all tested ventilation types. This outcome provides strong confirmation of the hypothesis that combining personal exhaust with physical barriers significantly lowers exposure to airborne contaminants. Computational fluid dynamics (CFD) simulations and experimental analyses confirmed that optimized design parameters—such as barrier height and exhaust flow rate—can maintain high efficiency in contaminant removal while reducing energy consumption and material use.

As a complementary addition to the core publications, this study addressed an important gap in evaluating environmental sustainability. Evaluation of infection control strategies was conducted using a dual assessment framework, incorporating both infection risk modelling and life cycle assessment (LCA). This dual-perspective analysis revealed a trade-off: strategies like disposable masks, while highly effective at reducing infection risk, imposed substantial environmental burdens due to their operational and material demands. In contrast, the integrated system of physical barriers and personal exhaust ventilation offered a well-balanced solution—achieving strong infection risk reduction with comparatively moderate environmental impact.

Overall, this thesis confirms most of the research hypotheses, while offering critical nuance to their application. In summary, the main findings of this thesis confirm that:

- Natural ventilation via smart windows improves IAQ and thermal comfort, but cannot alone ensure sufficient infection control, particularly in densely occupied spaces like classrooms.
- Multi-objective optimization of smart window operation and thermostat setpoints enables a balanced trade-off between energy use, thermal comfort, and indoor air quality across various climates.
- Controlling outdoor pollution penetration through an optimized hybrid ventilation significantly improves indoor air quality, energy use, and thermal comfort across various climates with different pollution levels.
- Physical barriers can alter airflow patterns and improve containment of exhaled aerosols, but their efficiency is highly dependent on the operation of air distribution systems and occupants' location.
- Combining physical barriers with personal exhaust ventilation, regardless of ventilation type and occupant location, significantly reduces airborne transmission by capturing contaminants at the source
- The resource-efficient design for integrated personal exhaust ventilation and physical barriers offered lower material and energy use while keeping high contaminant removal efficiency.
- A comparative life cycle assessment of infection mitigation strategies revealed that physical barriers with personal exhaust ventilation achieved the most balanced strategy, offering strong infection reduction with moderate environmental impact.

5.1. Future research directions

While this thesis advances knowledge in ventilation design and infection control strategies, several areas warrant further research to enhance the applicability and scalability of the proposed solutions. Future studies should focus on extending the current findings to real-world scenarios where occupant behaviour, movement, and external environmental conditions introduce additional complexity. Experimental field studies in classrooms and other densely occupied indoor environments would provide valuable validation of the proposed solutions beyond controlled laboratory settings. Further refinement of optimization algorithms, particularly with the integration of artificial intelligence (AI) and machine learning techniques, could enhance the adaptability of ventilation systems. AI-driven control systems could dynamically adjust ventilation rates, window openings, and exhaust flow rates in response to

real-time occupancy patterns and air quality data, optimizing system performance while minimizing energy use. Additionally, emerging new technologies, advanced filtration systems, and electrostatic precipitators should be explored in conjunction with the studied strategies to assess their combined efficacy in infection risk reduction. The environmental sustainability of ventilation and infection control strategies should also be examined in greater depth. Expanding life cycle assessment methodologies to include broader environmental impact categories—such as resource depletion, water use, and air pollution—could provide a more comprehensive understanding of the long-term implications of various IAQ management strategies. Moreover, incorporating long-term operational data from real-world deployments would enable more accurate assessments of the energy and maintenance costs associated with different approaches. Finally, interdisciplinary collaborations between engineers, public health professionals, architects, and policymakers are essential to ensure that future ventilation strategies are not only technically effective but also feasible for large-scale implementation. By integrating health-based design principles with sustainable engineering solutions, future research can continue to refine and optimize ventilation systems that safeguard indoor environments against airborne infections while promoting energy efficiency and environmental responsibility.

References

1. US EPA, O. U.S. Environmental Protection Agency Available online: https://www.epa.gov/home (accessed on 27 April 2025).
2. Spengler, J.D.; Chen, Q. INDOOR AIR QUALITY FACTORS IN DESIGNING A HEALTHY BUILDING. *Annual Review of Environment and Resources* **2000**, *25*, 567–600, doi:10.1146/annurev.energy.25.1.567.
3. Holden, K.A.; Lee, A.R.; Hawcutt, D.B.; Sinha, I.P. The Impact of Poor Housing and Indoor Air Quality on Respiratory Health in Children. *Breathe* **2023**, *19*, 230058, doi:10.1183/20734735.0058-2023.
4. Nero, A.V. Controlling Indoor Air Pollution. *Scientific American* **1988**, *258*, 42–49.
5. Kek, H.Y.; Mohd Saupi, S.B.; Tan, H.; Dzarfan Othman, M.H.; Nyakuma, B.B.; Goh, P.S.; Hamood Altowayti, W.A.; Qaid, A.; Abdul Wahab, N.H.; Lee, C.H.; et al. Ventilation Strategies for Mitigating Airborne Infection in Healthcare Facilities: A Review and Bibliometric Analysis (1993–2022). *Energy and Buildings* **2023**, *295*, 113323, doi:10.1016/j.enbuild.2023.113323.
6. Li, Y.; Cheng, P.; Jia, W. Poor Ventilation Worsens Short-range Airborne Transmission of Respiratory Infection. *Indoor Air* **2022**, *32*, doi:10.1111/ina.12946.
7. Berglund, B.; Brunekreef, B.; Knoppe, H.; Lindvall, T.; Maroni, M.; Molhave, L.; Skov, P. Effects of Indoor Air Pollution on Human Health. *Indoor Air* **1992**, *2*, 2–25, doi:10.1111/j.1600-0668.1992.02-21.x.
8. Persily, A.K.; Emmerich, S.J. Indoor Air Quality in Sustainable, Energy Efficient Buildings. *HVAC&R Research* **2012**, *18*, 4–20, doi:10.1080/10789669.2011.592106.
9. Kumar, P.; Singh, A.B.; Arora, T.; Singh, S.; Singh, R. Critical Review on Emerging Health Effects Associated with the Indoor Air Quality and Its Sustainable Management.

Science of The Total Environment **2023**, *872*, 162163, doi:10.1016/j.scitotenv.2023.162163.
10. Carslaw, N.; Bekö, G.; Langer, S.; Schoemaecker, C.; Mihucz, V.G.; Dudzinska, M.; Wiesen, P.; Nehr, S.; Huttunen, K.; Querol, X.; et al. A New Framework for Indoor Air Chemistry Measurements: Towards a Better Understanding of Indoor Air Pollution. *Indoor Environments* **2024**, *1*, 100001, doi:10.1016/j.indenv.2023.100001.
11. Pribadi, A.P.; Rauf, A.U.; Rahman, Y.M.R.; Haq, Z.F. Air Quality and Urban Sustainable Development- Current Issues and Future Directions. In *Sustainable Urban Environment and Waste Management*; Parray, J.A., Shameem, N., Haghi, A.K., Eds.; Urban Sustainability; Springer Nature Singapore: Singapore, 2025; pp. 23–51 ISBN 978-981-9611-39-3.
12. Peer Review History: Toxic Gases and Human Health: A Comprehensive Review of Sources, Health Effects, and Prevention Strategies – OPEN PEER REVIEW SUPPORT Company 2024.
13. Smith, B.; Nitschke, M.; Pilotto, L.; Ruffin, R.; Pisaniello, D.; Willson, K. Health Effects of Daily Indoor Nitrogen Dioxide Exposure in People with Asthma. *Eur Respir J* **2000**, *16*, 879–885, doi:10.1183/09031936.00.16587900.
14. Khan, A.; Kanwal, H.; Bibi, S.; Mushtaq, S.; Khan, A.; Khan, Y.H.; Mallhi, T.H. Volatile Organic Compounds and Neurological Disorders: From Exposure to Preventive Interventions. In *Environmental Contaminants and Neurological Disorders*; Akash, M.S.H., Rehman, K., Eds.; Emerging Contaminants and Associated Treatment Technologies; Springer International Publishing: Cham, 2021; pp. 201–230 ISBN 978-3-030-66375-9.
15. Alemayehu, Y.A.; Asfaw, S.L.; Terfie, T.A. Exposure to Urban Particulate Matter and Its Association with Human Health Risks. *Environ Sci Pollut Res* **2020**, *27*, 27491–27506, doi:10.1007/s11356-020-09132-1.
16. Morawska, L.; Tang, J.W.; Bahnfleth, W.; Bluyssen, P.M.; Boerstra, A.; Buonanno, G.; Cao, J.; Dancer, S.; Floto, A.; Franchimon, F.; et al. How Can Airborne Transmission of COVID-19 Indoors Be Minimised? *Environment International* **2020**, *142*, 105832, doi:10.1016/j.envint.2020.105832.
17. Snow, S.; Boyson, A.S.; Paas, K.H.W.; Gough, H.; King, M.-F.; Barlow, J.; Noakes, C.J.; Schraefel, M.C. Exploring the Physiological, Neurophysiological and Cognitive Performance Effects of Elevated Carbon Dioxide Concentrations Indoors. *Building and Environment* **2019**, *156*, 243–252, doi:10.1016/j.buildenv.2019.04.010.
18. Heinzerling, D.; Schiavon, S.; Webster, T.; Arens, E. Indoor Environmental Quality Assessment Models: A Literature Review and a Proposed Weighting and Classification Scheme. *Building and Environment* **2013**, *70*, 210–222, doi:10.1016/j.buildenv.2013.08.027.
19. EU Standard EN 16798-1:2019; Energy Performance of Buildings—Ventilation for Buildings—Part 1: Indoor Environmental Input Parameters for Design and Assessment of Energy Performance of Buildings Addressing Indoor Air Quality, Thermal Environment, Lighting and Acoustics—Module M1-6. European Committee for Standardization: Brussels, Belgium, 2019.
20. Polish Standard PN-83/B-03430/Az3 2000; Ventilation in Dwellings and Public Utility Buildings. Polish Committee for Standardization: Warsaw, Poland, 2000.
21. ASHRAE. ASHRAE Standard 62-2001; Ventilation for Acceptable Indoor Air Quality Atlanta. American Society of Heating, Refrigerating, and Air Conditioning Engineers, Inc.: Atlanta, Ga, USA, 2001.

22. Passe, U.; Battaglia, F. *Designing Spaces for Natural Ventilation: An Architect's Guide*; 0 ed.; Routledge, 2015; ISBN 978-0-203-58347-0.
23. Izadyar, N.; Miller, W. Ventilation Strategies and Design Impacts on Indoor Airborne Transmission: A Review. *Building and Environment* **2022**, *218*, 109158, doi:10.1016/j.buildenv.2022.109158.
24. NTNU Open: Natural Ventilation in Buildings : Architectural Concepts, Consequences and Possibilities Available online: https://ntnuopen.ntnu.no/ntnu-xmlui/handle/11250/231090 (accessed on 12 March 2025).
25. Chenari, B.; Dias Carrilho, J.; Gameiro Da Silva, M. Towards Sustainable, Energy-Efficient and Healthy Ventilation Strategies in Buildings: A Review. *Renewable and Sustainable Energy Reviews* **2016**, *59*, 1426–1447, doi:10.1016/j.rser.2016.01.074.
26. Li, H.; Lee, W.L.; Jia, J. Applying a Novel Extra-Low Temperature Dedicated Outdoor Air System in Office Buildings for Energy Efficiency and Thermal Comfort. *Energy Conversion and Management* **2016**, *121*, 162–173, doi:10.1016/j.enconman.2016.05.036.
27. Nair, A.N.; Anand, P.; George, A.; Mondal, N. A Review of Strategies and Their Effectiveness in Reducing Indoor Airborne Transmission and Improving Indoor Air Quality. *Environmental Research* **2022**, *213*, 113579, doi:10.1016/j.envres.2022.113579.
28. Merema, B.; Delwati, M.; Sourbron, M.; Breesch, H. Demand Controlled Ventilation (DCV) in School and Office Buildings: Lessons Learnt from Case Studies. *Energy and Buildings* **2018**, *172*, 349–360, doi:10.1016/j.enbuild.2018.04.065.
29. Peng, Y.; Lei, Y.; Tekler, Z.D.; Antanuri, N.; Lau, S.-K.; Chong, A. Hybrid System Controls of Natural Ventilation and HVAC in Mixed-Mode Buildings: A Comprehensive Review. *Energy and Buildings* **2022**, *276*, 112509, doi:10.1016/j.enbuild.2022.112509.
30. Clark, J.D.; Less, B.D.; Dutton, S.M.; Walker, I.S.; Sherman, M.H. Efficacy of Occupancy-Based Smart Ventilation Control Strategies in Energy-Efficient Homes in the United States. *Building and Environment* **2019**, *156*, 253–267, doi:10.1016/j.buildenv.2019.03.002.
31. Otoo, C.; Lu, T.; Lü, X. Application of Mixed-Mode Ventilation to Enhance Indoor Air Quality and Energy Efficiency in School Buildings. *Energies* **2024**, *17*, 6097, doi:10.3390/en17236097.
32. Pantelic, J.; Tham, K.W. Adequacy of Air Change Rate as the Sole Indicator of an Air Distribution System's Effectiveness to Mitigate Airborne Infectious Disease Transmission Caused by a Cough Release in the Room with Overhead Mixing Ventilation: A Case Study. *HVAC&R Research* **2013**, *19*, 947–961, doi:10.1080/10789669.2013.842447.
33. Elsaid, A.M.; Ahmed, M.S. Indoor Air Quality Strategies for Air-Conditioning and Ventilation Systems with the Spread of the Global Coronavirus (COVID-19) Epidemic: Improvements and Recommendations. *Environmental Research* **2021**, *199*, 111314, doi:10.1016/j.envres.2021.111314.
34. Sahu, A.K.; Verma, T.N.; Sinha, S.L. Numerical Simulation of Air Flow in Multiple Beds Intensive Care Unit of Hospital. *IJAME* **2019**, *16*, 6796–6807, doi:10.15282/ijame.16.2.2019.24.0511.
35. Tang, J.W.; Noakes, C.J.; Nielsen, P.V.; Eames, I.; Nicolle, A.; Li, Y.; Settles, G.S. Observing and Quantifying Airflows in the Infection Control of Aerosol- and Airborne-Transmitted Diseases: An Overview of Approaches. *Journal of Hospital Infection* **2011**, *77*, 213–222, doi:10.1016/j.jhin.2010.09.037.
36. Wu, J.; Xu, L.; Shen, J. Research on the Cross-Contamination in the Confined Conference Room with the Radiant Floor Heating System Integrated with the down-Supply Ventilation. *Heliyon* **2023**, *9*, e14389, doi:10.1016/j.heliyon.2023.e14389.

37. Varodompun, J.; Navvab, M. HVAC Ventilation Strategies: The Contribution for Thermal Comfort, Energy Efficiency, and Indoor Air Quality. *Journal of Green Building* **2007**, *2*, 131–150, doi:10.3992/jgb.2.2.131.
38. Xu, C.; Wei, X.; Liu, L.; Su, L.; Liu, W.; Wang, Y.; Nielsen, P.V. Effects of Personalized Ventilation Interventions on Airborne Infection Risk and Transmission between Occupants. *Building and Environment* **2020**, *180*, 107008, doi:10.1016/j.buildenv.2020.107008.
39. Yang, B.; Liu, Y.; Zhu, X.; Li, X. Personalized Ventilation Systems. In *Personal Comfort Systems for Improving Indoor Thermal Comfort and Air Quality*; Wang, F., Yang, B., Deng, Q., Luo, M., Eds.; Indoor Environment and Sustainable Building; Springer Nature Singapore: Singapore, 2023; pp. 113–127 ISBN 978-981-9907-17-5.
40. Olmedo, I.; Sánchez-Jiménez, J.L.; Peci, F.; Ruiz De Adana, M. Personal Exposure to Exhaled Contaminants in the near Environment of a Patient Using a Personalized Exhaust System. *Building and Environment* **2022**, *223*, 109497, doi:10.1016/j.buildenv.2022.109497.
41. Zhai, Z. (John); Metzger, I.D. Insights on Critical Parameters and Conditions for Personalized Ventilation. *Sustainable Cities and Society* **2019**, *48*, 101584, doi:10.1016/j.scs.2019.101584.
42. Sharma, A.; Omidvarborna, H.; Kumar, P. Efficacy of Facemasks in Mitigating Respiratory Exposure to Submicron Aerosols. *Journal of Hazardous Materials* **2022**, *422*, 126783, doi:10.1016/j.jhazmat.2021.126783.
43. Clase, C.M.; Fu, E.L.; Joseph, M.; Beale, R.C.L.; Dolovich, M.B.; Jardine, M.; Mann, J.F.E.; Pecoits-Filho, R.; Winkelmayer, W.C.; Carrero, J.J. Cloth Masks May Prevent Transmission of COVID-19: An Evidence-Based, Risk-Based Approach. *Annals of Internal Medicine* **2020**, *173*, 489–491, doi:10.7326/M20-2567.
44. Hall, S.; Johnson, P.; Bailey, C.; Gould, Z.; White, R.; Crook, B. Evaluation of Face Shields, Goggles, and Safety Glasses as a Virus Transmission Control Measure to Protect the Wearer Against Cough Droplets. *Annals of Work Exposures and Health* **2023**, *67*, 36–49, doi:10.1093/annweh/wxac047.
45. Brisbine, B.R.; Radcliffe, C.R.; Jones, M.L.H.; Stirling, L.; Coltman, C.E. Does the Fit of Personal Protective Equipment Affect Functional Performance? A Systematic Review across Occupational Domains. *PLoS ONE* **2022**, *17*, e0278174, doi:10.1371/journal.pone.0278174.
46. Dancer, S.J. Reducing the Risk of COVID-19 Transmission in Hospitals: Focus on Additional Infection Control Strategies. *Surgery (Oxford)* **2021**, *39*, 752–758, doi:10.1016/j.mpsur.2021.10.003.
47. Zhang, C.; Nielsen, P.V.; Liu, L.; Sigmer, E.T.; Mikkelsen, S.G.; Jensen, R.L. The Source Control Effect of Personal Protection Equipment and Physical Barrier on Short-Range Airborne Transmission. *Building and Environment* **2022**, *211*, 108751, doi:10.1016/j.buildenv.2022.108751.
48. Lee, H.; Awbi, H.B. Effect of Internal Partitioning on Indoor Air Quality of Rooms with Mixing Ventilation—Basic Study. *Building and Environment* **2004**, *39*, 127–141, doi:10.1016/j.buildenv.2003.08.007.
49. Wagner, J.; Sparks, T.L.; Miller, S.; Chen, W.; Macher, J.M.; Waldman, J.M. Modeling the Impacts of Physical Distancing and Other Exposure Determinants on Aerosol Transmission. *Journal of Occupational and Environmental Hygiene* **2021**, *18*, 495–509, doi:10.1080/15459624.2021.1963445.
50. Randall, K.; Ewing, E.T.; Marr, L.C.; Jimenez, J.L.; Bourouiba, L. How Did We Get Here: What Are Droplets and Aerosols and How Far Do They Go? A Historical

Perspective on the Transmission of Respiratory Infectious Diseases. *Interface Focus.* **2021**, *11*, 20210049, doi:10.1098/rsfs.2021.0049.
51. Ren, C.; Xi, C.; Wang, J.; Feng, Z.; Nasiri, F.; Cao, S.-J.; Haghighat, F. Mitigating COVID-19 Infection Disease Transmission in Indoor Environment Using Physical Barriers. *Sustainable Cities and Society* **2021**, *74*, 103175, doi:10.1016/j.scs.2021.103175.
52. Srikrishna, D. Can 10x Cheaper, Lower-Efficiency Particulate Air Filters and Box Fans Complement High-Efficiency Particulate Air (HEPA) Purifiers to Help Control the COVID-19 Pandemic? 2021.
53. Ng, B.F.; Xiong, J.W.; Wan, M.P. Application of Acoustic Agglomeration to Enhance Air Filtration Efficiency in Air-Conditioning and Mechanical Ventilation (ACMV) Systems. *PLoS ONE* **2017**, *12*, e0178851, doi:10.1371/journal.pone.0178851.
54. Stephens, B.; Novoselac, A.; Siegel, J.A. The Effects of Filtration on Pressure Drop and Energy Consumption in Residential HVAC Systems (RP-1299). *HVAC&R Research* **2010**, *16*, 273–294, doi:10.1080/10789669.2010.10390905.
55. Ding, Y.; Jiang, X.; Zhang, D.; Yao, Y.; Zhao, W.; He, Y. Analytical Model and Comprehensive Index Construction of Indoor Air Purification Effect Based on Dynamic Characteristics and Energy Efficiency. *Journal of Building Engineering* **2024**, *95*, 110098, doi:10.1016/j.jobe.2024.110098.
56. Kumar, P.; Martani, C.; Morawska, L.; Norford, L.; Choudhary, R.; Bell, M.; Leach, M. Indoor Air Quality and Energy Management through Real-Time Sensing in Commercial Buildings. *Energy and Buildings* **2016**, *111*, 145–153, doi:10.1016/j.enbuild.2015.11.037.
57. Radalj, A.; Nikšić, A.; Trajković, J.; Knezević, T.; Janković, M.; De Luka, S.; Djoković, S.; Mijatović, S.; Ilić, A.; Arandjelović, I.; et al. Combating Pathogens Using Carbon-Fiber Ionizers (CFIs) for Air Purification: A Narrative Review. *Applied Sciences* **2024**, *14*, 7311, doi:10.3390/app14167311.
58. Memarzadeh, F.; Olmsted, R.N.; Bartley, J.M. Applications of Ultraviolet Germicidal Irradiation Disinfection in Health Care Facilities: Effective Adjunct, but Not Stand-Alone Technology. *American Journal of Infection Control* **2010**, *38*, S13–S24, doi:10.1016/j.ajic.2010.04.208.
59. Luo, M.; De Dear, R.; Ji, W.; Bin, C.; Lin, B.; Ouyang, Q.; Zhu, Y. The Dynamics of Thermal Comfort Expectations: The Problem, Challenge and Impication. *Building and Environment* **2016**, *95*, 322–329, doi:10.1016/j.buildenv.2015.07.015.
60. Sekhar, S.C. Thermal Comfort in Air-Conditioned Buildings in Hot and Humid Climates - Why Are We Not Getting It Right? *Indoor Air* **2016**, *26*, 138–152, doi:10.1111/ina.12184.
61. Jayeoba, S.; Awojobi, E. Maintaining Optimal Indoor Air Quality: Pollutants Removal and Proper Ventilation in Mixed-Use Complexes. *AJESRE* **2024**, *16*, 60–70, doi:10.62154/ajesre.2024.016.010376.
62. Olesen, B.W.; Simone, A.; KrajcĺIik, M.; Causone, F.; Carli, M.D. Experimental Study of Air Distribution and Ventilation Effectiveness in a Room with a Combination of Different Mechanical Ventilation and Heating/Cooling Systems. *International Journal of Ventilation* **2011**, *9*, 371–383, doi:10.1080/14733315.2011.11683895.
63. Al Mindeel, T.; Spentzou, E.; Eftekhari, M. Energy, Thermal Comfort, and Indoor Air Quality: Multi-Objective Optimization Review. *Renewable and Sustainable Energy Reviews* **2024**, *202*, 114682, doi:10.1016/j.rser.2024.114682.
64. Torres, F.G.; De-la-Torre, G.E. Face Mask Waste Generation and Management during the COVID-19 Pandemic: An Overview and the Peruvian Case. *Science of The Total Environment* **2021**, *786*, 147628, doi:10.1016/j.scitotenv.2021.147628.

65. Singh, E.; Kumar, A.; Mishra, R.; Kumar, S. Solid Waste Management during COVID-19 Pandemic: Recovery Techniques and Responses. *Chemosphere* **2022**, *288*, 132451, doi:10.1016/j.chemosphere.2021.132451.
66. Pandit, P.; Maity, S.; Singha, K.; Annu; Uzun, M.; Shekh, M.; Ahmed, S. Potential Biodegradable Face Mask to Counter Environmental Impact of Covid-19. *Cleaner Engineering and Technology* **2021**, *4*, 100218, doi:10.1016/j.clet.2021.100218.
67. Stutman, M.B. Using Field Measurements of Air Filter Performance and HVAC Fan Energy Measurements to Select Air Filters with Lowest Life Cycle Cost. *Strategic Planning for Energy and the Environment* **2012**, *32*, 26–41, doi:10.1080/10485236.2012.10531826.
68. US Department of Energy Engineering Reference. In EnergyPlus™; Version 9.4.0, Documentation; US Department of Energy: Washington, DC, USA, 2020. **2020**, 1785.
69. Crawley, D.B.; Lawrie, L.K.; Winkelmann, F.C.; Buhl, W.F.; Huang, Y.J.; Pedersen, C.O.; Strand, R.K.; Liesen, R.J.; Fisher, D.E.; Witte, M.J.; et al. EnergyPlus: Creating a New-Generation Building Energy Simulation Program. *Energy and Buildings* **2001**, *33*, 319–331, doi:10.1016/S0378-7788(00)00114-6.
70. EnergyPlus Testing with HVAC Equipment Performance Tests CE300 to CE545 from ANSI/ASHRAE Standard 140-2011, June 2012, EnergyPlus Web Site Www.Energyplus.Gov.
71. Nihar, K.; Bhatia, A.; Garg, V. Optimal Control of Operable Windows for Mixed Mode Building Simulation in EnergyPlus. *IOP Conf. Ser.: Earth Environ. Sci.* **2019**, *238*, 012052, doi:10.1088/1755-1315/238/1/012052.
72. Cetin, K.S.; Fathollahzadeh, M.H.; Kunwar, N.; Do, H.; Tabares-Velasco, P.C. Development and Validation of an HVAC on/off Controller in EnergyPlus for Energy Simulation of Residential and Small Commercial Buildings. *Energy and Buildings* **2019**, *183*, 467–483, doi:10.1016/j.enbuild.2018.11.005.
73. Yusoff, Y.; Ngadiman, M.S.; Zain, A.M. Overview of NSGA-II for Optimizing Machining Process Parameters. *Procedia Engineering* **2011**, *15*, 3978–3983, doi:10.1016/j.proeng.2011.08.745.
74. Jalali, Z.; Noorzai, E.; Heidari, S. Design and Optimization of Form and Facade of an Office Building Using the Genetic Algorithm. *Science and Technology for the Built Environment* **2020**, *26*, 128–140, doi:10.1080/23744731.2019.1624095.
75. Asadi, E.; da Silva, M.G.; Antunes, C.H.; Dias, L. A Multi-Objective Optimization Model for Building Retrofit Strategies Using TRNSYS Simulations, GenOpt and MATLAB. *Building and Environment* **2012**, *56*, 370–378, doi:10.1016/j.buildenv.2012.04.005.
76. Ahmadianfar, I.; Heidari, A.A.; Noshadian, S.; Chen, H.; Gandomi, A.H. INFO: An Efficient Optimization Algorithm Based on Weighted Mean of Vectors. *Expert Systems with Applications* **2022**, *195*, 116516, doi:10.1016/j.eswa.2022.116516.
77. Sze To, G.N.; Chao, C.Y.H. Review and Comparison between the Wells–Riley and Dose-Response Approaches to Risk Assessment of Infectious Respiratory Diseases. *Indoor Air* **2010**, *20*, 2–16, doi:10.1111/j.1600-0668.2009.00621.x.
78. Riley, E.C.; Murphy, G.; Riley, R.L. AIRBORNE SPREAD OF MEASLES IN A SUBURBAN ELEMENTARY SCHOOL. *American Journal of Epidemiology* **1978**, *107*, 421–432, doi:10.1093/oxfordjournals.aje.a112560.
79. Gammaitoni, L. Using a Mathematical Model to Evaluate the Efficacy of TB Control Measures. *Emerg. Infect. Dis.* **1997**, *3*, 335–342, doi:10.3201/eid0303.970310.
80. Ai, Z.; Mak, C.M.; Gao, N.; Niu, J. Tracer Gas Is a Suitable Surrogate of Exhaled Droplet Nuclei for Studying Airborne Transmission in the Built Environment. *Build. Simul.* **2020**, *13*, 489–496, doi:10.1007/s12273-020-0614-5.

81. Villanueva, F.; Ródenas, M.; Ruus, A.; Saffell, J.; Gabriel, M.F. Sampling and Analysis Techniques for Inorganic Air Pollutants in Indoor Air. *Applied Spectroscopy Reviews* **2022**, *57*, 531–579, doi:10.1080/05704928.2021.2020807.
82. Hobeika, N.; García-Sánchez, C.; Bluyssen, P.M. Assessing Indoor Air Quality and Ventilation to Limit Aerosol Dispersion—Literature Review. *Buildings* **2023**, *13*, 742, doi:10.3390/buildings13030742.
83. Kierat, W.; Popiolek, Z. Dynamic Properties of Fast Gas Concentration Meter with Nondispersive Infrared Detector. *Measurement* **2017**, *95*, 149–155, doi:10.1016/j.measurement.2016.10.008.
84. CH TECHNOLOGIES Available online: https://chtechusa.com/products_tag_lg_collison-nebulizer.php (accessed on 11 December 2024).
85. Alford, R.H.; Kasel, J.A.; Gerone, P.J.; Knight, V. Human Influenza Resulting from Aerosol Inhalation. *Proceedings of the Society for Experimental Biology and Medicine* **1966**, *122*, 800–804, doi:10.3181/00379727-122-31255.
86. Nicas, M.; Nazaroff, W.W.; Hubbard, A. Toward Understanding the Risk of Secondary Airborne Infection: Emission of Respirable Pathogens. *Journal of Occupational and Environmental Hygiene* **2005**, *2*, 143–154, doi:10.1080/15459620590918466.
87. Shih, T.-H.; Liou, W.W.; Shabbir, A.; Yang, Z.; Zhu, J. A New *k*-ϵ Eddy Viscosity Model for High Reynolds Number Turbulent Flows. *Computers & Fluids* **1995**, *24*, 227–238, doi:10.1016/0045-7930(94)00032-T.
88. Sadrizadeh, S.; Tammelin, A.; Ekolind, P.; Holmberg, S. Influence of Staff Number and Internal Constellation on Surgical Site Infection in an Operating Room. *Particuology* **2014**, *13*, 42–51, doi:10.1016/j.partic.2013.10.006.
89. Riddle, A.; Carruthers, D.; Sharpe, A.; McHugh, C.; Stocker, J. Comparisons between FLUENT and ADMS for Atmospheric Dispersion Modelling. *Atmospheric Environment* **2004**, *38*, 1029–1038, doi:10.1016/j.atmosenv.2003.10.052.
90. Zhao, B.; Zhang, Y.; Li, X.; Yang, X.; Huang, D. Comparison of Indoor Aerosol Particle Concentration and Deposition in Different Ventilated Rooms by Numerical Method. *Building and Environment* **2004**, *39*, 1–8, doi:10.1016/j.buildenv.2003.08.002.
91. Zhang, Z.; Chen, Q. Experimental Measurements and Numerical Simulations of Particle Transport and Distribution in Ventilated Rooms. *Atmospheric Environment* **2006**, *40*, 3396–3408, doi:10.1016/j.atmosenv.2006.01.014.
92. Gao, N.P.; Niu, J.L. Modeling Particle Dispersion and Deposition in Indoor Environments. *Atmospheric Environment* **2007**, *41*, 3862–3876, doi:10.1016/j.atmosenv.2007.01.016.
93. Zukowska, D.; Melikov, A.K.; Popiolek, Z.J. Thermal Plume above a Simulated Sitting Person with Different Complexity of Body Geometry: Roomvent - 10th International Conference on Air Distribution in Rooms. *Roomvent 2007* **2007**, *3*, 191–198.
94. *Mundt, E., Mathisen, H. M., Nielsen, P. V., & Moser, A. (Eds.). (2004). Ventilation Effectiveness. REHVA Guidebook No. 2. REHVA.*;
95. Rowan, N.J.; Moral, R.A. Disposable Face Masks and Reusable Face Coverings as Non-Pharmaceutical Interventions (NPIs) to Prevent Transmission of SARS-CoV-2 Variants That Cause Coronavirus Disease (COVID-19): Role of New Sustainable NPI Design Innovations and Predictive Mathematical Modelling. *Science of The Total Environment* **2021**, *772*, 145530, doi:10.1016/j.scitotenv.2021.145530.
96. Norin, A.; Reenbom, E. A Business Model-LCA of Air Purifiers Comparing Sales and Rental Business Model in Sweden. **2024**.
97. Heijungs, R.; Kleijn, R. Numerical Approaches towards Life Cycle Interpretation Five Examples. *Int J LCA* **2001**, *6*, 141, doi:10.1007/BF02978732.

Appendices

In this section, the full-text papers, that were briefly described in Chapters 2 and 3, are presented. The papers are listed in the following order:

Paper 1: Grygierek, Krzysztof, **Seyedkeivan Nateghi**, Joanna Ferdyn-Grygierek, and Jan Kaczmarczyk. "Controlling and limiting infection risk, thermal discomfort, and low indoor air quality in a classroom through natural ventilation controlled by smart windows." Energies 16, no. 2 (2023): 592.

Paper 2: **Nateghi, Seyedkeivan**, and Jan Kaczmarczyk. "Multi-objective optimization of window opening and thermostat control for enhanced indoor environment quality and energy efficiency in contrasting climates." Journal of Building Engineering 78 (2023): 107617.

Paper 3: **Nateghi, Seyedkeivan**, Amirmohammad Behzadi, Jan Kaczmarczyk, Pawel Wargocki, and Sasan Sadrizadeh. "Optimal control strategy for a cutting-edge hybrid ventilation system in classrooms: Comparative analysis based on air pollution levels across cities." Building and Environment 267 (2025): 112295.

Paper 4: **Nateghi, Seyedkeivan**, Jan Kaczmarczyk, Ewa Zabłocka-Godlewska, and Wioletta Przystaś. "Investigating the Impact of Physical Barriers on Air Change Effectiveness and Aerosol Transmission Under Mixing Air Distribution." Building and Environment (2025): 112676.

Paper 5: **Nateghi, Seyedkeivan**, and Jan Kaczmarczyk. "Compatibility of integrated physical barriers and personal exhaust ventilation with air distribution systems to mitigate airborne infection risk." Sustainable Cities and Society 103 (2024): 105282.

Paper 6: **Nateghi, Seyedkeivan**, Shahrzad Marashian, Jan Kaczmarczyk, and Sasan Sadrizadeh. "Resource-efficient design of integrated personal exhaust ventilation and physical barriers for airborne transmission mitigation: A numerical and experimental evaluation." Building and Environment 268 (2025): 112336.

energies

MDPI

Article

Controlling and Limiting Infection Risk, Thermal Discomfort, and Low Indoor Air Quality in a Classroom through Natural Ventilation Controlled by Smart Windows

Krzysztof Grygierek [1], Seyedkeivan Nateghi [2], Joanna Ferdyn-Grygierek [2,*] and Jan Kaczmarczyk [2]

[1] Faculty of Civil Engineering, Silesian University of Technology, Akademicka 5, 44-100 Gliwice, Poland
[2] Faculty of Energy and Environmental Engineering, Silesian University of Technology, Konarskiego 20, 44-100 Gliwice, Poland
* Correspondence: joanna.ferdyn-grygierek@polsl.pl; Tel.: +48-32-237-29-12

Abstract: In this study, a controller method for window opening was developed to naturally ventilate a classroom with 30 occupants. The aim was to improve indoor environment quality and limit the probability of COVID infection risk simultaneously. The study was based on a building performance simulation using combined EnergyPlus, CONTAM, and Python programs. Seven cases with automatically opening windows were considered. Opening window parameters were optimized by genetic algorithms. It was shown that the optimized controller with indoor environment functions improved classroom ventilation and considerably decreased CO_2 concentration compared to a reference case where the windows were opened only during breaks, and the controller also improved occupants' thermal comfort. However, there was a noticeable increase in energy demand, caused by the increased air change rate. Introducing the probability of infection risk function to the controller did not reduce the transmission risk substantially, and the probability of infection transmission was high for 80% of the classroom occupancy time. The risk of infection changed only when additional actions were taken, such as introducing face masks, indoor air cleaners, or reducing the number of students present in the classroom. In these cases, it was possible to prevent the infection transmission for more than 90% of the lecture time (R0 < 1).

Keywords: ventilation; classroom; opening window; energy simulation; thermal comfort; CO_2 concentration; COVID risk

Citation: Grygierek, K.; Nateghi, S.; Ferdyn-Grygierek, J.; Kaczmarczyk, J. Controlling and Limiting Infection Risk, Thermal Discomfort, and Low Indoor Air Quality in a Classroom through Natural Ventilation Controlled by Smart Windows. *Energies* **2023**, *16*, 592. https://doi.org/10.3390/en16020592

Academic Editor: Álvaro Gutiérrez

Received: 10 December 2022
Revised: 29 December 2022
Accepted: 31 December 2022
Published: 4 January 2023

1. Introduction

Substantial research efforts have been made in recent decades to amend indoor air quality (IAQ) and thermal comfort to prepare healthful indoor environments for residents [1]. Based on the previous research findings, several standards determine thermal conditions and set adequate outdoor air supply rates to fulfill the hygienic requirements for acceptable air quality. Different indoor environment quality categories have been introduced in the standards based on the expectations of the residents [2,3]. The medium category is defined as the normal condition, and the high level of expectations is considered for special groups such as children and the elderly. After the advent of COVID-19 caused by the SARS-CoV-2 virus, keeping the building environment comfortable (by recommended standards) and healthy simultaneously has become challenging. Despite the availability of pharmaceutical treatments and vaccinations, debarment from virus transmission is the main way to cope with this issue [4]. It has been confirmed that COVID-19 is spread in the world through exhalation of infected persons and breathing in susceptible individuals. Consequently, viral transmission via aerosols that remain infective in the air has been considered [5,6]. Aerosols from exhalation can be distributed in different ways such as ordinary exhalation, talking, sneezing, coughing, or evaporation of respiratory droplets (microscopic aerosols). Accordingly, a susceptible individual has an infection risk if aerosols possess an adequate

virus amount [7,8]. Facemasks can be used to protect healthy people from preventing virus transmission [9,10]. However, wearing masks for many hours may frequently cause the breathing of air of poor quality [11]. The supply air change rate is a parameter to control viral concentration in the air inhaled by susceptible individuals, and it can diminish viral concentration in spaces with high occupancy density. Ventilation systems remove exhaled virus-laden air by lowering the overall indoor viral concentration. However, mechanical ventilation systems with a controlled air supply rate are not available in some relatively cold climates [12]. Hence, natural ventilation is considered as an energy-efficient and available resource to decrease infection probability via air subscription with susceptible individuals [13–15]. The air change rate in buildings with natural ventilation is unstable, often insufficient, and difficult to control [16]. Therefore, some recommendations of the World Health Organization, such as face masks and air purifiers, should be considered to cover the deficiencies of natural ventilation [17].

Continuing to address the importance of adequate ventilation, schools and classrooms are of major concern. Students remain most of their time in classrooms characterized by a high occupant density and often by insufficient air quality [18–20]. IAQ in classrooms is a universal subject in which disparate research and projects have been performed worldwide [21,22]. The principal aim in classrooms should be to maintain the comfort, health, and knowledge acquisition efficiency of students during lectures, which can be obtained by reaching acceptable levels of thermal comfort, air quality, and low infection risk. Students' activity and clothing thermal insulation do not change widely in classrooms [23]; thus, thermal comfort depends mainly on thermal parameters set by heating and ventilation systems. Previous studies have indicated that low ventilation rates negatively affect students' performance and increase absence [24,25]. A high concentration of the bioeffluent, indicated by CO_2 concentration, is the main reason for low perceived air quality in densely occupied places [26]. The problem is particularly evident in rooms with natural ventilation systems that cannot benefit from a constant air change rate to maintain good IAQ at any time students are present in the classroom. Due to the significant role window opening plays in increasing the air change rate, implementing automatic window control systems has been considered a promising IAQ control strategy [27]. Various studies have investigated smart windows to improve natural ventilation systems, indoor air quality, or thermal comfort. For example, Stazi et al. [28] analyzed the automatic window control system in a classroom by taking into account PMV and PPD comfort indicators and indoor air quality in a Mediterranean climate. Grygierek and Sarna [29] compared manually opening windows with automatic ones in a typical Polish single-family house. Research has shown that increasing the air change rate can significantly improve thermal comfort but has a significant effect on heating demand. Sorgato et al. [30] assessed the impact of occupant behavior in terms of the ventilation control of opening windows on thermal comfort and energy consumption related to the HVAC system in residential buildings in Brazil. The combined use of HVAC and natural ventilation (opening windows) was implemented using the Energy Management System, which enables advanced control during simulation in EnergyPlus. Psomas et al. [31] demonstrated that automated window control systems with integrated ventilation cooling strategies can significantly reduce thermal discomfort and the risk of overheating of dwellings during cooling periods in temperate climates. Tan and Deng [32] proposed and evaluated a natural ventilation strategy with optimized window control in a typical Australian residential building. By using flexible degrees of opening of the windows, the proposed strategy showed better performance in terms of maintaining the operative temperature in the room compared to the original open–close control. A large part of the research focuses on the analysis of the use of window opening as a passive building cooling technique, and only a few studies of window control systems considered the occupant health in buildings. Recently, Wang. et al. [33] showed that the simultaneous use of smart windows and air cleaners improved thermal comfort and decreased PM2.5 significantly, which created a healthier environment for people. Nevertheless, the focus has

been on the pollutant particulate matter, while the transmission of infection is of greater importance these days.

Successful school design is quite complex as it requires balancing various interrelated factors. In recent years, significant improvements have been made in the methods of optimizing school buildings with different ventilation systems, and genetic algorithms used to find high-performance design solutions have proven their effectiveness in solving complex classroom problems. For example, a study by Lakhdari et al. [34] showed how this approach can be used to optimize the thermal, lighting, and energy performance of a classroom in a hot and dry climate. Deblois and Ndiaye [35] implemented a multi-variable model to optimize the design of the hybrid ventilation system in four elementary classrooms by maximizing their occupied hours that utilize natural ventilation. Research by Acosta-Acosta and El-Rayes [36] developed a novel optimization model that provides the capability of optimizing the design in order to maximize occupant satisfaction in a classroom space in terms of the perception of human bioeffluent odor while minimizing construction cost. In turn, in a study by Arjmandi et al. [37], the performance of five different ventilation systems was tested to control the spread of airborne particles in a classroom, and then the best case was selected for the least likelihood of spreading infection. A multi-criteria optimization process was performed to assess the impact of design variables (air inlet width, air change rate, and supply air temperature) on thermal comfort.

Previous studies [38] have shown that natural ventilation is generally inadequate to obtain desirable IAQ conditions in classrooms, but installing a new centralized mechanical ventilation system is not always feasible. Therefore, the main objective of this study is to analyze the ability of natural ventilation enhanced by an automatic window-operating system driven by various control algorithms to guarantee a healthy and thermally comfortable environment in classrooms in a moderate climate. The analyses are based on numerical simulations of a multi-zone model of a fragment of a typical Polish school building. A co-simulation between EnergyPlus, CONTAM, and Python was used to control window opening and calculate the heat and mass flow in the building.

This study, in addition to considering IAQ and thermal comfort, deals with the possibility of reducing the concentration of airborne infections by controlling the opening of smart windows. Additionally, energy demand for the studied conditions was compared. The effect of additional actions, such as the introduction of portable air cleaners and wearing face masks, was also studied. The analyzed scenarios were compared based on their ability to reduce the number of hours with thermal discomfort, low indoor air quality, and high infection risk in an existing naturally ventilated classroom. Moreover, the effect of the analyzed scenarios on energy demand for the studied conditions was also presented.

2. Materials and Methods

2.1. Research Object

A typical Polish classroom with dimensions of 9 × 6 m and a height of 3.3 m was selected for the study. The building meets Polish requirements for the thermal insulation of walls and floors, the external brick walls are insulated with polystyrene (heat transfer coefficient U = 0.23 W/(m^2·K)), and beam and block floors are insulated with polystyrene insulation (U = 0.17 W/(m^2·K)) and double-glazed windows (U = 1.1 W/(m^2·K), solar heat gain coefficient is 0.64). The building has natural ventilation through leaks in windows and gravitational chimneys. In each classroom, there is one large window of 7.8 × 2.1 m (Figure 1a) consisting of twelve window sashes. The length of the window cracks is 42.6 m per window.

During classes (each lesson lasts 45 min, each break 15 min), there are 30 occupants present in the classroom every day (from Monday to Friday) from 8 am to 2 pm.

2.2. Software and Simulation Algorithm

A building performance simulation (BPS) was carried out under dynamic conditions using the EnergyPlus 9.4 (US Department of Energy, Washington, DC, USA) [39] and

CONTAM (National Institute of Standards and Technology, Gaithersburg, MD, USA) [40] programs, which are among the world's leading simulation software. EnergyPlus (EP) was used for thermal simulation and CONTAM was needed for inter-zone airflows calculations (this software has a model of a gravity chimney applied in this research). The programs were coupled, which allowed the transfer of data between them at each step of the simulation. This coupling was performed using CONTAM's developed inter-process communication application programming interface (API) and was accomplished via co-simulation based on the Functional Mock-up Interface (FMI). The process is described in detail in Ref. [40]. Each case was simulated with a 5 min time step for the whole school year (from September to June) using the TMY (typical meteorological year) climate data for Warsaw [41] (t_{min} = −12.2 °C, t_{max} = 33.1 °C, and t_{avg} = 8.2 °C).

Three options for opening the window were assumed (Figure 1): O1—one window sash tilted, O2—one window sash opened, and O3—one window sash tilted and one window sash opened (as a combination of the first two options). Opening more windows was not considered, to avoid too many air changes and outside noise. The opening and tilting of the window were carried out automatically by means of actuators and were adjusted by the controller. The controller consisted of two parts:

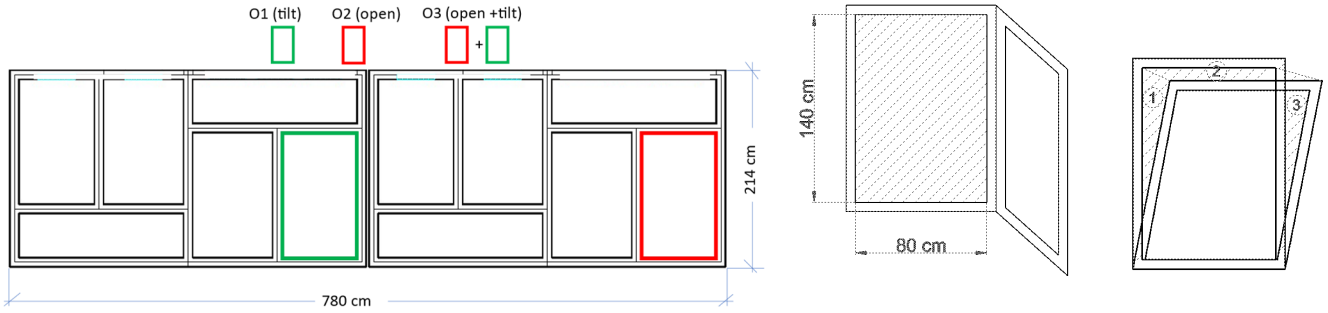

Figure 1. Scheme of window opening: (**a**) window construction, (**b**) open window, and (**c**) tilt window (sum of areas 1 to 3 was changed to two average openings 140 cm × 7 cm according to Pinto et al. [42]).

- Part I (connected with CO_2 concentration in classroom): the window was opened if the limit value of CO_2 concentration in the room was exceeded ($PPM_{\_o}$—optimized value). The type of window opening depended on the outside temperature (T_{out}). At low external temperatures, the window was only tilted (O1), and at high temperatures, one window was tilted and the other was opened (O3); for temperatures between low and high, option 2 was used. The external temperature range for window openings was optimized (T_{Out_o1}, dT_{Out_o1}). The summary of controller operation in part 1 is shown in Table 1.
- Part II (connected with indoor temperature). This part was used to limit overheating of the classroom. The setting of the windows depended on the indoor temperature in the classroom (T_{in}) and the outdoor temperature (T_{out}). The operation diagram is shown in Table 2 (optimized values are the ranges of outdoor temperatures (T_{Out_o2}, dT_{Out_o2}) and the corresponding indoor temperature limits (T_{in2_o}, T_{in2_o}, T_{in2_o}) at which the window is opened).

Table 1. Controller part I work algorithm.

If PPM	and If T_{Out}	Windows Opening Options
$\geq PPM\_o$	$<T_{Out\_o1}$	01
	$\geq T_{Out\_o1}$ and $< T_{Out\_o1} + dT_{Out\_o1}$	02
	$\geq T_{Out\_o1} + dT_{Out\_o1}$	03

Table 2. Controller part II work algorithm.

If T_{Out}	If $T_{in} \geq 21$ °C and If $T_{Out} < T_{in}$ and If T_{in}	Windows Opening Options
$<T_{Out\_o2}$	$\geq T_{in1\_o}$	01
$\geq T_{Out\_o2}$ and $< T_{Out\_o2} + dT_{Out\_o2}$	$\geq T_{in2\_o}$	02
$\geq T_{Out\_o2} + dT_{Out\_o2}$	$\geq T_{in3\_o}$	03

The window was opened if at least one part of the controller gave a signal to open the window. O2 and O3 settings were possible only from 7 am to 5 pm for safety reasons. At night, it was possible to tilt the window (O1) if the indoor temperature exceeded the limit value (T_{in2_nigh}—optimized value). The controller settings were obtained in the optimization process. It was carried out in the Python program [43] using the pymoo library [44], in which a single-criterion version of the genetic algorithms (GA) method [45] was selected for optimization. This method is based on natural selection, adaptation, and imitating biological evolution. As in genetics, they can cross information (genes) and combine and mutate them to provide a variety of solutions. In this study, design variables were represented by natural numbers (for discrete values). Values of design variables were initialized randomly from the allowable sets of variables:

$PPM\_o \in \{450, 500{:}100{:}1000\}$, $T_{Out\_o1} \in \{-6{:}2{:}10\}$, $dT_{Out\_o1} \in \{1{:}1{:}10\}$;
$T_{Out\_o2} \in \{22{:}1{:}30\}$, $dT_{Out\_o2} \in \{1{:}1{:}10\}$, T_{in1_o}, T_{in2_o}, $T_{in3\_o} \in \{21{:}1{:}30\}$;
$T_{in2\_night} \in \{25{:}1{:}30\}$.

Random selection, simulated binary crossover (SBX), and polynomial mutation (PM) were used in the evolution process. The objective function (Equation (1)) aimed to minimize the number of hours with poor conditions during lessons:

$$\min H(\mathbf{x}) = \min [H_{comfort}(\mathbf{x}) + H_{CO2}(\mathbf{x}) + H_{R0}(\mathbf{x})] \quad (1)$$

where the functions in square bracket are connected with:

(1) Thermal comfort ($H_{comfort}$):
   a. If the adaptive model of thermal comfort was used [2]—number of hours with thermal conditions within category IV.
   b. If the PMV-PPD model was used [2]—number of hours out of category III, i.e., PMV > 0.7 or PMV < −0.7.

(2) CO_2 concentration (H_{CO2})—number of hours with conditions within category IV: PPM > 1200, i.e., indoor concentration increased by 800 ppm above outdoor CO_2 concentration of 400 ppm.

(3) Infection risk (H_{R0})—number of hours with bad conditions: Reproduction number R0 > 1 (see Section 2.6).

x is a vector of design variables. In the article, these are the parameters of the controller for opening windows (described above). These values were changed in the optimization process. During the duration of the year-round simulations in the EP program, they were constant.

The scheme of the simulation programs coupling is presented in Figure 2.

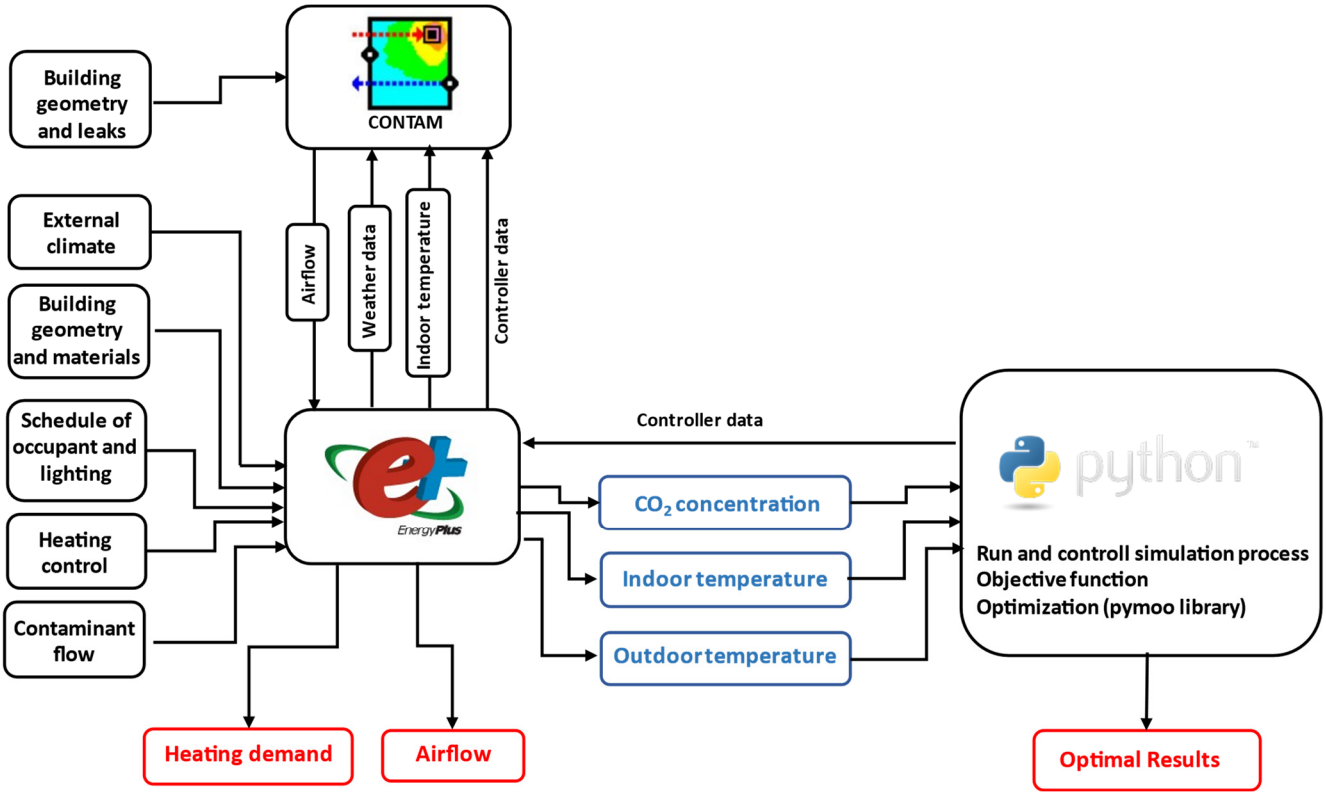

Figure 2. Co-simulation diagram.

2.3. Thermal Model

A fragment of the school building on the top floor with two classrooms (windows facing east and west) and part of the corridor between them were modeled to calculate inter-zone heat and air flows, as shown in Figure 3. The partitions were built in accordance with the construction described in Section 2.1. The Window 7.8 program [46] was used to determine the detailed data that describe the optical properties of the window panes (Pilkington OptifloatClear 4 mm, air 10% and argon 90%, Pilkington Optitherm S3 4 mm [47]).

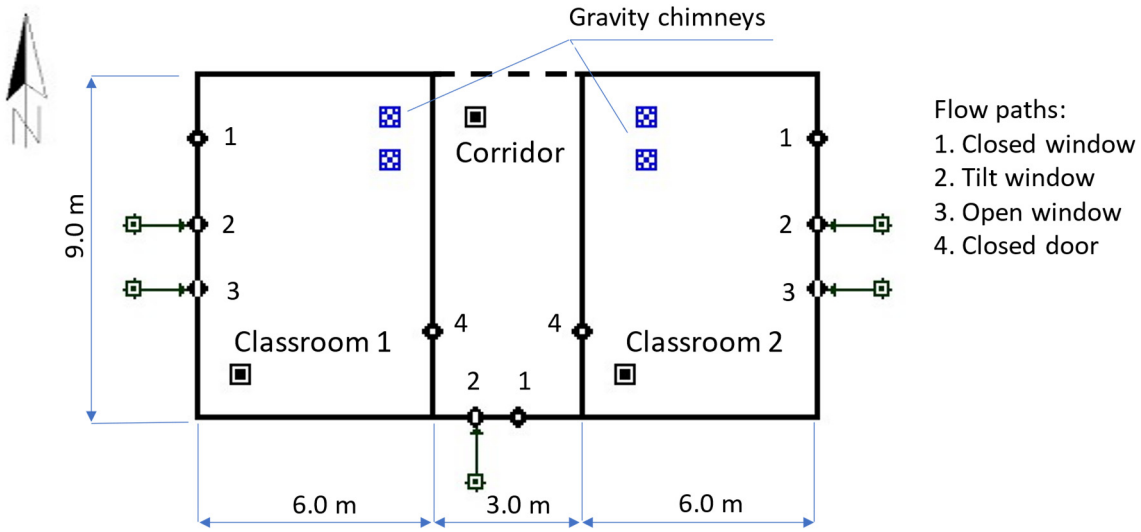

Figure 3. View of CONTAM model with marked airflow paths.

The following internal heat gains were taken into account: occupants: 95 W/occupant (including sensible heat 65%), lights (calculated using daylighting control system: artificial lighting was switched on depending on the intensity of natural lighting: only during the occupied hours and if the natural illuminance was lower than 250 lux).

An ideal controller for the heating system was assumed. The heating set-point was 21 °C (from 7 am to 4 pm) and 18 °C (in the rest of the day). In classrooms, the heating power was limited by a maximum heating capacity at the level of 3.0 kW.

2.4. Air and Contaminant Flows Model

The ventilation model took into account airflow through leaks in the building envelope and ventilation achieved through opening windows. In each classroom, two gravity chimneys were modeled (Figure 3). The airflow was calculated by taking into account the variable indoor temperature calculated in the EP program. The following airflow element types was taken into account:

- Powerlaw Model—One-Way Flow model [48] was adopted for closed windows. The tightness of windows and doors is described by Equation (2):

$$\dot{V} = a \cdot l \cdot (\Delta p)^n \quad (2)$$

where $\dot{V}$—airflow, a—airtightness factor, l—the length of the window cracks, n—exponent, and Δp—pressure difference.

According to [49], the following values of a and n were adopted:

– For windows, a = 0.1 $m^3/(m \cdot h \cdot Pa^{0.67})$, n = 0.67;
– For doors, a = 2.8 $m^3/(m \cdot h \cdot Pa^{0.5})$, n = 0.5; the door was closed all the time.

- Tilt Windows and Half-open Doors: Single Opening–Two-Way Flow model [48] was adopted for tilt and open windows. Contrary to the Powerlaw model, this takes into account the flow in two directions in one simulation time step. For the tilt window, the equivalent area of the opening was calculated from the equations given in the article by Pinto et al. [42].
- Gravitational Chimney: Darcy-Colebrook Resistance Model was assumed for chimneys [40]. The gravity chimneys were assumed as brick ones with dimensions of 27 × 14 cm, a roughness of 3 mm, and the sum of local loss coefficients of 3.4. The chimneys were extended above the roof to a height of 1.5 m. According to ASHRAE [3], it was assumed that each person staying at school emits 3.82 × 10^{-8} $m^3/(s \cdot W)$ of carbon dioxide. The concentration of carbon dioxide in the outdoor air was set constant at 400 ppm.

2.5. Air Cleaner

The air cleaner chosen for this study was a Winix Zero Pro, which is designed with HEPA filters that remove 99.97% of the particles with 0.3 µm size. The device is appropriate for large rooms as the selected volume flow (CADR) is 330 m^3/h in "High" mode, which generates tolerable noise during school lectures (40 dB) [50].

2.6. Infection Risk Calculation

The probability of infection risk was calculated for students in the classroom based on their various activities by the Wells–Riley model [51]. In the Wells–Riley model, the viral load released is introduced by the quantum emission rate (E). This study assumed this for each student sitting, light moving, and speaking during lectures. Therefore, weighted averages of E were equal to 58 quanta/h. The quanta concentration was 0 at beginning of the first class (QC_0) and increased with time until the end of the student's presence in the

classroom. The time development of the average quanta concentration $QC_{(t)}$ (quanta/m^3) in the classroom can be obtained from Equation (3).

$$QC_{(t)} = \frac{E \cdot I \cdot (1 - \eta_i)}{V \cdot \lambda} + \left(QC_0 - \frac{E \cdot I}{V \cdot \lambda} \right) \cdot e^{-t \cdot \lambda} \quad (3)$$

where V, I, η_i, and λ represent the volume of the room (m^3), number of infected individuals, facial mask efficiency for the infected person, and first-order loss rate coefficient, respectively. The quanta is reduced not only by facial mask efficiency, but also due to ventilation (λv), filtration (k_f), deposition (λ_{dep}), and airborne virus decay (k). Hence, λ is defined as summed effects of these values (Equation (4)).

$$\lambda = \lambda v + \lambda_{dep} + k + k_f \quad (4)$$

As this study considers natural ventilation, λv changes according to actual window opening and outdoor weather conditions. Based on previous studies, the surface deposition loss rate was estimated as equal to 0.31 h^{-1} [52] and airborne virus decay was evaluated as equal to 0.63 h^{-1} [53]. Filtration removal rate can be calculated as k_f = CADR/V. The CADR (m^3/h) is the clean air delivery rate achieved by portable air cleaners with HEPA filters defined in Section 2.5. The filtration removal rate for one air cleaner assumed in this study was equal to 330 m^3/h and k_f = 1.85 when two air cleaners were used. The infection risk $R(t)$ is the probability of infection in a closed space of susceptible individuals at a specific time (t). It can be obtained from Equation (5), which is based on the Wells–Riley model [54] and was improved by Gammaitoni–Nucci [55]. Infection risk depends on the inhalation rate (Q_i) of susceptible persons, which was estimated as 0.71 m^3/h for each student based on their activities in the classroom. If all susceptible students wear masks, the facial mask efficiency (η_s) reduces the quanta inhaled. A perfect mixing of indoor air with a constant source was assumed to use the calculated average, $QC_{(t)}$, which increases with time.

$$R(t_1) = n \left(1 - e^{-Q_i (1 - \eta_s) \int_0^{t_1} QC_{(t)} dt} \right) \quad (5)$$

A plausible probability level for the classroom can be defined based on the reproduction number R0, which is calculated from the ratio of new infections to the initial infectious individuals. To control the epidemic, keeping the basic reproduction number lower than 1 (R0 < 1) has been recommended.

2.7. Selected Cases

Seven cases, summarized in Table 3, were analyzed. A base case, Case 1, assumes fully opening one window only during break time, which is a common situation in classrooms. Case 2 considers that one window can be tilted and/or the second one fully opened automatically according to indoor environment quality functions (CO_2 concentration and thermal comfort). In Case 3, one window is able to tilt, fully open, or both tilt one and open the other window simultaneously, while the controller considers all objective functions (thermal comfort, CO_2 concentration, and infection risk). Case 4 is a repetition of Case 3 with the students wearing 50% filtration masks. Cases 5 and 6 also repeat Case 4 while the classroom is equipped with one and two air cleaners, respectively. The air cleaners provide 330 m^3/h of clean air, which adds to the loss rate coefficient (k_f) in Equation (4). As the last case, Case 7 also repeats Case 4 while only half of the students attend the class in person.

Table 3. Test cases conducted in the study.

Case	Controller Basis	Number of People	Mask	Clean Air Delivery Rate by Air Cleaner (CADR, m^3/h)
1	Opening window during breaks	30	No	–
2	Objective function: (1) Thermal comfort; (2) CO_2 concentration.	30	No	–
3	Objective function: (1) Thermal comfort; (2) CO_2 concentration; (3) Infection risk.	30	No	–
4		30	Yes	–
5		30	Yes	330
6		30	Yes	2×330
7		15	Yes	–

3. Results

The result is divided into four primary segments to indicate the operation of the optimal controller of the window and various objective functions in seven selected cases. First, optimized controller performance was investigated. The second part refers to indoor air quality during the lecture, which includes CO_2 concentration and air change rate data. The third part presents the indoor operative temperature, which is the main parameter that affects thermal comfort in this study. The last part, which was dedicated to the infection risk, presents the distribution of reproduction number (R0).

3.1. Optimal Controller Operation

The designed controller, which optimized the window opening by considering indoor environment objective functions and using the genetic algorithm, made significant changes in the window opening and, consequently, CO_2 concentration and indoor temperature. The changes were displayed for window status, air change rate, CO_2 concentration, and indoor operative temperature on a special day (March 6). March 6 was selected as the coldest day that the controller could open the window in all options (tilt, open, tilt and open). Figure 4 shows that by using the optimized controller (Case 2), the window opened for a longer time than in Case 1. In addition, the window opening increased as the end of lecture time approached. Thus, in some hours, windows were both tilted and fully opened, while in Case 1, the controller opened the window (fully open) for 15 min constantly until the end of the students' presence in the classroom.

According to Figure 5, the outdoor temperature on March 6 varied between 3 and 10 °C. Therefore, window opening resulted in a decrease in indoor temperature. In case 1, despite temperature fluctuations with a larger range than in Case 2, the indoor operative temperature was higher than in Case 2 at all hours.

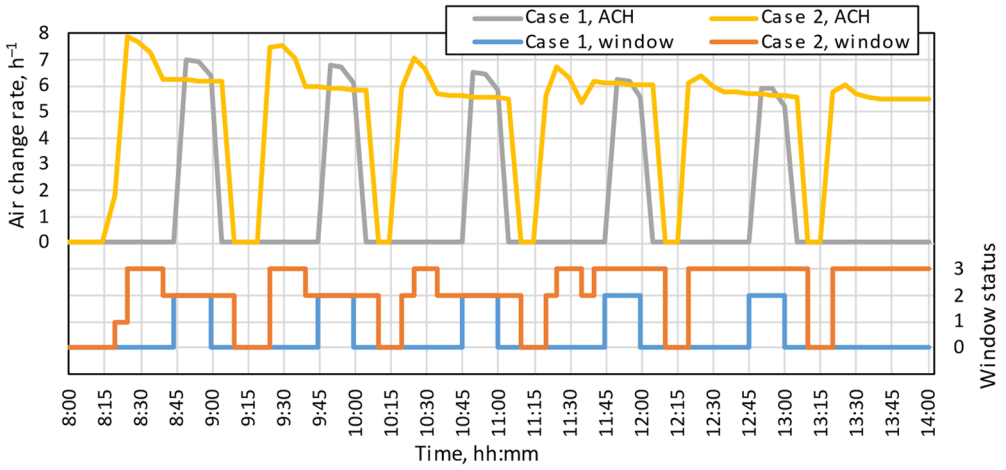

Figure 4. Air change rate and window opening status during 6 March; 0, 1, 2, and 3 represent closed, tilted, fully opened, and tilted and fully opened together, respectively.

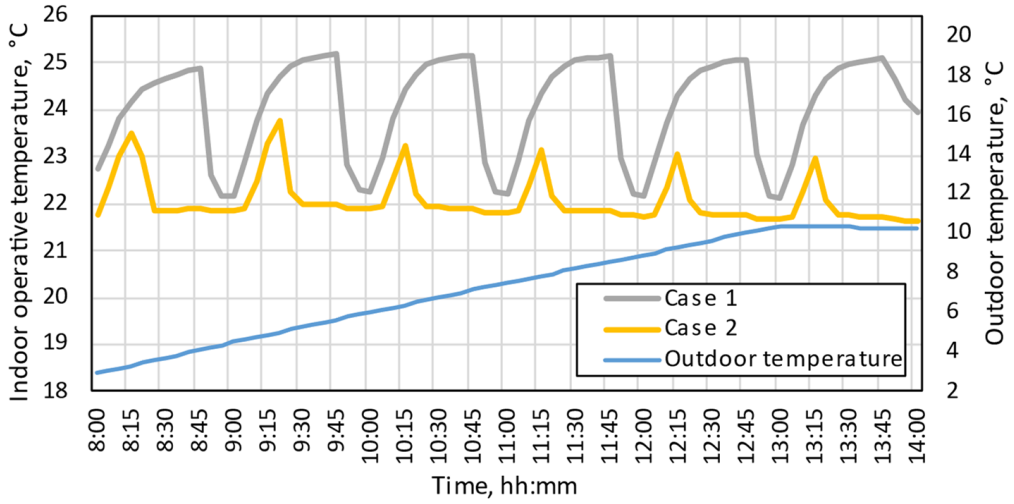

Figure 5. Indoor operative temperature and outdoor temperature during 6 March.

The effect of the optimized controller on the reduction in CO_2 concentration on 6th March was investigated. Figure 6 shows that in case 1, the CO_2 concentration at the end of each class, before the break time, reached the peak value and passed 2500 ppm. Meanwhile, after optimizing the controller with indoor environment quality functions, the CO_2 concentration varied between 600 ppm and 1200 ppm. Therefore, using the optimized controller was very effective in reducing CO_2 concentration.

The window status for one year is briefly shown in Table 4 for different cases. The window was opened only 3% of the time (break times) before optimization (case 1). After optimization, windows were opened or tilted for approximately 40% of the time, and also the time when students were not present. Tilting is the dominant opening area and an important factor to control objective functions. Despite adding masks and air cleaners in cases 4 to 6, and reducing the number of students in case 7, the performance of the controller in window opening was almost the same.

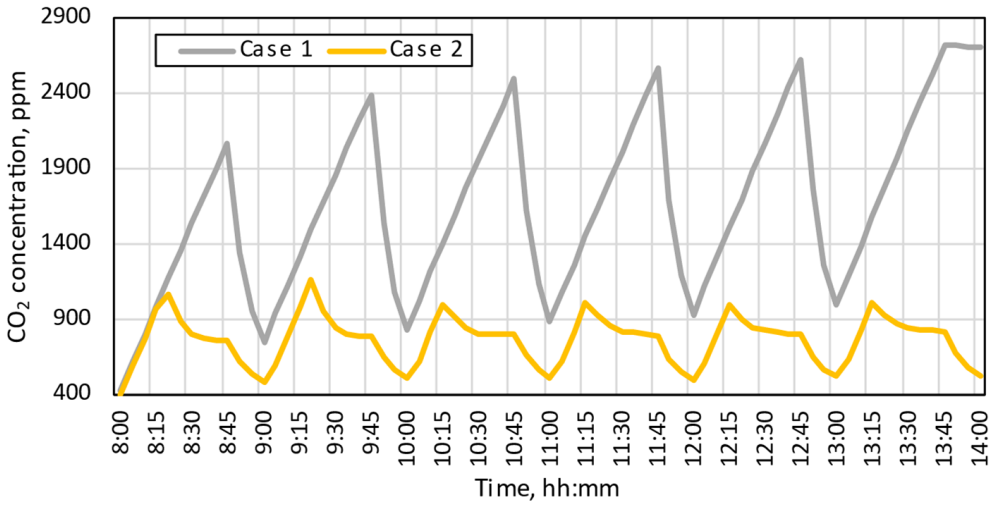

Figure 6. CO_2 concentration during 6 March.

Table 4. Percentage of time with different window status in all cases.

Window State	Case 1	Case 2	Case 3	Case 4	Case 5	Case 6	Case 7
Tilt	0%	29%	31%	30%	30%	30%	30%
Open	3%	5%	2%	4%	4%	6%	4%
Tilt and Open	0%	6%	10%	8%	7%	5%	6%
Closed	97%	60%	57%	58%	59%	59%	60%

3.2. Air Quality

Figure 7 presents the cumulative distribution of CO_2 concentration in the classroom (only occupied time). Considering that in Case 1, the window was opened only during breaks without considering the optimization of objective functions, the CO_2 concentration increased to 2900 ppm. Solutions applied in Cases 2 to 6 performed relatively similar, but substantially better than Case 1. In these cases, for 80% of the time when students were in the classroom, the CO_2 concentration was between 400 ppm and 950 ppm. In Case 7, as the number of students was reduced to 15, more than 90% of the students' attendance time had a concentration of less than 900 ppm.

The air change rate (ACH) is the second investigated parameter that affects CO_2 concentration and the indoor air quality. Figure 8 shows the distribution of ACH values based on time (only occupied time). As for CO_2 concentration, except for Case 1, other cases had similar performance. In Case 1, at all the times when students were in the classroom, the ACH value was less than 1 h^{-1}. In contrast, the air change rate in Cases 2 to 7 had significant fluctuations, reaching up to 12 h^{-1} in some hours.

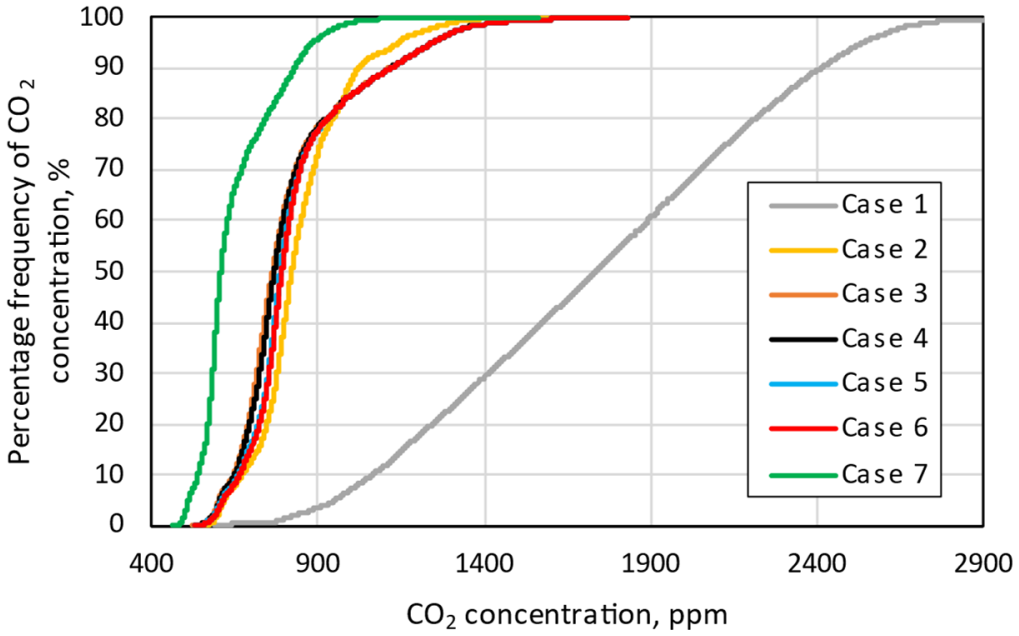

Figure 7. Cumulative distribution of CO_2 concentration frequency during the occupied classroom.

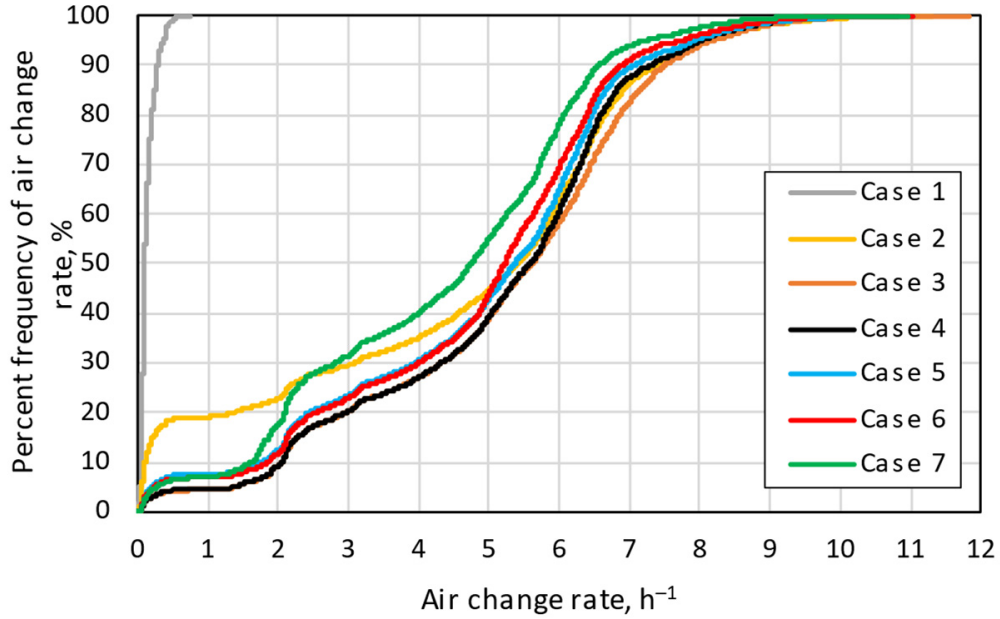

Figure 8. Cumulative distribution of air change rate during the occupied classroom.

3.3. Thermal Environment

According to Figure 9, the indoor operative temperature in the classroom in Case 1 for 30% of the time was above 30 °C. This was due to the fact that the windows stayed closed during the classes and were opened only during breaks, even in September and June, when it was warm outside. In practice, during these periods in classrooms, windows are usually also open during lessons, which significantly reduces the indoor temperature. In the theoretical case, when there are 30 occupants in the room and the windows are closed, the temperature due to internal heat gains and solar gains may even exceed 40 °C. In Cases 2 to 7 (windows can be opened during lessons), for approximately 70% of the time when students were in the classroom, the temperature was between 20 and 25 °C.

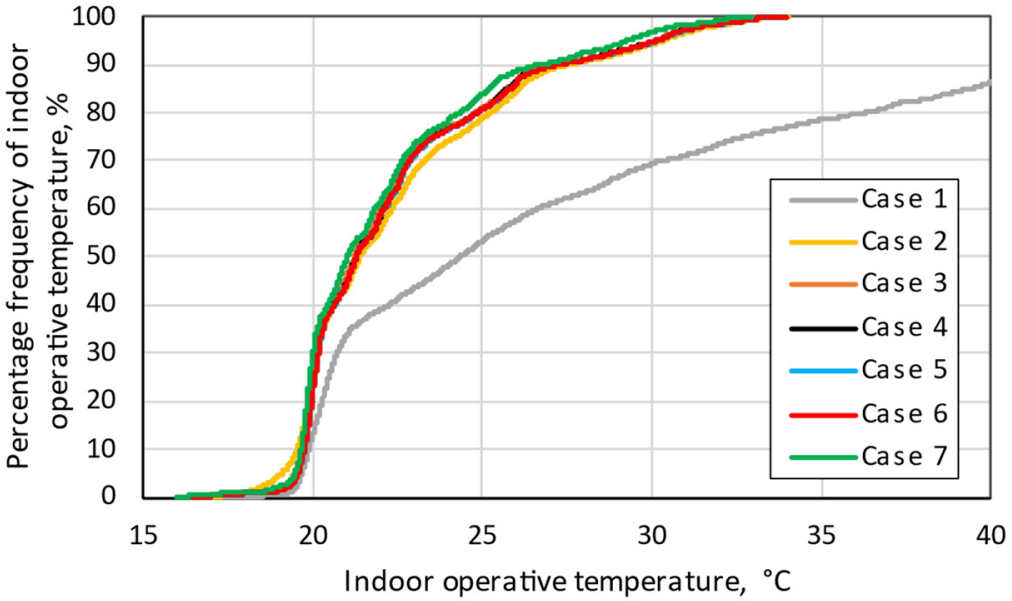

Figure 9. Cumulative distribution of indoor operative temperature during the occupied classroom.

3.4. Infection Risk

To evaluate if the proposed controller reduces the infection risk in addition to improving the indoor environment, it was necessary to investigate the reproduction number (R0) distribution during classes, i.e., in the students' presence time. According to Figure 10, the use of the window opening controller reduced the probability of infection risk to some extent. In Case 1, the distribution of R0 was close to linear from 0 to 11. The reproduction values also reached 11 in Case 2, but for 90% of the time, R0 was less than 5. In Case 3, despite the optimization of the window controller considering the probability of infection transmission, no specific change in the R0 distribution was observed. In Cases 4 to 7, the improvements were clearly obvious. The reproduction number did not exceed 2 and, most of the time, it was smaller than 1 in Cases 5 to 7.

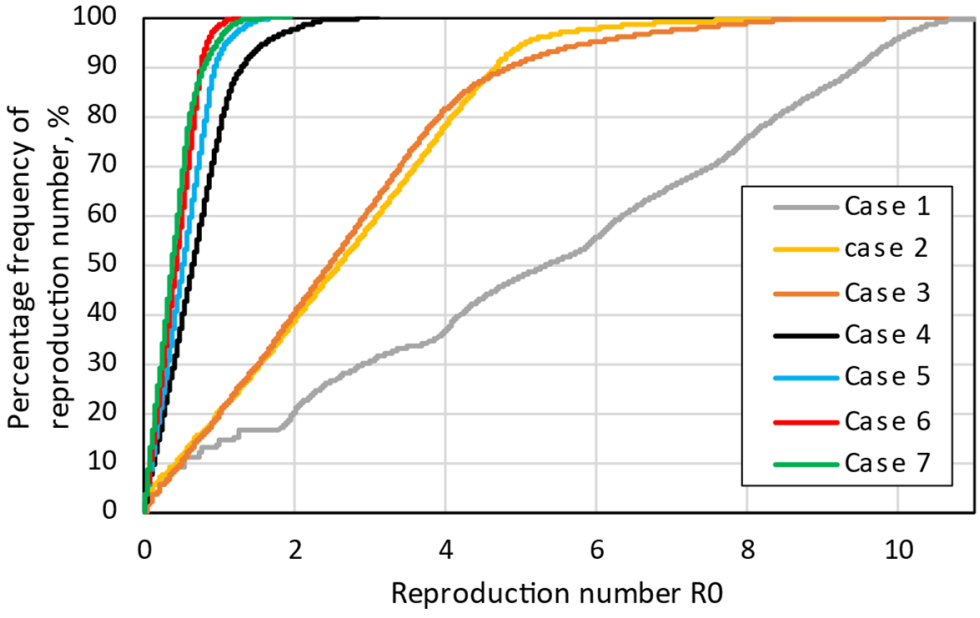

Figure 10. Cumulative distribution of reproduction number (R0).

4. Discussion

In this study, a new controller method for the window opening was developed and optimized to improve the natural ventilation of the classroom. The ultimate aim was to maintain good indoor air quality and thermal comfort, as well as to limit the probability of infection risk for the time when students were present in the classroom. The optimized controller by indoor environment functions compared to the base case, in which the windows were opened only during breaks, showed a noticeable improvement in indoor air quality. The results for thermal comfort, CO_2 concentration, and air change rate all improved. On the other hand, there was a noticeable increase in energy demand, caused by increasing ACH.

4.1. Indoor Environment Quality Optimization

Previous studies suggested that the use of controllers is effective on thermal comfort, and their proper usage makes a substantial improvement in the overall thermal comfort of occupants [56]. Based on European standards [2], there are different expectation levels of the building's occupants from the indoor air environment including "High", "Medium", and "Moderate", which are placed in three categories [2]. A normal level could be medium, and a high level may be used for special occupants such as children or old persons. As a lower level will not provide any health risk, this study used the moderate level of expectation (category III) for controller optimization to be able to cover all the objective functions. Case 1, in which one window sash was fully opened during each break, did not provide thermal comfort conditions in the classroom. Figure 11 demonstrates that annually, 44% of the time when students were in the classroom are out of the recommended thermal comfort categories range (IV), including 39% of the time when the room was overheated due to high operative temperature in warmer periods, as described in Section 3.2. In Case 2 where the window opening was controlled by indoor environment quality functions (thermal comfort and CO_2 concentration), only 18% of the total time occupants were present in the classroom was outside the recommended categories of thermal comfort. During the lesson (i.e., during the time when internal heat gains occurred), the classroom was passively cooled by the outside air supplied through the open window. The window was opened for 25% of the time of the school season, in contrast to Case 1 where it was only 3% (always during breaks). In addition, 26% of the occupied time was placed in the highest level of expectation (category I), while in Case 1, only 10% of the time fell in the first category. As Cases 3 to 7 had a very similar performance to Case 2, they were omitted in Figure 11.

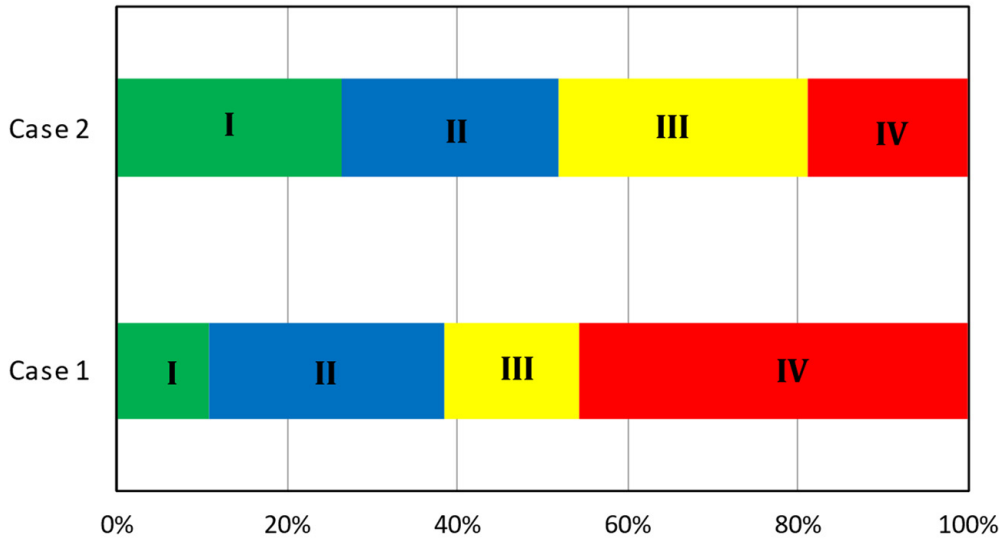

Figure 11. Percentage of thermal comfort index in different categories.

On the other hand, the influx of a large amount of outside air into the room (sometimes over 10 h^{-1}), during periods of low external temperatures, significantly decreased the indoor air temperature, even below 10 °C in the case of ventilation during breaks (Case 1) and to 14 °C in Case 2, which was a source of great discomfort during the lessons. There were 56 "too cold" hours in Case 1 and 96 "too cold" hours in Case 2, which accounted for 5% and 10% of occupancy time, respectively. In Case 1, the windows were closed immediately after the break, but it took several minutes to warm up the room due to the limited maximum power of the heating system.

Using the automatic window opener to reduce the CO_2 concentration is a relatively common approach that has been experimentally and numerically investigated already. Heebøll et al. [57] investigated that, in the case of using an automatic window along with mechanical ventilation, a significant reduction in CO_2 concentration occurred compared to manually opening the window and using the heat recovery system. In this study, the automatic window was the only available way to naturally ventilate the classroom. The European standard referring to the equilibrium concentration and CO_2 emission introduces three categories, which suggest maintaining the CO_2 concentration maximum at 550 ppm, 800 ppm, and 1350 ppm above the outdoor CO_2 level (in this study, 400 ppm was assumed) [2]. As an important objective function, this study considered category II for the controller setting in the optimization process. Figure 12 displays that the changes after optimization were significant in terms of CO_2 concentration. For 49% of time in Case 1, it was placed out of defined categories (IV). Meanwhile, for almost all hours of Case 2, the CO_2 concentration was maintained within the defined standard categories. In addition, for 80% of the time, the CO_2 concentration was in category I (400–950 ppm), while in Case 1, requirements for category I were fulfilled for only 5% of the time.

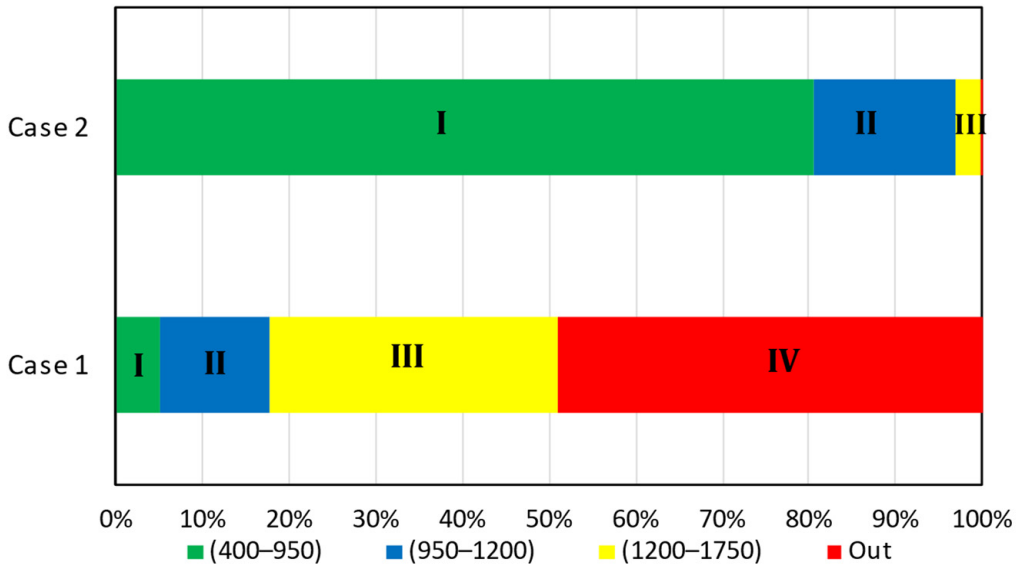

Figure 12. Percentage of carbon dioxide concentration in different categories.

Although the air change rate is not one of the objective functions, this value significantly changes after optimization of thermal comfort and CO_2 concentration. On the other hand, it is necessary to have a sufficient air change rate in the room to comply with hygiene issues. Considering 30 people in the classroom, the ventilation airflow rate should be 600 m^3/h according to the Polish standard [58], 482 m^3/h according to [3] (assuming category III and low emission from building), and 524 m^3/h according to [2], which corresponds to 3.4 h^{-1}, 2.7 h^{-1}, and 2.9 h^{-1}, respectively. As shown in Figure 8, ACH was less than 1 h^{-1} in all hours in Case 1, which is not proper hygienically. Case 2 experienced entirely different conditions. ACH was higher than 3.4 h^{-1} for approximately 70% of

the time when students were in the classroom. Although the window opening control approach based on indoor environment led to a significant improvement in air change rate, still considerable fluctuations of ACH value were observed. In some hours, the ACH reached even 12 h^{-1}. In addition, for approximately 20% of the students' presence time in the classroom, ACH was lower than 1 h^{-1}. Hence, mechanical ventilation is necessary to ensure a steady, constant exchange of air.

4.2. Infection Risk Optimization

Unlike CO_2 concentration, the use of the controller did not have much effect on reducing the probability of infection risk in the classroom. Case 3, where the infection risk objective was added to the controller optimization, had a similar performance to Case 2 (without considering COVID in the controller) in reducing the probability of infection risk. Figure 10 indicates that only for 14% of the lecture time, the reproduction number was lower than 1 when the window was opened during breaks (Case 1). In Case 3, the controller slightly increased this amount to 20.2%. However, for 79.8% of lecture time, R0 was still higher than 1, which does not provide a safe condition for infection risk inside the room. Therefore, it is necessary to take other actions, in addition to optimization of smart windows performance, to limit the probability of infection risk.

Many studies have investigated the effect of masks on reducing the possibility of virus transmission [59]. However, the sufficiency of this solution depends also on other parameters than only mask characteristics. This includes ventilation rate, exposure time, number of susceptible people, and number of infected persons [60]. In this study, masks with 50% filtration efficiency were intended for students in Cases 4 to 7. Using masks (Case 4) significantly reduced hours with a high probability of infection. However, for 23% of the lecture time, R0 was still higher than 1. Therefore, in classrooms with controlled natural ventilation, wearing masks with 50% efficiency alone is not enough.

Air cleaners are effective in the elimination of particles and aerosols from the air in closed spaces [61]. Hence, for Case 5 and Case 6, one and two air purifiers were assumed in the classroom, respectively. The air cleaners were especially effective when used along with occupants wearing face masks; the time when reproduction number R0 was above 1 was reduced to less than 10%, which is desirable. The best performance in terms of limiting virus transmission was observed in Case 6, where two air purifiers with 330 m^3/h CADR were in operation. For this case, only 1.6% of the time included a higher probability of infection risk (R0 > 1). Although air cleaners were effective for reducing the risk of infection in classes, they should be applied carefully as they generate noise (40 dB). The location of the air cleaner in the classroom should also be considered [62].

After the emergence of COVID-19, holding online classes became especially prevalent. However, over time, due to the reduction in the pandemic and the low efficiency of students' learning, they returned to classes, and classes were held with the maximum number. This study probes hybrid classes to control the probability of infection transmission as well as students' learning efficiency. Case 7 assumes that the class is held with only 15 students present in the class. Therefore, half of the students participate in the class virtually. In this case, where the students were considered with 50% filtration masks, they experienced high infection risk (R0 > 1) for only 4% of the lecture class.

4.3. Energy Analyses

This study also examined energy demand for heating as a consequence of window opening. Figure 13 shows a summary of the unfavorable indoor environment conditions observed for each studied case together with the heat demand. The lowest demand was noted for the reference case (Case 1) in which the controller opened the window only during break times. This case, however, had the most undesirable conditions in terms of low air quality and high probability of infection transmission, which is discussed in previous sections. The introduction of the smart windows with optimized indoor air parameters

(Case 2) improved air quality conditions in the classroom, but a substantial increase in heating demand was indicated (about 190%).

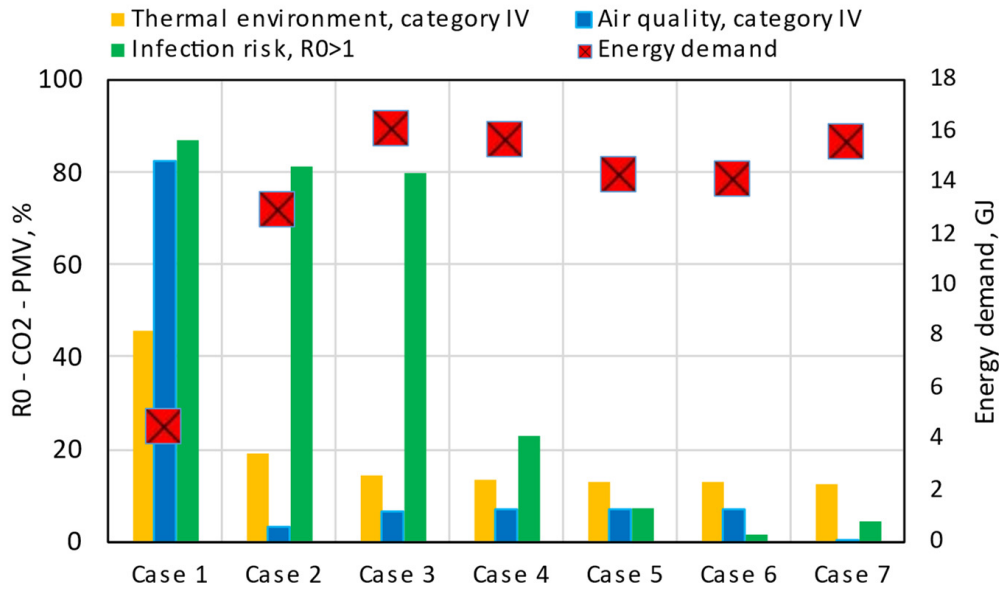

Figure 13. Summary of all objective functions performed in the cases: the percentage of hours that each function is out of acceptable range (left axis) and annual energy demand (right axis).

Introducing infection risk to the optimization process in the controller (Case 3) increased even more the heat demand (about 260% compared to Case 1), which was caused by the further increase in air change rates. This had some positive but only small effect on lowering the probability of infection transmission and CO_2 concentration.

Introducing face masks for the students and especially air cleaners significantly decreased the risk of infection. The energy demand in these cases also decreased slightly. In the case when students used masks (Case 4), heating demand fell only slightly by 0.5 GJ, which is 3%. Air cleaners in Cases 5 and 6 partially reduced the risk of infection; therefore, the optimized system opened the window less often, which reduced the heat demand by 1.5 GJ, which was 10% of the value in Case 4. To sum up, the energy demand for heating, CO_2 concentration, and thermal comfort in Cases 5 and 6 that used different numbers of air cleaners had a similar performance, and the only variable function was the probability of infection risk. Case 6, with an R0 lower than 1 for 98% of the time, had the best performance in reducing infection risk. In Case 7, as the number of people in the classroom decreased, it not only reduced the probability of infection risk desirably but also the number of hours to 0 when the CO_2 concentration was outside the standard category. However, in the absence of air cleaners, the energy demand slightly increased.

It should be noted the heat demand output obtained in simulations covered only the demand for heating. Air cleaners need electricity for operation. The power of a single air cleaner applied in this study was 21 W; thus, one air cleaner operating constantly during occupancy hours will consume approximately 20 kWh and should be added to the total energy demand. Nevertheless, indoor air cleaning strategies are necessary to reduce the risk of infection in classrooms, especially with natural ventilation.

Electrical energy for the automatic window opening system was not included in the analysis. The window actuators require relatively little electrical power, but nevertheless, this energy can influence the optimal solution.

5. Conclusions

Clean air is a basic requirement for human health and well-being. The key to protecting occupants against the negative impact of air pollution is improving ventilation. Schools are usually low-rise buildings (2 to 3 floors) and most of the classrooms are on the top floor, where the length of gravitational ventilation ducts is very short. Therefore, the natural ventilation systems used in school rooms (especially in windless periods) are unable to provide the required airflow, and the CO_2 concentration can periodically reach even 10,000 ppm [63], if the windows are not opened all day. The situation can be improved by the regular airing of classrooms, which can be supported by a smart window opening system that was developed in this study.

The analysis of the simulation results showed that for the typical classroom in Poland the following conclusions can be drawn:

- The regular opening of windows only during breaks does not ensure acceptable environment quality in the classroom—the thermal environment is low for more than 45% of time and air quality for more than 80%.
- Smart windows with controllers substantially improve thermal comfort and increase air change rate; thus, air quality is also improved, but the risk of infection is reduced only slightly. The introduction of the "infection risk" objective to controller optimization (Case 3) has very little effect on reducing the probability of infection risk.
- The inflow of cool air through an open window causes a significant increase in the heating power in the rooms, and in periods of low external temperature, it can cause a local decrease in the indoor temperature in the rooms (in this study, even below 14 °C).
- The frequent opening of windows during a day significantly increases heating demand (in this study, heating demand increased 3 times compared to the case when windows are only opened during school breaks). Therefore, mechanical ventilation is necessary to ensure a constant air exchange, which, at the same time, allows the use of heat recovery from the air removed from the room; however, the introduction of such a system is problematic in existing schools and requires large investments.
- In order to reduce infection risk substantially, wearing masks and operating effective air cleaners are necessary (these applications can decrease the time with high infection risk to 1.6%).
- Decreasing the number of students in the classroom, as it was expected, helps to further decrease the risk of infection (in this study, the time with high infection risk decreases to 4.2%).
- The results show that classrooms that possess windows with optimized controllers by indoor environment and infection risk functions, along with air cleaners and masks for students, are able to control air quality, thermal comfort, and infection risk.

6. Limitations and Future Works

- Considering that the present study was limited to only one climate and one typical school, it will be interesting to study the controller performance in different climates and compare the results.
- The expansion of controller parameters and the optimization of functions, especially those that would be affected by window opening, can be advantageous in the future. Energy demand and other indoor air pollutants such as particulate matter (PM) are the major influential issues involved with opening windows.
- The presented analysis concerned the effect of controller operation on energy demand, but the economic issues were not addressed.
- As the model considered the classroom with fully mixed indoor air to use the calculation for quanta concentration, an experimental study with local measurement is recommended to investigate conditions in the real state.

Author Contributions: Conceptualization, J.K. and S.N.; methodology, K.G., J.F.-G., J.K. and S.N.; software, K.G.; formal analysis, S.N. and J.K.; writing—original draft preparation, S.N., J.K. and J.F.-G.; writing—review and editing, K.G. All authors have read and agreed to the published version of the manuscript.

Funding: This research received no external funding.

Institutional Review Board Statement: Not applicable.

Informed Consent Statement: Not applicable.

Data Availability Statement: Not applicable.

Acknowledgments: The work was supported by the Polish Ministry of Education and Science within the research subsidy.

Conflicts of Interest: The authors declare no conflict of interest.

References

1. Šujanová, P.; Rychtáriková, M.; Sotto Mayor, T.; Hyder, A. A Healthy, Energy-Efficient and Comfortable Indoor Environment, a Review. *Energies* **2019**, *12*, 1414. [CrossRef]
2. *EU Standard EN 16798-1:2019*; Energy Performance of Buildings—Ventilation for Buildings—Part 1: Indoor Environmental Input Parameters for Design and Assessment of Energy Performance of Buildings Addressing Indoor Air Quality, Thermal Environment, Lighting and Acoustics—Module M1-6. European Committee for Standardization: Brussels, Belgium, 2019.
3. ASHRAE. *ASHRAE Standard 62-2001*; Ventilation for Acceptable Indoor Air Quality Atlanta. American Society of Heating, Refrigerating, and Air Conditioning Engineers, Inc.: Atlanta, Ga, USA, 2001.
4. Srivastava, S.; Khokhar, F.; Madhav, A.; Pembroke, B.; Shetty, V.; Mutreja, A. COVID-19 Lessons for Climate Change and Sustainable Health. *Energies* **2021**, *14*, 5938. [CrossRef]
5. Allam, M.; Cai, S.; Ganesh, S.; Venkatesan, M.; Doodhwala, S.; Song, Z.; Hu, T.; Kumar, A.; Heit, J.; Study Group, C.; et al. COVID-19 Diagnostics, Tools, and Prevention. *Diagnostics* **2020**, *10*, 409. [CrossRef]
6. Lewis, D. Is the Coronavirus Airborne? Experts Can't Agree. *Nature* **2020**, *580*, 175. [CrossRef] [PubMed]
7. Gralton, J.; Tovey, E.R.; McLaws, M.-L.; Rawlinson, W.D. Respiratory Virus RNA Is Detectable in Airborne and Droplet Particles: Viral RNA in Airborne and Droplet Particles. *J. Med. Virol.* **2013**, *85*, 2151–2159. [CrossRef]
8. Santarpia, J.L.; Herrera, V.L.; Rivera, D.N.; Ratnesar-Shumate, S.; Reid, S.P.; Ackerman, D.N.; Denton, P.W.; Martens, J.W.S.; Fang, Y.; Conoan, N.; et al. The size and culturability of patient-generated SARS-CoV-2 aerosol. *J. Expo. Sci. Environ. Epidemiol.* **2022**, *32*, 706–711. [CrossRef] [PubMed]
9. Makison Booth, C.; Clayton, M.; Crook, B.; Gawn, J.M. Effectiveness of Surgical Masks against Influenza Bioaerosols. *J. Hosp. Infect.* **2013**, *84*, 22–26. [CrossRef]
10. O'Dowd, K.; Nair, K.M.; Forouzandeh, P.; Mathew, S.; Grant, J.; Moran, R.; Bartlett, J.; Bird, J.; Pillai, S.C. Face Masks and Respirators in the Fight Against the COVID-19 Pandemic: A Review of Current Materials, Advances and Future Perspectives. *Materials* **2020**, *13*, 3363. [CrossRef]
11. Domínguez-Amarillo, S.; Fernández-Agüera, J.; Cesteros-García, S.; González-Lezcano, R.A. Bad Air Can Also Kill: Residential Indoor Air Quality and Pollutant Exposure Risk during the COVID-19 Crisis. *Int. J. Environ. Res. Public. Health* **2020**, *17*, 7183. [CrossRef]
12. Zhao, Y.; Sun, H.; Tu, D. Effect of Mechanical Ventilation and Natural Ventilation on Indoor Climates in Urumqi Residential Buildings. *Build. Environ.* **2018**, *144*, 108–118. [CrossRef]
13. Jo, S.; Hong, J.; Lee, S.-E.; Ki, M.; Choi, B.Y.; Sung, M. Airflow Analysis of Pyeongtaek St Mary's Hospital during Hospitalization of the First Middle East Respiratory Syndrome Patient in Korea. *R. Soc. Open Sci.* **2019**, *6*, 181164. [CrossRef] [PubMed]
14. Kulkarni, H.; Smith, C.M.; Lee, D.D.H.; Hirst, R.A.; Easton, A.J.; O'Callaghan, C. Evidence of Respiratory Syncytial Virus Spread by Aerosol. Time to Revisit Infection Control Strategies? *Am. J. Respir. Crit. Care Med.* **2016**, *194*, 308–316. [CrossRef] [PubMed]
15. Rule, A.M.; Apau, O.; Ahrenholz, S.H.; Brueck, S.E.; Lindsley, W.G.; de Perio, M.A.; Noti, J.D.; Shaffer, R.E.; Rothman, R.; Grigorovitch, A.; et al. Healthcare Personnel Exposure in an Emergency Department during Influenza Season. *PLoS ONE* **2018**, *13*, E0203223. [CrossRef] [PubMed]
16. Zhang, H.; Yang, D.; Tam, V.W.Y.; Tao, Y.; Zhang, G.; Setunge, S.; Shi, L. A Critical Review of Combined Natural Ventilation Techniques in Sustainable Buildings. *Renew. Sustain. Energy Rev.* **2021**, *141*, 110795. [CrossRef]
17. World Health Organization. *Roadmap to Improve and Ensure Good Indoor Ventilation in the Context of COVID-19*; World Health Organization: Geneva, Switzerland, 2021; ISBN 978-92-4-002128-0.
18. Schibuola, L.; Scarpa, M.; Tambani, C. Natural Ventilation Level Assessment in a School Building by CO_2 Concentration Measures. *Energy Procedia* **2016**, *101*, 257–264. [CrossRef]
19. Schibuola, L.; Tambani, C. Indoor Environmental Quality Classification of School Environments by Monitoring PM and CO_2 Concentration Levels. *Atmos. Pollut. Res.* **2020**, *11*, 332–342. [CrossRef]

20. Santamouris, M.; Synnefa, A.; Asssimakopoulos, M.; Livada, I.; Pavlou, K.; Papaglastra, M.; Gaitani, N.; Kolokotsa, D.; As-Simakopoulos, V. Experimental Investigation of the Air Flow and Indoor Carbon Dioxide Concentration in Classrooms with Intermittent Natural Ventilation. *Energy Build.* **2008**, *40*, 1833–1843. [CrossRef]
21. European Commission Joint Research Centre; Institute for Health and Consumer Protection.; European Commission; Di-Rectorate General for Health and Consumers; Regional Environmental Centre for Central and Eastern Europe. *SINPHONIE: Guidelines for Healthy Environments within European Schools*; Publications Office: Luxembourg, 2014.
22. Seppanen, O.A.; Fisk, W.J.; Mendell, M.J. Association of Ventilation Rates and CO_2 Concentrations with Health And Other Responses in Commercial and Institutional Buildings. *Indoor Air* **1999**, *9*, 226–252. [CrossRef]
23. Daum, D.; Haldi, F.; Morel, N. A Personalized Measure of Thermal Comfort for Building Controls. *Build. Environ.* **2011**, *46*, 3–11. [CrossRef]
24. Clements-Croome, D.J.; Awbi, H.B.; Bakó-Biró, Z.; Kochhar, N.; Williams, M. Ventilation Rates in Schools. *Build. Environ.* **2008**, *43*, 362–367. [CrossRef]
25. Coley, D.A.; Greeves, R.; Saxby, B.K. The Effect of Low Ventilation Rates on the Cognitive Function of a Primary School Class. *Int. J. Vent.* **2007**, *6*, 107–112. [CrossRef]
26. Lu, X.; Pang, Z.; Fu, Y.; O'Neill, Z. The Nexus of the Indoor CO_2 Concentration and Ventilation Demands Underlying CO_2-Based Demand-Controlled Ventilation in Commercial Buildings: A Critical Review. *Build. Environ.* **2022**, *218*, 109116. [CrossRef]
27. Cho, H.; Cabrera, D.; Sardy, S.; Kilchherr, R.; Yilmaz, S.; Patel, M.K. Evaluation of Performance of Energy Efficient Hybrid Ventilation System and Analysis of Occupants' Behavior to Control Windows. *Build. Environ.* **2021**, *188*, 107434. [CrossRef]
28. Stazi, F.; Naspi, F.; Ulpiani, G.; Di Perna, C. Indoor Air Quality and Thermal Comfort Optimization in Classrooms Developing an Automatic System for Windows Opening and Closing. *Energy Build.* **2017**, *139*, 732–746. [CrossRef]
29. Grygierek, K.; Sarna, I. Impact of Passive Cooling on Thermal Comfort in a Single-Family Building for Current and Future Climate Conditions. *Energies* **2020**, *13*, 5332. [CrossRef]
30. Sorgato, M.J.; Melo, A.P.; Lamberts, R. The Effect of Window Opening Ventilation Control on Residential Building Energy Consumption. *Energy Build.* **2016**, *133*, 1–13. [CrossRef]
31. Psomas, T.; Fiorentini, M.; Kokogiannakis, G.; Heiselberg, P. Ventilative Cooling through Automated Window Opening Control Systems to Address Thermal Discomfort Risk during the Summer Period: Framework, Simulation and Parametric Analysis. *Energy Build.* **2017**, *153*, 18–30. [CrossRef]
32. Tan, Z.; Deng, X. An Optimised Window Control Strategy for Naturally Ventilated Residential Buildings in Warm Climates. *Sustain. Cities Soc.* **2020**, *57*, 102118. [CrossRef]
33. Wang, Y.; Cooper, E.; Tahmasebi, F.; Taylor, J.; Stamp, S.; Symonds, P.; Burman, E.; Mumovic, D. Improving Indoor Air Quality and Occupant Health through Smart Control of Windows and Portable Air Purifiers in Residential Buildings. *Build. Serv. Eng. Res. Technol.* **2022**, *43*, 571–588. [CrossRef]
34. Lakhdari, K.; Sriti, L. Birgit Painter Parametric Optimization of Daylight, Thermal and Energy Performance of Middle School Classrooms, Case of Hot and Dry Regions. *Build. Environ.* **2021**, *204*, 108173. [CrossRef]
35. Deblois, J.C.; Ndiaye, D. CFD-Assisted Design and Optimization of Solar Chimneys for Elementary School Classrooms. In Proceedings of the 14th Conference of International Building Performance Simulation Association, Hyderabad, India, 7–9 December 2015; pp. 818–825.
36. Acosta-Acosta, D.F.; El-Rayes, K. Optimal Design of Classroom Spaces in Naturally-Ventilated Buildings to Maximize Occupant Satisfaction with Human Bioeffluents/Body Odor Levels. *Build. Environ.* **2020**, *169*, 106543. [CrossRef]
37. Arjmandi, H.; Amini, R.; Khani, F.; Fallahpour, M. Minimizing the Respiratory Pathogen Transmission: Numerical Study and Multi-Objective Optimization of Ventilation Systems in a Classroom. *Therm. Sci. Eng. Prog.* **2022**, *28*, 101052. [CrossRef]
38. Schibuola, L.; Tambani, C. High Energy Efficiency Ventilation to Limit COVID-19 Contagion in School Environments. *Energy Build.* **2021**, *240*, 110882. [CrossRef] [PubMed]
39. Engineering Reference. *EnergyPlusTM*; Version 9.4.0; Documentation; US Department of Energy: Washington, DC, USA, 2020.
40. Dols, W.S.; Polidoro, B.J. *CONTAM User Guide and Program Documentation Version 3.4*; National Institute of Standards and Technology: Gaithersburg, MD, USA, 2020.
41. Typical Meteorological Years and Statistical Climatic Data for the Area of Poland for Energy Calculations of Buildings—Open Data. Available online: https://Dane.Gov.Pl/Pl/Dataset/797,Typowe-Lata-Meteorologiczne-i-Statystyczne-Dane-Klimatyczne-Dla-Obszaru-Polski-Do-Obliczen-Energetycznych-Budynkow (accessed on 28 November 2022).
42. Pinto, M.; Viegas, J.; Freitas, V. Summer Cross Ventilation in Residential Buildings. In Proceedings of the Energy for Sustainability International Conference 2017 Designing Cities & Communities for the Future, Funchal, Portugal, 8–10 February 2017.
43. EnergyPlus Python API 0.1 Documentation. Available online: https://nrel.github.io/EnergyPlus/api/python/ (accessed on 28 November 2022).
44. Blank, J.; Deb, K. Pymoo: Multi-Objective Optimization in Python. *IEEE Access* **2020**, *8*, 89497–89509. [CrossRef]
45. Goldberg, D. *Genetic Algorithms in Search, Optimization and Machine Learning*; Addison-Wesley Publishing Company, Inc.: Boston, MA, USA, 1989; ISBN 978-0201157673.
46. Mitchell, R.; Kohler, C.; Curcija, D.; Zhu, L.; Vidanovic, S.; Czarnecki, S.; Arasteh, D. WINDOW 7 User Manual. Lawrence Berkeley National Laboratory, March 2019. Available online: https://Windows.Lbl.Gov/Tools/Window/Documentation (accessed on 14 December 2021).

47. Pilkington. Available online: https://www.Pilkington.Com/Pl-Pl/Pl/Produkty/Funkcje-Szkla/Izolacja-Cieplna/Pilkington-Insulight-Therm (accessed on 15 December 2021).
48. Dols, W.S.; Emmerich, S.J.; Polidoro, B.J. Coupling the Multizone Airflow and Contaminant Transport Software CONTAM with EnergyPlus Using Co-Simulation. *Build. Simul.* **2016**, *9*, 469–479. [CrossRef]
49. Polish Ministry of Infrastructure. *Regulation of the Minister of Infrastructure of 12 April 2002 on the Technical Conditions That Should Be Met by Buildings and Their Location; Journal of Laws of the Republic of Poland No 75, Item. 690, (with Recast)*; Polish Ministry of Infrastructure: Warsaw, Poland, 2002. (In Polish)
50. Fernández de Mera, I.G.; Granda, C.; Villanueva, F.; Sánchez-Sánchez, M.; Moraga-Fernández, A.; Gortázar, C.; de la Fuente, J. HEPA Filters of Portable Air Cleaners as a Tool for the Surveillance of SARS-CoV-2. *Indoor Air* **2022**, *32*, e13109. [CrossRef]
51. Sze To, G.N.; Chao, C.Y.H. Review and Comparison between the Wells–Riley and Dose-Response Approaches to Risk Assessment of Infectious Respiratory Diseases. *Indoor Air* **2010**, *20*, 2–16. [CrossRef]
52. Diapouli, E.; Chaloulakou, A.; Koutrakis, P. Estimating the Concentration of Indoor Particles of Outdoor Origin: A Review. *J. Air Waste Manag. Assoc.* **2013**, *63*, 1113–1129. [CrossRef]
53. van Doremalen, N.; Bushmaker, T.; Morris, D.H.; Holbrook, M.G.; Gamble, A.; Williamson, B.N.; Tamin, A.; Harcourt, J.L.; Thornburg, N.J.; Gerber, S.I.; et al. Aerosol and Surface Stability of SARS-CoV-2 as Compared with SARS-CoV-1. *N. Engl. J. Med.* **2020**, *382*, 1564–1567. [CrossRef]
54. Riley, E.C.; Murphy, G.; Riley, R.L. Airborne Spread of Measles In A Suburban Elementary School. *Am. J. Epidemiol.* **1978**, *107*, 421–432. [CrossRef]
55. Gammaitoni, L. Using a Mathematical Model to Evaluate the Efficacy of TB Control Measures. *Emerg. Infect. Dis.* **1997**, *3*, 335–342. [CrossRef]
56. Raja, I.A.; Nicol, J.F.; McCartney, K.J.; Humphreys, M.A. Thermal Comfort: Use of Controls in Naturally Ventilated Buildings. *Energy Build.* **2001**, *33*, 235–244. [CrossRef]
57. Heebøll, A.; Wargocki, P.; Toftum, J. Window and Door Opening Behavior, Carbon Dioxide Concentration, Temperature, and Energy Use during the Heating Season in Classrooms with Different Ventilation Retrofits—ASHRAE RP1624. *Sci. Technol. Built Environ.* **2018**, *24*, 626–637. [CrossRef]
58. *Polish Standard PN-83/B-03430/Az3 2000*; Ventilation in Dwellings and Public Utility Buildings. Polish Committee for Standardization: Warsaw, Poland, 2000. (In Polish)
59. Howard, J.; Huang, A.; Li, Z.; Tufekci, Z.; Zdimal, V.; van der Westhuizen, H.-M.; von Delft, A.; Price, A.; Fridman, L.; Tang, L.-H.; et al. An Evidence Review of Face Masks against COVID-19. *Proc. Natl. Acad. Sci. USA* **2021**, *118*, e2014564118. [CrossRef]
60. Morawska, L.; Allen, J.; Bahnfleth, W.; Bluyssen, P.M.; Boerstra, A.; Buonanno, G.; Cao, J.; Dancer, S.J.; Floto, A.; Franchimon, F.; et al. A Paradigm Shift to Combat Indoor Respiratory Infection. *Science* **2021**, *372*, 689–691. [CrossRef] [PubMed]
61. Buising, K.L.; Schofield, R.; Irving, L.; Keywood, M.; Stevens, A.; Keogh, N.; Skidmore, G.; Wadlow, I.; Kevin, K.; Rismanchi, B.; et al. Use of Portable Air Cleaners to Reduce Aerosol Transmission on a Hospital Coronavirus Disease 2019 (COVID-19) Ward. *Infect. Control Hosp. Epidemiol.* **2022**, *43*, 987–992. [CrossRef] [PubMed]
62. Duill, F.F.; Schulz, F.; Jain, A.; Krieger, L.; van Wachem, B.; Beyrau, F. The Impact of Large Mobile Air Purifiers on Aerosol Concentration in Classrooms and the Reduction of Airborne Transmission of SARS-CoV-2. *Int. J. Environ. Res. Public. Health* **2021**, *18*, 11523. [CrossRef] [PubMed]
63. Popiołek, Z.; Ferdyn-Grygierek, J. Efficiency of Heating and Ventilation in School Buildings before and after Retrofitting. In Proceedings of the 3rd International Seminar Healthy Buildings, Sofia, Bulgaria, 18 November 2005.

Journal of Building Engineering 78 (2023) 107617

Contents lists available at ScienceDirect

Journal of Building Engineering

journal homepage: www.elsevier.com/locate/jobe

Multi-objective optimization of window opening and thermostat control for enhanced indoor environment quality and energy efficiency in contrasting climates

Seyedkeivan Nateghi *, Jan Kaczmarczyk

Department of Heating, Ventilation and Dust Removal Technology, Faculty of Energy and Environmental Engineering, Silesian University of Technology, 44-100, Gliwice, Poland

ARTICLE INFO

Keywords:
Window opening
Multi objective optimization
Energy demand
CO_2 concentration
Thermal comfort
JEPlus +EA

ABSTRACT

In this study, a triple-objective model-based optimization of a controlled opening window's specifications and thermostat control setpoints was investigated. Numerical simulations were performed employing EnergyPlus, and multi-criteria optimization of objective functions and decision parameters was accomplished by jEPlus + EA using Non-dominated Sorting Genetic Algorithm (NSGA-II). Controlled window optimization was carried out for a typical classroom, and the results were evaluated for two contrast climates. The decision variables are indoor temperature set points for opening control, thermostat set points, and the window opening area. The annual energy demand, the average CO_2 concentration, and the predicted percentage of dissatisfaction (PPD) were also regarded as objective functions to be simultaneously minimized. Max-min normalization and selecting final answers from the Pareto front were performed by the weighted sum method. By operating the suggested parameters, executing the optimized control strategy on the window opening resulted in indoor environmental quality improvement and a substantial decrease in energy demand, which had been selected as objective functions. The results show that using a controller based on indoor temperature instead of time significantly improved indoor air quality but greatly increased energy consumption. By performing optimization, in more than 50% of the time, all objective functions were controlled simultaneously for both selected climates. In total, the optimized window and thermostat controller performed desirable in both climates.

1. Introduction

It has been proven that the contemporary population spends most of their time in buildings, and the low quality of indoor may pose a risk for human health [1,2]. Vulnerability to high CO_2 concentration in a closed space causes different health consequence. Headaches, breathing difficulties, tiredness, and sweating are common health effects, especially in the educational environment with populated places [3]. On the other hand, the emergence of new infectious diseases like Covid-19 from SARS-CoV-2 has also added the probability of infection transmission to the problems caused by poor indoor air quality [4]. In recent years, significant progress has been made in improving indoor air quality (IAQ), enhancing people's awareness and education about IAQ, and identifying the key factors that impact IAQ [5]. Also, some standards were defined as thermal requirements, and various categories were presented based

* Corresponding author.
E-mail address: Seyedkeivan.Nateghi@polsl.pl (S. Nateghi).

https://doi.org/10.1016/j.jobe.2023.107617
Received 4 June 2023; Received in revised form 10 August 2023; Accepted 18 August 2023
Available online 20 August 2023

on the occupants' expectations [6,7]. Ventilation is one of the known and reliable ways to improve indoor air quality [8]. In addition, ventilation systems help to eliminate viruses by reducing viral concentration [9]. However, many buildings in countries with continental or cold climates do not have mechanical ventilation systems and usually use natural ventilation. Natural ventilation provides an unstable air change rate, which is corelated to actual outdoor weather conditions. Besides, depending on the type of climate, natural ventilation increases energy demand and may disrupt thermal comfort of occupants. In a tropical climate, overheating and increasing cooling demand, and in continental climates, overcooling and increased heating demand are problems that are faced in buildings with natural ventilation.

In this regard, several studies investigated and designed automatic windows to control the opening of the window and the air change rate in buildings [10]. Stavrakakis et al. [11] introduced a novel computational approach to optimize window openings for thermal comfort through the predicted mean vote (PMV) index. They concluded that the suggested approach prepares the optimal window, which correlates to the thermal comfort for various activity levels of occupants. Besides paying attention to proper ventilation, classrooms are of the greatest importance due to the high density of occupants and insufficient air quality [12]. By optimizing a window controller, Grygierek et al. [13] simultaneously controlled indoor air quality, thermal comfort, and infection transmission probability in a classroom. They indicated that window controllers optimized by indoor environment quality and infection risk functions can maintain acceptable indoor environment quality and decrease virus transmission if students wear face masks and air cleaners in classrooms. However, the energy demand was not considered in the optimization process. The research gaps in the study can be filled by optimizing objective functions including energy demand, indoor CO_2 concentration, and thermal comfort, which takes into account economic, environmental, and hygienic concerns.

The selection of specific parameters for optimizing the window controller is crucial to achieving optimal indoor environmental quality and energy efficiency. The window area plays a vital role in determining the indoor/outdoor air exchange rate, directly influencing indoor air quality and energy demand. By optimizing the open area, we can strike a balance between adequate ventilation and energy conservation, enhancing the overall indoor environment. Furthermore, the interplay between the window controller and the indoor temperature is essential. External climatic conditions, such as heat gain during warm periods and heat loss during colder periods affects how the window controller respond to indoor environmental functions. The heating and cooling set point thermostat values dictate when the cooling and heating systems start and stop operation. Properly determining these values is critical, as they significantly impact the energy demand and thermal comfort levels within the building. By fine-tuning the set point thermostats, we can strike a balance between maintaining comfortable indoor conditions and minimizing energy consumption. The selection of these parameters was driven by their profound influence on indoor environmental quality, energy demand, and thermal comfort. On the other hand, parameters optimized through objective functions for a building in one specific climate might not be directly transferable to other climates. The operational characteristics of a window controller designed for one climate would likely differ significantly when applied in a different climate. Given this crucial consideration, it became imperative to explore and understand the importance of studying different climates.

A special issue that should be considered in multi-objective optimization is the detection of optimal answers based on the importance of the objective functions. Most studies assume equal or constant magnitude for all objective functions during the optimization process [14]. Naderi et al. [15] conducted a multi-objective simulation-based optimization study, focusing on architectural specifications and control parameters for a smart shading blind. The research aimed to simultaneously minimize three objective functions: annual total building energy consumption, predicted percentage of dissatisfied (PPD), and discomfort glare index (DGI). Nateghi et al. [16] introduced a holistic approach to multi-criteria optimization, addressing the energy demands of a multi-story hotel building, resulting in both economic and environmental benefits. The optimization process involves considering three objectives: heating, cooling, and electrical equipment energy consumption with equal weight allocated to each factor. While in some cases, there is a priority, and some functions are placed in low-importance groups or even ignored. Energy demand is one of the functions that can be a priority when countries' governments are involved with providing energy in winter or even hot summers. The other objective function that could pose high importance is CO_2 concentration. The high concentration of bioeffluent in populated and closed spaces leads to poor indoor air quality, specified by CO_2 concentration [17]. Also, in some period, there might be an outbreak of airborne infection diseases. In such situation, controlling virus transmission and it is prioritized over thermal comfort conditions. The strategy of controllers for the opening window is another point that should be noticed and carefully chosen. Window controllers can open or close the window based on different parameters. Schedule, indoor temperature, outdoor temperature, and CO_2 concentration are the most common parameters for the window controller [18]. Determining and designing a general, useable, and understandable controller strategy makes it more feasible for industries to construct proposed automatic windows in the future.

This study investigated the objective functions of indoor air quality, thermal comfort, and energy demand by performing a multi-objective optimization for a classroom with 30 students. Window area, thermostat set point temperatures, and also minimum and maximum indoor temperature that the controller let the window open were considered as optimization parameters in this study. Optimization was accomplished in two different climates, continental and tropical, to make the application of this study more general. In addition, the comparison of the behaviour of the optimization functions in different climates determines the influence of weather data in controlling desirable indoor environmental quality and energy demand. EnergyPlus for energy simulation and JEPlus + EA for the optimization process were employed in this study. In the JEPlus + EA environment, the "Non-dominated Sorting Genetic Algorithm" (NSGA-II) was used to optimize described parameters. The optimum and ultimate answers were selected among Pareto solutions using the weighted sum method based on the function's importance.

2. Methodology

This section presents an introduction to the software employed for conducting the building energy simulation, followed by the implementation of a dedicated numerical model for validation purposes, in conjunction with an experimental study utilizing the selected methodology. Additionally, a comprehensive exposition is provided on the multi-objective optimization method and decision theory, with a detailed elucidation of the NSGA algorithm and the weighted sum method.

2.1. Building energy simulation software

The simulation of building implementation under dynamic conditions was performed employing EnergyPlus 9.4 [19] and SketchUp simulation software. The SketchUp plugin was employed to design the geometry of the building and the thermal area. EnergyPlus building energy simulation program was used to design the thermophysical specifications of the classroom, lighting, natural ventilation, an idealized energy system with heating or cooling loads, and its zone thermostat. EnergyPlus employs the thermal balance model to estimate the thermal performance of the construction [20]. EnergyPlus features plenty of abilities, but it is impossible to execute any optimization by EnergyPlus, therefore, JEPlus + EA which is an online optimization engine was applied for optimization in this study. Java programming language provides this software. Also, JEPlus from EnergyPlus was employed to determine the design parameters (decision variables) and output (objective functions).

2.2. Multi-objective optimization

The controller settings, thermostat, and window opening area were optimized through a multi-objective optimization process using the JEPlus + EA program [21]. The Non-dominated Sorting Genetic Algorithm [22] (NSGA-II) method was chosen for optimization. The objective functions were selected to minimize the average CO_2 concentration, predicted percentage of dissatisfied (PPD), and total energy demand during a school year. Since multi-objective optimization problems involve optimizing multiple objective functions simultaneously, it is common for these objective functions to vary in opposite directions. As a result, improving one objective function may come at the cost of degrading another. This leads to a situation where there are multiple solutions that satisfy the optimization problem, and none of them are necessarily unique. In multi-objective optimization, the Pareto front refers to the set of non-dominated solutions, where no solution is better than another in all objective functions. The Pareto front provides the engineer with a range of solutions that achieve the best trade-off between conflicting objectives, allowing them to limit their focus to the most effective solutions [23,24]. Owing to the development of plenty of design parameter arrangements, an optimization algorithm is required to assess various conditions and introduce the responses. Non-dominated Sorting Genetic Algorithm (NSGA-II) is widely used in multi-objective optimization, which optimizes each objective without being overwhelmed by any other answers at the same time. Since in this algorithm, there is no limit for using various variables (continuous or discrete), NSGA-II was used in this study. In a file in ''rvx'' format, the outputs of Energy Plus were written as objective functions. Hence, in this research, in addition to the different control strategies executed on the opening of the window, optimization related to the descriptive parameters has also been done. In this way, the proper control strategy for opening the window was selected and the window opening threshold, thermostat set points and the opening area were adjusted to the most optimal mode according to the algorithm. The most appropriate approach to multi-criteria decision-making is the Weighted Sum Method (WSM). WSM calculates the multiplication of normalized objective functions by their weighting coefficients to transform a multi-objective vector minimization issue of objective functions into a numeric issue [25]. WSM is calculated by Ref. [26] Eq. (2):

$$f_{ws}(x) = \sum_{i=1}^{3} a_i \frac{f_i(x) - f_i(x)^{min}}{f_i(x)^{max} - f_i(x)^{min}} \tag{2a}$$

where $f_i(x)$ is the objective function including energy demand, CO_2 concentration and PPD. $f_i(x)^{max}$ and $f_i(x)^{min}$ represent the maximum and minimum of each objective functions and, a_i is also the objective function weighting coefficient that represents

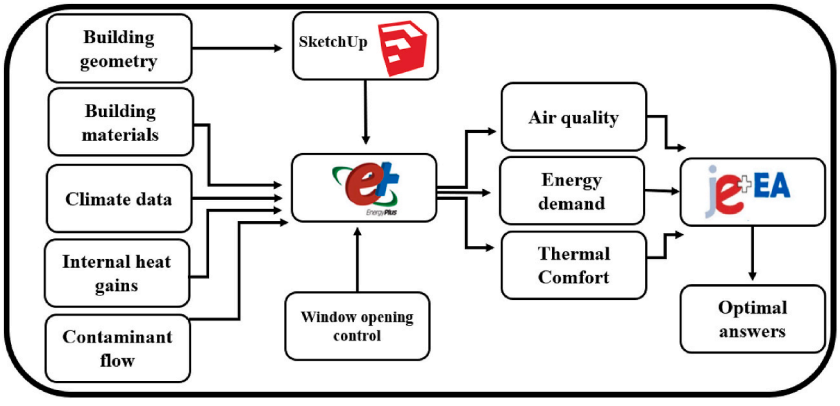

Fig. 1. Flow chart of the procedure used to find the optimal answers.

importance of each function. Fig. 1 indicates the flow chart of the procedure and simulation programs used for the assessment of multi objective optimization.

3. Modelling simulation

3.1. Numerical procedure and validation

A comparative analysis was conducted between a numerical model developed in EnergyPlus and experimental data obtained from a study by Lei, Zhangping et al. [27]. The aforementioned study investigated the impact of varying window opening areas on CO_2 concentration within a dormitory located in Beijing. Experimental measurements were carried out in a room occupied by six individuals. The findings revealed that when the window opening area was 0.011 m^2, the CO_2 concentrations remained relatively stable for a duration of 7 h. Conversely, with an increased opening area of 0.11 m^2, the CO_2 concentrations decreased to levels below 1000 ppm within a span of 3 h. In the numerical model, the stack with open area approach was implemented in EnergyPlus to accurately calculate the natural ventilation resulting from the window opening. The ventilation airflow rate was determined as a function of wind speed, thermal stack effect, and the size of the opening area. Equation (1) was employed to estimate the ventilation rate [19]:

$$Q = C_D A \sqrt{\frac{2gh\Delta T}{T_{in}}} \tag{1}$$

C_D, A and h represent discharge coefficient, opening area (m^2) and height of opening (m). Also ΔT is the temperature difference between indoor and outdoor environments.

Fig. 2 demonstrates the degree of concordance between our numerical investigation and the referenced study in terms of similarity. The findings indicate a noteworthy resemblance between the present study and the mentioned work, thereby validating the information obtained through this analysis, particularly regarding the examination of diverse window-opening areas. The minor deviations observed can be attributed to variations in building materials, weather data precision, time steps, and measurement errors. It is important to note that these disparities are negligible, and their presence is well within acceptable limits.

3.2. Building description

To assess the effectiveness of a multi-objective optimization process and the designed controller parameters were evaluated by implementing the selected method in a classroom with typical dimensions of 9 × 6 × 3.3 m, located on the top floor of a 3 stories school building. The classroom had east and west-facing windows and a double-layer, clear-glazing window with a U value of 1.1 W/(m^2•K) was used for the study. The beam and block floors were insulated with polystyrene insulation, with a heat transfer coefficient of U = 0.17 W/(m^2•K). The classroom was designed with three large windows, measuring 2.5 × 2.15 m which the window controller has the ability to open the window with any desired area from 0 to 16 m^2. The occupancy of classroom consisted of 30 individuals who followed a schedule with lessons lasting 45 min and breaks lasting 15 min. It was estimated that there were internal heat gains of 95 W per occupant, and artificial lighting was utilized when the natural illuminance levels dropped below 250 lux. The ventilation model considered airflow through leaks in the building based on wind speed and natural ventilation attained via window openings. The building modelled by EnergyPlus is shown in Fig. 3. While Warsaw and Bangkok have distinct climate zones, the classroom model possesses several features that make it versatile and well-suited for implementation in both locations. The use of high U-value for windows demonstrates a commitment to energy efficiency and thermal insulation. Such windows can effectively retain heat during cold winters, reducing energy consumption for heating. Similarly, in tropical climates, these windows can block excess heat from entering the classroom, thus reducing the reliance on cooling systems. Also, the large considered windows offer abundant natural light, fostering a positive learning environment for students in both cities.

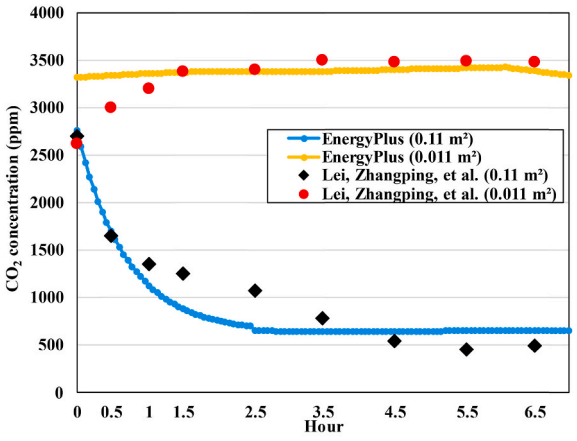

Fig. 2. Comparative Analysis of Data: Present numerical Study and Lei, Zhangping et al.

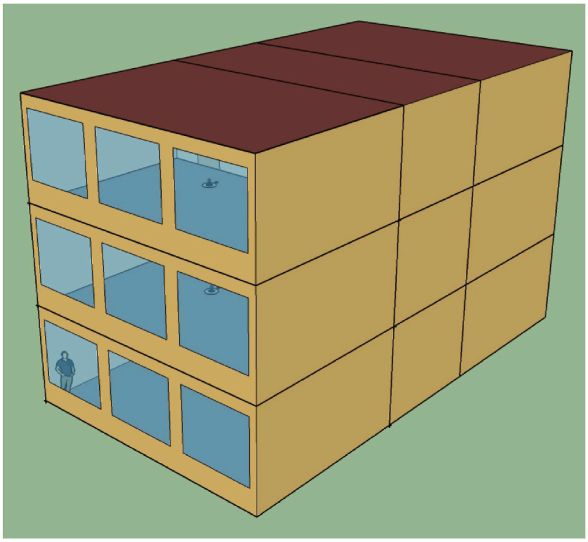

Fig. 3. The schematic diagram of the building model for the present study.

3.3. Climate & clothing level

Two cities with contrast climates were considered based on Köppen-Geiger climate categorization [28] in the study. Warsaw was selected as humid continental climate which represent cold weather along with heating load requirement during the year. Bangkok was selected as tropical climate which depute hot weather with cooling load requirement during the year. The choice of continental and tropical climates is justified by their global relevance, wide applicability, contrasting characteristics, and the practical implications of addressing climate-specific challenges. Continental climates experience significant temperature variations between seasons, necessitating tailored heating and cooling strategies. In contrast, tropical climates pose challenges related to controlling indoor humidity and managing intense solar heat gains. Characteristics of selected cities are given in Table 1.

The calculations were conducted throughout the school period spanning from September to June. Fig. 4 displays the monthly outdoor air temperature data for Warsaw and Bangkok. Based on the analysis of the data, it was observed that Bangkok city necessitates a cooling load throughout all the months considered, whereas Warsaw city requires a heating load during the same period. The relatively consistent average temperature during the months considered for Bangkok led to the adoption of a clothing insulation level of 0.5 for students based on standards [31]. Conversely, for Warsaw, a clothing insulation level of 1 was considered appropriate due to the heating load requirement, with a slight increase to 1.2 in December, January, and February.

3.4. Window opening control

Previous studies proved that window opening based on a fixed schedule time is unable to control indoor environment quality [13]. In the case where the window was open only during students' breaks, the indoor air quality was outside the standard range most of the time. Nateghi et al. investigated opening the window every 5 min, which significantly improved air quality but disturbed thermal comfort [32]. A Time-dependent controller, which only opens the window during break times, avoids increasing energy demand. However, it is expected to perform poorly regarding indoor air quality. Nevertheless, a time-dependent controller was used as the base case to compare with the optimal cases. The time-dependent controller includes two parameters: the maximum and minimum indoor temperature at which the window can be opened. Outside the set interval, the controller automatically closes the window. According to previous studies, this time-dependent controller is expected to improve indoor air quality, unlike time-based control. At the same time, a time-dependent controller increases energy demand significantly. The important thing about the time-dependent controller is the simplicity of changing the parameters set to open or close the window. Therefore, this study uses the second type of control to perform optimization to control all objective functions at the same time.

3.5. Objective process

Three optimization functions, consisting of the annual energy demand, average CO_2 concentration, and average PPD index of the classroom, were considered to simultaneously improve the classroom's energy performance and indoor environment quality. The

Table 1
Characteristics of the representative cities [29,30].

City	Latitude (°N)	Longitude (°E)	Climate	Elevation (m)
Warsaw	52.23 °N	21.01 °E	Humid continental	100
Bangkok	13.75 °N	100.5 °E	Tropical	1.5

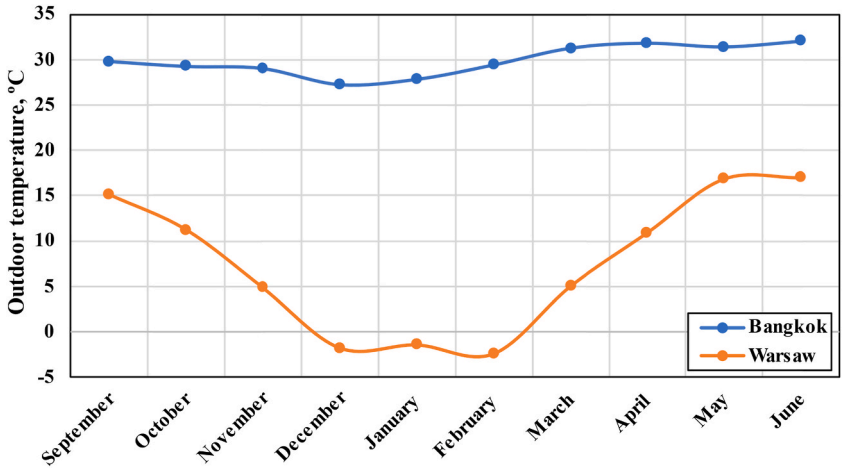

Fig. 4. Average monthly outdoor temperatures in Warsaw and Bangkok.

optimization issue includes five continuous parameters: the minimum and maximum indoor temperature that the controller lets the window be opened (P1&P2), the heating and cooling set point thermostat (P3&P4), and the window area (P5). Table 2 displays the applied decision parameters, their initial value and the range of their changes.

Based on the experience of earlier studies [33], the control parameters of the NSGA-II were chosen. Population size, maximum generation number, crossover rate and mutation rate were considered as 10, 200, 100% and 20% respectively with the initial analysis of convergence.

3.6. Selected cases

When the optimization was terminated and a Pareto optimal answer was acquired, the decision-making procedure should be executed to ascertain a final favoured answer. Engineering expertise, characteristics of the system, the objective functions' relative importance, and the optimal answers' sensitivity to the described parameters are some factors that could effect on making the decision for finding final optimum answers. In this way, design parameters can be chosen by engineers based on their primary needs and benefits. This study employed WSM to choose the final optimum answer from all Pareto solutions. Based on Eq. (2), importance of three objectives were determined. a_1, a_2 and a_3 represents energy demand, CO_2 concentration and PPD respectively. According to the purpose of the study and the significance of each objective function, three optimal cases with different weights for the objective functions were designed. The first and second cases, which were introduced as the basic cases, differed only in controlling the window's opening. The first case was designed based on the time-dependent controller of the window and considered opening only in break times classroom. The second case was designed based on the initial values of the minimum and maximum indoor temperatures for keeping the window open. For both base cases 1 and 2, the initial values were used for the window opening area and control of the thermostat (Table 2). As the first optimal case, the third case considered all the objective functions with the same weight ($1/3$). The fourth case was designed according to the high importance of energy demand. In this case, the coefficient of energy demand was 0.5, and the coefficient of the other two objective functions was considered 0.25. The fifth case, considering the coefficient of 0.5 for the average CO_2 concentration, was used for cases where indoor air quality, health issues, and residents' health were a priority. No remarkable improvement in thermal comfort was achieved in the case with the high importance of thermal comfort ($a_3 = 1/2$) in compared to case 3 ($a_3 = 1/3$). Therefore, the case with the high importance of thermal comfort was ignored. The selected cases were briefly described in Table 3.

$$a_1 + a_2 + a_3 = 1 \tag{2b}$$

4. Results

This part demonstrates the results of multi-criteria optimization based on the simulation of the selected objective functions for two

Table 2
Properties of the decision parameters.

Parameter	Object Controller	Description parameter	Unit	Range[a]	Base value
P1	Window	Minimum indoor temperature for keeping the window open	(°C)	(17–23)	21
P2	Window	Maximum indoor temperature for keeping the window open	(°C)	(23–28)	25
P3	Thermostat	Heating setpoint	(°C)	(17–23)	21
P4	Thermostat	Cooling setpoint	(°C)	(23–28)	25
P5	Window	Open area	m^2	[0,16)	1

[a] All defined ranges are Continues.

Table 3
Selected cases based on WSM coefficient.

	Case	Controller type	Coefficient a_1	Coefficient a_2	Coefficient a_3
Base cases	1	Time	–	–	–
	2	Indoor Temperature	–	–	–
Optimized cases	3	Indoor Temperature	$\frac{1}{3}$	$\frac{1}{3}$	$\frac{1}{3}$
	4	Indoor Temperature	$\frac{1}{2}$	$\frac{1}{4}$	$\frac{1}{4}$
	5	Indoor Temperature	$\frac{1}{4}$	$\frac{1}{2}$	$\frac{1}{4}$

climates (Warsaw and Bangkok). One issue that is possible in three-objective problems to find the system's characteristics and performance is to examine and compare pairs of objective functions. Therefore, to analyze the interactions of the objective functions, the criteria were selected in pairs from the three existing objective functions. The optimization procedure created information on the examined arrangements and selected a series of optimal answers, which were the Pareto front. Figs. 5 and 6 incorporate the multi-criteria optimization results of the NSGA-II in the shape of Pareto solutions, which distinctly disclose the interaction and opposition between pairs of objective functions. These responses are optimal points selected by the response discretization method. All pair objective functions have their optimal value and depend on the third function. The red points are the responses of the base cases (1 and 2), which are far from the other optimal answers. The blue, yellow, and green points are the selected answers for cases 3, 4, and 5, respectively. As it is evident in the graphs, the blue dots, which are the answer to case 3, were placed in the middle of the answers due to the equal importance of all the objective functions. Also, the yellow points indicate the desirable values for minimizing energy demand, while the green points represent the desirable values for reducing CO_2 concentration. It is generally observed that as one of the objectives decreases, the other objective increase. Therefore, it is not feasible to minimize all the objective functions simultaneously. Of course, due to the complexity of the functions and the correlation of each objective function, the Pareto diagrams were different for different climates and objective functions. In Warsaw, the answers selected by the software when showing the relationship of thermal comfort with CO_2 concentration and energy demand were almost placed on a vertical line. However, the Non-linear regression curve for the selected responses was almost similar to the other curves. Also, for Bangkok, the energy demand and thermal comfort functions did not act in conflict, and the logarithmic curve of the regression was ascending.

The definition of energy demand involves the sum of heating and cooling demand. However, in Bangkok, there is no heating demand throughout the year, while in Warsaw, heating demand significantly contributes to the total energy demand. Hence, the energy demand pattern follows a complex trajectory. Moreover, all decision parameters aimed at optimizing objective functions exhibit strong correlations. Specifically, P1 is reliant on the value of P3, while P2 is closely correlated to P4.

After max-min normalization, final optimum answers were determined based on the weighted coefficient of each case. Fig. 7 presents the optimum design parameters of selected cases in two cities with different climates. The following general results were obtained for each parameter. In comparison to the base cases (1&2).

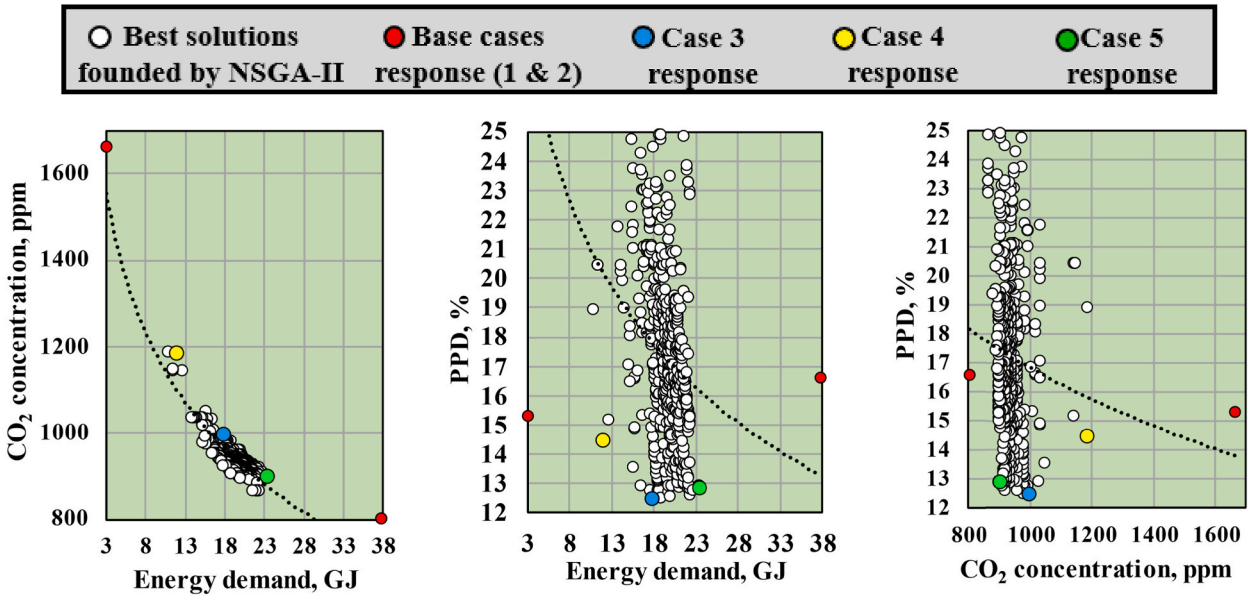

Fig. 5. Pareto front of the triple-objective optimization based on objective functions at Warsaw.

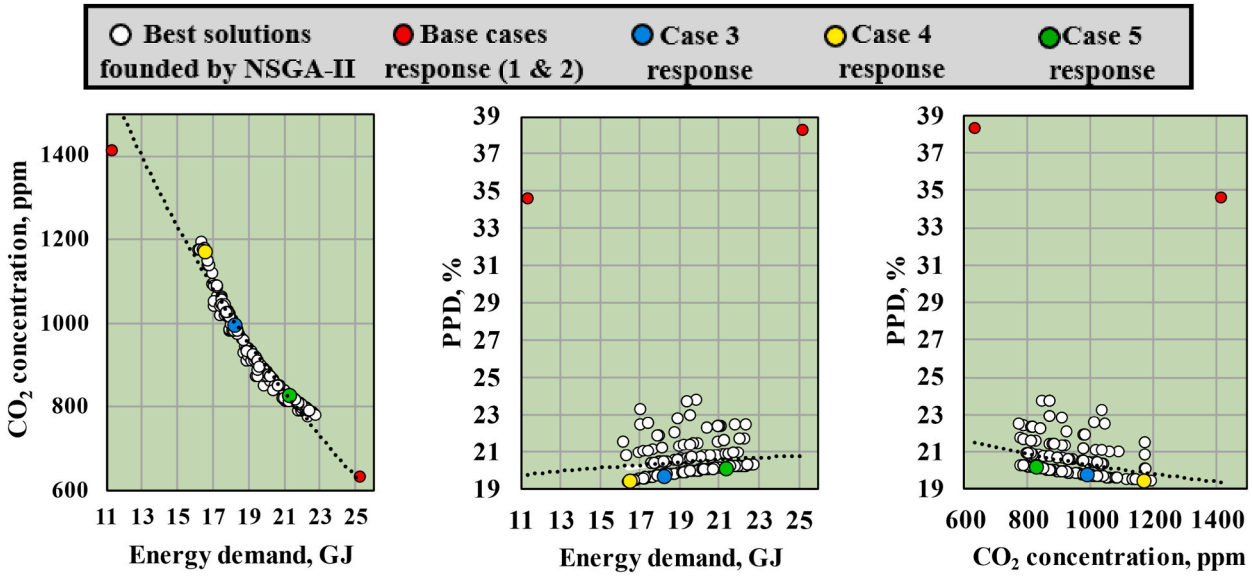

Fig. 6. Pareto front of the triple-objective optimization based on objective functions at Bangkok.

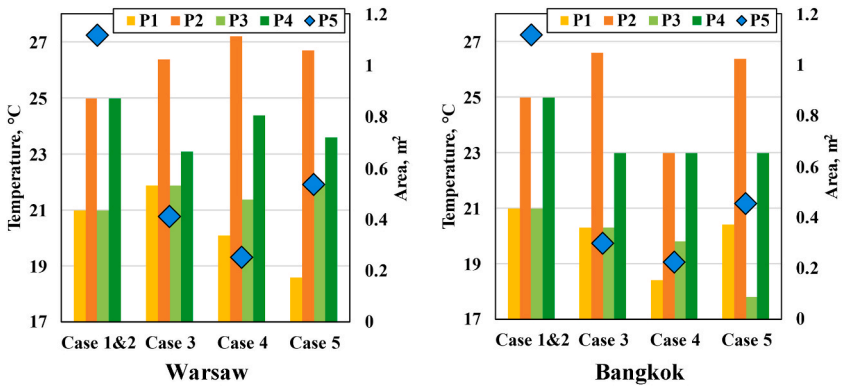

Fig. 7. Optimum design parameters of selected cases.

- P1: The minimum indoor temperature required for opening the window decreased in all optimum cases except for case 3 in Warsaw, which increased from 21 °C to 22 °C.
- P2: The maximum indoor temperature required for opening the window increased in all optimum cases except for case 4 in Bangkok, which decreased from 25 °C to 23 °C.
- P3: The heating setpoint thermostat for Warsaw increased, and for Bangkok decreased in all optimum cases.
- P4: Cooling setpoint thermostat decreased in all optimum cases in both cities.
- P5: The opening area of the window decreased in all optimum cases, especially in case 4, when energy demand was a priority.

The process of optimization and selection among millions of potential solutions has been performed. However, it is understood that there may be some exceptions that are acceptable and can be disregarded.

5. Discussion

In this section, the impact of decision parameters on the energy performance and indoor environment quality of classrooms was extensively analyzed for all selected cases across varying climatic conditions. A window controller based on indoor temperature was designed and optimized along with thermostat control to enhance natural ventilation in the classroom, with the ultimate aim of improving indoor air quality, thermal comfort, and reducing annual energy demand. In comparison to base cases where windows and energy systems were operated using initial values, the controlled window and thermostat optimized via the chosen objective functions demonstrated considerable enhancement in minimizing function values. The three subsequent sections discuss the results obtained for energy demand, air quality and thermal comfort.

5.1. Energy demand

The significance of energy demand arises from the combination of energy costs and the anticipated high energy consumption resulting from the operation of the temperature-based controller (case 2). This high energy demand can be attributed to prolonged window openings and fluctuating indoor temperatures. Unlike indoor environmental quality functions, energy demand lacks specific standards and classifications. However, the capacity of energy systems can be determined based on factors such as geographical area and climate. A previous study [34], considered a heating capacity of 6.5 kW for the designed classroom in Warsaw, which represents the dominant energy type required during school hours. In the case of the classroom in Bangkok, a cooling capacity of 8 kW was deemed necessary to meet the cooling demand. Fig. 8 presents the cumulative distribution of energy demand in classrooms located in Bangkok and Warsaw.

For both cities, Case 1 exhibited the highest energy efficiency in terms of energy demand, while Case 2 was the least efficient. In an attempt to minimize energy demand during student attendance, Case 3 aimed to optimize all objective functions with equal importance. However, even in this scenario, the energy demand exceeded the capacity of the cooling or heating systems for a significant portion of the time when students were present (30% in Warsaw and 8% in Bangkok). Conversely, Case 4, which prioritized energy demand, demonstrated the best performance among the optimized cases. Consequently, approximately 98% and 92% of the total time for the Warsaw and Bangkok cases, respectively, were able to meet the heating and cooling capacity requirements of the designated energy systems.

5.2. Air quality

The second objective function in multi-objective optimization, which is of great importance, was indoor air quality. CO_2 concentration was selected as indoor air quality index in this study. European standards have defined indoor environment categories, for air quality the categories are based on CO_2 concentration. There are several categories specific to children, the elderly, or people with respiratory difficulties, considering different amounts of CO_2 concentration higher than the CO_2 concentration of outdoor environments (400 ppm). The first category considers 550 ppm, the second, 800 ppm, and the third category allows 1350 ppm higher than the outdoor concentration. In this study, the second category which allows CO_2 concentration of 800 ppm higher than the outdoor concentration was given to the optimization software as a standard measure of indoor air quality. Higher value is not recommended for schools, and lower value may make it difficult for the controller to control other objective functions. Fig. 9 shows that Case 1 in both selected cities did not perform well in controlling indoor air quality. For Warsaw 34% and Bangkok 28% of the total time, the CO_2 concentration was in category 4, which is outside all defined categories (above 1750 ppm). The interesting point is that Case 2 performed best in both selected cities without optimization, and indoor air quality decreased after multi-objective optimization. More than 90% of the time, in both selected cities, the CO_2 concentration was in category 1, which is a desirable result. However, the results indicate that in case 2, excessive window opening disrupts thermal comfort conditions and leads to a drastic increase in energy demand during most hours. The optimized cases had less time in the first category. However, 87–98% of the total time was in the defined categories (I,II,III). Case 5, which gives more importance to indoor air quality than other objective functions, had the best performance among the optimized cases. For Warsaw, 6% and for Bangkok, only 3% of the total time, the CO_2 concentration was placed in the category IV.

5.3. Thermal comfort

Thermal comfort is the last objective function to be discussed. In this study, the PPD index, which predicts the percentage of dissatisfied people, was used as a criterion for calculating thermal comfort. Various categories have been determined for the PPD index based on the expectations and ages of occupants. Considering that the thermal comfort function is optimized along with two other important objective functions, the broadest category for thermal comfort was considered, based on which the PPD value should not be greater than 25. In this case, at least 75% of the people in the classroom have sufficient satisfaction in terms of thermal comfort. Fig. 10 indicated the cumulative dispersion of the PPD index when people were in the classroom in the two cities of Warsaw and Bangkok. As

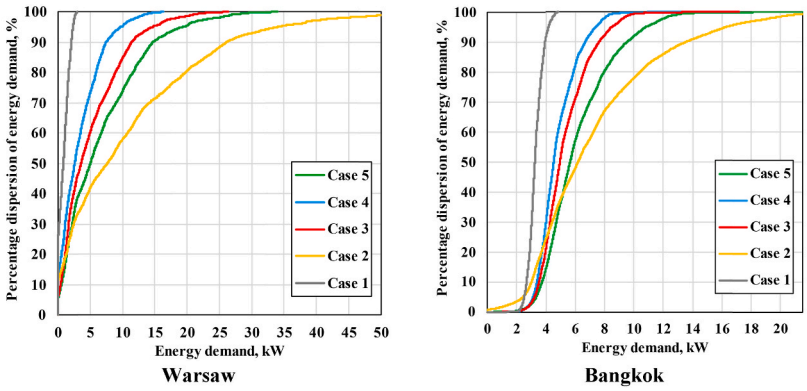

Fig. 8. Cumulative distribution of Energy demand frequency during the occupied classroom.

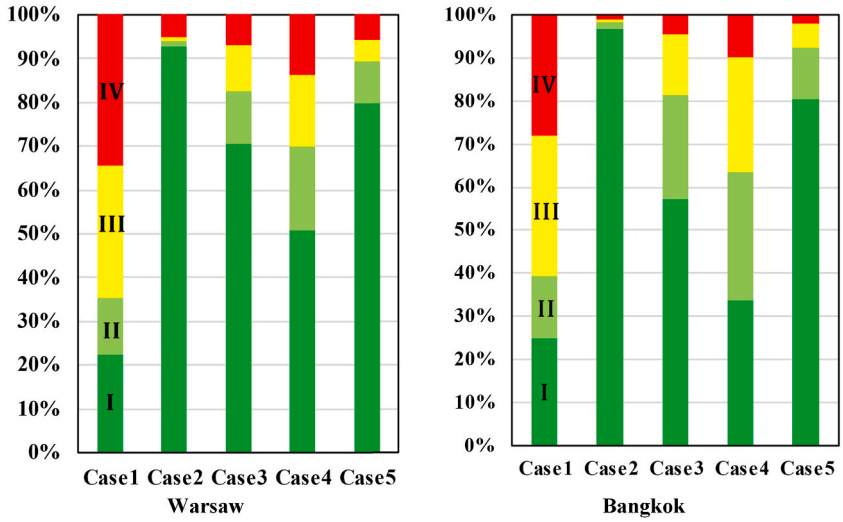

Fig. 9. Percentage bar of carbon dioxide concentration in different categories.

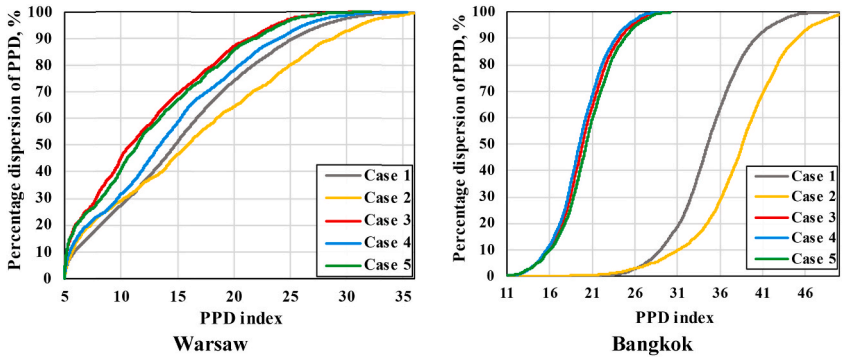

Fig. 10. Cumulative distribution of PPD index frequency during the occupied classroom.

expected, Case 1 did not perform well in both cities. However, the situation was more critical for Bangkok, where more than 90% of the time, the PPD index was higher than 25%. According to the weather conditions in the two considered cities, an index above 25% will be too cold for Warsaw and too hot for Bangkok.

Contrary to expectations, using the controller with initial assumed values (Case 2) not only did not improve the thermal comfort but also performed worse than Case 1 in Warsaw and Bangkok. After optimization, thermal comfort performance improved in all three cases considered for two climates. The performance improvement in Bangkok was more noticeable than in Warsaw. More than 90% of cases 3, 4, and 5 were in the thermal comfort range. For Warsaw, cases 3 and 5 performed almost the same and far better than case 4.

5.4. Summary

Acceptable values for all objective functions were determined based on selected standards and capacities. For indoor air quality, CO_2 concentration below 1200 ppm was targeted and PPD index of below 25% was considered for thermal comfort. In terms of energy demand, according to the difference in outdoor temperature in the two selected climates, 8 kW for Bangkok and 6.5 kW for Warsaw were allocated as the capacity of cooling and heating systems respectively. This study aimed to increase the hours so that all the functions are within the acceptable range. However, because the selected functions are entirely in conflict with each other, it was impossible to place them within the acceptable range throughout the year. Fig. 11 summarises the results obtained from this study for the cities of Warsaw and Bangkok.

The summary of results for Warsaw shows that in case 4, more than others, all the objective functions were within the acceptable range (53%). Despite the optimization efforts, in 40% of cases, one of the objective functions was still outside the acceptable range. Additionally, in 7% of the total time, at least two objective functions exceeded the standard range. Notably, in Case 4, which prioritized minimizing energy demand, this objective function was more often within the acceptable range compared to the two other optimized cases. Cases 3 and 5 had similar results, but Case 5 which prioritized minimizing CO_2 concentration, achieved standard air quality for a longer duration.

For Bangkok, Case 3 had the best operation with controlling all objective functions for 58% of the time. However, one objective

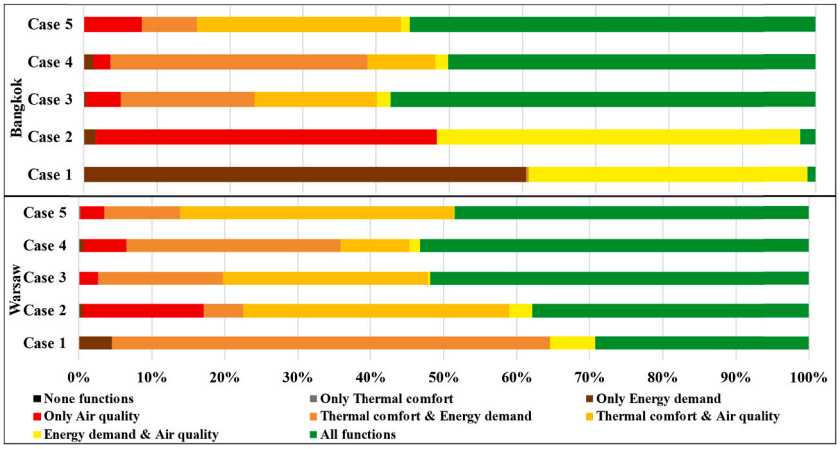

Fig. 11. Summary of result of objective functions: The percentage of hours that each function remains within an acceptable range based on standards.

function was out of standard range for 36% of the time. Also, at least two objective functions were uncontrollable in 6% of the time. Cases 4 and 5 performed similarly but had relatively successful objective function control. The base cases (1 and 2) had the least successful performance, with at least one objective function outside the acceptable range for over 95% of the total time. Thus, despite Case 2's excellent indoor air quality control performance, the optimization process improved the performance of the window controller and the thermostat in the simultaneous control of the objective functions.

5.5. Challenges and future directions

This study examined an identical classroom model with consistent attributes across two cities characterized by diverse climates. While the classroom model exhibits a range of qualities that lend it adaptability to both climate contexts, it's worth noting that the distinctive structural attributes of buildings in each country could present challenges in line with their respective economic and social circumstances. However, the incorporation of high U-value windows underscores a dedicated focus on energy efficiency and thermal insulation. These windows effectively trap warmth during colder seasons, thereby reducing energy consumption related to heating. Correspondingly, in tropical climates, these windows function to impede excessive heat ingress, consequently diminishing reliance on cooling systems. Moreover, the considerable size of the windows contributes abundant natural light, cultivating a positive learning atmosphere for students in any country. As a result, the outcomes obtained for Warsaw and Bangkok, which represent climates necessitating both heating and cooling throughout the year, have the potential to be extrapolated to varying global climates, provided there's meticulous consideration of climate-specific prerequisites. Also, numerous parameters and strategies were held constant or excluded in the simulation and optimization model due to simplification. To further enhance future studies, it is recommended to explore the significant impact of strategies like shading on energy demand and thermal comfort. Additionally, optimizing parameters such as building and window orientations, which were kept constant in this study, could yield valuable insights for improved building performance.

6. Conclusion

This study addresses the significance of enhancing indoor air quality within densely populated classroom environments, which are often plagued by elevated CO_2 emissions. Natural ventilation offers a promising remedy, yet it may not suffice to deliver the necessary airflow. Controlled window opening systems present a solution by activating windows as needed. However, this approach poses challenges in terms of energy demand and occupant thermal comfort, particularly in extreme climates. The exploration of multi-objective optimization for controlled windows and thermostat setpoints, centered around CO_2 concentration, thermal comfort, and energy demand, yielded several noteworthy conclusions.

- Adoption of a temperature-based window controller significantly improved indoor air quality while substantially escalating energy demand.
- The optimization process underscored the importance of scaling down the area of controlled windows in both Warsaw and Bangkok from the initial value.
- Optimization algorithm considered elevating the heating thermostat setpoint in Warsaw (22 °C) and lowering it in Bangkok (18 °C). Cooling thermostat setpoints were adjusted downward in both climates based on the optimization process (23 °C).
- Decreasing the minimum indoor temperatures (19 °C) and increasing maximum indoor temperatures (27 °C) required for opening windows resulted in improved performance of window controller.
- While optimized scenarios showed a minor decrease in indoor air quality compared to temperature-based control (Case 2), the trade-off was justified by substantial gains in thermal comfort and energy efficiency. This trend was consistent for both climates.
- Optimized solutions considerably improved thermal comfort in all cases for Bangkok, with modest enhancements observed in Warsaw.

- For energy efficiency prioritization (Case 4), optimized window controller and thermostat setpoints effectively met heating and cooling demands for 98% and 92% of the total time in Warsaw and Bangkok, respectively.
- Over 50% of total time in both climates exhibited all objective functions within acceptable limits after optimization.

In conclusion, the application of optimized window controllers and thermostat setpoints demonstrated commendable performance across the chosen climates, resulting in enhancements in indoor air quality, thermal comfort, and energy efficiency.

Declaration of competing interest

The authors declare that they have no known competing financial interests or personal relationships that could have appeared to influence the work reported in this paper.

Data availability

No data was used for the research described in the article.

References

[1] M.H. Forouzanfar, L. Alexander, H.R. Anderson, V.F. Bachman, S. Biryukov, M. Brauer, R. Burnett, D. Casey, M.M. Coates, A. Cohen, et al., Global, regional, and national comparative risk assessment of 79 behavioural, environmental and occupational, and metabolic risks or clusters of risks in 188 countries, 1990–2013: a systematic analysis for the global burden of disease study 2013, Lancet 386 (2015) 2287–2323, https://doi.org/10.1016/S0140-6736(15)00128-2.
[2] N.E. Klepeis, W.C. Nelson, W.R. Ott, J.P. Robinson, A.M. Tsang, P. Switzer, J.V. Behar, S.C. Hern, W.H. Engelmann, The national human activity pattern survey (nhaps): a resource for assessing exposure to environmental pollutants, J. Expo. Sci. Environ. Epidemiol. 11 (2001) 231–252, https://doi.org/10.1038/sj.jea.7500165.
[3] Direct human health risks of increased atmospheric carbon dioxide, Nature Sustainability Available online: https://www.nature.com/articles/s41893-019-0323-1#citeas. (Accessed 7 February 2023).
[4] K. Azuma, U. Yanagi, N. Kagi, H. Kim, M. Ogata, M. Hayashi, Environmental factors involved in SARS-CoV-2 transmission: effect and role of indoor environmental quality in the strategy for COVID-19 infection control, Environ. Health Prev. Med. 25 (2020) 66, https://doi.org/10.1186/s12199-020-00904-2.
[5] K.W. Tham, Indoor air quality and its effects on humans—a review of challenges and developments in the last 30 years, Energy Build. 130 (2016) 637–650, https://doi.org/10.1016/j.enbuild.2016.08.071.
[6] ASHRAE, ASHRAE Standard 62-2001, Ventilation for Acceptable Indoor Air Quality Atlanta, American Society of Heating, Refrigerating, and Air Conditioning Engineers, Inc., 2001.
[7] ASHRAE. ASHRAE, Standard 62-2001; Ventilation for Acceptable Indoor Air Quality Atlanta, American Society of Heating, Refrigerating, and Air Conditioning Engineers, Inc., Atlanta, Ga, USA, 2001.
[8] N.A. Megahed, E.M. Ghoneim, Indoor air quality: rethinking rules of building design strategies in post-pandemic architecture, Environ. Res. 193 (2021), 110471, https://doi.org/10.1016/j.envres.2020.110471.
[9] L. Morawska, J.W. Tang, W. Bahnfleth, P.M. Bluyssen, A. Boerstra, G. Buonanno, J. Cao, S. Dancer, A. Floto, F. Franchimon, et al., How can airborne transmission of COVID-19 indoors Be minimised? Environ. Int. 142 (2020), 105832 https://doi.org/10.1016/j.envint.2020.105832.
[10] E.M. Saber, I. Chaer, A. Gillich, B.G. Ekpeti, Review of intelligent control systems for natural ventilation as passive cooling strategy for UK buildings and similar climatic conditions, Energies 14 (2021) 4388, https://doi.org/10.3390/en14154388.
[11] G.M. Stavrakakis, P.L. Zervas, H. Sarimveis, N.C. Markatos, Optimization of window-openings design for thermal comfort in naturally ventilated buildings, Appl. Math. Model. 36 (2012) 193–211, https://doi.org/10.1016/j.apm.2011.05.052.
[12] R.M.S.F. Almeida, V.P. de Freitas, Indoor environmental quality of classrooms in southern European climate, Energy Build. 81 (2014) 127–140, https://doi.org/10.1016/j.enbuild.2014.06.020.
[13] K. Grygierek, S. Nateghi, J. Ferdyn-Grygierek, J. Kaczmarczyk, Controlling and limiting infection risk, thermal discomfort, and low indoor air quality in a classroom through natural ventilation controlled by smart windows, Energies 16 (2023) 592, https://doi.org/10.3390/en16020592.
[14] I. Costa-Carrapiço, R. Raslan, J.N. González, A systematic review of genetic algorithm-based multi-objective optimisation for building retrofitting strategies towards energy efficiency, Energy Build. 210 (2020), 109690, https://doi.org/10.1016/j.enbuild.2019.109690.
[15] E. Naderi, B. Sajadi, M.A. Behabadi, E. Naderi, Multi-objective simulation-based optimization of controlled blind specifications to reduce energy consumption, and thermal and visual discomfort: case studies in Iran, Build. Environ. 169 (2020), 106570, https://doi.org/10.1016/j.buildenv.2019.106570.
[16] S. Nateghi, A. Mansoori, M.A.E. Moghaddam, J. Kaczmarczyk, Multi-objective optimization of a multi-story hotel's energy demand and investing the money saved in energy supply with solar energy production, Energy Sustain. Dev. 72 (2023) 33–41, https://doi.org/10.1016/j.esd.2022.11.010.
[17] X. Lu, Z. Pang, Y. Fu, Z. O'Neill, The nexus of the indoor CO2 concentration and ventilation demands underlying CO2-based demand-controlled ventilation in commercial buildings: a critical review, Build. Environ. 218 (2022), 109116, https://doi.org/10.1016/j.buildenv.2022.109116.
[18] V. Fabi, R.V. Andersen, S.P. Corgnati, B.W. Olesen, A methodology for modelling energy-related human behaviour: application to window opening behaviour in residential buildings, Build. Simulat. 6 (2013) 415–427, https://doi.org/10.1007/s12273-013-0119-6.
[19] US department of energy engineering reference, in: EnergyPlus™; Version 9.4.0, Documentation vol. 2020, US Department of Energy, Washington, DC, USA, 2020, p. 1785.
[20] D.B. Crawley, L.K. Lawrie, F.C. Winkelmann, W.F. Buhl, Y.J. Huang, C.O. Pedersen, R.K. Strand, R.J. Liesen, D.E. Fisher, M.J. Witte, et al., EnergyPlus: creating a new-generation building energy simulation program, Energy Build. 33 (2001) 319–331, https://doi.org/10.1016/S0378-7788(00)00114-6.
[21] Yi Zhang, Use JEPlus as an efficient building design optimisation tool, in: CIBSE ASHRAE Technical Symposium vol. 18, Imperial College London, 2012.
[22] S. Chatterjee, K. Abhishek, S.S. Mahapatra, S. Datta, R.K. Yadav, NSGA-II approach of optimization to study the effects of drilling parameters in AISI-304 stainless steel, Procedia Eng. 97 (2014) 78–84, https://doi.org/10.1016/j.proeng.2014.12.227.
[23] E. Asadi, M.G. da Silva, C.H. Antunes, L. Dias, A multi-objective optimization model for building retrofit strategies using TRNSYS simulations, GenOpt and MATLAB, Build. Environ. 56 (2012) 370–378, https://doi.org/10.1016/j.buildenv.2012.04.005.
[24] Y. Zhai, Y. Wang, Y. Huang, X. Meng, A multi-objective optimization methodology for window design considering energy consumption, thermal environment and visual performance, Renew. Energy 134 (2019) 1190–1199, https://doi.org/10.1016/j.renene.2018.09.024.
[25] J. Ryu, S. Kim, H. Wan, Pareto front approximation with adaptive weighted sum method in multiobjective simulation optimization, in: Proceedings of the Proceedings of the 2009 Winter Simulation Conference (WSC), IEEE, Austin, TX, USA, December, 2009, pp. 623–633.
[26] M. Karmellos, A. Kiprakis, G. Mavrotas, A multi-objective approach for optimal prioritization of energy efficiency measures in buildings: model, software and case studies, Appl. Energy 139 (2015) 131–150, https://doi.org/10.1016/j.apenergy.2014.11.023.
[27] Z. Lei, C. Liu, L. Wang, N. Li, Effect of natural ventilation on indoor air quality and thermal comfort in dormitory during winter, Build. Environ. 125 (2017) 240–247, https://doi.org/10.1016/j.buildenv.2017.08.051.
[28] M.C. Peel, B.L. Finlayson, T.A. McMahon, Updated world map of the köppen-geiger climate classification, Hydrol. Earth Syst. Sci. 11 (2007) 1633–1644, https://doi.org/10.5194/hess-11-1633-2007.

[29] Climates classification by wincenty okołowicz - vivid maps, Available online: https://vividmaps.com/climates-classification-by-wincenty/. (Accessed 22 July 2023).
[30] S. Sinsakul, Late quaternary geology of the lower central plain, Thailand, J. Asian Earth Sci. 18 (2000) 415–426, https://doi.org/10.1016/S1367-9120(99)00075-9.
[31] EU Standard EN 16798-1, Energy performance of buildings—ventilation for buildings—Part 1: indoor environmental input parameters for design and assessment of energy performance of buildings addressing indoor air quality, in: Thermal Environment, Lighting and Acoustics—Module M1-6, European Committee for Standardization, Brussels, Belgium, 2019, 2019.
[32] Seyed Keivan Nateghi, Kaczmarczyk Jan, Control of virus infection, thermal comfort and energy demand in a school classroom with natural ventilation, in: International Conference Green Energy and Environmental Technology, vol. 27, 2022, p. 29 (July, Rome, Italy).
[33] Y. Yusoff, M.S. Ngadiman, A.M. Zain, Overview of NSGA-II for optimizing machining process parameters, Procedia Eng. 15 (2011) 3978–3983, https://doi.org/10.1016/j.proeng.2011.08.745.
[34] C. van Dronkelaar, D. Cóstola, R.A. Mangkuto, J.L.M. Hensen, Heating and cooling energy demand in underground buildings: potential for saving in various climates and functions, Energy Build. 71 (2014) 129–136, https://doi.org/10.1016/j.enbuild.2013.12.004.

Building and Environment 267 (2025) 112295

Contents lists available at ScienceDirect

Building and Environment

journal homepage: www.elsevier.com/locate/buildenv

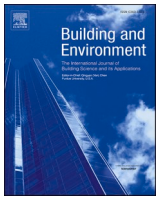

Optimal control strategy for a cutting-edge hybrid ventilation system in classrooms: Comparative analysis based on air pollution levels across cities

Seyedkeivan Nateghi [a,b,*], Amirmohammad Behzadi [b], Jan Kaczmarczyk [a], Pawel Wargocki [c], Sasan Sadrizadeh [b,d]

[a] Department of Heating, Ventilation and Dust Removal Technology, Faculty of Energy and Environmental Engineering, Silesian University of Technology, Gliwice, Poland
[b] Department of Civil and Architectural Engineering, KTH Royal Institute of Technology, Stockholm, Sweden
[c] Department of Environmental and Resource Engineering, Technical University of Denmark, Copenhagen, Denmark
[d] School of Business, Society, and Engineering, Mälardalen University, Västerås, Sweden

ARTICLE INFO

Keywords:
Smart controllers
Hybrid ventilation
Air quality
EnergyPlus
Multi-objective optimization
Window opening

ABSTRACT

Natural ventilation has the potential to enhance indoor air quality in classrooms with elevated CO_2 levels, although it may introduce outdoor pollutants. This study introduces a novel controller for automatic windows that simultaneously monitors outdoor air pollution and temperature, synchronizing window openings with mechanical ventilation system to create a comfortable, healthy, and energy-efficient indoor environment. The practicality of the proposed controller is assessed for a classroom in Delhi, Warsaw, and Stockholm, each with contrasting climates and outdoor pollution levels, specifically PM2.5 and NO_2. The controller parameters are optimized for each city using a non-dominated sorting genetic algorithm (NSGA-II) to find the best trade-off between thermal comfort, CO_2 levels, and energy consumption. The results show that the controller successfully met the indoor air quality standards in all cities; however, its operation was significantly influenced by the climate and pollution levels. While natural ventilation was utilized for 44% and 31% of the year in Warsaw and Stockholm, respectively, it was used for only 11% of the year in Delhi, the most polluted city. The optimization process significantly reduced energy use across all cities while also successfully reducing indoor CO_2 concentrations. Although thermal comfort decreased slightly, it remained within acceptable thermal comfort conditions.

1. Introduction

Indoor air quality is of paramount importance, especially given the modern lifestyle that confines individuals indoors for extended periods, exposing them to potential health hazards [1,2]. Elevated CO_2 levels in enclosed spaces lead to various health issues, from headaches to fatigue, particularly in densely populated educational settings and classrooms [3,4]. The recent emergence of infectious diseases, exemplified by the COVID-19 pandemic, has emphasized the importance of addressing airborne transmission risks alongside existing challenges related to indoor air quality [5]. In recent years, there has been substantial progress in improving indoor air quality (IAQ), raising public awareness, and identifying key IAQ factors [6]. Thermal standards have been established based on occupants' expectations [7]. Ventilation is one of the strategies for enhancing IAQ and reducing viral concentrations [8]. While mechanical ventilation causes high energy demand, numerous studies have explored and developed automatic window systems to regulate window openings and control the air change rate in buildings [9].

Tan and Deng [10] proposed an optimized window control strategy for naturally ventilated residential buildings in warm climates, which enhances ventilation performance and occupant comfort. This strategy demonstrated significant improvements in maintaining indoor temperatures and reducing deviations from neutral operative temperatures by over 30% compared to traditional control methods. Grygierek et al. [11] developed a smart window controller aimed at improving indoor air quality and reducing infection risk in classrooms. Their study highlighted that while natural ventilation enhanced CO_2 reduction and thermal comfort, it was insufficient on its own to significantly lower infection risk, indicating that additional strategies are needed for comprehensive indoor environmental management [1]. Using extra fans during window openings could be beneficial to enhance the

* Corresponding author at: Department of Heating, Ventilation and Dust Removal Technology, Faculty of Energy and Environmental Engineering, Silesian University of Technology, Gliwice 44-100, Poland.
E-mail address: Seyedkeivan.Nateghi@polsl.pl (S. Nateghi).

https://doi.org/10.1016/j.buildenv.2024.112295
Received 31 May 2024; Received in revised form 4 October 2024; Accepted 7 November 2024
Available online 16 November 2024

effectiveness of natural ventilation. Prior research by Nateghi et al. [12] explored temperature-based window controllers in diverse climates for classrooms, optimizing indoor air quality, energy use, and thermal comfort. However, the challenge of outdoor pollution infiltrating buildings during window opening persists. In 2016, more than half the global population resided in urban regions [13,14], where air pollutants such as PM2.5 and NO_2 pose significant health risks [15–17]. By 2050, this urban population is expected to rise to 70% [18,19]. In 2019, numerous individuals were exposed to PM2.5 [20,21] and NO_2 [16] concentrations, surpassing the World Health Organization's Air Quality Guidelines, indicating widespread health hazards [22]. Most of Europe's urban population experienced PM2.5 and NO_2 levels exceeding the WHO's 2005 limit values [23,24]. These pollutants not only impact outdoor air quality but also pose a significant threat to indoor air quality [25]. The increasing daily air pollution in large cities underscores the importance of considering outdoor pollution in studies related to the indoor environment.

Considering outdoor pollution criteria in automatic window controllers further restricts the use of natural ventilation, making the implementation of mechanical ventilation more important. However, the building sector is a major contributor to primary energy consumption and greenhouse gas emissions, responsible for 39% and 36%, respectively [26]. This is largely due to the widespread use of mechanical ventilation, which is further strained by window openings. Improving energy efficiency is essential, and one effective strategy is the implementation of hybrid ventilation. This strategy integrates natural ventilation with mechanical systems, providing fresh air only when windows are closed. This method can reduce dependency on mechanical systems while ensuring indoor environmental quality [27]. Rabani, M., & Petersen, A. J [28] explored a hybrid ventilation control method for a mixed-mode office environment in Norway. This system combines natural ventilation with a balanced mechanical ventilation system managed by demand control ventilation (DCV). The study showed that hybrid ventilation method meets thermal comfort and CO_2 level standards while decreasing energy usage. Wang et al. [29] developed a framework that integrates hybrid systems to effectively reduce indoor PM2.5 concentrations while maintaining thermal comfort and minimizing additional energy use [1]. Their study demonstrated that this hybrid approach not only enhances indoor air quality but also offers significant health benefits at a low energy cost.

A hybrid ventilation system should be designed to address a series of critical factors, including indoor air quality, energy consumption, and thermal comfort. Balancing objectives related to indoor air quality and energy use requires careful parameter selection for opening windows to achieve the desired indoor environmental quality and energy efficiency [30]. The relationship between window opening, outdoor temperature, and outdoor pollution levels is particularly important. External climate factors, such as heat gain during warm periods, heat loss during cold periods, and outdoor pollution levels, affect how window openings interact with indoor environmental conditions. Furthermore, the setpoint values for heating and cooling thermostats play a crucial role in determining when the mechanical ventilation systems activate and deactivate. Setting these values accurately is essential due to their significant impact on the building's energy consumption and thermal comfort [31]. Therefore, optimizing parameters for window opening, ventilation, and thermostat settings is crucial to adapting strategies to local climate and pollution conditions, ensuring both energy efficiency and indoor air quality are effectively managed. However, optimized parameters for a building in one city might not be suitable for another city with different climate and pollution conditions. Moreover, the operational characteristics of a pollution-temperature-based controller could vary significantly when applied in a different city with unique environmental factors. Recognizing this, exploring and comprehending the significance of studying various cities with diverse climates and pollution levels became essential.

Despite significant advances in indoor air quality management, there remains a notable gap in addressing the simultaneous control of outdoor pollution infiltration within indoor environments while implementing natural ventilation. Existing research primarily focuses on enhancing indoor air quality through natural ventilation, such as window openings, to manage high CO_2 levels in dense spaces like classrooms or decrease energy consumption. However, this approach inadvertently exposes occupants to harmful outdoor pollutants, including NO_2 and PM2.5, compromising overall indoor air quality and health. There is a need for a novel controller that dynamically synchronizes window openings with mechanical ventilation, considering both outdoor pollution levels and temperature. Furthermore, optimization of this controller, which adapts to varying climate conditions and pollution levels, is essential. Controlling outdoor pollution without such an optimized system may disturb thermal comfort, increase indoor CO_2 levels, or lead to higher energy consumption. This underscores the importance of an integrated approach that can be applied across diverse global settings.

This study fills the existing gap by employing an air pollution-driven control strategy for a window controller that integrates a hybrid ventilation system for a classroom with 30 students. The research was conducted in three major cities—Delhi, Warsaw, and Stockholm—to enhance the study's generalizability. Comparing the performance of the proposed design in these diverse climates reveals the impact of weather data and outdoor pollution on controlling indoor environmental quality and energy demand. The window controller operates based on outdoor pollution criteria and outdoor temperature. The controller's thresholds for outdoor contaminants adhere to the standards of the selected countries, while outdoor temperature thresholds were determined through multi-objective optimization. Additionally, thermostat setpoint temperatures were used as key parameters for optimization. The objective functions aim to minimize average CO_2 concentration, pollutant penetration, predicted percentage of dissatisfaction (PPD), and total energy use. The window opening is synchronized with a ventilation system that utilizes a packaged terminal heat pump for hybrid ventilation. When mechanical ventilation is off and windows are open, a running exhaust fan ensures sufficient ventilation through natural means. Indoor air quality, energy demand, and thermal comfort were assessed and compared with base scenarios to showcase the efficiency and potential of the proposed design. EnergyPlus was employed for energy simulations, and JEPlus + EA was used to conduct the optimization process. The Non-dominated Sorting Genetic Algorithm (NSGA-II) was utilized to identify optimal solutions, which were then selected from the Pareto front using the weighted sum method, considering the relative importance of each objective.

2. Methods

2.1. Building energy simulation tools

In this research, the SketchUp plugin was used to create the building and thermal area geometry. The EnergyPlus software was then employed to define the classroom's thermophysical properties, including aspects like lighting, ventilation, and a template heat pump for heating and cooling loads [32]. EnergyPlus operates using a thermal balance model to predict the thermal performance of buildings [33]. For this study, a Unitary Packaged Terminal Heat Pump model was utilized to simulate the unitary heating and cooling system. Previous comparisons with other whole-building energy analysis tools for identical test cases have shown that EnergyPlus delivers reliable results in line with other simulation programs [34].

2.2. Contaminant modelling

To model the contaminant and predict the contaminant concentration, a transient well-mixed mass balance model was used as follows [32,35]:

$$V\frac{dC_f^t}{dt} = \sum_{i=1}^{N_{sink}} R_{f,i}C_f + \dot{m}\left(C_{f,z,i} - C_{f,z}^t\right) + \dot{m}\left(C_{f,\infty} - C_f^t\right) + \dot{m}\left(C_{f,sup} - C_f^t\right) + S_f\left(C_f^{t-\delta t}\right) \quad (1)$$

$V\frac{dC_f^t}{dt}$ is the term for generic contaminant storage in zone air (ppm.kg/s). $\sum_{i=1}^{N_{sink}} R_{f,i}C_f$ represents the summation of removal rates from sinks on both zone and interior surfaces (ppm.kg/s). $\dot{m}\left(C_{f,z,i} - C_{f,z}^t\right)$ denotes the generic transfer of contaminants resulting from interzone air mixing (ppm.kg/s). $\dot{m}\left(C_{f,\infty} - C_f^t\right)$ signifies the generic transfer of contaminants due to infiltration and ventilation of outdoor air (ppm.kg/s). $\dot{m}\left(C_{f,sup} - C_f^t\right)$ represents the generic contaminant transfer resulting from the system's supply (ppm.kg/s), and $S_f\left(C_f^{t-\delta t}\right)$ stands for the generic rate of contaminant generation or removal based on the generic contaminant level in zone air from the previous time step.

2.3. Energy management system (EMS)

The Energy Management System (EMS) within EnergyPlus is a powerful tool utilized in this study to implement diverse control strategies for operable windows and synchronize them with the ventilation system [36,37]. EMS is able to empower users to create customized high-level supervisory control routines, overriding specific aspects of the EnergyPlus modeling [38].

2.4. Multi objective optimization

Implementing multi-objective optimization is imperative for addressing conflicting goals related to energy use and indoor environmental quality [39]. For instance, achieving optimal air quality may come at the expense of increased energy consumption, highlighting the need for a balanced approach. In this study, the JEPlus + EA program which is an online optimization engine utilizes the Non-dominated Sorting Genetic Algorithm (NSGA-II) for optimization [40–43]. Java programming language provides this software. Also, JEPlus from EnergyPlus was employed to determine the design parameters (decision variables) and output (objective functions). In indoor environment optimization, the genetic algorithm approach addresses conflicting objectives. This robust technique efficiently balances competing factors such as energy use, indoor air quality, and thermal comfort. The genetic algorithm operates in response space, generating a Pareto frontier diagram to showcase optimal points [44,45]. The NSGA-II algorithm, applied due to its versatility with various variables, operates on EnergyPlus outputs in ''rvx'' format. The configuration parameters for the NSGA-II algorithm, including population size, maximum number of generations, crossover rate, and mutation rate, are carefully considered based on past researches and the specificities of the current study's physics [40,46,47]. In multi-objective optimizations, the algorithm offers a set of optimal choices on a curve that is not superior to each other. The curve is the Pareto front [48,49], addressing conflicting objective functions. The best points are determined through statistical methods, with the total weighted average method being a common choice in this study [50,51]. This method is calculated based on Eq. (2):

$$f_{ws}(x) = \sum_{i=1}^{n} a_i \frac{f_i(x) - f_i(x)^{min}}{f_i(x)^{max} - f_i(x)^{min}} \quad (2)$$

where $f_i(x)$ are the objective functions and $f_i(x)^{max}$ and $f_i(x)^{min}$ are the minimum and maximum of each objective function, respectively. a_i is also the weight coefficient.

3. Case study

3.1. Building model description

A classroom with dimensions of 9 × 6 × 3.3 meters on the top floor of a three-story school building was designed. A segment of the building, including two classrooms (with windows-oriented east and west) and part of the corridor, was modeled to analyze inter-zone heat and air flows, as depicted in Fig. 1(a). The classrooms featured double-layer, clear-glazing windows with a U value of 1.1 W/(m²•K). The floors, constructed with beam and block, were insulated using polystyrene, yielding a heat transfer coefficient of U = 0.17 W/(m²•K). Each classroom had three large windows measuring 2.5 × 2.15 meters, equipped with controllers capable of adjusting the window opening area. The classrooms were occupied by 30 individuals who adhered to a schedule of 45-minute lessons and 15-minute breaks. Calculations were performed for the school year from September to June, with the outdoor CO_2 level set at 400 ppm and individual CO_2 emission rates factored. Considering the seated students with low activity, they would produce 0.23772 l/min CO_2 gas per metabolic equivalent [52]. It was estimated that each occupant had a low level of activity, with an internal heat gain of 95 W. Due to Delhi's relatively stable average temperature during the study period, a clothing insulation level of 0.5 for students was chosen in accordance with standard guidelines [53]. Conversely, for Stockholm and Warsaw, a higher clothing insulation level of 1 was used to meet heating requirements, with a slight increase to 1.2 during the colder months of December, January, and February.

Artificial lighting was employed when natural light levels fell below 250 lux. The natural ventilation model accounted for airflow through leaks and window openings, influenced by wind speed. An exhaust fan providing 300 CFM (Cubic Feet Per Minute), enhances natural ventilation, was considered when mechanical ventilation is off, and windows are open. For mechanical ventilation, a packaged terminal heat pump (PTHP) is considered, comprising an outdoor air mixer, direct expansion (DX) cooling coil, DX heating coil, supply air fan, and a supplemental heating coil [34]. The PTHP is controlled by a thermostat located in the classroom and will be determined through multi-objective optimization for each city. Since the outdoor air mixer can introduce polluted air into the classroom, a filter with a 0.14 m3/s removal rate from sinks was incorporated into the heating, ventilation, and air-conditioning (HVAC) systems. This removal filter can operate as both mechanical and chemical filters to reduce PM2.5 and NO_2 concentrations, respectively [54,55]. The filter's efficiency starts at 90% and gradually decreases to 50% after six months. It has been scheduled to replace the filter after six months, as shown in Fig. 1(b). While the simulated building is crafted to accommodate diverse climatic conditions, the classroom design encompasses characteristics that enhance its versatility and suitability in both environments. The integration of windows with a high U-value underscores a commitment to promoting energy efficiency and enhancing thermal insulation. In colder regions, these windows effectively retain warmth during the winter months, thereby reducing reliance on heating systems. Conversely, in warmer areas, they serve to block excessive heat ingress, consequently diminishing the necessity for cooling mechanisms. Moreover, the expansive windows facilitate the ingress of natural light, fostering a welcoming and optimal educational setting for students in both regions.

3.2. Climate & pollution of selected cities

Three cities with distinct climates and different pollution levels were considered in the study. Delhi was selected as a subtropical climate [56] with the highest air pollution level among the selected cities. Delhi's outdoor air pollution makes it a compelling case study for investigating innovative indoor air control solutions, offering the potential to significantly improve the health and well-being of its millions of residents. As illustrated in Fig. 2, the prevailing hot weather on most days in Delhi

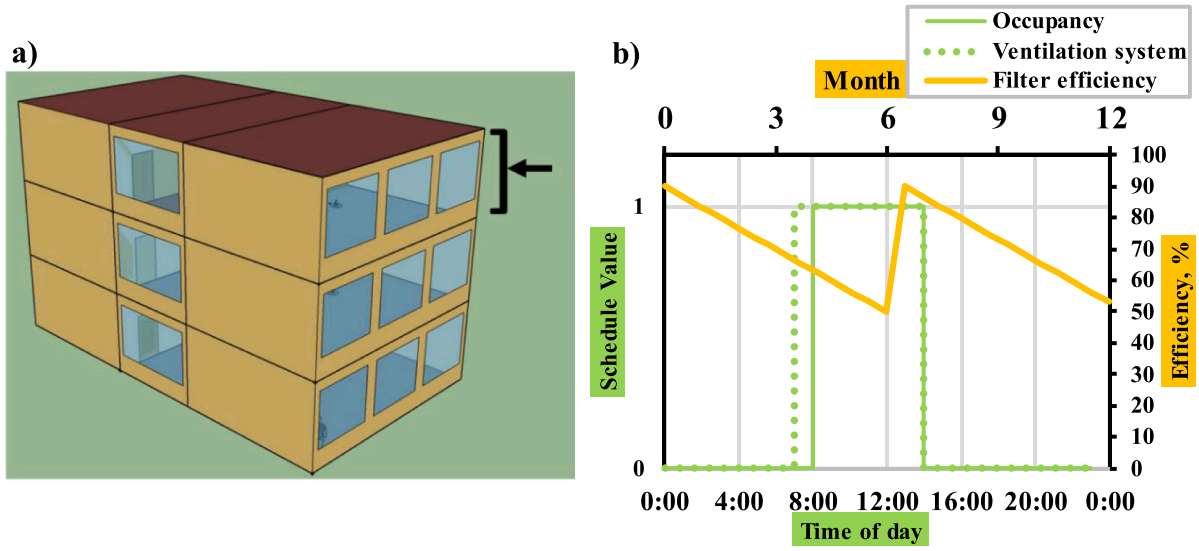

Fig. 1. (a) EnergyPlus geometric model and (b) schedule values defined for occupancy, ventilation system, and filter efficiency of the classroom.

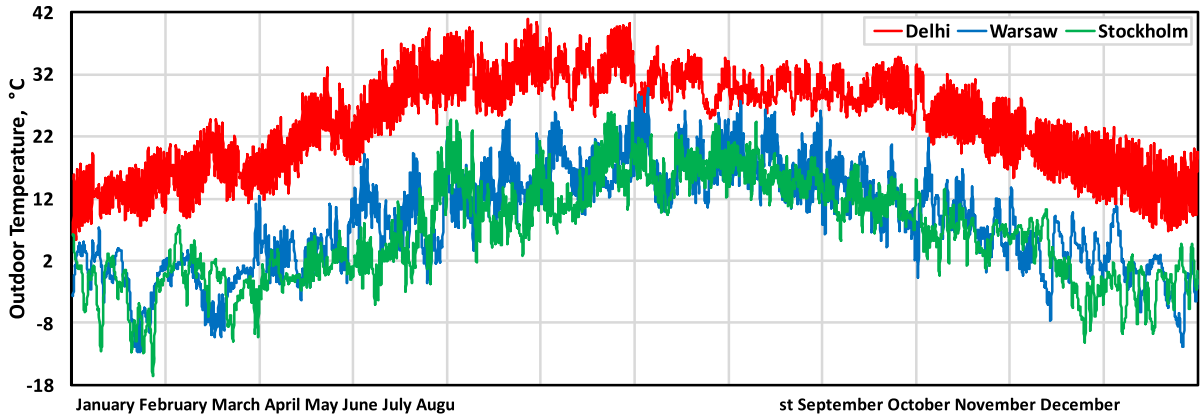

Fig. 2. Annual outdoor temperatures in Delhi, Warsaw, and Stockholm [57].

makes this city require a cooling load. Stockholm was selected because of its humid continental climate, which has the lowest level of air pollution among the selected cities. Opting for Stockholm, with low pollution levels, is pivotal in showcasing the broad applicability of our indoor pollution control strategy. Demonstrating indoor air pollution control effectiveness in a clean city like Stockholm, the aim is to underscore the universal utility of the approach, presenting it as a valuable solution applicable across diverse urban settings worldwide. The consistent cold climate experienced in Stockholm on most days necessitates a heating load in the city. Warsaw was selected because of its humid continental climate, the same as Stockholm, and providing a relevant case study for the authors. Positioned between Stockholm and Delhi in terms of pollution levels, Warsaw serves as an intermediary case, allowing us to assess the adaptability and effectiveness of our strategy in a city with moderate pollution. Like Stockholm, Warsaw's prevailing cold weather underscores the necessity for cooling load, aligning it with the climatic considerations of the study.

The selection of continental and subtropical climates is warranted by their worldwide significance, broad suitability, distinct features, and the pragmatic implications of tackling climate-specific issues despite variations in outdoor pollution levels. Continental climates undergo notable temperature fluctuations throughout the seasons, requiring tailored approaches for heating and cooling. In tropical climates, managing indoor humidity and coping with significant solar heat gain are major challenges. The representative cities and their respective climate characteristics, categorized according to the Köppen-Geiger climate classification system [56] are summarized in Table 1.

Standards define acceptable indoor pollutant levels. Different standards were applied for each city, given the varying concentration ranges of pollutants across selected cities. Efforts were made to select the pollutant acceptance levels according to the pollution levels of each city. As shown in Table 2, notably high pollution levels were adopted as the threshold for Delhi by considering the Central Pollution Control Board's national ambient air quality standards [60]. For Warsaw and Stockholm, the EU air quality standards [61] and WHO global air quality guidelines [62] were respectively selected. Although Warsaw and Stockholm are both European Union member states, two different standards were used in this study. According to the sensitivity analysis, this study considered standards specific to each city in order to achieve the best outputs in terms of air quality, energy consumption, thermal comfort, and the

Table 1
Characteristics of the representative cities [58,59].

City	Latitude (°N)	Longitude (°E)	Climate	Elevation (m)
Delhi	28.7 °N	77.10 °E	Hot Semi-Arid	293
Warsaw	52.23 °N	21.01 °E	Humid continental	100
Stockholm	59.33 °N	18.07 °E	Humid continental	28

Table 2
Permissible Pollution Thresholds.

City	Standard	PM2.5 (μg/m^3)	NO_2 (μg/m^3)
Delhi	Central Pollution Control Board (CPCB)	60	80
Warsaw	EU air quality standards	25	40
Stockholm	WHO global air quality guidelines	15	25

performance of the introduced controller method. In all cases, the standards chosen were based on daily average or 24-h mean concentrations.

The outdoor PM2.5 and NO_2 concentration was set to the temporal hour-average values monitored in Delhi [63], Warsaw [64] and Stockholm [65]. The red lines in Figs. 3 and 4 represent the defined threshold concentration of each city based on their selected standards. Given that the established standard values for PM2.5 are lower than those for NO_2 across all selected cities, instances of PM2.5 concentration reaching critical levels are more frequent. In Delhi, one of the most polluted cities, the standard threshold is 60 μg/m^3. From October to June, PM2.5 concentration tends to be notably high. Since the school year extends from September to the end of June, controlling PM2.5 levels becomes particularly challenging throughout the academic calendar. In Warsaw, where the standard threshold value is 40 μg/m^3, high PM2.5 concentration is observed in January, March, November, and December. Despite selecting the lowest PM2.5 standard value for Stockholm, only March, and to some extent April and September, necessitate protection from indoor penetration.

As for NO_2, standard values are 80 μg/m^3 for Delhi, 40 μg/m^3 for Warsaw, and 25 μg/m^3 for Stockholm. In Delhi, NO_2 concentration remains high from October to June, mirroring the pattern observed with PM2.5. Conversely, in Warsaw, elevated NO_2 levels are recorded mainly in January, March, April, November, and December. In Stockholm, March stands out as the critical month in terms of NO_2 concentration.

3.3. Window opening & hybrid ventilation control mode

In Fig. 5, outdoor pollution indicators (PM2.5 and NO_2) and outdoor temperature data serve as sensors, feeding information to the EMS for interpretation. The EMS, in turn, directs actuators to make real-time adjustments to building systems, forming a closed-loop system for dynamic optimization of energy usage and maintenance of optimal indoor environmental conditions. The EMS, through actuators, enforces control strategies based on three conditions, including two outdoor pollution thresholds aligned with selected countries' standard values and also, outdoor temperature thresholds determined through multi-objective optimization. The defined actuators, mechanical and natural ventilation, operate under distinct conditions to ensure the effectiveness of the hybrid ventilation system. Therefore, EMS prevents the simultaneous operation of natural and mechanical systems. Mechanical ventilation is switched off and natural ventilation is activated only when all three specified conditions are met. If any of these conditions are not fulfilled, mechanical ventilation will be activated, and natural ventilation will be deactivated. A running exhaust fan was considered in the model when mechanical ventilation is off, and windows are open to ensure sufficient ventilation through natural ventilation.

3.4. Optimization process

Three objective functions were employed to enhance the energy efficiency and indoor environmental quality of the classroom. The first objective (a_1) is annual average CO_2 concentration, the second one (a_2) is annual energy usage and the third one (a_3) is annual average Predicted Percentage of Dissatisfied (PPD) index. The optimization algorithm aims to minimize all three objective functions simultaneously. In this study, equal importance was assigned to each objective function ($a_1 = a_2 = a_3 = \frac{1}{3}$) when selecting the optimal solutions. The algorithm optimizes controller settings related to outdoor temperature thresholds and thermostat setpoint parameters to achieve the minimum values for the objective functions. The optimization task involved four continuous parameters: P1 and P2, which determined the minimum and maximum outdoor temperature thresholds for activating natural ventilation (window opening) and deactivating the ventilation system, respectively, through the EMS control strategy. The heating and cooling set point thermostat related to the ventilation system (P3&P4) are also defined as the third and fourth parameters. Table 3 shows the decision variables and their respective ranges.

Drawing from insights gleaned in prior research [40], the selection process for the NSGA-II control parameters was informed. Parameters such as crossover rate, maximum generation count, mutation rate, and population size were meticulously deliberated, resulting in 10, 200, 100%, and 20%, respectively. These choices were reached following an initial examination of convergence dynamics. Fig. 6 illustrates the flow chart of the simulation progress, energy management system, and multi-objective optimization.

4. Results and discussion

The results were initially acquired by multi-objective optimization conducted independently for three cities are presented, with the aim of enhancing the performance of the defined objective functions while controlling air pollution. The Pareto optimal solutions were identified, and the controller settings were optimized for each city based on its specific design parameters. First, the optimization outcomes and the selected Pareto optimal solutions are discussed. Next, the overall performance of the hybrid ventilation systems is examined. This is followed

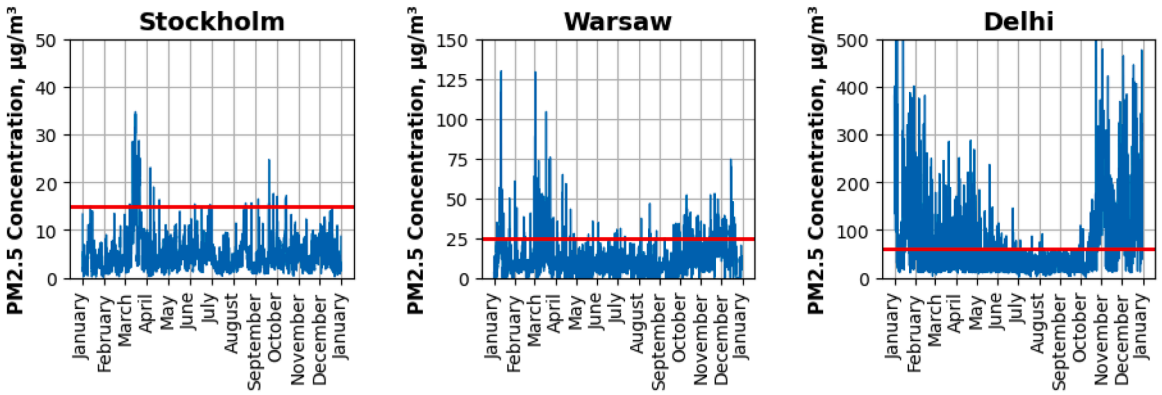

Fig. 3. Monitored annual hour-average outdoor PM2.5 concentration in Delhi, Warsaw, and Stockholm. Red lines represent standard thresholds.

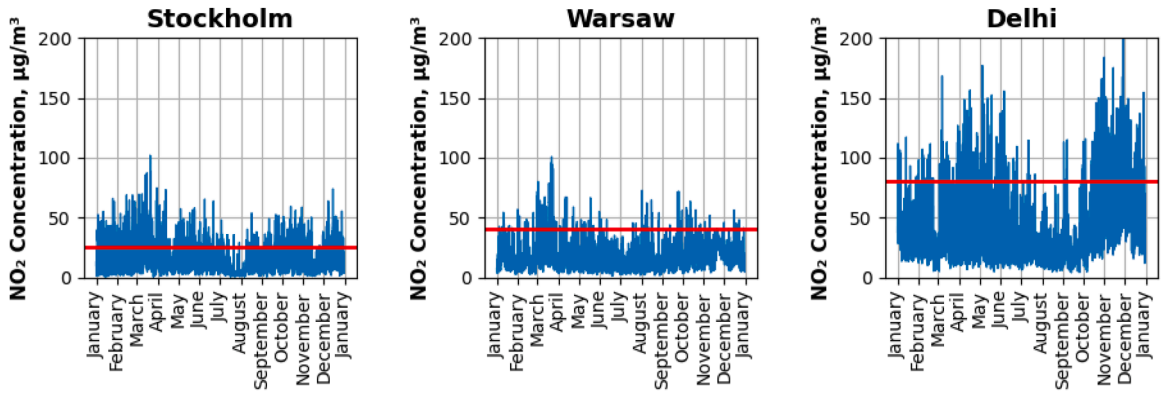

Fig. 4. Monitored annual hour-average outdoor NO_2 concentration in Delhi [60], Warsaw, and Stockholm. Red lines represent standard thresholds.

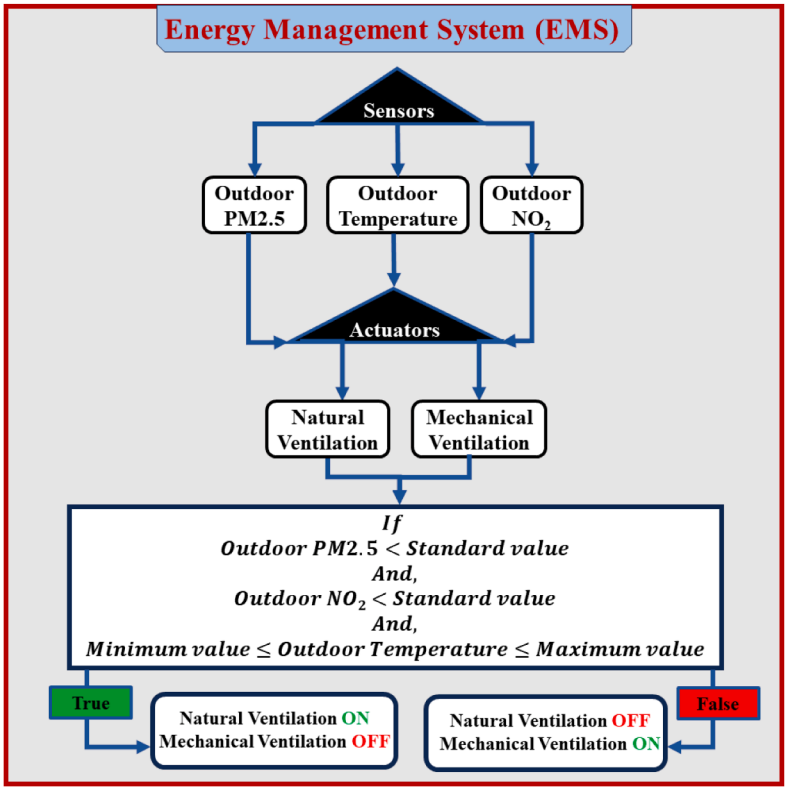

Fig. 5. Schematic of the developed energy management system.

Table 3
The domain of decision variables for the optimization.

Parameter	Object	Description parameter	Unit	Range
P1	EMS	Minimum outdoor temperature for keeping the window open	(°C)	(0–21)
P2	EMS	Maximum outdoor temperature for keeping the window open	(°C)	(21–35)
P3	Ventilation system	Heating setpoint	(°C)	(16–21)
P4	Ventilation system	Cooling setpoint	(°C)	(21–27)

by an analysis of the infiltration of PM2.5 and NO_2 into the indoor environment. The energy consumption associated with the optimized strategies is then evaluated, and the indoor CO_2 levels achieved with the optimized settings are assessed. Finally, the thermal comfort conditions maintained within the indoor spaces are reviewed.

4.1. Multi-objective optimization

The multi-objective optimization seeks to identify and explore the Pareto frontier curve, which illustrates a collection of optimal solutions. The secondary objective involves determining the most favorable compromise among three competing objectives, where attaining one goal may require sacrificing other metrics. Fig. 7 displays two-dimensional Pareto frontier diagrams illustrating the CO_2 concentration, PPD thermal comfort index, and energy consumption based on the NSGI-II algorithm for three distinct geographical locations: Delhi, Warsaw, and Stockholm. The x-axis represents the PPD thermal comfort index, the y-axis represents CO_2 concentration (in ppm), and the color bar represents energy consumption (in kWh). Each subfigure illustrates the optimal trade-off points, providing a comprehensive view of the

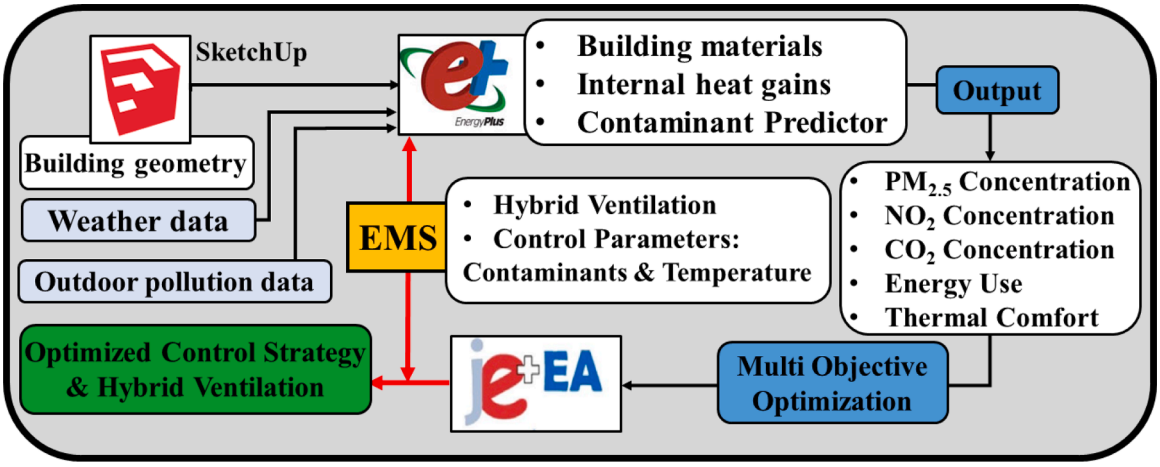

Fig. 6. Flowchart diagram of the applied method.

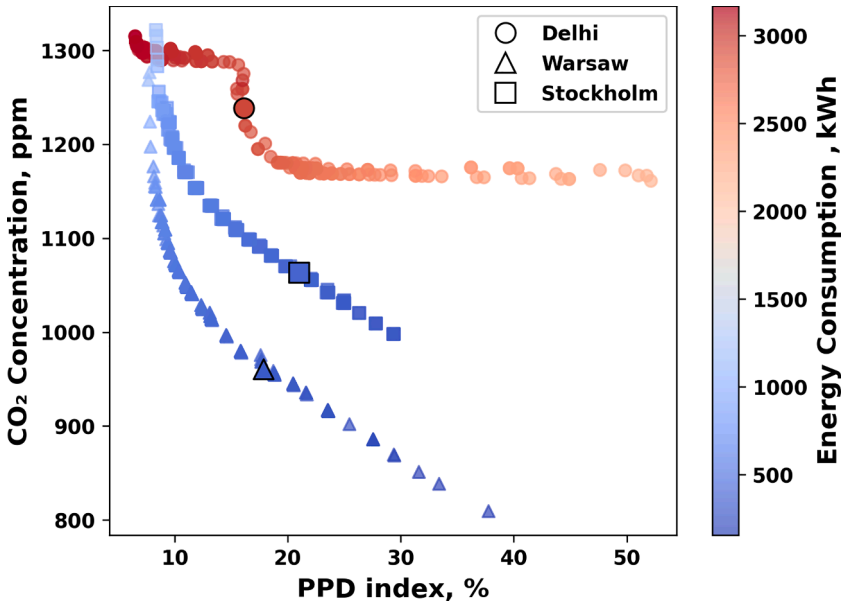

Fig. 7. The Pareto frontier diagram of CO_2 concentration, PPD index, and energy consumption in examined cities.

interactions among these three crucial factors. Simultaneous minimization of all objective functions proves unfeasible due to their complexity and interdependencies. The Pareto diagrams exhibit variations across various cities with different climates and pollution levels. The weighted sum method was utilized to prioritize a range of options according to their resemblance to an ideal solution, with elevated scores indicating superior performance. Bold symbols highlight the selected optimal answers obtained by the weighted sum approach. In all cities, energy consumption peaks when Predicted Percentage of Dissatisfied (PPD) values are at their lowest, indicating that maintaining optimal comfort levels in various climates demands significant energy expenditure. At the same time, this leads to higher CO_2 concentrations, highlighting the trade-off between energy use and indoor air quality. Delhi, known for its hot climate and high pollution levels, faces significant challenges in reconciling energy usage with CO_2 levels. The severe pollution limits opportunities for window opening, making it difficult to decrease CO_2 levels. As a result, Delhi often sacrifices reducing CO_2 levels to prioritize thermal comfort. Conversely, Warsaw, characterized by a colder climate and cleaner air than Delhi, effectively maintains low levels of both CO_2 concentration and energy consumption due to more opportunities for window opening. Stockholm, with its Pareto line between Delhi and Warsaw, still faces challenges in managing CO_2 levels due to its severely cold climate, which limits window opening. However, Stockholm performs better than Delhi because the clean air does not restrict window opening as much as in Delhi. Therefore, Stockholm maintains a more balanced approach despite its cold climate, though it still has more constraints than Warsaw.

Fig. 8 presents the parameter values for selected optimal solutions based on Eq. (2) for all cities. They are compared with the base case parameter values, representing the condition where only mechanical ventilation operates during the simulation without using the smart controller. Therefore, the base cases do not provide values for the minimum and maximum outdoor temperatures required to keep the smart window open (P1 & P2). In the base case, the heating and cooling set points (P3 & P4) were chosen from standard values defined according to resident expectations, based on the EU standard for energy performance in HVAC systems in buildings [66]. Each value was selected based on climate's city and energy load requirements. Initially, the same setpoints were considered for all three cities. However, the results for Delhi, including hybrid ventilation performance were not satisfactory. Consequently, a brief sensitivity analysis was conducted to optimize these values. Specifically, for Warsaw and Stockholm, the

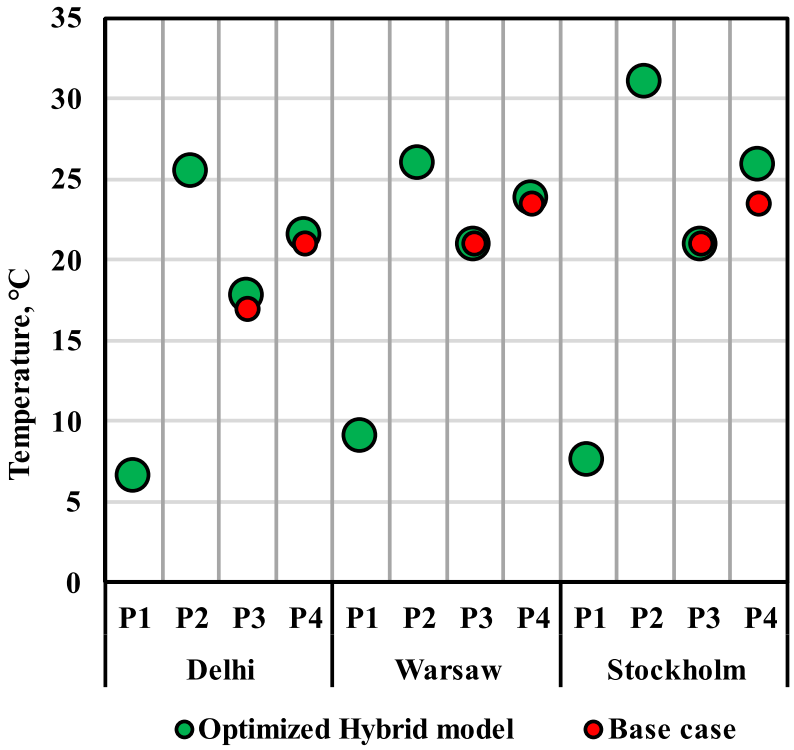

Fig. 8. Design parameters of the optimum model and base case. P1: Minimum outdoor temperature for keeping the window open, P2: Maximum outdoor temperature for keeping the window open, P3: Heating setpoint, P4: Cooling setpoint.

heating and cooling setpoints (P3 & P4) were set to 21°C and 23.5°C, respectively. For Delhi, a lower setpoint provided more favourable results. After conducting the sensitivity analysis within the allowable range, the setpoints were adjusted to 17°C for heating and 21°C for cooling, resulting in more favourable outcomes. After optimization, P3 and P4 did not change significantly. However, for Stockholm, the cooling set point was set to a higher value. Additionally, the maximum outdoor temperature for keeping the window open (P2) in Stockholm was higher than in the other two cities, at 31°C, while it was around 26°C for Warsaw and Delhi. The minimum outdoor temperature for keeping the window open (P1) was selected within the 7-9°C range for all cities.

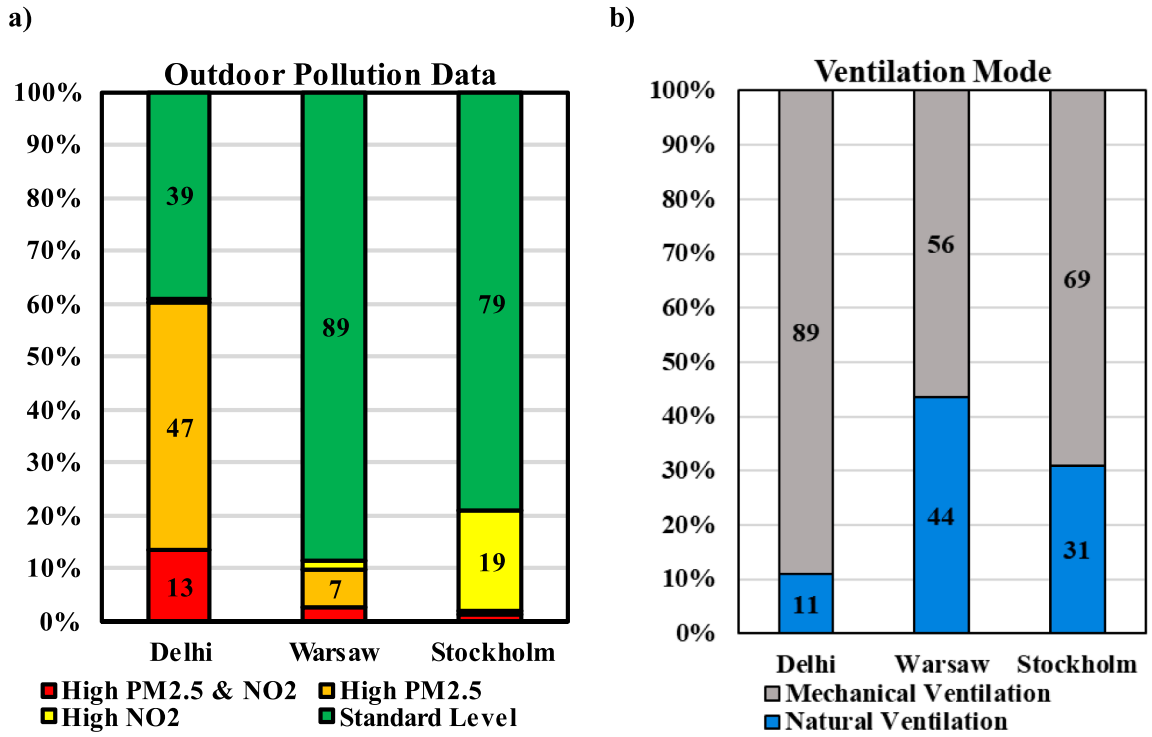

Fig. 9. The percentage bar of hour-average pollution data and ventilation mode in examined cities.

4.2. Hybrid ventilation performance

Following multi-objective optimization, the performance of optimized controller for the studied cities is analyzed in detail to see how the system works if properly designed. While each controller had different thresholds of PM2.5 and NO_2 concentrations for the respective city, the operation of the designed strategy also varied depending on the city's pollution data. Additionally, each controller had different thresholds for outdoor temperature based on the city's climate, as determined by optimization. As shown in Fig. 9 (a), in Delhi, only 39% of the year, the outdoor air quality meets the standard level. The figure also illustrates that the air quality met the standard in Warsaw and Stockholm for 89% and 79% of the year, respectively. Therefore, there was a strong limitation on window openings in Delhi compared to the other two cities. Even though Stockholm is cleaner than Warsaw, the standard in Warsaw is less strict, resulting in a higher percentage of the year meeting the air quality standards. Correlatively, Fig. 9 (b) shows that the controller allowed the windows to open for natural ventilation for only 11% of the year in Delhi. This value was 44% for Warsaw and 31% for Stockholm, signifying that the natural ventilation mode was highly correlated with outdoor pollution data. A closer look at the figure demonstrates that the annual duration for keeping the windows open in Warsaw is longer than in Stockholm, despite Warsaw being more polluted. In addition to wider pollution thresholds, another reason for the longer window-opening duration in Warsaw is the more frequent occurrence of outdoor temperatures within the allowable range set by the optimized controller. However, if identical thresholds were chosen for pollution and temperature, Stockholm would have the highest probability and Delhi the lowest probability of utilizing natural ventilation.

4.3. Pollution infiltration under optimized hybrid model

Fig. 10 presents the cumulative distribution of PM2.5 concentration across the selected cities under the optimal condition. In Delhi, where the standard indoor PM2.5 concentration is 60 μg/m³ (represented by the blue vertical line), approximately 99% of the year, classroom's air quality met the desired standards. Similarly, this trend was observed consistently throughout the year for classrooms in Warsaw and Stockholm with 25 μg/m³ and 15 μg/m³ standard indoor PM2.5 respectively. The figure further shows that during 63%, 10%, and 4% of the year, outdoor PM2.5 concentrations exceeded standard levels in Delhi, Warsaw, and Stockholm, respectively.

Fig. 11 compares the cumulative indoor and outdoor NO_2 concentration distribution for all cities. According to the figure, in Delhi, where the standard indoor NO_2 concentration is 80 μg/m³, the classroom consistently maintained the desired air quality throughout the year. Additionally, NO_2 concentrations remained below standard values for the year in all three cities, indicating full compliance with regulatory standards. Notably, outdoor NO_2 concentrations exceeded standard levels during 14%, 5%, and 20% of the year in Delhi, Warsaw, and Stockholm, respectively.

4.4. Analysis of optimized objective functions

This section describes the optimization process aimed at minimizing objective function values. Additionally, an extensive analysis of how decision parameters influenced the energy performance and indoor environmental quality of classrooms in the three selected cities is provided. Fig. 12 depicts the energy use of all cities under base cases and optimized models. To better compare the performance of the designed controller system and the optimization effectiveness, another case is also given (Optimized Non-Hybrid model) that is optimized but does not synchronize the introduced controller and mechanical ventilation system to implement the hybrid system. In the base case, which relies solely on a mechanical ventilation system, Delhi shows the highest energy consumption with an annual use of 3154 kWh. This is significantly higher compared to Warsaw (1113 kWh) and Stockholm (1040 kWh), reflecting the greater energy demands due to Delhi's climatic conditions. The optimized non-hybrid model slightly reduces energy consumption compared to the base case in Delhi. However, this model significantly increases energy use in Warsaw and Stockholm. This sharp increase is due to the windows being open during cold seasons while the mechanical ventilation system is operating simultaneously. This underscores the importance of implementing a hybrid control strategy to achieve

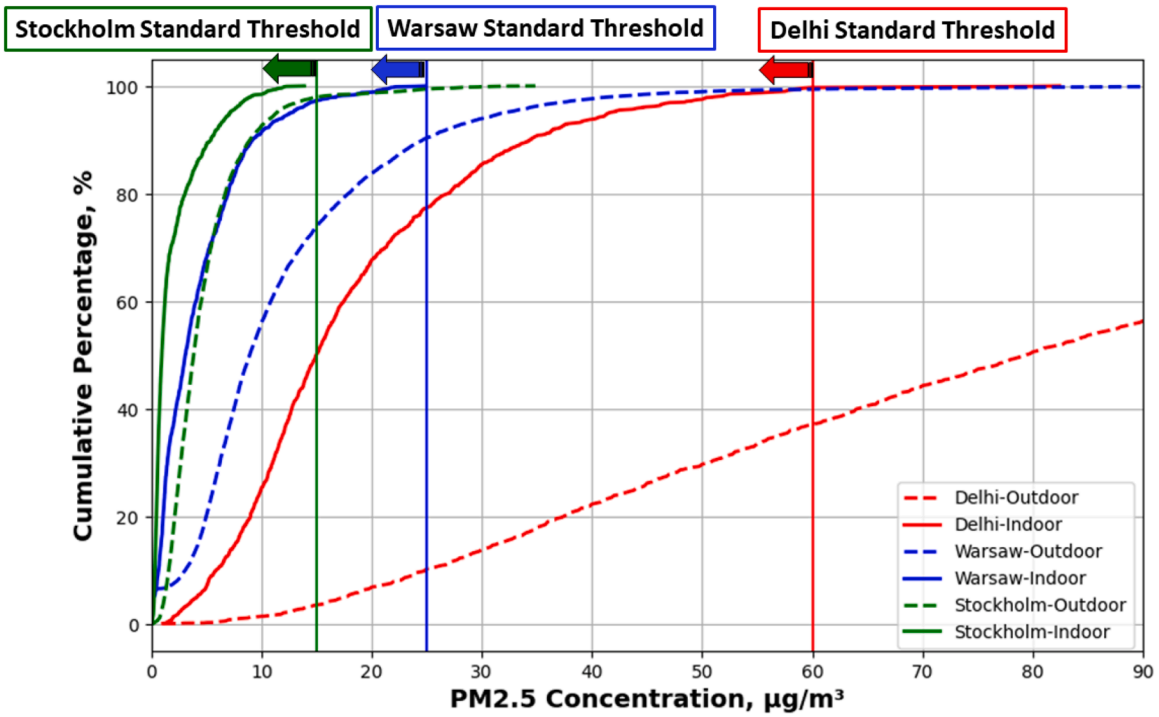

Fig. 10. Cumulative distribution of $PM_{2.5}$ concentration in examined cities.

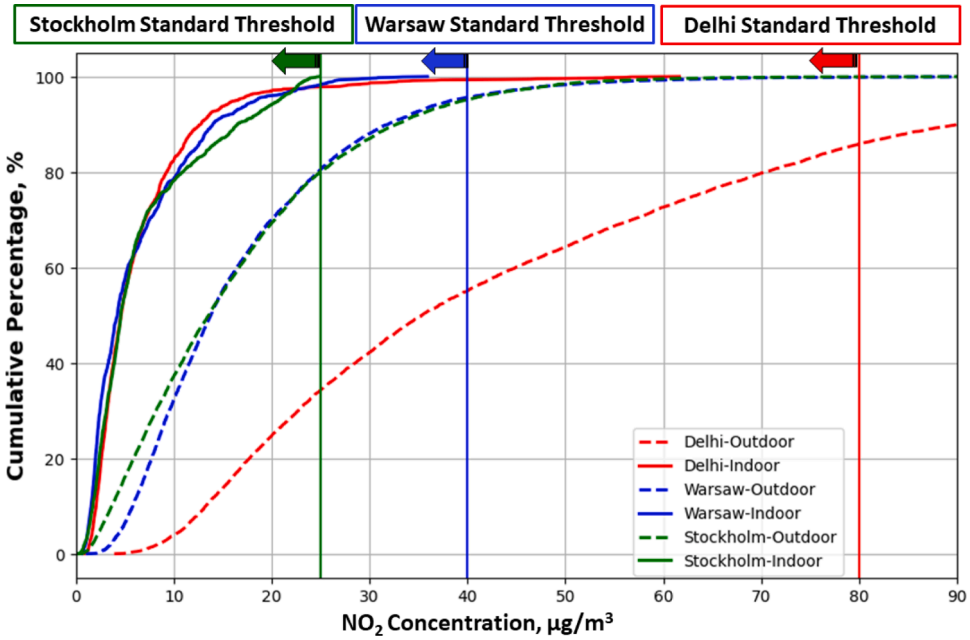

Fig. 11. Cumulative distribution of NO_2 concentration in examined cities.

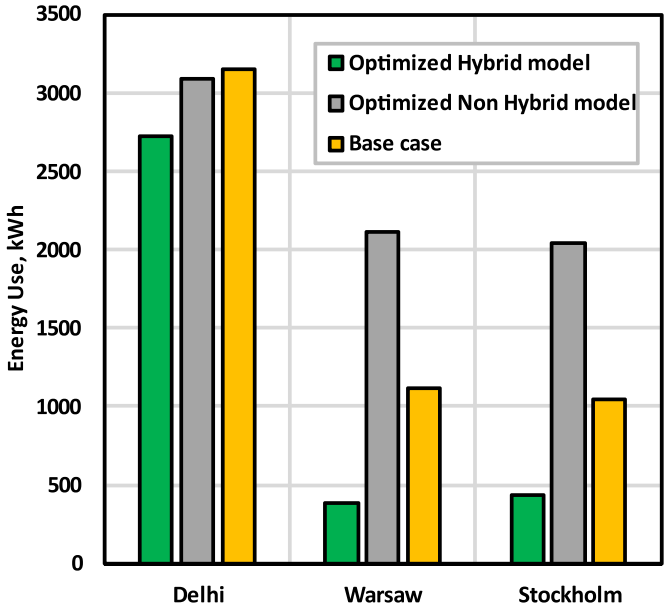

Fig. 12. Comparison of annual energy use in examined cities.

optimal energy savings while maintaining indoor environmental quality. The optimized hybrid model demonstrates the most effective energy-saving strategy. In Delhi, this model reduces energy consumption to 2722 kWh, indicating energy saving compared to both the base case and the optimized non-hybrid model. Similarly, in Warsaw and Stockholm, the optimized hybrid model achieves the lowest energy consumption, with values well below those of the other models. Specifically, Warsaw's energy use is approximately 381 kWh, and Stockholm's is around 438 kWh under the hybrid optimized model. These results highlight the effectiveness of the hybrid model in reducing energy consumption across different climatic conditions.

CO_2 concentration, a crucial indicator of indoor air quality, is the second objective function. The optimization process aimed to minimize the average CO_2 concentration to enhance indoor air quality. European standards delineate indoor environment classifications according to CO_2 concentration, accommodating various demographic groups such as elderly, children, or individuals with respiratory conditions. These classifications establish thresholds above the outdoor CO_2 concentration level of 400 ppm, with the initial category set at 550 ppm, the subsequent at 800 ppm, and the third permitting up to 1350 ppm higher than outdoor levels. Fig. 13 compares the cumulative distribution of CO_2 concentration during the occupied classrooms under the base case (only mechanical ventilation) and the designed optimal hybrid system in different cities. According to the figure, for all six cases, indoor air quality concerning CO_2 concentration remained within the widest Category (III) for the entire year. The base cases in all cities exhibited nearly identical performance. The indoor CO_2 concentration fell into category II for only 17% of the entire year, with the remainder categorized as category III. The optimal cases demonstrated improved performance in terms of indoor CO_2 concentration across all cities. Due to more favorable outdoor temperature and wider pollution thresholds, Warsaw experienced lower indoor CO_2 concentrations than the other two cities throughout the year. In Warsaw, 43% of the year, CO_2 concentration was within Category I, 12% in Category II, and 45% in Category III. Stockholm showed similar trends, with 30% in Category I, 14% in Category II, and 56% in Category III. Conversely, Delhi faces more stringent limitations, with only 8% in Category I, 14% in Category II, and 78% in Category III. These variations underscore the influence of local climate and pollution conditions on indoor air quality outcomes, emphasizing the importance of the hybrid ventilation strategies in different urban contexts.

Thermal comfort is the last but not least significant objective function that must be satisfied with minimal energy use and CO_2 concentration thanks to the multi-objective optimization. The Predicted Percentage Dissatisfied (PPD) index, predicting the percentage of dissatisfied individuals, served as the metric for assessing thermal comfort. The PPD index is categorized based on occupant expectations and age groups and should not exceed 25%, considering the widest category defined by European standards [66]. This threshold ensures that at least 75% of occupants experience satisfactory thermal comfort. For this, Fig. 14 illustrates the cumulative distribution of the PPD index. Considering the climatic conditions of the selected cities, a PPD index above 25% would signify conditions that are too cold for Warsaw and Stockholm and too warm for Delhi. According to the figure, the base cases achieved the desired results in all cities by keeping the PPD index

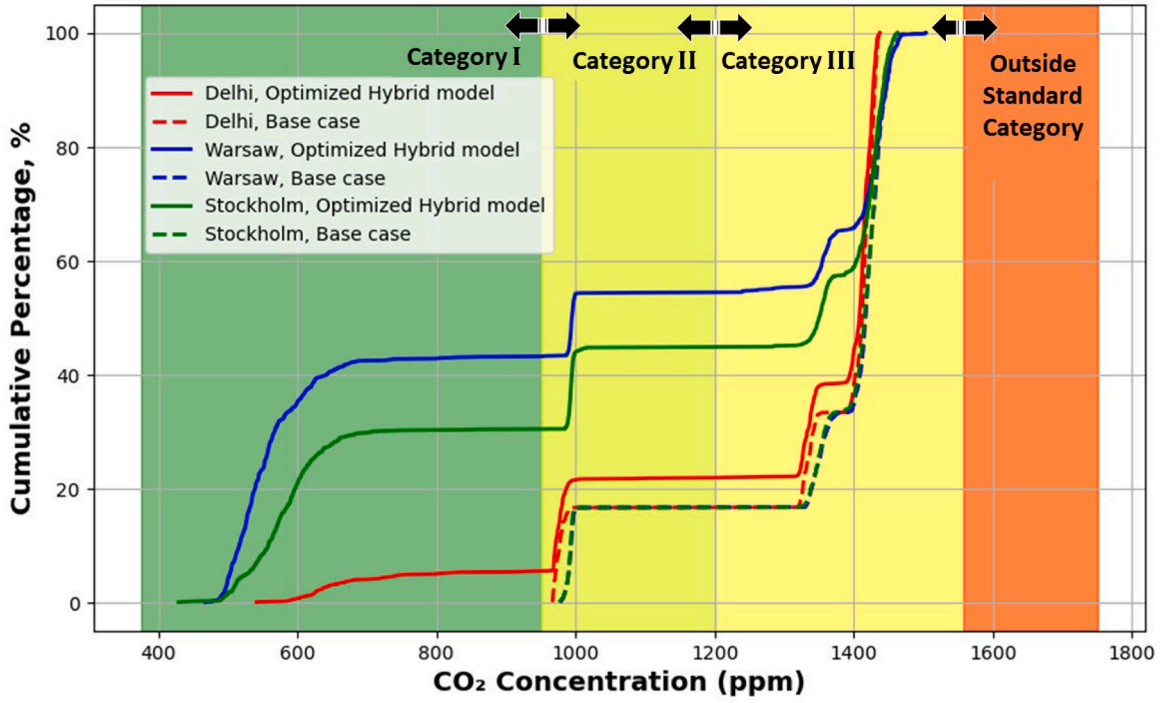

Fig. 13. Cumulative distribution of CO_2 concentration during the occupied classrooms in examined cities.

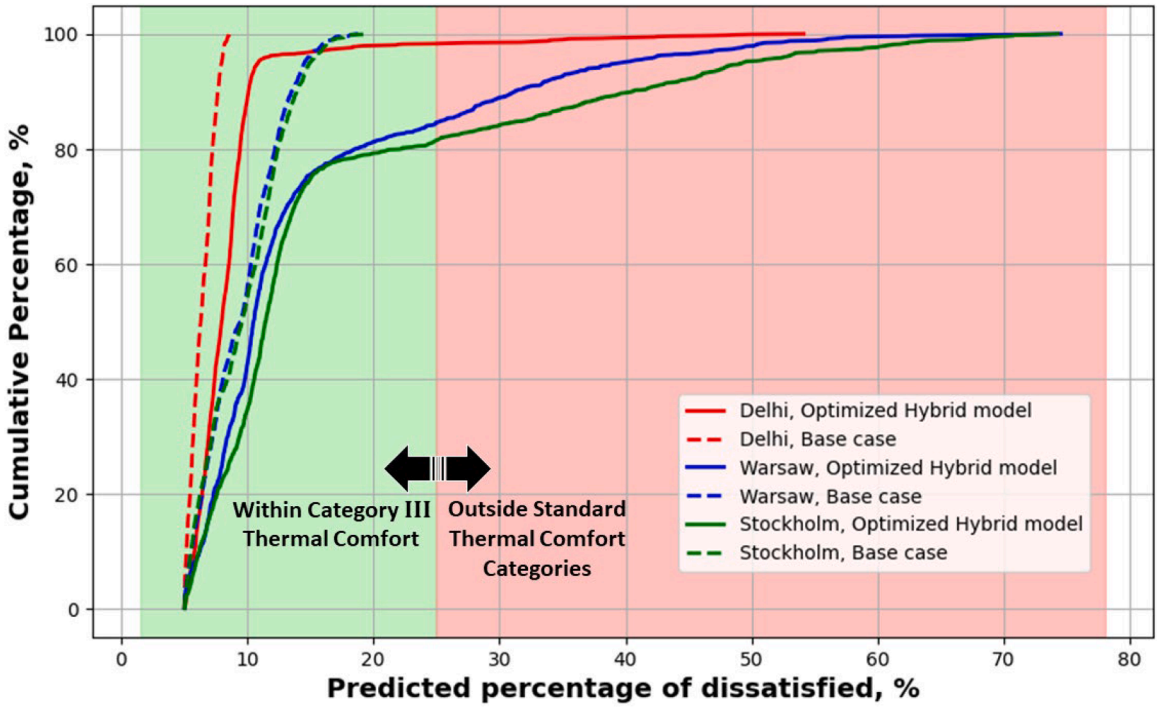

Fig. 14. Cumulative distribution of PPD index during the occupied classrooms in examined cities.

below 10% in Delhi and below 20% in Warsaw and Stockholm throughout the entire year. However, the base cases used more energy than the optimized hybrid models since mechanical ventilation was used frequently the whole year. Following optimization process to decrease energy use and CO_2 concentration, thermal comfort performance slightly declined in optimized hybrid models compared to the base cases across all cities. Warsaw's performance was closely similar to Stockholm's, with occupants reporting acceptable thermal comfort for over 80% of the year, likely due to the higher probability of open windows in these cities. Conversely, thermal comfort was acceptable for 99% of the year in the optimized case of Delhi, where windows were less frequently opened.

5. Challenges and future directions

- By incorporating the Adaptive model alongside the Fanger model, future studies can explore the impact of occupants' adaptive behaviors on thermal comfort perception, especially in educational settings. In that case, individuals have the flexibility to adjust their clothing or activities in response to indoor conditions.
- The current study is limited to specific climatic and pollution conditions in Delhi, Warsaw, and Stockholm. These locations were chosen to represent a range of climates and pollution levels. Future studies should consider a broader range of geographic locations, environmental conditions, and pollution levels to validate the system's universal effectiveness.
- The performance of the hybrid ventilation system is highly sensitive to the setpoints for PM2.5 and NO_2. Our sensitivity analysis revealed that stricter pollutant setpoints significantly reduce the usage of natural ventilation, which is a key component of the system's energy efficiency strategy. Ensuring outdoor air quality is crucial for maximizing the benefits of natural ventilation. Future works can explore adaptive setpoint strategies that can dynamically adjust based on real-time outdoor air quality and occupant requirements. This approach could effectively optimize the balance between energy consumption, thermal comfort, and indoor air quality.
- With global temperatures on the rise and the increasing frequency of extreme weather events, it is critical to evaluate how the system will perform under future climate scenarios. This includes not only temperature increases but also changes in pollution patterns and the frequency of extreme weather events. Simulation results under projected IPCC temperature increases for 2050 and 2100 suggest that higher temperatures may require further system optimization to maintain thermal comfort and indoor air quality. Adaptive strategies that can respond to these changes will be essential for maintaining system efficacy in future climates.

6. Conclusion

This study has successfully developed and optimized a novel hybrid ventilation system that effectively balances indoor air quality, thermal comfort, and energy consumption in classrooms across three cities with distinct climates and pollution levels. The multi-objective optimization process, employing the NSGA-II algorithm, identified Pareto optimal solutions that provided the best trade-offs among these objectives for each city. The main conclusions could be summarized below:

- The multi-objective optimization reveals that balancing objective functions including thermal comfort, CO_2 concentration, and energy consumption involves trade-offs that vary significantly across different climates. Maintaining low energy consumption and CO_2 levels proves challenging in hot, polluted environments like Delhi.
- Optimization of heating and cooling setpoints, along with the criteria for opening smart windows based on outdoor temperatures, can significantly impact the energy performance and indoor environmental quality of buildings in different climates. Delhi, with its hot climate and high pollution levels, benefits from lower heating and cooling setpoints and a lower outdoor temperature threshold for window opening to improve objective functions. In contrast, Warsaw and Stockholm, with their colder climates, can afford higher setpoints and a higher outdoor temperature threshold for window openings.
- The controller's operation in synchronizing mechanical and natural ventilation was significantly influenced by the specific climate and pollution levels of each city, with natural ventilation being utilized more frequently in Warsaw and Stockholm compared to Delhi. In Delhi, natural ventilation was utilized for 11% of the year, compared to 44% in Warsaw and 31% in Stockholm.
- The controller can effectively maintain indoor air quality standards for PM2.5 and NO_2 concentrations in all cities, despite the varying levels of outdoor pollution and climatic conditions.
- The optimized hybrid model significantly improves energy efficiency compared to the base case across all three cities. Specifically, in Delhi, the hybrid model reduces energy consumption by approximately 13 % from the base case. In Warsaw, energy use is reduced by about 65 %, and in Stockholm, it decreases by approximately 57 % compared to the base case.
- The optimized hybrid models greatly improve CO_2 levels compared to the base case. While base cases in all cities mostly stayed in the lowest air quality category (Category III), the optimized systems performed better. In Warsaw and Stockholm, these systems notably increased the time spent in the best air quality category (Category I), while in Delhi, the improvements were smaller but still noticeable.
- Although the optimized hybrid systems led to a slight increase in the PPD index, which means thermal comfort decreased slightly compared to the base case, the comfort levels were still acceptable. Delhi maintained acceptable thermal comfort for 99% of the year, while Warsaw and Stockholm had it for over 80% of the year.

CRediT authorship contribution statement

Seyedkeivan Nateghi: Writing – original draft, Visualization, Validation, Methodology, Formal analysis. **Amirmohammad Behzadi:** Writing – review & editing, Writing – original draft, Visualization, Formal analysis. **Jan Kaczmarczyk:** Supervision, Funding acquisition, Data curation. **Pawel Wargocki:** Writing – review & editing, Supervision, Data curation. **Sasan Sadrizadeh:** Supervision, Data curation, Conceptualization.

Declaration of competing interest

The authors declare that they have no known competing financial interests or personal relationships that could have appeared to influence the work reported in this paper.

Data availability

Data will be made available on request.

References

[1] P. Wolkoff, K. Azuma, P. Carrer, Health, work performance, and risk of infection in office-like environments: the role of indoor temperature, air humidity, and ventilation, Int. J. Hyg. Environ. Health 233 (2021) 113709, https://doi.org/10.1016/j.ijheh.2021.113709.
[2] B. Kozielska, A. Mainka, M. Żak, D. Kaleta, W. Mucha, Indoor air quality in residential buildings in Upper Silesia, Poland, Build. Environ. 177 (2020) 106914, https://doi.org/10.1016/j.buildenv.2020.106914.
[3] O. Toyinbo, Indoor Environmental Quality Pupils' Health and Academic Performance—A Literature Review, Buildings 13 (2023) 2172, https://doi.org/10.3390/buildings13092172.
[4] L.-R. Jia, J. Han, X. Chen, Q.-Y. Li, C.-C. Lee, Y.-H. Fung, Interaction between thermal comfort, indoor air quality and ventilation energy consumption of educational buildings: a comprehensive review, Buildings 11 (2021) 591, https://doi.org/10.3390/buildings11120591.
[5] B.R. Rowe, A. Canosa, A. Meslem, F. Rowe, Increased airborne transmission of COVID-19 with new variants, implications for health policies, Build. Environ. 219 (2022) 109132, https://doi.org/10.1016/j.buildenv.2022.109132.
[6] S. Mahajan, P. Kumar, J.A. Pinto, A. Riccetti, K. Schaaf, G. Camprodon, V. Smári, A. Passani, G. Forino, A citizen science approach for enhancing public understanding of air pollution, Sustain. Cities. Soc. 52 (2020) 101800, https://doi.org/10.1016/j.scs.2019.101800.
[7] P. Kumar, A. Sharma, Study on importance, procedure, and scope of outdoor thermal comfort –a review, Sustain. Cities. Soc. 61 (2020) 102297, https://doi.org/10.1016/j.scs.2020.102297.
[8] A. Zivelonghi, M. Lai, Mitigating Aerosol Infection Risk in School Buildings: The Role of Natural Ventilation, Volume, Occupancy and CO_2 Monitoring, Building Environ. 204 (2021) 108139, https://doi.org/10.1016/j.buildenv.2021.108139.
[9] E.M. Saber, I. Chaer, A. Gillich, B.G. Ekpeti, Review of intelligent control systems for natural ventilation as passive cooling strategy for UK buildings and similar

climatic conditions, Energies. (Basel) 14 (2021) 4388, https://doi.org/10.3390/en14154388.
[10] Z. Tan, X. Deng, An optimised window control strategy for naturally ventilated residential buildings in warm climates, Sustain. Cities. Soc. 57 (2020) 102118, https://doi.org/10.1016/j.scs.2020.102118.
[11] K. Grygierek, S. Nateghi, J. Ferdyn-Grygierek, J. Kaczmarczyk, Controlling and limiting infection risk, thermal discomfort, and low indoor air quality in a classroom through natural ventilation controlled by smart windows, Energies. (Basel) 16 (2023) 592, https://doi.org/10.3390/en16020592.
[12] S. Nateghi, J. Kaczmarczyk, Multi-objective optimization of window opening and thermostat control for enhanced indoor environment quality and energy efficiency in contrasting climates, J. Build. Eng. 78 (2023) 107617, https://doi.org/10.1016/j.jobe.2023.107617.
[13] P. Sicard, E. Agathokleous, S.C. Anenberg, A. De Marco, E. Paoletti, V. Calatayud, Trends in urban air pollution over the last two decades: a global perspective, Sci. Total Environ. 858 (2023) 160064, https://doi.org/10.1016/j.scitotenv.2022.160064.
[14] R. Javadi, N. Nasrollahi, Urban green space and health: the role of thermal comfort on the health benefits from the urban green space; a review study, Build. Environ. 202 (2021) 108039, https://doi.org/10.1016/j.buildenv.2021.108039.
[15] E. McDuffie, R. Martin, H. Yin, M. Brauer, Global burden of disease from major air pollution sources (GBD MAPS): a global approach, Res. Rep. Health Eff. Inst. 2021 (2021) 210.
[16] S.C. Anenberg, A. Mohegh, D.L. Goldberg, G.H. Kerr, M. Brauer, K. Burkart, P. Hystad, A. Larkin, S. Wozniak, L. Lamsal, Long-term trends in urban NO2 concentrations and associated paediatric asthma incidence: estimates from global datasets, Lancet Planet. Health 6 (2022) e49–e58, https://doi.org/10.1016/S2542-5196(21)00255-2.
[17] M. Pascal, M. Corso, O. Chanel, C. Declercq, C. Badaloni, G. Cesaroni, S. Henschel, K. Meister, D. Haluza, P. Martin-Olmedo, et al., Assessing the public health impacts of urban air pollution in 25 European cities: results of the Aphekom project, Sci. Total Environ. 449 (2013) 390–400, https://doi.org/10.1016/j.scitotenv.2013.01.077.
[18] Nations, U. United Nations | Peace, dignity and equality
on a healthy planet 2024 Available online: https://www.un.org/en/ (accessed on 17 March 2024).
[19] Y. Zheng, S. Du, X. Zhang, L. Bai, H. Wang, Estimating carbon emissions in urban functional zones using multi-source data: a case study in Beijing, Build. Environ. 212 (2022) 108804, https://doi.org/10.1016/j.buildenv.2022.108804.
[20] V.A. Southerland, M. Brauer, A. Mohegh, M.S. Hammer, A. Van Donkelaar, R. V. Martin, J.S. Apte, S.C. Anenberg, Global urban temporal trends in fine particulate matter (PM2·5) and attributable health burdens: estimates from global datasets, Lancet Planet. Health (6) (2022) e139–e146, https://doi.org/10.1016/S2542-5196(21)00350-8.
[21] A. Benchrif, A. Wheida, M. Tahri, R.M. Shubbar, B. Biswas, Air quality during three Covid-19 lockdown phases: AQI, PM2.5 and NO2 assessment in cities with more than 1 million inhabitants, Sustain. Cities. Soc. 74 (2021) 103170, https://doi.org/10.1016/j.scs.2021.103170.
[22] L. Bai, W. Chen, Z. He, S. Sun, J. Qin, Pollution characteristics, sources and health risk assessment of polycyclic aromatic hydrocarbons in PM2.5 in an office building in Northern Areas, China, Sustain. Cities. Soc. 53 (2020) 101891, https://doi.org/10.1016/j.scs.2019.101891.
[23] European Environment Agency. Air quality in Europe: 2011 report. Publications Office of the European Union, 2011.
[24] S. Liu, A. Gautam, X. Yang, J. Tao, X. Wang, W. Zhao, Analysis of improvement effect of PM2.5 and gaseous pollutants in Beijing based on self-organizing map network, Sustain. Cities. Soc. 70 (2021) 102827, https://doi.org/10.1016/j.scs.2021.102827.
[25] A. Steinemann, P. Wargocki, B. Rismanchi, Ten questions concerning green buildings and indoor air quality, Build. Environ. 112 (2017) 351–358, https://doi.org/10.1016/j.buildenv.2016.11.010.
[26] A.S. Ahmad, M.Y. Hassan, M.P. Abdullah, H.A. Rahman, F. Hussin, H. Abdullah, R. Saidur, A review on applications of ANN and SVM for building electrical energy Consumption Forecasting, Renewable Sust. Ener. Rev. 33 (2014) 102–109, https://doi.org/10.1016/j.rser.2014.01.069.
[27] R.Z. Homod, K.S.M. Sahari, H.A.F. Almurib, Energy saving by integrated control of natural ventilation and HVAC systems using model guide for comparison, Renew. Energy 71 (2014) 639–650, https://doi.org/10.1016/j.renene.2014.06.015.
[28] M. Rabani, A.J. Petersen, Detailed assessment of hybrid ventilation control system in a mixed-mode building in cold climate, J. Phys. Conf. Ser. 2600 (2023) 102006, https://doi.org/10.1088/1742-6596/2600/10/102006.
[29] Y. Wang, E. Cooper, F. Tahmasebi, J. Taylor, S. Stamp, P. Symonds, E. Burman, D. Mumovic, Improving indoor air quality and occupant health through smart control of windows and portable air purifiers in residential buildings, Build. Serv. Eng. Res. Technol. 43 (2022) 571–588, https://doi.org/10.1177/01436244221099482.
[30] S. Taheri, P. Hosseini, A. Razban, Model predictive control of heating, ventilation, and air conditioning (HVAC) systems: a state-of-the-art review, J. Build. Eng. 60 (2022) 105067, https://doi.org/10.1016/j.jobe.2022.105067.
[31] Q. Li, L. Zhang, L. Zhang, X. Wu, Optimizing energy efficiency and thermal comfort in building green retrofit, Energy 237 (2021) 121509, https://doi.org/10.1016/j.energy.2021.121509.
[32] US Department of Energy Engineering Reference, EnergyPlus™, US Department of Energy, Washington, DC, USA, 2020, p. 1785. Version 9.4.0, Documentation2020.
[33] D.B. Crawley, L.K. Lawrie, F.C. Winkelmann, W.F. Buhl, Y.J. Huang, C.O. Pedersen, R.K. Strand, R.J. Liesen, D.E. Fisher, M.J. Witte, et al., EnergyPlus: creating a new-generation building energy simulation program, Energy Build. 33 (2001) 319–331, https://doi.org/10.1016/S0378-7788(00)00114-6.
[34] Henninger, R.H. and M.J. Witte, 2015a. EnergyPlus testing with HVAC equipment performance tests CE300 to CE545 from ANSI/ASHRAE Standard 140-2011. EnergyPlus Version 7.2.0, 2012. U.S. Department of Energy, Energy Efficiency and Renewable Energy Office of Building Technologies Washington, D.C.
[35] A. Rackes, M.S. Waring, Modeling impacts of dynamic ventilation strategies on indoor air quality of offices in six US cities, Build. Environ. 60 (2013) 243–253, https://doi.org/10.1016/j.buildenv.2012.10.013.
[36] K. Nihar, A. Bhatia, V. Garg, Optimal control of operable windows for mixed mode building simulation in EnergyPlus, IOP Conf. Ser.: Earth Environ. Sci. 238 (2019) 012052, https://doi.org/10.1088/1755-1315/238/1/012052.
[37] H. Zhang, Building Energy Management and Demand Response, Nanyang Technological University, 2019.
[38] K.S. Cetin, M.H. Fathollahzadeh, N. Kunwar, H. Do, P.C. Tabares-Velasco, Development and validation of an HVAC on/off controller in EnergyPlus for energy simulation of residential and small commercial buildings, Energy Build. 183 (2019) 467–483, https://doi.org/10.1016/j.enbuild.2018.11.005.
[39] T. Hong, J. Kim, M. Lee, A multi-objective optimization model for determining the building design and occupant behaviors based on energy, economic, and environmental performance, Energy 174 (2019) 823–834, https://doi.org/10.1016/j.energy.2019.02.035.
[40] Y. Yusoff, M.S. Ngadiman, A.M. Zain, Overview of NSGA-II for optimizing machining process parameters, Procedia Eng. 15 (2011) 3978–3983, https://doi.org/10.1016/j.proeng.2011.08.745.
[41] S. Chatterjee, K. Abhishek, S.S. Mahapatra, S. Datta, R.K. Yadav, NSGA-II approach of optimization to study the effects of drilling parameters in AISI-304 stainless steel, Procedia Eng. 97 (2014) 78–84, https://doi.org/10.1016/j.proeng.2014.12.227.
[42] B. Sajadi, M. Mirnaghi, M. Akhavan-Behabadi, N. Delgarm, A. Goudarzi, Simulation-based optimization of smart windows performance using coupled EnergyPlus - NSGA-II - ANP method, Energy Equip. Syst. 9 (2021), https://doi.org/10.22059/ees.2021.243024.
[43] A. Vukadinović, J. Radosavljević, A. Đorđević, M. Protić, N. Petrović, Multi-objective optimization of energy performance for a detached residential building with a sunspace using the NSGA-II genetic algorithm, Solar Energy 224 (2021) 1426–1444, https://doi.org/10.1016/j.solener.2021.06.082.
[44] Z. Jalali, E. Noorzai, S. Heidari, Design and optimization of form and facade of an office building using the genetic algorithm, Sci. Technol. Built. Environ. 26 (2020) 128–140, https://doi.org/10.1080/23744731.2019.1624095.
[45] T. Goel, R. Vaidyanathan, R.T. Haftka, W. Shyy, N.V. Queipo, K. Tucker, Response surface approximation of pareto optimal front in multi-objective optimization, Comput. Methods Appl. Mech. Eng. 196 (2007) 879–893, https://doi.org/10.1016/j.cma.2006.07.010.
[46] E. Naderi, B. Sajadi, M.A. Behabadi, E. Naderi, Multi-objective simulation-based optimization of controlled blind specifications to reduce energy consumption, and thermal and visual discomfort: case studies in Iran, Build. Environ. 169 (2020) 106570, https://doi.org/10.1016/j.buildenv.2019.106570.
[47] R.A. Lara, E. Naboni, G. Pernigotto, F. Cappelletti, Y. Zhang, F. Barzon, A. Gasparella, P. Romagnoni, Optimization tools for building energy model calibration, Energy Procedia 111 (2017) 1060–1069, https://doi.org/10.1016/j.egypro.2017.03.269.
[48] E. Asadi, M.G. da Silva, C.H. Antunes, L. Dias, A multi-objective optimization model for building retrofit strategies using TRNSYS simulations, GenOpt and MATLAB, Build. Environ. 56 (2012) 370–378, https://doi.org/10.1016/j.buildenv.2012.04.005.
[49] Y. Zhai, Y. Wang, Y. Huang, X. Meng, A multi-objective optimization methodology for window design considering energy consumption, thermal environment and visual performance, Renew. Energy 134 (2019) 1190–1199, https://doi.org/10.1016/j.renene.2018.09.024.
[50] I. Ahmadianfar, A.A. Heidari, S. Noshadian, H. Chen, A.H. Gandomi, INFO: an efficient optimization algorithm based on weighted mean of vectors, Expert. Syst. Appl. 195 (2022) 116516, https://doi.org/10.1016/j.eswa.2022.116516.
[51] S. Wang, S. Ali, T. Yue, M. Liaaen, Integrating weight assignment strategies with NSGA-II for supporting user preference multiobjective optimization, IEEE Trans. Evol. Computat. 22 (2018) 378–393, https://doi.org/10.1109/TEVC.2017.2778560.
[52] ASHRAE, ASHRAE Standard 62-2001, Ventilation for Acceptable Indoor Air Quality Atlanta, American Society of Heating, Refrigerating, and Air Conditioning Engineers, Inc, 2001.
[53] European Committee for Standardization. Energy Performance of Buildings—Ventilation for Buildings—Part 1: Indoor Environmental Input Parameters for Design and Assessment of Energy Performance of Buildings Addressing Indoor Air Quality, Thermal Environment, Lighting and Acoustics—Module M1-6, European Committee for Standardization, Brussels, Belgium, 2019.
[54] K. Partti-Pellinen, O. Marttila, A. Ahonen, O. Suominen, T. Haahtela, Penetration of nitrogen oxides and particles from outdoor into indoor air and removal of the pollutants through filtration of incoming air: nitrogen oxides and particles from outdoor into indoor air, Indoor Air 10 (2000) 126–132, https://doi.org/10.1034/j.1600-0668.2000.010002126.x.
[55] A. Reyes-Lingjerde. Reduction in NO_2-concentration across ventilation filters in an office building located close to heavy traffic. Master thesis, The University of Bergen, 2016.

[56] M.C. Peel, B.L. Finlayson, T.A. McMahon, Updated world map of the Köppen-Geiger climate classification, Hydrol. Earth Syst. Sci. 11 (2007) 1633–1644, https://doi.org/10.5194/hess-11-1633-2007.
[57] U.S. Department of Energy. EnergyPlus Weather Data. Available online: https://energyplus.net/weather (accessed on 17 November 2024).
[58] Vivid Maps. Climates Classification by Wincenty Okołowicz. Available online: https://vividmaps.com/climates-classification-by-wincenty/ (accessed on 17 November 2024).
[59] S. Sinsakul, Late quaternary geology of the lower central plain, Thailand, J. Asian Earth Sci. 18 (2000) 415–426, https://doi.org/10.1016/S1367-9120(99)00075-9.
[60] TransportPolicy.net. India: Air Quality Standards. Available online: https://www.transportpolicy.net/standard/india-air-quality-standards/ (accessed on 17 November 2024).
[61] TransportPolicy.net. EU: Air Quality Standards. Available online: https://www.transportpolicy.net/standard/eu-air-quality-standards/ (accessed on 17 November 2024).
[62] WHO global air quality guidelines. Particulate matter (PM2.5 and PM10), ozone, nitrogen dioxide, sulfur dioxide and carbon monoxide. Geneva: World Health Organization; 2021. Licence: CC BY-NC-SA 3.0 IGO.
[63] Central Pollution Control Board (CPCB). Introduction to the Central Pollution Control Board. Available from: https://cpcb.nic.in/Introduction/ [accessed 17 November 2024].
[64] Chief Inspectorate for Environmental Protection. Available from: https://www.gios.gov.pl/pl/ [accessed 17 November 2024].
[65] World Air Quality Index Project. Air Pollution: Real-time Air Quality Index (AQI) for Stockholm, St. Eriksgatan 83. Available from: https://aqicn.org/city/sweden/stockholm-st-eriksgatan-83/ [accessed 17 November 2024].
[66] EU Standard EN 16798-1:2019, Energy Performance of Buildings—Ventilation for Buildings—Part 1: Indoor Environmental Input Parameters for Design and Assessment of Energy Performance of Buildings Addressing Indoor Air Quality, Thermal Environment, Lighting and Acoustics—Module M1-6, European Committee for Standardization, Brussels, Belgium, 2019.

Building and Environment 272 (2025) 112676

Contents lists available at ScienceDirect

Building and Environment

journal homepage: www.elsevier.com/locate/buildenv

Investigating the impact of physical barriers on air change effectiveness and aerosol transmission under mixing air distribution

Seyedkeivan Nateghi [a,*], Jan Kaczmarczyk [a], Ewa Zabłocka-Godlewska [b], Wioletta Przystaś [b]

[a] Department of Heating, Ventilation and Dust Removal Technology, Faculty of Energy and Environmental Engineering, Silesian University of Technology, Gliwice, Poland
[b] Department of Air Protection, Faculty of Energy and Environmental Engineering, Silesian University of Technology, Gliwice, Poland

ARTICLE INFO

Keywords:
Physical barrier
Airborne transmission
Air change effectiveness
Bioaerosol

ABSTRACT

This research investigated the effectiveness of desk partitions in reducing airborne infection risks in classroom environments. Experiments were conducted in a controlled test chamber with two designs of mixing air distribution systems (MV1 and MV2). Nebulized aerosols and bioaerosols were utilized in the presence of physical barriers to simulate the transmission of exhaled droplets from a source of infection and to assess this transmission among individuals sitting near this source. In addition, local air change effectiveness (ACE) was evaluated based on age of air measurements using CO_2 tracer gas decay method. Results showed that air change effectiveness without partitions were higher than with partitions for both systems, indicating that partitions create an obstacle for effective ventilation air distribution. Moreover, MV1 exhibited significant ACE reductions at some points with partitions, while MV2 maintained high ACE values across all points. For aerosol measurements, MV2 achieved high concentration reduction rates (C_R) around 0.8 across all points, whereas MV1 exhibited mixed results, with some points showing negative C_R values due to airflow obstruction. For bioaerosol generation bacteria *Micrococcus luteus* was used. Sampling of bioaerosol measured *Micrococcus luteus* concentrations, 4- and 45-minutes post-generation. MV2 system was more effective in reducing bacterial concentrations with partitions, while MV1 showed variable results, with partitions reducing concentrations at some points but increasing them at others. Overall, MV2 demonstrated superior performance in maintaining lower contaminant concentrations, especially for environments requiring prevention measures or where maintaining well-mixed air is difficult.

1. Introduction

In response to various pandemics, considerable attention has been directed towards minimizing infection transmission, particularly within building environments. Airborne transmission may take place either through direct contact between individuals in close proximity (short-range transmission) or indirectly via the blending of exhaled pathogens with the air in the room (long-range transmission) [1]. Indirect transmission becomes especially significant in areas with insufficient ventilation and high levels of occupancy over prolonged periods of exposure [2]. The World Health Organization (WHO) has implemented various policies and guidelines to curb virus spread in public spaces [3,4]. The widespread application of physical barriers, owing to their low cost and easy implementation, has been a key preventive measure [5]. However, it is crucial to recognize that while physical barriers offer advantages, such as affordability, they also bring the limitations [6]. One notable limitation is the potential disruption to air distribution, which can affect their efficacy in reducing infection risk [7]. It is also important to note that while physical barriers can reduce airborne transmission, they do not completely eliminate the risk [8].

Prior research has explored the effectiveness of physical barriers in mitigating respiratory droplet transmission. Lee and Awbi examined the impact of internal partitioning on air quality and ventilation in rooms with mixing ventilation [9]. They found that partition location and height affect air distribution and contaminant spread. Liu, Xiaoping, et al. investigated the impact of internal partitions on indoor airflow and contaminant distribution suggest that 1.5 m (W) × 1 m (H) baffles can significantly alter indoor airflow distribution [10]. Chen et al. conducted a study examining the influence of barrier heights on aerosol particle spread in an open office environment [11]. Their findings indicated that a minimum barrier height of 60 cm above the desk surface is necessary for effectively preventing virus transmission. However, for workstations farther from the exhaust outlet, the effectiveness of physical barriers in reducing transmission was found to be less pronounced. In a densely

* Corresponding author.
E-mail address: seyedkeivan.nateghi@polsl.pl (S. Nateghi).

https://doi.org/10.1016/j.buildenv.2025.112676
Received 16 October 2024; Received in revised form 22 January 2025; Accepted 4 February 2025
Available online 5 February 2025

occupied canteen, Zhang et al. conducted experimental investigations on the impact of physical partitions on the risk of short-distance cross-infection [12]. Results showed that physical partitions effectively mitigated short-distance airborne transmission, reducing the infection risk. However, the presence of physical partitions also led to the accumulation of expiratory air within compartments, raising considerations for air quality management. Similarly, Dacunto et al. studied aerosol dispersion in a university classroom by employing three-sided clear dividers attached to student desk surfaces [13]. They found that increasing desk spacing reduced potential exposure, and dividers were particularly effective at reducing aerosol concentrations at instructor locations.

These studies underscore the importance of physical barriers in reducing infection transmission while emphasizing the need to consider factors such as room air distribution and ventilation conditions. [14]. Although the efficacy of physical barriers has been demonstrated, there is limited understanding of how different air distribution patterns and ventilation systems influence their performance.

Previous studies conducted under controlled laboratory conditions have utilized various methods to examine the transmission of infections between people. Some studies have applied tracer gas to simulate the spread of airborne pathogens [15], while others have generated aerosols to mimic real-world conditions [16,17]. Even fewer studies have employed bioaerosols, which are crucial for a realistic assessment of airborne infection risks. Previous studies have shown that understanding bioaerosol dynamics is crucial for accurate assessment of airborne infection risks [18,19]. King et al. [20] demonstrated the feasibility of using computational fluid dynamics (CFD) to accurately predict bioaerosol deposition patterns in different hospital room layouts. This study underscored the effectiveness of physical barriers in reducing cross-contamination. However, a comprehensive comparison of different methods has not yet been conducted to evaluate their respective impacts on airborne transmission experiments. Investigating the variations of aerosols and bioaerosols in transmission of infections could provide deeper insights into the mechanisms of infection spread and the effectiveness of mitigation strategies. Such comparisons are essential to optimize experimental setups and enhance the accuracy of infection risk assessments in various indoor environments.

This study aims to comprehensively evaluate the effectiveness of desk partitions in combination with two designs of mixing air distribution systems to reduce airborne infection risks in classroom settings. The study examines aerosol particle concentration reduction by releasing nebulized NaCl aerosols to simulate the transmission of exhaled droplets. Measurements were taken at various points near the infection source to evaluate the effectiveness of the partitions and air distribution systems in reducing aerosol concentrations. Furthermore, bioaerosol sampling and analysis were conducted to mimic the spread of infectious particles. Bioaerosols created from bacteria *Micrococcus luteus* strain were sprayed in the test chamber, and concentrations were measured to determine how the partitions and ventilation systems impact on the bioaerosol spread. Additionally, the study investigates the Air change effectiveness (ACE) of both systems, utilizing the tracer gas decay method to assess their performance in managing indoor air quality. The focus is on determining whether the partitions influence the airflow patterns and thus local air change efficiency. In particular, the aim of this study is to provide information on ventilation systems operation in environments that incorporate physical barriers, ultimately aiming to enhance infection control methods in educational settings.

2. Methods

2.1. Test room and ventilation systems

Experiments were conducted in a 9 × 6 × 3.3 m ($L \times W \times H$) test chamber. Three desks were arranged linearly, spaced 0.55 m apart and centrally positioned within the test chamber, as illustrated in Fig. 1. The

Fig. 1. Photo of designed partitions and two dummies at a desk.

design and construction of transparent partitions for desktop placement were meticulously executed. These partitions included a front panel measuring 65 × 138 cm ($H \times L$) and three side panels: two at the desk edges and one dividing the two seating areas. This configuration ensures each occupant has an enclosed space, acting as a physical barrier to minimize the transmission of airborne particles between adjacent individuals [21]. The height and width of the partitions adequately cover the occupants' breathing zones, making them a potentially effective preventive measures in educational settings.

To simulate the effect of occupants on air flow pattern in the room, six heated dummies were utilized, with two placed at each desk, each carrying a sensible heat load of 60 W, which corresponds to low-seating-activity. Each dummy took the form of a 1.10 m tall cylindrical steel tube with a diameter of 0.40 m, resulting in a surface area of 1.63 m^2, equivalent to that of a 15-year-old child. The cylinders were painted grey. The test room incorporated two different mixing ventilation systems with unique configurations as depicted in Fig. 2. The setup consisted of a single pollutant source, simulating an infected person, and five measurement points (P1-P5) representing susceptible individuals. Airborne particle concentrations were monitored at the breathing height of dummies, approximately 1.1 m above the ground.

For the first one denoted as MV1, four ceiling air terminal devices were positioned on both sides of the room. These devices integrated both air supply and exhaust. The air supply was directed downward through square diffusers, while exhaust air was extracted through grilles located above the supply. The second one (MV2), characterized by four ceiling swirl air diffusers positioned on both sides of the room. MV2 involved supplying air through square diffusers that swirl the air downwards, while exhaust air was extracted through a circle air exhaust terminal located near the ceiling level. Fig. 3 illustrates the configuration of supply diffusers for the two selected mixing ventilation systems.

In all measurement cases, indoor space was ventilated using 148 L/s of fresh air, resulting in an air change rate of 3 h^{-1}. The variations during the tests were ±10 L/s. The supply air temperature was kept at 20 ± 1

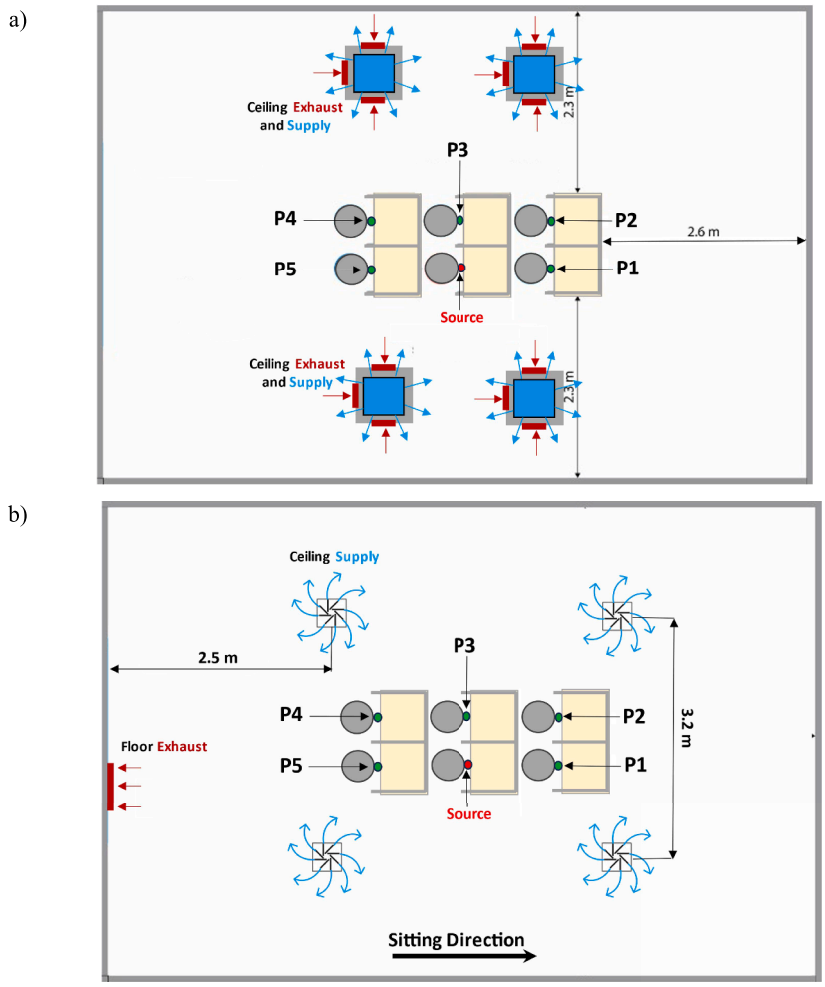

Fig. 2. Test room with mixing ventilations and experimental setup illustration, (a): MV1 (b): MV2. One infected occupant (Red circle) and 5 susceptible occupants (Gray circles).

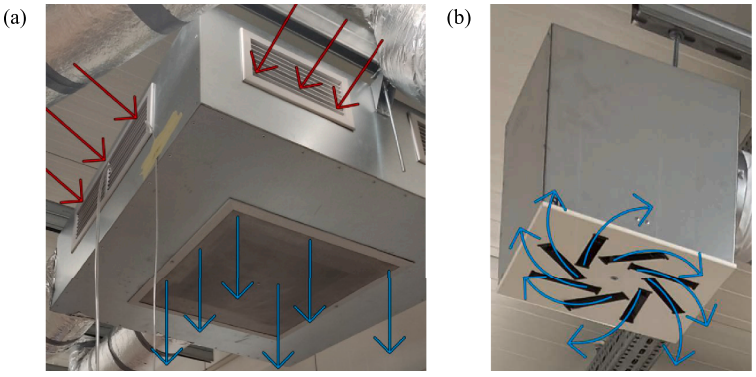

Fig. 3. Configuration of air terminal devices used for diffuse, (a): MV1 (b): MV2.

°C. In all studied cases, the average room air temperature was 22 ± 1 °C and relative humidity at 40 ± 10%.

2.2. Tracer gas dosing and measurement

Carbon dioxide was utilized as a tracer gas to study the effectiveness of MV to deliver clean ventilation air at the occupants' locations. CO_2 was chosen for its inert properties and relevance to indoor air quality assessment. The simplest technique employed was the decay method, also known as the step-down method. This method involves injection of CO_2 tracer gas into the enclosed space under investigation. The tracer gas was thoroughly mixed with the ambient air, simulating a uniform distribution throughout the environment. After the injection phase, the CO_2 dosing was stopped, and gas concentration measurements were conducted at five distinct points (Fig. 2) within the space and one exhaust location. P1 to P5 were chosen to ensure accurate representation of areas potentially affected by physical barriers. In the case of insufficient air mixing the location of exhaust is particularly important, as it affects Air change effectiveness (ACE). The Testo 160 sensors were used to record the CO_2 concentration in 1 min interval. The measuring

range of the sensors was from 0 to 5000 ppm, with uncertainty of ± 50 ppm.

2.3. Aerosol generation and measurement

In previous research, the Collision nebulizer has been successfully employed to produce aerosols for virus assays [22]. In this study, a Collison nebulizer with 3 jets [23] was employed along with a solution of sodium chloride (NaCl) to simulate droplets in human exhalation. According to Nicas et al. [24], respiratory fluid droplets can be likened to NaCl solution. The solution comprised 1 gram of NaCl dissolved in a solvent mixture of 250 cm^3, consisting of 50% distilled water and 50% isopropyl alcohol by volume. The solution was proved to properly simulate the evaporative behavior of human saliva and provide a more accurate representation of its composition [25]. Atomization occurred at a pressure of 20 psi, resulting in droplets with a geometric mean diameter (GMD) of 0.7 μm and a geometric standard deviation (GSD) ranging from 1.22 to 1.35. The Collison nebulizer produces a log-normal distribution of droplet sizes ranging from 0.05 μm to 20 μm under typical operating conditions [23]. This range aligns well with the size spectrum of respiratory droplets generated during human exhalation [26]. While the mean diameter of 0.7 μm represents the finer fraction of exhaled droplets, it is crucial for assessing airborne transmission risks, as smaller droplets remain suspended for longer durations and can travel farther in indoor environments. The aerosolized droplets, blended with clean air, emanated from the nebulizer inlet positioned precisely at the top of the dummy mimicking the mouth location of a subject. The ejection air velocity from the nebulizer was calculated to be approximately 2 m/s. Five measurement points (Fig. 1) were designated at the mouths of the exposed dummies. An aerodynamic particle sizer (PCE), capable of detecting particles ranging from 0.3 to 10 Âμm , was employed to measure both particle counts and aerodynamic diameters at 1-minute intervals. PM2.5 was measured and used in the analysis due to its relevance in evaluating indoor air quality and health impacts.

2.4. Bioaerosol generation and sampling method

Bacteria belonging to *Micrococcus luteus* were used as a model organism to prepare suspensions for bioaerosols generation. Bioaerosols were generated using the same method as aerosol generation, ie, Collison Nebulizer, ensuring that in all tests the droplets were of similar size. The bacteria concentration in the suspensions was adjusted to 150 × 10ˆ6 CFU/ml. This concentration was determined and verified using McFarland standards and by measuring the optical density at a wavelength of 600 nm using a Hitachi UV–Vis spectrophotometer. Bioaerosols were emitted continuously for 4 mins using the Collison nebulizer, which operated at an air flow rate of 6 L/min to disperse the suspension into the room. Samples of bioaerosols were collected by the impact method using the AirIdeal 3P sampler (Biomerieux). The first measurement of microorganism concentration was performed immediately after the 4-minute nebulization. The second measurement was taken 45 mins after the bioaerosol emission had ended. All measurements were done in triplicate. The research was conducted in a room, which had been previously sterilized with 60 mins of UV light (250–270 nm) before starting the research. Measurements were taken at three points (P1, P3, P5) which localization is presented in the Fig. 2. Trypticase Soy Agar (BTL) plates were used for bacteria growth, and samples were incubated for 48 h at a temperature of 37 °C. The number of bacteria was counted using a bacterial counter, and results were presented as CFU/m^3. The efficiency of the ventilation system in the classroom, with and without partitions, was evaluated by comparing the differences in microorganism numbers between sampling points.

3. Results

The results are divided into three main sections: Ventilation Effectiveness, Aerosol Particle Concentration Reduction, and Bioaerosol Analysis. Each category is analyzed under two different air distribution systems (MV1 and MV2), both with and without partitions. The data collected provides insights into how different air distributions and the presence of physical barriers impact indoor air quality and infection transmission.

3.1. Air change effectiveness

Effectiveness of ventilation to provide clean air was evaluated based on local Air Change Effectiveness Index [27]. It was calculated as the ratio of the age of air in the exhaust duct (τ_e) to the local mean age of air at a measured location (τ_m):

$$ACE = \frac{\tau_e}{\tau_m} \quad (1)$$

The higher the ACE values, the more effective the ventilation system is in that area. In this study, the CO_2 concentrations were obtained during a decay test, where the decay of tracer gas concentration over time was measured at different points. As depicted in Fig. 4, measurements were conducted under two air distribution systems (MV1 and MV2) and two conditions (with physical barriers and without physical barriers). The results show that local ACE values without partitions obtained higher values for both MV1 and MV2 systems, indicating good mixing and relatively effective ventilation. However, there are variations across the points, particularly in MV1 where points P4 and P5 show slightly lower ACE values. Introducing physical barriers (PB) generally results in lower local ACE values, suggesting that PB might create obstacles that reduce ventilation effectiveness in some areas. For MV1, points P1 to P3 exhibit ACE values close to 1 in both conditions, indicating good ventilation performance, although slightly reduced with PB. Points P4 and P5 show a noticeable drop in local ACE values with PB, highlighting the hindrance caused by partitions in these specific areas. In contrast, the MV2 system maintains consistently high ACE values across all points, even with PB, indicating a more robust and capable performance. Despite the reduction in local ACE with PB in MV2, these values are still high compared to MV1. Overall, the MV2 system shows more uniform and effective local ACE values and is less affected by the introduction of partitions, suggesting it might be a better choice for environments where partitions are necessary for preventing infection transmission.

3.2. Aerosol concentration reduction

The aerosol measurements were conducted under two air distribution systems (MV1 and MV2). Particle concentrations were measured at five points near the infection source, where the exposed individuals were positioned. The average particle concentration value at each point was calculated under 45 mins steady-state conditions. At each point, there were two values representing two different conditions, comprising with and without partitions. Fig. 5 illustrates the concentration reduction rate (C_R) of aerosol particles under two different air distribution systems, MV1 and MV2, at five points (P1 to P5) near the infection source where exposed individuals were situated. The C_R was determined by comparing the particle concentration with and without the use of partitions, following the equation:

$$C_R = \frac{C_{Without\ PB} - C_{With\ PB}}{C_{Without\ PB}} \quad (2)$$

Under the MV1 system, P1 and P2 showed a moderate positive concentration reduction rate, indicating that partitions were somewhat effective in reducing the particle concentration in these areas. Specifically, C_R values were around 0.4. P3 had a slight positive reduction rate, close to 0.3, demonstrating minimal improvement with the partitions. At the same time, the standard deviations calculated using error propagation techniques were relatively high at these three points (P1, P2, P3).

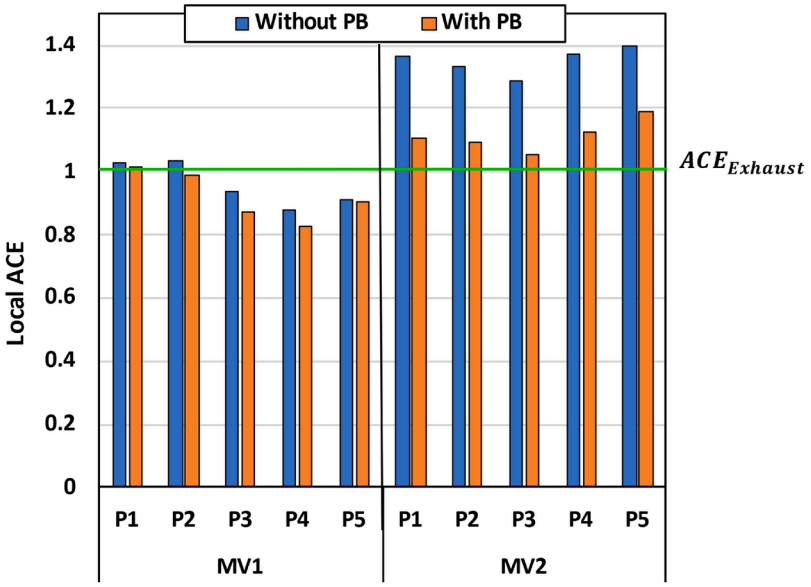

Fig. 4. Local air change effectiveness (ACE) at points P1-P5 comparison across air distribution systems and physical barriers (PB).

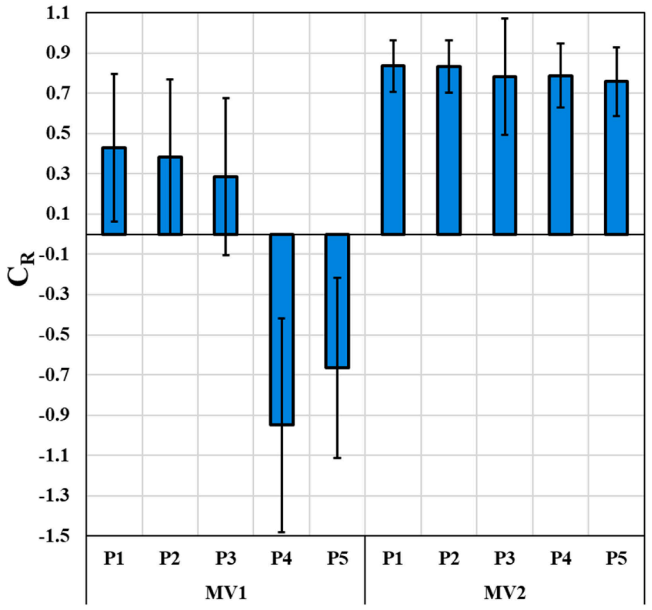

Fig. 5. Comparison of aerosol concentration reduction rates (C_R) across air distribution systems and prevention measures.

Error propagation involves assessing how uncertainties in input variables impact the uncertainty of the final result. This high variability reduces the certainty of the positive effect of the partitions. P4 and P5 exhibited negative C_R values, with P4 showing a significant negative value of approximately −0.95 and P5 around −0.65. This suggests that in these locations, the partitions were ineffective and possibly even detrimental, leading to higher particle concentrations than without partitions. Moreover, the standard deviation at P4 was too high, indicating significant variability. In contrast, the MV2 system consistently showed high positive C_R values across all five points. P1, P2, and P3 had C_R values of around 0.8, indicating a substantial reduction in particle concentration with the use of partitions. P4 and P5 also demonstrated strong positive C_R values, slightly lower but still significant at around 0.7 and 0.6 respectively. This indicates that under the MV2 system, partitions were highly effective in reducing aerosol particle concentrations. The results for aerosol measurements highlight a stark contrast between the two air distribution systems. The MV2 system, which likely involves more effective air circulation and distribution, shows that the use of partitions can significantly reduce aerosol concentrations near the infection source. This suggests that the MV2 system is more conducive to the effective use of partitions in mitigating airborne transmission risks. On the other hand, the MV1 system's mixed results indicate that partitions alone may not be sufficient to reduce aerosol concentrations and could even exacerbate the situation in certain locations. This underscores the importance of optimizing the overall ventilation strategy in conjunction with physical barriers.

3.3. Bioaerosol sampling and analysis

The bioaerosol sampling involved measuring the concentration of *Micrococcus luteus* strain at three locations near the infection source (P1, P3, P5), where individuals were exposed. Measurements were taken immediately after 4-minute bioaerosol generation and also 45 mins after bioaerosol generation had ended at each point. Fig. 6 illustrates two values at each point, depicting conditions with and without partitions. The analysis of bioaerosol concentrations immediately after 4 mins emission provides a clear comparison of the effectiveness of the two ventilation systems (MV1 and MV2) in reducing airborne bacterial concentrations and their spreading, both with and without the presence of partitions. For MV1, without partitions, the bacterial concentrations after 4 mins bioaerosol emission were 1089 CFU/m^3 at P1, 693 CFU/m^3 at P3, and 987 CFU/m^3 at P5. With PB, the concentrations changed to 423 CFU/m^3 at P1, 1569 CFU/m^3 at P3, and 1363 CFU/m^3 at P5. While partitions significantly reduced the concentration at P1, they caused an increase at P3 and P5. The increased concentrations at P3 and P5 suggest that the partitions might have redirected airflow, causing a build-up of bacteria in those areas. Therefore, partitions in MV1 potentially obstructed the airflow, thereby reducing the effectiveness of the ventilation in dispersing and removing bioaerosols. The standard deviations were also considerably high, indicating significant variability and possible inefficiency in well-mixing and distributing the air uniformly in the presence of partitions. For MV2, without partitions, the bacterial concentrations at 4 mins of emission were 731 CFU/m^3 at P1, 679 CFU/m^3 at P3, and 648 CFU/m^3 at P5. With partitions, these concentrations were reduced to 273 CFU/m^3 at P1 and 340 CFU/m^3 at P5 but increased to 777 CFU/m^3 at P3. This shows that partitions effectively reduced concentrations at P1 and P5. At P3 under MV2, particle concentrations increased after the addition of partitions. However, the high standard

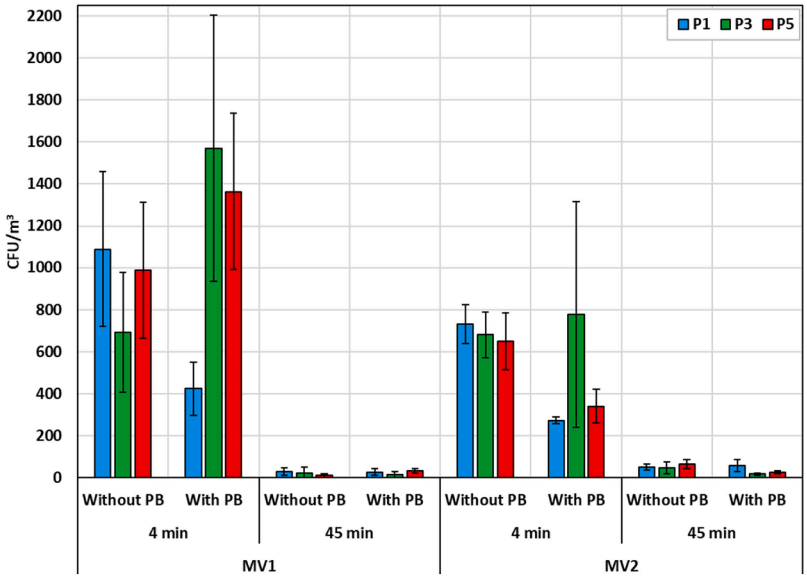

Fig. 6. Comparison of bioaerosol concentrations at different points with and without PB under MV1 and MV2 systems.

deviation at this point made the concentration measurements less certain. Furthermore, the increase in concentration at P3 under MV2 was smaller compared to P3 under MV1. Obtained results suggest that in the case of MV2 the presence of partitions helped stabilize the airflow and reduce bacterial concentration more efficiently. The standard deviations in MV2, although present, were smaller compared to MV1, suggesting a more stable and effective air mixing and bioaerosol removal capability, even with partitions in place. For measurements 45 mins after the bioaerosol emission ceases, a significant reduction in bacterial concentrations was observed for both systems. Bacteria concentrations decreased substantially across all points with and without partitions in comparison with the results just after emission. In MV1 system, after 45 mins the use of partitions led to lower concentrations at most points, with less variability. MV1 not only helped in immediate reduction but also maintained lower concentrations over time, with reduced variability as indicated by lower standard deviations. This indicates that while both systems effectively reduced bacterial concentrations over time, MV2 with partitions consistently showed better performance in maintaining lower concentrations and reduced variability.

The data conclusively show that MV2 is superior in maintaining lower and more consistent bacterial concentrations across different points in the room, both with and without partitions. This indicates a higher efficiency in ventilation and better compatibility with physical barriers. The smaller standard deviations observed in MV2 further underscore its effectiveness in providing a well-mixed environment, which is crucial for minimizing infection risks in enclosed spaces. Conversely, MV1′s performance was notably hindered by the presence of partitions, highlighting its limited capability in ensuring effective air distribution and particulate removal under such conditions.

4. Discussion

This study aimed to evaluate the effectiveness of desk partitions under two different mixing air distribution systems in reducing airborne infection risks in classroom settings. The results indicate that desk partitions can effectively reduce infection transmission, but their effectiveness heavily relies on the design of the ventilation system. This is consistent with findings from previous studies [13,28], which emphasize the necessity of proper ventilation to enhance the protective effects of physical barriers. The design of the ventilation system is important for optimizing ventilation effectiveness and consequently mitigating infection risk. Although both studied ventilation systems operated on the principle of mixing ventilation and had two air inlets on both sides of the benches, as shown in Fig. 2, their effectiveness in removing pollutants differed in areas not directly under the inlet. The MV2 system, which maintained high Air change effectiveness (ACE) and consistent reduction in aerosol and bioaerosol concentrations, outperformed the MV1 system, highlighting the role of well-designed ventilation systems in mitigating airborne infection transmission risks [29]. The observed differences between the MV1 and MV2 systems can be attributed to their distinct airflow patterns and mixing efficiencies. MV1 directs airflow downward with a lower inlet air velocity of 0.4 m/s.

The ceiling-mounted exhaust terminals positioned directly above the supply diffusers intensify this configuration's limitations, often creating localized recirculation zones [30]. These zones, particularly near physical barriers, lead to stagnant areas and poor ventilation effectiveness and areas where contaminants can accumulate. Consequently, while MV1 may effectively ventilate the areas on both sides of the benches, it struggles to deliver fresh air to the benches in the central part of the room, where physical barriers further obstruct direct airflow. In contrast, MV2 employs swirl air diffusers with a higher initial inlet air velocity of 2.3 m/s. The swirling motion introduced by these diffusers promotes enhanced air mixing and a more uniform airflow distribution throughout the classroom. Previous studies have demonstrated that swirl diffusers are particularly effective in preventing stagnant zones and ensuring better contaminant removal compared to standard downward diffusers [31,32]. Despite having diffusers positioned on the sides of the room, MV2 effectively distributes fresh air to the central regions, ensuring adequate ventilation at critical measurement points. Additionally, the centralized exhaust terminal in MV2 further enhances pollutant removal by minimizing recirculation zones and directing airflow more efficiently. The superior performance of MV2 in reducing both aerosol and bioaerosol concentrations, even in the presence of physical barriers, underscores its compatibility with partitioned environments. CFD simulations from a related study reinforce these observations, showing that MV2′s swirling airflow pattern mitigates recirculation zones and promotes efficient air mixing, ensuring effective ventilation in challenging scenarios [33]. Moreover, the higher air velocity of MV2 not only improves the reach of fresh air but also reduces the likelihood of pollutant accumulation in localized areas.

Fig. 7 shows the concentration reduction rates (C_R) for aerosols and bioaerosols under the MV1 and MV2 systems at three measurement points (P1, P3, and P5). At P1, both MV1 and MV2 systems were effective in reducing particle concentrations, but MV2 showed a higher

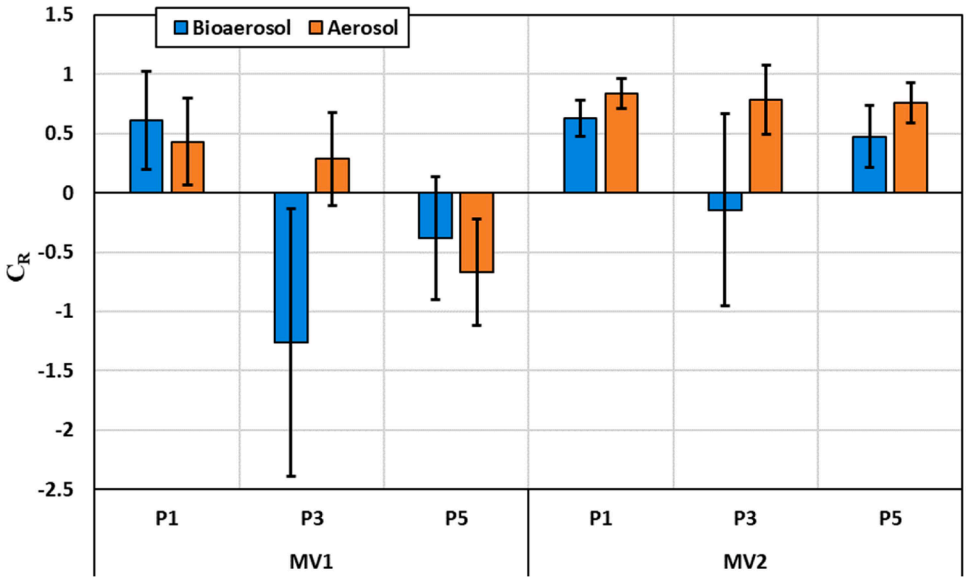

Fig. 7. Comparison of aerosol and bioaerosol concentration reduction (C_R) across air distribution systems and prevention measures.

overall reduction in both aerosols and bioaerosols, reflecting better management of airflow and particle dispersion. At P3, a notable difference in performance between the two ventilation systems and also in aerosol and bioaerosol concentrations is observed. For aerosols, MV1 exhibited a positive C_R value, indicating a reduction in concentration, whereas MV2 had a significantly higher positive C_R value, showcasing its superior capability in reducing aerosol concentrations beside the source pollution. In contrast, bioaerosol C_R values were negative for both systems, with MV1 having a significantly more negative value compared to MV2. The negative C_R values for bioaerosols in both systems suggest challenges in managing particles with biological properties, which may settle or adhere to surfaces more easily [34]. On the other hand, standard deviations for bioaerosols at P3 were notably high for both MV1 and MV2, indicating significant variability and further emphasizing the difficulty in consistently reducing bioaerosol concentrations. At P5, MV1 showed a negative C_R value for aerosols and bioaerosols, indicating an increase in concentration behind the source, which suggests that the airflow pattern of MV1 may be obstructed by the partitions, leading to particle accumulation. In contrast, MV2 maintained a positive C_R value for aerosols and bioaerosols, demonstrating an effective reduction in aerosol and bioaerosol concentration. This further supports the superior performance of the MV2 system in managing airflow and reducing particle concentrations even in the presence of partitions.

The comparison between aerosols and bioaerosols under the two ventilation systems revealed distinct results, which can be interpreted through the different nature of aerosols and bioaerosols: Aerosols (NaCl solution) and bioaerosols (*Micrococcus luteus*) have different physical and chemical properties. Aerosols are primarily influenced by factors like particle size, density, and the ability to remain suspended in air. Bioaerosols, created by biological particles, are bigger in size and heavier. Moreover, due to the cell surface hydrophobicity and electrostatic charge are more affected by environmental factors such as humidity and temperature, what affect their sedimentation and adhesion properties. Their ability to settle or be resuspended can differ significantly in different conditions [35,36]. Moreover, methodologies for measuring aerosols and bioaerosols differ. Aerosol measurements were taken using an aerodynamic particle sizer at regular intervals, while bioaerosol concentrations were measured with Aerobiocollector and then using a bacterial counter after growth on agar plates. This difference in methodology can contribute to variations in detected concentrations and reduction efficiency between aerosols and bioaerosols. Despite these differences with aerosols, the bioaerosol method remains a reliable indicator for investigating infection transmission and provides insight into the behavior of real biological particles, posing a health risk, under varying conditions.

5. Challenges and limitations

The study examined only two ventilation designs, MV1 and MV2, which, while mixing ventilation is representative of the most common systems, do not encompass the full range of possible configurations. Additionally, the location of supply and exhaust ventilation may significantly influence airflow patterns and pollutant removal.

Indoor pollutant concentration distribution is strongly influenced by the room arrangement, such as desk location, placement of physical barriers, and the position of the infected occupant. In this study, the infected occupant was consistently positioned at a fixed point, and the selected measurement points were strategically chosen to evaluate the performance of the ventilation systems in mitigating airborne transmission in these high-risk areas. However, the fixed location of desks and partitions limited the ability to explore different classroom layouts, which could affect airflow and transmission dynamics. Variations in the location of the infected individual or exposed occupants could also influence the results by altering airflow patterns and particle dispersion, particularly near physical barriers or ventilation inlets and outlets. Future studies should consider varying occupant configurations, desk layouts, and placements to provide broader insights into the impact of such variables on ventilation performance and infection control strategies.

The use of heated dummies with simplified cylindrical geometries presents a limitation in capturing the full complexity of human anatomy. Although this design accurately generates enthalpy and buoyancy fluxes, as supported by Zukowska et al. [37], it does not simulate respiratory activities such as breathing or coughing. This restricts the ability to fully replicate the dynamic interactions of human occupants with airflow and pollutant dispersion, which should be considered in future studies.

6. Conclusion

The study comprehensively evaluated the effectiveness of desk partitions in combination with two distinct mixing air distribution systems (MV1 and MV2) to reduce airborne infection risks in classroom settings.

The results indicated that the performance of these preventive measures is significantly influenced by the efficiency of ventilation and the airflow patterns generated by the ventilation systems. Key findings include:

- The use of desk partitions proved effective in reducing infection transmission by minimizing direct airflow between individuals. However, this effectiveness is highly dependent on the design of the ventilation system, which plays a crucial role in managing airflow and particle dispersion in indoor environments.
- The study highlighted significant differences in the performance of mixing ventilation designs, as exemplified by the MV1 and MV2 systems when used with partitions. The MV2 system consistently maintained high Air change effectiveness (ACE) and significantly reduced both aerosol and bioaerosol concentrations. In contrast, the MV1 system exhibited decreased ACE and increased particle concentrations at specific points, indicating its lower effectiveness in environments with physical barriers. Overall, the superior air mixing and distribution capabilities of the MV2 system underscore the importance of optimizing mixing ventilation to maintain lower contaminant levels in various settings.
- The observed differences in concentration reductions between aerosols and bioaerosols across the air distribution systems and measurement points highlight the complex interplay of factors such as particle properties, and measurement techniques. This underscores the importance of properly tailored methods for controlling different types of airborne particles in indoor environments. Furthermore, the study suggests that using bioaerosol methods to investigate infection transmission is appropriate and effective, similar to the use of aerosols. However, bioaerosols require specific handling and analysis due to their more complex biological composition.

Overall, this study underscores the importance of designing ventilation systems and understanding their airflow patterns, particularly in environments that incorporate physical barriers, to ensure effective infection control. Future studies should explore further optimizations and configurations of ventilation systems to enhance their effectiveness in various indoor settings.

CRediT authorship contribution statement

Seyedkeivan Nateghi: Writing – original draft, Investigation, Funding acquisition, Formal analysis. **Jan Kaczmarczyk:** Writing – review & editing, Supervision, Methodology, Conceptualization. **Ewa Zabłocka-Godlewska:** Writing – review & editing, Resources, Methodology, Investigation. **Wioletta Przystaś:** Writing – review & editing, Resources, Methodology, Investigation.

Declaration of competing interest

The authors declare that they have no known competing financial interests or personal relationships that could have appeared to influence the work reported in this paper.

Acknowledgements

The work was supported by the Polish Ministry of Education and Science within the research subsidy.

Data availability

No data was used for the research described in the article.

References

[1] Transmissibility and Transmission of Respiratory Viruses | Nature Reviews Microbiology Available online: https://www.nature.com/articles/s41579-021-00535-6 (accessed on 19 November 2023).
[2] Z. Asif, Z. Chen, S. Stranges, X. Zhao, R. Sadiq, F. Olea-Popelka, C. Peng, F. Haghighat, T. Yu, Dynamics of SARS-CoV-2 spreading under the influence of environmental factors and strategies to tackle the pandemic: a systematic review, Sustain. Cities Soc. 81 (2022) 103840, https://doi.org/10.1016/j.scs.2022.103840.
[3] Advice for the Public on COVID-19 – World Health Organization Available online: https://www.who.int/emergencies/diseases/novel-coronavirus-2019/advice-for-public (accessed on 9 January 2025).
[4] Leading Health Agencies Outline Updated Terminology for Pathogens That Transmit through the Air Available online: https://www.who.int/news/item/18-04-2024-leading-health-agencies-outline-updated-terminology-for-pathogens-that-transmit-through-the-air (accessed on 9 January 2025).
[5] A. Eykelbosh. A Rapid Review of the Use of Physical Barriers in Non-Clinical Settings and COVID-19 Transmission, National Collaborating Centre for Environmental Health, Vancouver, 2021.
[6] C.M. Rooney, J. McIntyre, L. Ritchie, M.H. Wilcox, Evidence review of physical distancing and partition screens to reduce healthcare acquired SARS-CoV-2, Infect. Prev. Pract. 3 (2021) 100144, https://doi.org/10.1016/j.infpip.2021.100144.
[7] T. Jefferson, C. Del Mar, L. Dooley, E. Ferroni, L.A. Al-Ansary, G.A. Bawazeer, M. L. Van Driel, R. Foxlee, A. Rivetti, Physical interventions to interrupt or reduce the spread of respiratory viruses: systematic review, BMJ 339 (2009) b3675, https://doi.org/10.1136/bmj.b3675. –b3675.
[8] M. Bagherirad, P. Trevan, M. Globan, E. Tay, N. Stephens, E. Athan, Transmission of tuberculosis infection in a commercial office, Med. J. Aust. 200 (2014) 177–179, https://doi.org/10.5694/mja12.11750.
[9] H. Lee, H.B. Awbi, Effect of internal partitioning on indoor air quality of rooms with mixing ventilation—basic study, Build. Environ. 39 (2004) 127–141, https://doi.org/10.1016/j.buildenv.2003.08.007.
[10] X. Liu, X. Wu, L. Chen, R. Zhou, Effects of internal partitions on flow field and air contaminant distribution under different ventilation modes, Int. J. Environ. Res. Public Health 15 (2018) 2603, https://doi.org/10.3390/ijerph15112603.
[11] C. Ren, C. Xi, J. Wang, Z. Feng, F. Nasiri, S.-J. Cao, F. Haghighat, Mitigating COVID-19 infection disease transmission in indoor environment using physical barriers, Sustain. Cities Soc. 74 (2021) 103175, https://doi.org/10.1016/j.scs.2021.103175.
[12] J. Ye, Z. Ai, C. Zhang, A new possible route of airborne transmission caused by the use of a physical partition, J. Build. Eng. 44 (2021) 103420, https://doi.org/10.1016/j.jobe.2021.103420.
[13] P. Dacunto, D. Moser, A. Ng, M. Benson, Classroom aerosol dispersion: desk spacing and divider impacts, Int. J. Environ. Sci. Technol. 19 (2022) 1057–1070, https://doi.org/10.1007/s13762-021-03564-z.
[14] C. Zhang, P.V. Nielsen, L. Liu, E.T. Sigmer, S.G. Mikkelsen, R.L. Jensen, The source control effect of personal protection equipment and physical barrier on short-range airborne transmission, Build. Environ. 211 (2022) 108751, https://doi.org/10.1016/j.buildenv.2022.108751.
[15] Z. Ai, C.M. Mak, N. Gao, J. Niu, Tracer gas is a suitable surrogate of exhaled droplet nuclei for studying airborne transmission in the built environment, Build. Simul. 13 (2020) 489–496, https://doi.org/10.1007/s12273-020-0614-5.
[16] M. Ehsanifar, Airborne aerosols particles and COVID-19 transition, Environ. Res. 200 (2021) 111752, https://doi.org/10.1016/j.envres.2021.111752.
[17] J.W. Tang, C.J. Noakes, P.V. Nielsen, I. Eames, A. Nicolle, Y. Li, G.S. Settles, Observing and quantifying airflows in the infection control of aerosol- and airborne-transmitted diseases: an overview of approaches, J. Hosp. Infect. 77 (2011) 213–222, https://doi.org/10.1016/j.jhin.2010.09.037.
[18] W. Przystaś, E. Zabłocka-Godlewska, S.K. Nateghi, J. Kaczmarczyk, Effect of the Time of Bioaerosol Emission on Potential Exposure to Microorganisms in the Class Room with and Without Operating Mechanical Ventilation, RWTH Aachen University, 2023.
[19] E. Zabłocka-Godlewska, W. Przystaś, J. Kaczmarczyk, S.K. Nateghi, Preliminary Study of Bioaerosol Dispersion in Classroom Space, RWTH Aachen University, 2023.
[20] M.-F. King, C.J. Noakes, P.A. Sleigh, M.A. Camargo-Valero, Bioaerosol deposition in single and two-bed hospital rooms: a numerical and experimental study, Build. Environ. 59 (2013) 436–447, https://doi.org/10.1016/j.buildenv.2012.09.011.
[21] S.K. Nateghi, J. Kaczmarczyk, A. Lipczynska, Potential of physical barriers integrated with personal exhaust ventilation in decreasing airborne infection risk for people, J. Phys.: Conf. Ser. 2600 (2023) 102020, https://doi.org/10.1088/1742-6596/2600/10/102020.
[22] R.H. Alford, J.A. Kasel, P.J. Gerone, V. Knight, Human influenza resulting from aerosol inhalation, Proc. Soc. Exp. Biol. Med. 122 (1966) 800–804, https://doi.org/10.3181/00379727-122-31255.
[23] CH TECHNOLOGIES Available online: https://chtechusa.com/products_tag_lg_collison-nebulizer.php (accessed on 11 December 2024).
[24] M. Nicas, W.W. Nazaroff, A. Hubbard, Toward understanding the risk of secondary airborne infection: emission of respirable pathogens, J. Occup. Environ. Hyg. 2 (2005) 143–154, https://doi.org/10.1080/15459620590918466.
[25] C. Xu, X. Wei, L. Liu, L. Su, W. Liu, Y. Wang, P.V. Nielsen, Effects of personalized ventilation interventions on airborne infection risk and transmission between occupants, Build. Environ. 180 (2020) 107008, https://doi.org/10.1016/j.buildenv.2020.107008.

[26] R.S. Papineni, F.S. Rosenthal, The size distribution of droplets in the exhaled breath of healthy human subjects, J. Aerosol Med. 10 (1997) 105–116, https://doi.org/10.1089/jam.1997.10.105.
[27] E. Mundt, H.M. Mathisen, P.V. Nielsen, A. Moser, Ventilation Effectiveness. REHVA Guidebook No.2, REHVA, 2004.
[28] Epple, P.; Steppert, M.; Florschütz, M.; Dahlem, P. Partition walls as effective protection from bio-aerosols in classrooms – an experimental investigation. *GMS Hygiene and Infection Control; 16:Doc09* 2021, doi:10.3205/DGKH000380.
[29] N. Izadyar, W. Miller, Ventilation strategies and design impacts on indoor airborne transmission: a review, Build. Environ. 218 (2022) 109158, https://doi.org/10.1016/j.buildenv.2022.109158.
[30] Y.E. Cetin, M. Avci, O. Aydin, Influence of ventilation strategies on dispersion and removal of fine particles: an experimental and simulation study, Sci. Technol. Built. Environ. 26 (2020) 349–365, https://doi.org/10.1080/23744731.2019.1701332.
[31] Eddy Rusly, Mirek Piechowski, CFD modelling for swirl diffuser and its implications on air change effectiveness assessment to green star's IEQ-2, in: Proceedings of Building Simulation, 2011.
[32] P. Mishra, Swirl diffuser design and performance characteristics for air flow in air conditioning of an automobile-a review, Int. J. Innov. Res. Dev. 4 (2015) 67–75, *volume*.
[33] S. Nateghi, S. Marashian, J. Kaczmarczyk, S. Sadrizadeh, Resource-efficient design of integrated personal exhaust ventilation and physical barriers for airborne transmission mitigation: a numerical and experimental evaluation, Build. Environ. 268 (2025) 112336, https://doi.org/10.1016/j.buildenv.2024.112336.
[34] C.Y.H. Chao, M.P. Wan, A study of the dispersion of expiratory aerosols in unidirectional downward and ceiling-return type airflows using a multiphase approach, Indoor Air 16 (2006) 296–312, https://doi.org/10.1111/j.1600-0668.2006.00426.x.
[35] B. Ghosh, H. Lal, A. Srivastava, Review of bioaerosols in indoor environment with special reference to sampling, analysis and control mechanisms, Environ. Int. 85 (2015) 254–272, https://doi.org/10.1016/j.envint.2015.09.018.
[36] A.C.K. Lai, L.T. Wong, K.W. Mui, W.Y. Chan, H.C. Yu, An experimental study of bioaerosol (1–10 Mm) deposition in a ventilated chamber, Build. Environ. 56 (2012) 118–126, https://doi.org/10.1016/j.buildenv.2012.02.027.
[37] D. Zukowska, A.K. Melikov, Z.J. Popiolek, Thermal plume above a simulated sitting person with different complexity of body geometry: roomvent - 10th international conference on air distribution in rooms, Roomvent 3 (2007) 191–198.

Sustainable Cities and Society 103 (2024) 105282

Contents lists available at ScienceDirect

Sustainable Cities and Society

journal homepage: www.elsevier.com/locate/scs

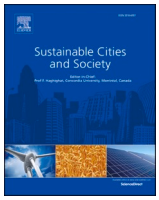

Compatibility of integrated physical barriers and personal exhaust ventilation with air distribution systems to mitigate airborne infection risk

Seyedkeivan Nateghi *, Jan Kaczmarczyk

Department of Heating, Ventilation and Dust Removal Technology, Faculty of Energy and Environmental Engineering, Silesian University of Technology, 44-100 Gliwice, Poland

ARTICLE INFO

Keywords:
Physical barrier
Personal exhaust
Ventilation mode
Airborne transmission

ABSTRACT

This study investigated the effectiveness of integrating desk partitions and personal exhaust ventilation to mitigate airborne infection risks in areas where people sit closely together. Experiments were conducted in a test chamber equipped with different air distribution systems, including two different mixing and one displacement ventilation. N_2O tracer gas was utilized to study airborne transmission between occupants. Results showed effectiveness of preventive measures varied depending on air distributions. In the absence of preventive measures, mixing ventilation systems exhibited higher infection risk compared to displacement ventilation. After the introduction of physical barriers, N_2O concentration increased at two measurement points in presence of one of the mixing ventilation systems. In contrast, the other mixing ventilation and displacement ventilation showed a reduction in N_2O concentration, up to 63 % and 43 %, respectively, depending on measurement points. Combination of physical barriers and personal exhaust ventilation consistently reduced N_2O concentration by 34 % to 83 %, depending on measurement point's location and type of air distribution. Furthermore, higher airflow rates of personal exhaust increased efficiency of proposed strategy in limiting infection risk. This study supports employing physical barriers and personal exhaust ventilation to reduce airborne infection risks. Tailoring preventive measures to specific air distribution system is crucial.

1. Introduction

In response to the worldwide challenge posed by COVID-19 pandemic, there has been a significant focus on mitigating the transmission of infections, particularly in building environments. The urgency of the current global health crisis underscores the need for comprehensive solutions applicable across diverse regions (Balogun et al., 2020). The World Health Organization (WHO) has introduced various policies and guidelines to prevent virus transmission in public places (*World Health Organization. Infection Prevention and Control during Health Care When COVID-19 Is Suspected: Interim Guidance, 19 March 2020. World Health Organization;, 2020.*, n.d.). People who have contracted the virus release viral particles attached to the saliva in the air when they speak, cough, or sneeze (V et al., 2020). Airborne transmission can occur directly between individuals in close proximity (short-range transmission) or indirectly through the mixing of exhaled pathogens with room air (long-range transmission) (Asif et al., 2022). Indirect transmission is particularly critical in spaces with inadequate ventilation and high occupancy levels during extended periods of exposure (Leung, 2021). Physical barriers have been widely employed as a preventive measure due to their affordability and ease of implementation (*Eykelbosh A. A Rapid Review of the Use of Physical Barriers in Non-Clinical Settings and COVID-19 Transmission. Vancouver, BC: National Collaborating Centre for Environmental Health (NCCEH). 2021 Nov.*, n.d.), especially in spaces where occupants stay close to each other. However, it is important to acknowledge that physical barriers can also introduce limitations, such as potential disruptions to air distribution, which can impact their effectiveness in reducing infection risk. Previous studies have examined the efficacy of physical barriers in reducing respiratory droplet transmission (Rooney et al., 2021).

Chen et al. conducted a study to assess the impact of barrier heights on the spread of aerosol particles in an open office environment (Ren et al., 2021). Their findings revealed that a minimum barrier height of 60 cm above the desk surface is necessary to effectively prevent the transmission of viruses. However, for workstations located further away from the outlet, the effectiveness of physical barriers in reducing transmission was found to be less significant. In a densely occupied canteen, Zhang et al. conducted experimental investigations to examine

* Corresponding author.
E-mail address: seyedkeivan.nateghi@polsl.pl (S. Nateghi).

https://doi.org/10.1016/j.scs.2024.105282
Received 7 October 2023; Received in revised form 16 February 2024; Accepted 16 February 2024
Available online 17 February 2024

the effect of physical partitions on the risk of short-distance cross--infection (Ye et al., 2021). The results demonstrated that partitions were effective in mitigating short-distance airborne transmission, thereby reducing the risk of infection. However, the presence of physical partitions also resulted in the accumulation of expiratory air within the compartments, which may have implications for air quality management. Similarly, Dacunto et al. investigated the dispersion of aerosols in a university classroom by implementing three-sided clear dividers attached to student desk surfaces (Dacunto et al., 2022). The use of partitions resulted in a decrease in overall contaminant concentrations in most cases compared to desks without partitions. Mentioned studies highlighted the importance of physical barriers in reducing infection transmission, but they also emphasize the need to consider factors such as barrier height, room air distribution, and ventilation conditions (Zhang et al., 2022). It is important to note that while physical barriers can reduce airborne transmission, they do not completely eliminate the risk (Bagherirad et al., 2014).

While physical barriers play a significant role in reducing direct airborne transmission, personalized ventilation (PV) systems recently have been used extensively as a separate strategy to address mitigating infection transmission (Izadyar & Miller, 2022). PV systems provide targeted clean air by supplying fresh air or exhausting exhaled air of occupants, offering enhanced protection from infection transmission in short-range scenarios (W. Liu et al., 2021). Previous studies have investigated the efficacy of PV systems in reducing airborne transmission risks (Katramiz et al., 2022). Liu et al. conducted a study to explore the potential of personalized ventilation (PV) in reducing the risk of cross-infection between occupants in close proximity within indoor environments (W. Liu et al., 2021). The PV system, with adjustable flow rates, HEPA filtration, and a circular nozzle emulating aircraft cabin or coach airflow patterns, was optimized for improved thermal comfort and ventilation efficiency. The findings revealed that PV was effective in decreasing the infection risk for individuals when compared to relying solely on mixing ventilation. Notably, the side-by-side orientation was identified as a crucial factor in airborne risk control with PV, as it facilitated the lateral diffusion of infectious droplets toward adjacent occupants. Some well-designed PV systems provide an excellent approach to controlling infection risks by Personalized Exhaust (PE) (Pantelic & Tham, 2011). Yang et al. introduced an innovative personalized ventilation (PV) – personalized exhaust (PE) system that was designed to effectively remove exhaled air from the vicinity of an infected individual (Yang et al., 2015). The personalized ventilation (PV) system was delivered outdoor air via PV air terminal devices, complemented by two distinct PE-integrated chairs, namely Shoulder-PE and Top-PE, each equipped with adjustable local exhaust devices, ensuring the inhaled air quality in the controlled environment. The results demonstrated that the combined PV-PE system, implemented for a healthy person, resulted in the lowest intake fraction of contaminated air. Furthermore, when considering the infected person alone, utilizing the PE system alone yielded superior performance compared to solely relying on the PV system for the healthy individual. In an experimental study, Karam et al. proposed the integration of a localized chair exhaust device with a downward piston ventilation system in an educational setting (Karam et al., 2022). They found that to ensure practical use in educational spaces, the DPV system should be operated at a rate of 60 L/s per person, accompanied by a localized chair exhaust operating at rate of 20 L/s. This configuration maintained a high level of protection provided by the downward piston ventilation system while achieving significant energy savings, reducing the overall system energy consumption by 51 % compared to the reference case which was the operation of downward piston ventilation without the implementation of the localized chair exhaust devices. Mentioned studies highlight the effectiveness of PE systems in mitigating infection transmission and emphasize their distinct role in addressing indirect transmission. The local exhaust might significantly enhance system efficiency in all environments, particularly when the personal exhaust is located close to the occupants (Pantelic et al., 2009). While previous studies have made significant strides in understanding the efficacy of physical barriers and personalized ventilation systems in reducing infection transmission risks, it's important to acknowledge certain aspects that have remained unexplored. Notably, past research has primarily focused on the effectiveness of these strategies separately. Additionally, comparing the compatibility of various air distribution methods in airborne transmission within densely populated spaces has not been systematically studied. Evaluating the compatibility of a new approach under various environmental conditions enhances the credibility and sustainability of the solution making the study more comprehensive (Amirzadeh et al., 2023).

This study aims to contribute insights applicable on a global scale by investigating the potential of two possible strategies for mitigating airborne transmission risk, i.e. physical barriers and personal exhaust ventilation, specifically in densely populated spaces such as public buildings, clinical environments, schools, and offices. Different ventilation systems, including mixing and displacement will be examined, to evaluate the impact of various air distribution methods on airborne transmission. Additionally, the compatibility of each air distribution system will be assessed with the proposed prevention strategies designed to reduce infection risk. This study investigates the potential of physical barriers in mitigating infection transmission as well as proposes a new approach that combines physical barriers and personal exhaust ventilation. To assess the efficiency of this innovative system, experiments were conducted at different flow rates. Six heated dummies were used to simulate seated occupants and employed tracer gas to replicate the behaviour of fine droplet nuclei exhaled by an infected person. Concentration measurements of N_2O were taken at three points near the source location to assess the effectiveness of the proposed strategy in reducing airborne contaminant concentrations and consequently transmission risks. Overall, this research contributes to the global effort in combating the spread of airborne infections, with the ultimate goal of enhancing global health resilience in the face of the ongoing pandemic and potential future threats.

2. Methodology

2.1. Experimental setup

Experimental investigations were carried out within a test chamber measuring 9 × 6 × 3.3 m. Three desks were arranged in a row with 0.55 m between them. The desks were positioned centrally within the test chamber, as shown in Fig. 1. Six heated dummies, two at each desk, were used to simulate the presence of occupants with low seating activity each with a sensible heat load of 60 W. Each dummy was constructed as a 1.10 m in height cylindrical steel tube with 0.40 m in diameter, resulting in a surface area of 1.63 m^2, which corresponds to a 15-year-old child. The cylinder was painted grey.

The test room was equipped with three different air distribution systems: two designs of mixing ventilation and one displacement ventilation system. Only one system was installed and studied at a time. Mixing air distribution system denoted as MV_1, employs an air fabric supply duct with small nozzles located centrally above the desks and the exhaust grill placed at a floor level. This setup is shown in Fig. 2a. The other mixing ventilation system, referred to as MV_2, employs a distinctive configuration. In this setup, four ceiling air terminal devices are positioned on both sides of the room, as indicated in Fig. 2b. Each terminal device integrates both air supply air and air exhaust. The air was supplied with a square diffuser downwards and the exhaust air was extracted with the grilles located above the supply. Lastly, the third air distribution system adopts the Displacement Ventilation (DV) approach. In this configuration, two displacement diffusers were placed on the floor in the front corners, see Fig. 2c. The air was exhausted with grills located at the ceiling in the back side of the room.

In this study, all experimental trials were conducted in the same

Fig. 1. Photo of the test room with desks and heated dummies.

controlled environment and chamber indicated in Fig. 1. The variations depicted in Fig. 2 solely arise from the distinct ventilation systems employed, allowing for a comprehensive assessment of their individual effects on airborne infection risks.

2.2. Design of physical barriers (PB) and personal exhaust (PE) system

Transparent partitions were meticulously designed and constructed to be placed on the desktops, as illustrated in Fig. 3. Each partition consisted of a front panel measuring 65 × 138 cm and three side panels, two at the desk edges and one separating occupants. A plenum box was attached to the front side of a partition. It had a narrow slot opening, with a height of 1 cm and the whole table width. The slot was used to extract the air at the tabletop level. The plenum box was attached to exhaust duct with a flow measuring device and variable motor fan removing the air outside the test chamber. The authors successfully implemented the designed system in a previous study (Nateghi et al., 2023).

2.3. Tracer gas dosing and measurements

In order to mimic airborne viruses, present in the exhaled air of an infected individual, N_2O (nitrous oxide) was used as a tracer gas. Tracer gas simulations are effective for replicating the movement of particles smaller than 3–5 μm, such as droplet nuclei released from respiratory tracts. (Ai et al., 2020). A constant flow of N_2O at rate of 0.532 L/min obtained by mass flow controller (Bürkert Communicator) was mixed with air and supplied through an 8 mm opening tube at a constant airflow rate of 14 L/min. The meticulous mass flow controller, ensuring a constant flow of the tracer gas independent of pressure and flow resistance, enhances the accuracy and reliability of dosing experiment. The end of the tube was placed on the edge of the cylinder representing "infected" occupant. To quantify the concentration of the tracer gas, Fast Concentration Meters (FCMs), utilizing non-dispersive infrared absorption (NDIR) technology, were employed at a sampling rate of 4 Hz and a time constant of 0.8 s. NDIR-based FCMs measure the absorption of infrared light to accurately and continuously analyse the concentration of N_2O. Only instruments based on NDIR absorption method are fast enough to follow the respiration cycle. NDIR provides tracer gas concentration measurements with an uncertainty of ±20.0 ppm at a 95 % confidence level (Kierat & Popiolek, 2017). The instruments were intercalibrated before and after measurements to reduce the measuring error.

2.4. Experimental procedure and conditions

To evaluate the efficacy of the developed system, various scenarios were analysed and compared. The baseline cases, without any preventive measures, were used as a reference point to assess the impact of different preventive measures. The effectiveness of these measures was evaluated under three different air distribution principles (MV_1, MV_2, and DV), considering the use of partitions alone as well as the integration of partitions with a personal exhaust system. Under all the indoor space was ventilated using 148 L/s of fresh air, resulting in an air change rate of 3 h^{-1}. The variations during the tests were ±10 L/s. The supply air temperature was kept at 20 ± 1 °C. In all studied cases, the average room air temperature was set at 22 ± 1 °C and relative humidity at 40 ± 10%. The efficiency of the personal exhaust ventilation was investigated at 9 L/s/person for all three ventilation systems tested. In case of MV_2 there were two additional air flow rates of 4, and 12 L/s per person tested. While using personal exhaust ventilation, the air extraction was balanced by matching the ventilation rate of the main exhaust system with the personal exhaust flow rate. Table 1 provides a comprehensive overview of the various scenarios and their corresponding configurations.

Measurements of N_2O concentration were conducted continuously at the three locations of the occupants in the closest proximity to the source of infection. The sampling tube was placed approximately 1.1 m above the floor at a distance of 0.02 m from the cylinder. The measuring points are labelled as 1, 2, and 3 (Fig. 1). Each measurement lasted at least 1 h. Concentration data were recorded continuously, but only data obtained under steady state of N_2O concentration were taken for the analysis. Fig. 4 illustrates the monitored N_2O concentration at all points during each ventilation system. The initial step involved measuring N_2O concentration without preventive measures until reaching the equilibrium concentration value, which was the longest period. Subsequently, physical barriers and personal exhaust were introduced, respectively, until steady states were achieved. The recorded signals exhibited moderate fluctuations and deviations in concentration levels due to noise and brief instabilities caused by minor turbulence within the flow (Kierat & Popiolek, 2017).

3. Results

Fig. 5 presents the average N_2O concentration values at equilibrium obtained at three points under various scenarios. Concentrations differed between the conditions studied and between measured points. In general, higher N_2O concentrations were obtained in rooms without any prevention mean, ie without partition and personal exhaust. An exception was found in MV_1, where the introduction of partitions alone

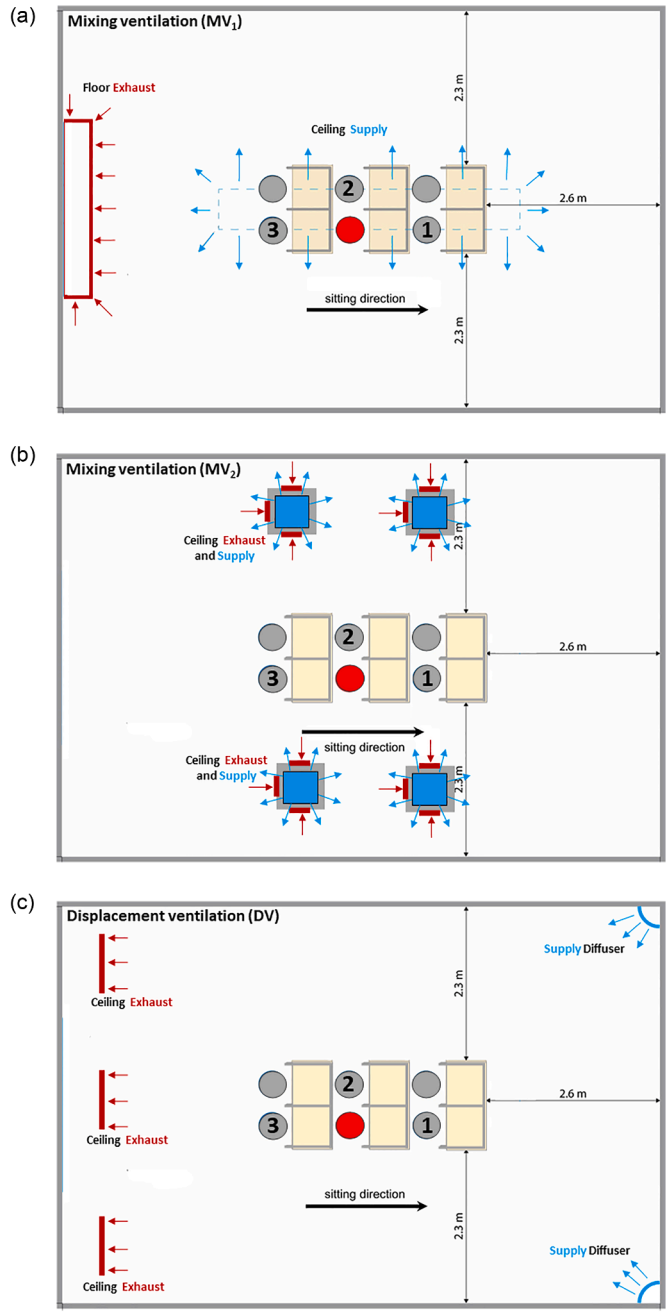

Fig. 2. Test room arrangement. (a): Mixing ventilation, MV_1. (b): Mixing ventilation, MV_2. (c): Displacement ventilation, DV. Red circle is infected and grey circles are susceptible occupants. 1, 2, and 3 indicate measurement points.

worsened the condition at points 2 and 3 compared to the condition without physical barriers.

To comprehensively evaluate the impact of the ventilation system and the applied prevention methods at each exposure individual location, i.e. each measuring point was analysed separately. The analysis was conducted using the equilibrium N_2O concentration value at each point related to the local maximum equilibrium value according to Eq. (1):

$$N_i = \frac{c_i}{c_{max,i}} \tag{1}$$

in which N_i represents the normalized equilibrium concentration value for point i, c_i is the equilibrium N_2O concentration (ppm) for point i, and $c_{max,i}$ is the maximum equilibrium N_2O concentration value (ppm) in point i. The normalization method based on local maximum value was chosen for its simplicity and effectiveness, providing a dimensionless index for meaningful comparisons across scenarios. By expressing concentrations as fractions of the maximum observed at specific points, this approach yielded a specific value for different prevention measures and air distribution, which was comparable on the same scale for each point. The higher N_i index indicates the greater likelihood of cross-infection. Since the normalization is based on the local maximum equilibrium concentration, the analysis of the results is presented separately for each measurement point. At each point, there were nine values representing nine different conditions (comprising three air distribution systems for each of the three prevention measures). An index with a maximum value of 1 is obtained for each point representing the local maximum equilibrium value.

3.1. Point 1

The individual, positioned in front of the pollution source, was considered as the first measurement point. The ventilation system MV_1, devoid of any additional prevention measures, exhibited the highest normalized concentration value (N_1=1) as shown in Fig. 6. Two other air distribution systems also registered elevated values in the absence of prevention measures. Adding only physical barriers (PE=0) yielded varying outcomes, contingent upon the type of air distribution system employed. Incorporating PB with MV_1 had minimal impact on reducing the risk of infection transmission. Conversely, in the MV_2 and DV air distribution systems, the normalized concentration of N_2O was notably reduced to 0.53 and 0.44, respectively. Implementing physical barriers in combination with personal exhaust ventilation (PE=9 L/s per person) led to a significant reduction of normalized N_2O concentration in all three air distributions. Displacement ventilation demonstrated the best performance in limiting likelihood of cross-infection by reducing normalized concentration to 0.23.

3.2. Point 2

The second point of assessment focused on the vulnerable individual beside the infection source, where the infected individual and an exposed person were seated together at a shared desk. As indicated in Fig. 7, the lowest normalized concentration among scenarios without applied prevention measures was observed in displacement ventilation condition. In the configuration involving designed physical barriers, a divider was employed to separate the local environment for two occupants at a common desk. The separator yielded favourable conditions for air distributions MV_2 and DV, reducing the normalized concentration compared to scenarios without any protective measures. However, in air distribution MV_1, the partitions not only failed to reduce the normalized concentration but increased this value significantly leading to increased probability of being infected. Consequently, the highest normalized concentration at Point 2 (N_2 =1) was observed when partitions were utilized in air distribution MV_1. Similar to Point 1, the implementation of personal exhaust ventilation integrated with partitions resulted in a reduction in N_2O concentration in all three air distributions. The lowest normalized concentration was observed in displacement ventilation when partitions were employed in conjunction with personal exhaust flow rate of 9 L/s per person (N_2=0.07).

3.3. Point 3

The third assessment point concentrated on the individual situated behind the source of infection. Investigation of location behind the infection source was crucial because implementation of partitions could change air flow distribution. In contrast to points 1 and 2, the lowest normalized concentration among the air distributions without any preventions was observed in mixing ventilation system MV_2, as shown in Fig. 8. Within the implemented physical barrier setup (PE=0), notable

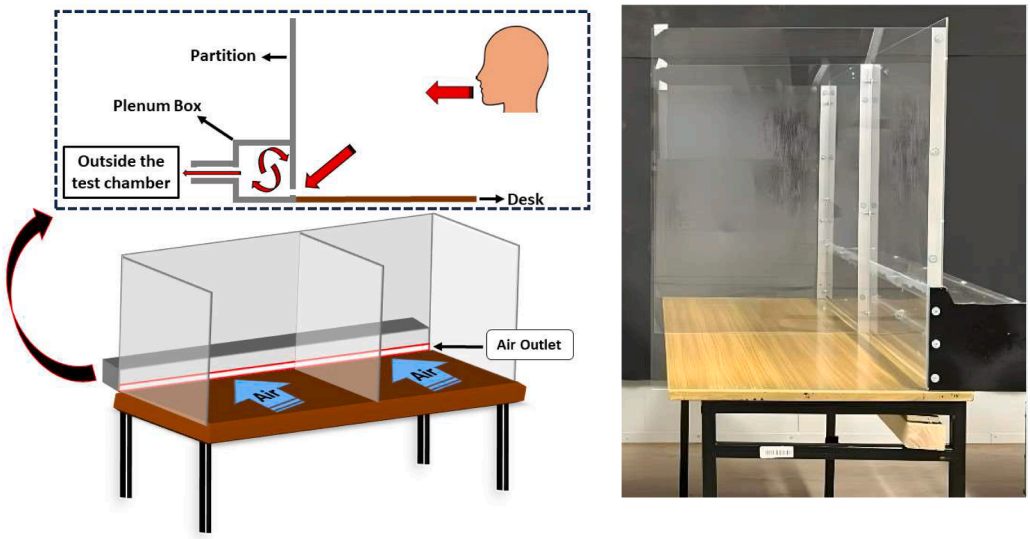

Fig. 3. Real setup picture (right) and diagram (left) depicting a two-person desk with integrated partitions and a personal exhaust system.

Table 1
Overview of measurement scenarios.

Ventilation principle	Physical barrier (PB)	PE flow rate (L/s per person)
MV_1	×	×
	ü	0, 9
MV_2	×	×
	ü	0, 4, 9, 12
DV	×	×
	ü	0, 9

reduction of normalized concentration was observed in DVand MV_2 compared to scenarios without any protective measures. However, similar to point 2, the physical barriers failed to decrease the normalized concentration in air distribution MV_1, but also led to increase N_3 to 1, due to airflow blockage and alteration. As a result, the highest normalized concentration at Point 3 was observed when only partitions were employed in MV_1. The utilization of partitions combined with personal exhaust ventilation (PE=9), reduced the concentration at Point 3 across all three air distributions. The lowest normalized concentration occurred in air distribution MV_2 when partitions was combined with personal exhaust ventilation (N_3=0.22). However, contrary to expectations, the normalized N_2O concentration was relatively high in conditions where DV was employed. It is justifiable that in displacement ventilation, exhaled air containing N_2O is lifted by the convective flow above the dummy and directed toward the room air exhaust at the back of the room.

3.4. Personal exhaust flow rate

The assessment of the effect of airflow rate of personal exhaust on mitigating the risk of transmission was conducted for MV_2. In the previous section, where an air flow rate of 9 L/s per person was used for PE, it was shown that personal exhaust ventilation has a significant effect on reducing the risk of infection transmission. Comparing the efficiency of different flow rates helps to improve the proposed system in terms of reducing the risk of infection transmission. Fig. 9 illustrates the concentration of N_2O at various points by manipulating the airflow rate of the personal exhaust (PE) system. In the case of the lowest PE flow rate (4 L/s), the highest concentrations were observed at point 1, which represents the location in front of the infection source. Points 2 and 3 exhibited relatively similar concentrations across all airflow rates. Increasing the PE flow rate from 4 to 9 L/s per person, resulted in a relative decrease in N_2O concentration at all three points. Subsequently, when the flow rate was further increased from 9 to 12 L/s, N_2O concentration experienced a steeper decline, reaching the range of 5 ppm at all points. Considering the negligible impact on N_2O concentration at higher flow rates, higher flow rates were disregarded.

4. Discussion

Analyses were conducted with the aim of evaluating the effectiveness of prevention strategies and compatibility of different air distributions in reducing airborne infection risks. Due to the applied tracer gas method the analysis focused on the transmission of small droplet nuclei. Three measurement points close to the infection source were selected, as they represent highly exposed individuals. N_2O tracer gas has been widely employed in previous research due to its advantages, which include low background concentration, inertness, and non-toxicity at low concentration levels(M. Bivolarova et al., 2017; Cermak & Melikov, 2007; Kierat et al., 2018; Nielsen et al., 2011, 2012; Qian et al., 2006). Moreover, it does not substantially change the characteristics of exhaled air, as it has the same density as CO_2. Lipczyńska, et al. employed N_2O in the inhaled air of the thermal manikin and used the measured concentration values to calculate infection probability (Lipczynska et al., 2022). The decrease in N_2O concentration indicates a reduced risk of transmitting infections, as the concentration values measured can be linked to the probability of infection transmission (Shao & Li, 2020).

4.1. Without prevention

The study investigated one displacement and two mixing air distribution systems. By including two different mixing ventilation designs, the study aimed to assess how variations in the location and arrangement of supply and exhaust components within the room might impact contaminant distribution. When comparing different air distribution systems without any preventive measures, significant variations in infection risk were observed. Mixing ventilation systems exhibited the higher infection risk, while displacement ventilation system demonstrated the lowest. At Points 1 and 3, located in front of and behind the pollution source, MV_1 exhibited the highest N_2O concentration, reaching 66 ppm and 45 ppm, respectively. MV_1, which directed airflow from above individuals, led to the dispersion of tracer gas both in front of and behind the infected person. The point positioned beside the source, recorded the highest N_2O concentration in MV_2, reaching 58 ppm. MV_2, supplying airflow from the sides of the infected person, resulted in lateral dispersion of N_2O. In contrast, DV, which introduced airflow

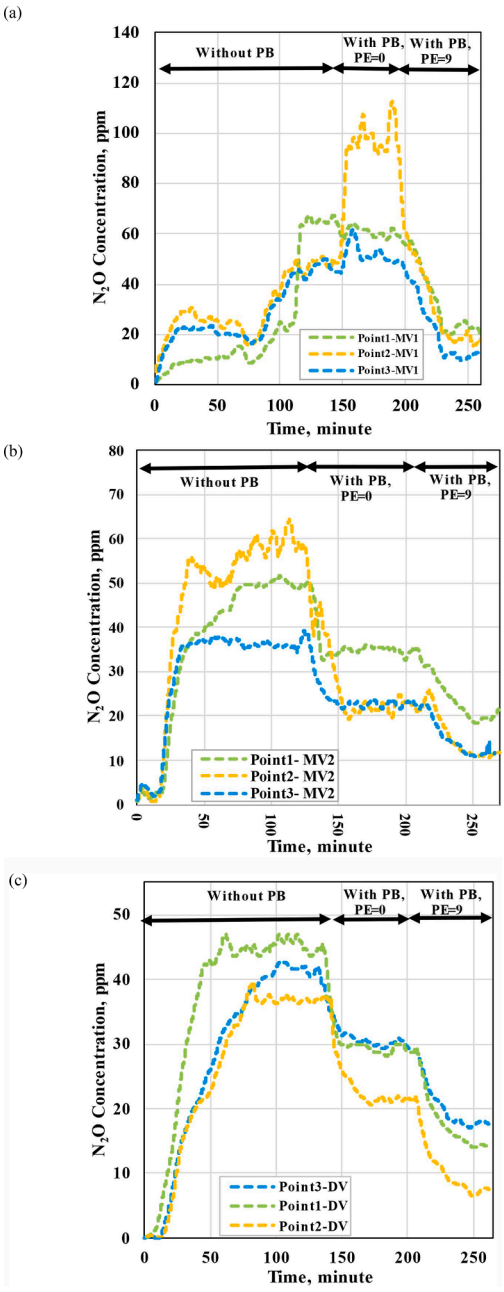

Fig. 4. Monitored N2O concentration. (a): MV1, (b): MV2, (c): DV.

from the back of occupants, maintained the lowest N_2O concentration at Points 1 and 2. This phenomenon can be attributed to a specific flow pattern associated with displacement ventilation, where clean air from the floor level is drawn into the convective flow around the heated dummy. To further validate these findings, CFD simulation can offer stronger confirmation of this hypothesis (Kosutova et al., 2018; Lin et al., 2005; Serra & Semiao, 2009). Overall, displacement ventilation maintained the lowest N_2O concentrations across measurement points, establishing it as the most effective air distribution system in reducing contamination risk. In the comparison of the two mixing ventilation systems, MV_1 consistently exhibited higher concentrations than MV_2, indicating that MV_1 was the least effective among the three air distribution systems. Supporting our results, Yonggao et al. found that when the exhaust of the displacement ventilation system is positioned at the ceiling, it outperforms mixing ventilation in reducing airborne infection risk (Yin et al., 2009).

4.2. *Physical barrier (PE=0)*

There is no doubt that a physical barrier proves effective in obstructing an individual's exhalation, thus serving as a valuable measure for significantly reducing the likelihood of cross-infection among individuals seated closely together. Additionally, the utilization of partitions offers increased surfaces for virus-laden droplets to adhere to. Wang et al. (Wang et al., 2021) identified that expiratory droplets could settle on the partition surfaces. Nevertheless, the findings of our current investigation also indicate that partitions lead to the accumulation of exhaled air within the compartment partially enclosed by the partition and the desk, a phenomenon supported by a computational analysis conducted by Liu et al. (Z. Liu et al., 2021). While partitions effectively mitigate short-range exposure, they do not reduce the dispersion of exhaled air into the room, thereby maintaining the risk of long-distance airborne transmission resulting from increased room concentration. In MV_1, point 2, where an infected individual and an exposed person were seated together, partitions as a preventive measure proved to be ineffective. Interestingly, adding partitions not only failed to reduce the N_2O concentration but also led to a doubling in N_2O concentration due to airflow blockage. As in previous studies where the side-by-side direction was identified as critical (W. Liu et al., 2021), presented results underscore the high potential of infection transmission of side-by-side occupants when using physical barriers strategy. Also at Point 3, located behind the infection source, presented similar challenges due to the potential airflow alterations caused by partitions. Physical barriers applied in the room with the mixing (MV_1) air distribution system caused an 8 % increase in N_2O concentration at Point 3, and 7 % reduction at Point 1, indicating limited effectiveness. This highlights the importance of considering airflow dynamics and the specific characteristics of the air distribution system when implementing partitions. However, the other two systems exhibited strong compatibility with the

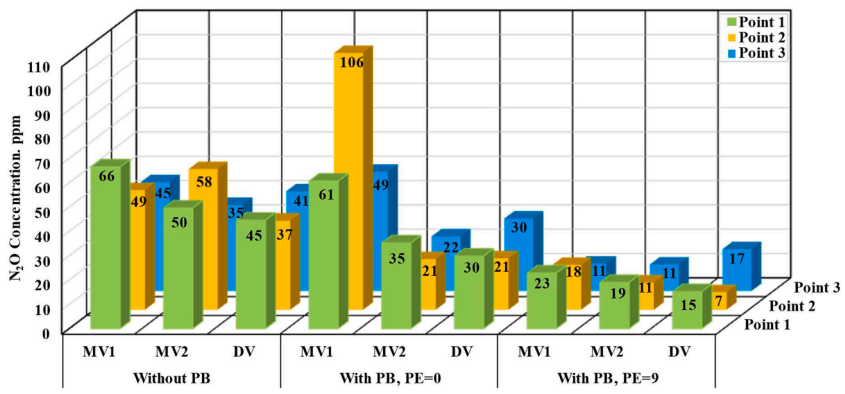

Fig. 5. N_2O concentrations measured at three points in three examined scenarios.

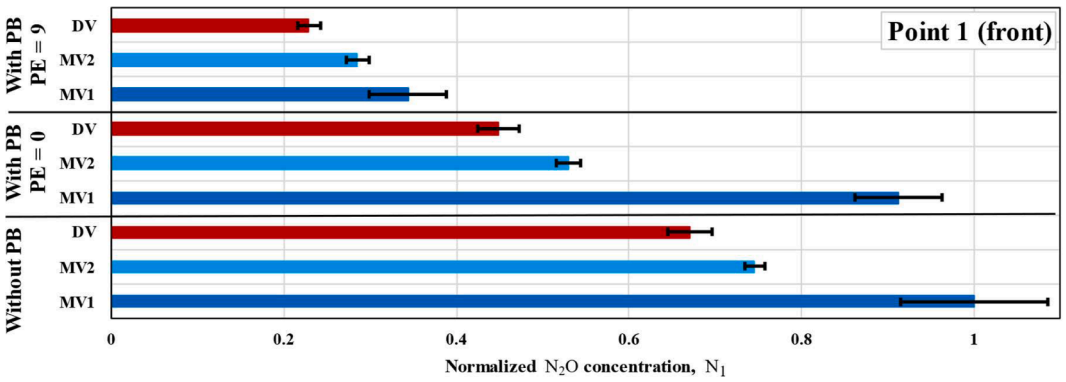

Fig. 6. Normalized N_2O concentrations in front of source (Point 1).

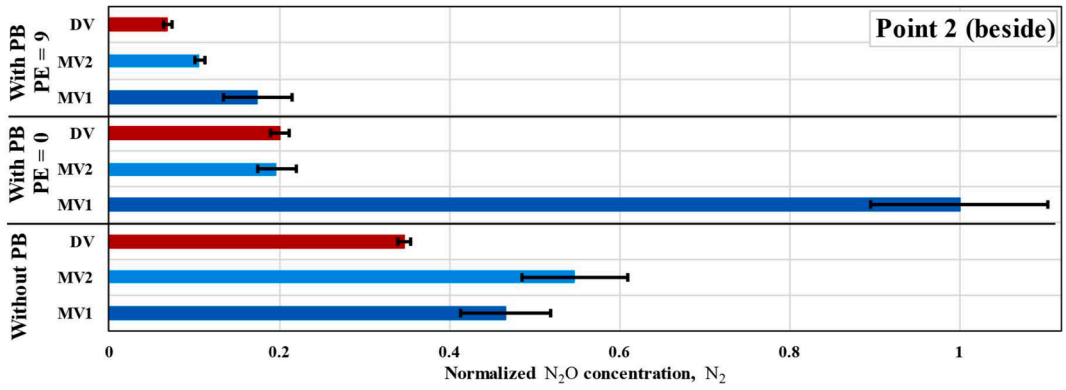

Fig. 7. Normalized N_2O concentrations next to the source (Point 2).

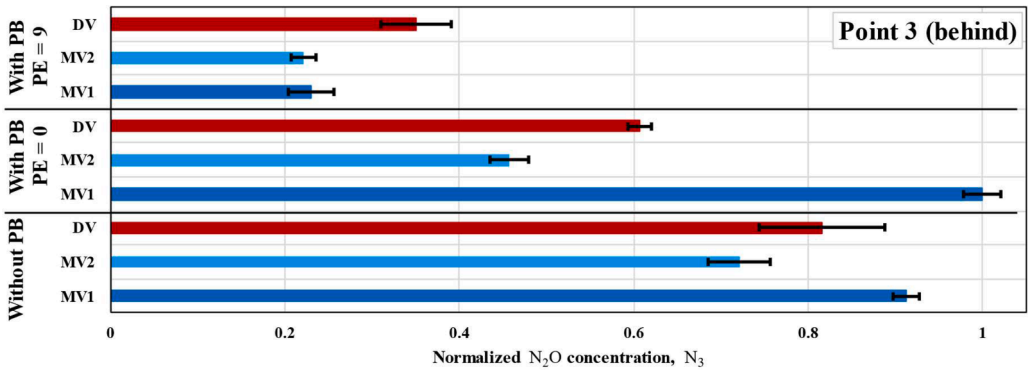

Fig. 8. Normalized N_2O concentrations behind the source (Point 3).

implemented partitions. In MV_2, the use of partitions resulted in a reduction of the N_2O concentration at points 1, 2, and 3 by 30 %, 63 %, and 37 %, respectively. Similarly, in the DV system, adding partitions reduced the N_2O concentration at all points. N_2O concentration reduction at points 1, 2, and 3 when using only partitions was 33 %, 43 %, and 25 %, respectively. The effectiveness of partitions depends on the specific characteristics of the air distribution system. Overall, as highlighted by Ren et al., the implementation of physical barriers can diminish the likelihood of infection risk, contingent upon a comprehensive understanding of the ventilation system's impact on airflow and pollutant concentration (Ren et al., 2021).

4.3. Integrated physical barriers and personal exhaust

Due to the accumulation of exhaled air within the compartment partially enclosed by the partition and the desk, there is a need for suction devices to reduce the dispersion of exhaled air, in addition to providing protection. The PE suction effect helps in reducing spread of contaminants and cross-contamination risks, as endorsed by Karam, Jennifer, et al., who used two outlets above the manikin's shoulders (Karam et al., 2022). Another localized exhaust design proposed by Bivolarova et al. (M. P. Bivolarova et al., 2023) was a wearable exhaust placed even closer to the contaminant source - mouth. Applying such designs in practice in many cases, such as schools, may be problematic. In this study a personal exhaust is integrated with physical barrier. It has an outlet slot located at the desk level, which does not restrict the occupants' movements and does not limit the view. Results for mixing ventilation MV_1 indicate that the integration of personal exhaust ventilation is crucial for enhancing the effectiveness of physical barriers in reducing airborne infection risks. While adding partitions, N_2O

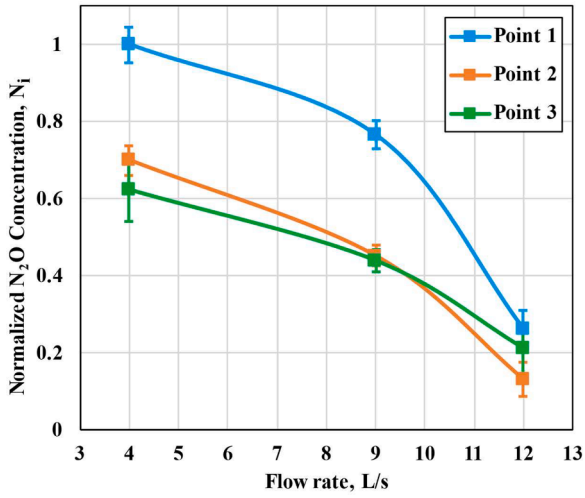

Fig. 9. Normalized N_2O concentrations for different PE flow rates.

concentration at point 2 increased more than twice (from 49 to 106 ppm), the integration of personal exhaust ventilation substantially reduced it by factor 2.5. N_2O concentration reduction trend was observed in all points while operating MV_2 and DV. Remarkably, N_2O concentration values were at the same level across all measured points for the three distinct air distribution systems. The introduction of partitions, while disrupting air mixing by creating barriers, led to localized increase in tracer gas concentration at specific points. However, when the personal exhaust system was operating, its concentrations at all nine measured points were significantly lower compared to the previous cases and showed minimal variation within the space. Consequently, the proposed design demonstrated acceptable compatibility with all three air distribution systems.

To conduct a comprehensive assessment of the proposed system's efficiency, it is imperative to examine the importance of the PE airflow rate. As expected, when the PE flow rate was set at 4 L/s, the normalized concentration exhibited the highest value at each measurement point, indicating the highest infection risk. Increase in PE flow rate to 9 L/s resulted in a noticeable concentration decrease. Specifically, at points 1, 2, and 3, the normalized concentration decreased by 23 %, 35 %, and 30 % respectively. With further exhaust flow rate increase to 12 L/s, the normalized concentration experienced even steeper decline. It decreases by 65 %, 71 %, and 52 % at points 1, 2, and 3, respectively.

The measurement results confirmed that a higher PE airflow rate unquestionably increases occupant protection. An increased air flow may suggest higher energy consumption for its transport. In this case, however, increased airflow of PE was connected with the appropriate decrease of overall exhaust ventilation airflow rate, thus the total flow of air exhausted from the test chamber remained the same. In the proposed approach the PE substitutes the conventional method of exhausting air through the main ventilation system. It facilitates the precise and more efficient removal of pollutants at their source. Nevertheless, it's imperative to emphasize that personal ventilation systems, owing to their complex feature, generally may comprise higher costs compared to the total volume ventilation system.

4.4. Limitations and future studies

- The use of tracer gas in the study accurately represents smaller aerosols (M. Bivolarova et al., 2017) influenced by air distribution, but it does not capture the behaviour of larger droplets that have different aerodynamic properties and can settle (Ai et al., 2020). Therefore, it is recommended to employ various methods such as aerosol or particle generation, to gain a comprehensive understanding of the entire aerosol spectrum.
- The measurements were conducted under steady-state conditions, which only partially reflect the complexities observed in practical scenarios where people move and have different head orientations. It is suggested to conduct further research to incorporate dynamic factors in order to more accurately simulate conditions individuals encounter in practice.
- The dosing of tracer gas with exhaled air was simplified to constant exhalation for the sake of the experiment's convenience. Computational fluid dynamics (CFD) analyses have indicated that a simplified constant exhalation model can effectively be utilized for spatial analyses (Bulińska & Buliński, 2017). Nevertheless, it is important to consider more advanced dosing models, encompassing parameters such as coughing, sneezing, etc., in future studies (Nishihara et al., 2023).
- The study chose the normalized concentration index as a measure to assess the exposure risk for an individual. This index is useful for making quick and straightforward predictions regarding pathogen exposure but does not account for the specific infectivity of a particular disease agent. Although various infection risk assessment models are commonly used to project infection risk over time, they consider factors such as pathogen infectivity, viability, and concentration in respiratory fluids. However, these models were not taken into consideration in this study due to the absence of a pandemic scenario.
- Future research should focus on a more completed experimental setup and optimizing various parameters such as the dimension of partitions and the personal exhaust outlet to maximize their effectiveness in mitigating airborne infection risks across different air distribution systems.

5. Conclusion

This study investigated effective strategies for mitigating airborne transmission risks in densely populated spaces between occupants staying in close proximity. Three locations of susceptible occupants in relation to the infected person were considered: in front, side and back. Various ventilation systems, including two mixing ventilation (MV_1 and MV_2) and one displacement ventilation (DV) were examined to assess their compatibility with infection prevention strategies. Preventive measures including a new proposed combination of the physical barrier with personal exhaust ventilation were examined. Analysing the measurement results, the following findings have been obtained:

- In the absence of any additional prevention methods, the displacement ventilation system demonstrated superior performance compared to the two examined mixing ventilation systems in terms of reducing the risk of infection for occupants seated in close proximity to an infected individual.
- The application of a physical barrier alone, without the use of personal exhaust, in rooms with different ventilation systems had varying effects depending on the occupant's location and the specific ventilation system. Conditions improved for all locations in the case of systems MV_2 and DV. However, for MV_1, the conditions deteriorated, especially for occupants seated beside the infected person.
- Integration of physical barriers and personal exhaust ventilation demonstrated a more substantial reduction of infection risk in all three air distributions. Within MV_1, the infection risk was significantly reduced, aligning it with MV_2 and DV, which consistently showed lower risks.
- Comparing the performance of different air distribution systems, MV_2 and DV demonstrated better performance compared to MV_1 in the probability of infection transmission.
- Increasing the flow rate of personal exhaust ventilation further reduces the risk of infection transmission at all points and improves the proposed strategy's efficiency.

- Overall, the result of this study suggests the combination of physical barriers and personal exhaust ventilation as a promising effective way to reduce airborne infection risks and highlights the importance of considering the specific air distribution system when implementing preventive measures.

CRediT authorship contribution statement

Seyedkeivan Nateghi: Writing – original draft, Investigation, Funding acquisition, Formal analysis, Data curation. **Jan Kaczmarczyk:** Writing – review & editing, Supervision, Methodology, Conceptualization.

Declaration of competing interest

The authors declare the following financial interests/personal relationships which may be considered as potential competing interests: Seyedkeivan Nateghi reports was provided by Silesian University of Technology.

Data availability

No data was used for the research described in the article.

Acknowledgments

This research was supported by the Excellence Initiative - Research University program implemented at the Silesian University of Technology in 2023/24 academic year.

References

Ai, Z., Mak, C. M., Gao, N., & Niu, J. (2020). Tracer gas is a suitable surrogate of exhaled droplet nuclei for studying airborne transmission in the built environment. *Building Simulation, 13*(3), 489–496. https://doi.org/10.1007/s12273-020-0614-5

Amirzadeh, M., Sobhaninia, S., Buckman, S. T., & Sharifi, A. (2023). Towards building resilient cities to pandemics: A review of COVID-19 literature. *Sustainable Cities and Society, 89*, Article 104326. https://doi.org/10.1016/j.scs.2022.104326

Asif, Z., Chen, Z., Stranges, S., Zhao, X., Sadiq, R., Olea-Popelka, F., & Yu, T. (2022). Dynamics of SARS-CoV-2 spreading under the influence of environmental factors and strategies to tackle the pandemic: A systematic review. *Sustainable Cities and Society, 81*, Article 103840. https://doi.org/10.1016/j.scs.2022.103840

Bagherirad, M., Trevan, P., Globan, M., Tay, E., Stephens, N., & Athan, E. (2014). Transmission of tuberculosis infection in a commercial office. *Medical Journal of Australia, 200*(3), 177–179. https://doi.org/10.5694/mja12.11750

Balogun, A. L., Marks, D., Sharma, R., Shekhar, H., Balmes, C., Maheng, D., & Salehi, P. (2020). Assessing the Potentials of Digitalization as a Tool for Climate Change Adaptation and Sustainable Development in Urban Centres. *Sustainable Cities and Society, 53*, Article 101888. https://doi.org/10.1016/j.scs.2019.101888

Bivolarova, M., Ondráček, J., Melikov, A., & Ždímal, V. (2017). A comparison between tracer gas and aerosol particles distribution indoors: The impact of ventilation rate, interaction of airflows, and presence of objects. *Indoor Air, 27*(6), 1201–1212. https://doi.org/10.1111/ina.12388

Bivolarova, M. P., Kierat, W., Hvidkjær, S., Stengade, K. A., Illum, T., Boe Gad, S., & Melikov, A. K. (2023). Reduced personal exposure to airborne cross-infection using wearable exhaust ventilation. *E3S Web of Conferences, 396*, 02032. https://doi.org/10.1051/e3sconf/202339602032

Bulińska, A., & Buliński, Z. (2017). A CFD analysis of different human breathing models and its influence on spatial distribution of indoor air parameters. *Computer Assisted Methods in Engineering and Science, 22*(3), 3.

Cermak, R., & Melikov, A. (2007). Protection of Occupants from Exhaled Infectious Agents and Floor Material Emissions in Rooms with Personalized and Underfloor Ventilation. *HVAC&R Research, 13*(1), 23–38. https://doi.org/10.1080/10789669.2007.10390942

Dacunto, P., Moser, D., Ng, A., & Benson, M. (2022). Classroom aerosol dispersion: Desk spacing and divider impacts. *International Journal of Environmental Science and Technology, 19*(2), 1057–1070. https://doi.org/10.1007/s13762-021-03564-z

Eykelbosh, A. (2021 Nov). A rapid review of the use of physical barriers in non-clinical settings and COVID-19 transmission. *Vancouver, BC: National Collaborating Centre for Environmental Health (NCCEH)*. n.d.

Izadyar, N., & Miller, W. (2022). Ventilation strategies and design impacts on indoor airborne transmission: A review. *Building and Environment, 218*, Article 109158. https://doi.org/10.1016/j.buildenv.2022.109158

Karam, J., Katramiz, E., Ghali, K., & Ghaddar, N. (2022). Downward piston ventilation assisted with a localized—Chair exhaust for mitigation of pathogen transport in educational spaces. *Journal of Building Engineering, 58*, Article 105066. https://doi.org/10.1016/j.jobe.2022.105066

Katramiz, E., Ghaddar, N., & Ghali, K. (2022). Novel personalized chair-ventilation design integrated with displacement ventilation for cross-contamination mitigation in classrooms. *Building and Environment, 213*, Article 108885. https://doi.org/10.1016/j.buildenv.2022.108885

Kierat, W., Bivolarova, M., Zavrl, E., Popiolek, Z., & Melikov, A. (2018). Accurate assessment of exposure using tracer gas measurements. *Building and Environment, 131*, 163–173. https://doi.org/10.1016/j.buildenv.2018.01.017

Kierat, W., & Popiolek, Z. (2017). Dynamic properties of fast gas concentration meter with nondispersive infrared detector. *Measurement, 95*, 149–155. https://doi.org/10.1016/j.measurement.2016.10.008

Kosutova, K., Van Hooff, T., & Blocken, B. (2018). CFD simulation of non-isothermal mixing ventilation in a generic enclosure: Impact of computational and physical parameters. *International Journal of Thermal Sciences, 129*, 343–357. https://doi.org/10.1016/j.ijthermalsci.2018.03.001

Leung, N. H. L. (2021). Transmissibility and transmission of respiratory viruses. *Nature Reviews Microbiology, 19*(8), 528–545. https://doi.org/10.1038/s41579-021-00535-6

Lin, Z., Chow, T. T., Wang, Q., Fong, K. F., & Chan, L. S. (2005). Validation of CFD Model for Research into Displacement Ventilation. *Architectural Science Review, 48*(4), 305–316. https://doi.org/10.3763/asre.2005.4838

Lipczynska, A., Bivolarova, M. P., Guo, L., Kierat, W., & Melikov, A. K. (2022). Airborne infection probability in relation of room air distribution: An experimental investigation. *E3S Web of Conferences, 356*, 05014. https://doi.org/10.1051/e3sconf/202235605014

Liu, W., Liu, L., Xu, C., Fu, L., Wang, Y., Nielsen, P. V., & Zhang, C. (2021a). Exploring the potentials of personalized ventilation in mitigating airborne infection risk for two closely ranged occupants with different risk assessment models. *Energy and Buildings, 253*, Article 111531. https://doi.org/10.1016/j.enbuild.2021.111531

Liu, Z., Li, R., Wu, Y., Ju, R., & Gao, N. (2021b). Numerical study on the effect of diner divider on the airborne transmission of diseases in canteens. *Energy and Buildings, 248*, Article 111171. https://doi.org/10.1016/j.enbuild.2021.111171

Nateghi, S. K., Kaczmarczyk, J., & Lipczynska, A. (2023). Potential of physical barriers integrated with personal exhaust ventilation in decreasing airborne infection risk for people. *Journal of Physics: Conference Series, 2600*(10), Article 102020. https://doi.org/10.1088/1742-6596/2600/10/102020

Nielsen, P. V., Olmedo, I., de Adana, M. R., Grzelecki, P., & Jensen, R. L. (2012). Airborne cross-infection risk between two people standing in surroundings with a vertical temperature gradient. *HVAC&R Research, 18*(4), 552–561. https://doi.org/10.1080/10789669.2011.598441

Nielsen, P. V., Olmedo, I., Ruiz de Adana, M., Grzelecki, P., & Jensen, R. L. (2011). Airborne Cross-Infection Risk Between Two People in a Displacement Ventilated Room: ASHRAE IAQ Conference 2010. *IAQ 2010: Airborne Infection Control*.

Nishihara, T., Li, H., Kuga, K., & Ito, K. (2023). Seamless numerical analysis of transient infectious droplet dispersion and inhalation exposure—In silico study. *Building and Environment, 244*, Article 110748. https://doi.org/10.1016/j.buildenv.2023.110748

Pantelic, J., Sze-To, G. N., Tham, K. W., Chao, C. Y. H., & Khoo, Y. C. M. (2009). Personalized ventilation as a control measure for airborne transmissible disease spread. *Journal of The Royal Society Interface, 6*(suppl_6). https://doi.org/10.1098/rsif.2009.0311.focus

Pantelic, J., & Tham, K. W. (2011). Assessment of the ability of different ventilation systems to serve as a control measure against airborne infectious disease transmission using Wells-Riley approach. *Scopus*. https://scholarbank.nus.edu.sg/handle/10635/45912.

Qian, H., Li, Y., Nielsen, P. V., Hyldgaard, C. E., Wong, T. W., & Chwang, A. T. Y. (2006). Dispersion of exhaled droplet nuclei in a two-bed hospital ward with three different ventilation systems. *Indoor Air, 16*(2), 111–128. https://doi.org/10.1111/j.1600-0668.2005.00407.x

Ren, C., Xi, C., Wang, J., Feng, Z., Nasiri, F., Cao, S. J., & Haghighat, F. (2021). Mitigating COVID-19 infection disease transmission in indoor environment using physical barriers. *Sustainable Cities and Society, 74*, Article 103175. https://doi.org/10.1016/j.scs.2021.103175

Rooney, C. M., McIntyre, J., Ritchie, L., & Wilcox, M. H. (2021). Evidence review of physical distancing and partition screens to reduce healthcare acquired SARS-CoV-2. *Infection Prevention in Practice, 3*(2), Article 100144. https://doi.org/10.1016/j.infpip.2021.100144

Serra, N., & Semiao, V. (2009). Comparing displacement ventilation and mixing ventilation as HVAC strategies through CFD. *Engineering Computations, 26*(8), 950–971. https://doi.org/10.1108/02644400910996844

Shao, X., & Li, X. (2020). COVID-19 transmission in the first presidential debate in 2020. *Physics of Fluids, 32*(11), Article 115125. https://doi.org/10.1063/5.0032847

V, A. A. R., R, V., & Haghighat, F (2020). The contribution of dry indoor built environment on the spread of Coronavirus: Data from various Indian states. *Sustainable Cities and Society, 62*, Article 102371. https://doi.org/10.1016/j.scs.2020.102371

Wang, C. T., Fu, S. C., & Chao, C. Y. H. (2021). Short-range bioaerosol deposition and recovery of viable viruses and bacteria on surfaces from a cough and implications for respiratory disease transmission. *Aerosol Science and Technology, 55*(2), 215–230. https://doi.org/10.1080/02786826.2020.1837340

World Health Organization. (2020). Infection prevention and control during health care when COVID-19 is suspected: Interim guidance, 19 March 2020. *World Health Organization*. n.d.

Yang, J., Sekhar, S. C., Cheong, K. W. D., & Raphael, B. (2015). Performance evaluation of a novel personalized ventilation-personalized exhaust system for airborne infection control. *Indoor Air, 25*(2), 176–187. https://doi.org/10.1111/ina.12127

Ye, J., Ai, Z., & Zhang, C. (2021). A new possible route of airborne transmission caused by the use of a physical partition. *Journal of Building Engineering, 44*, Article 103420. https://doi.org/10.1016/j.jobe.2021.103420

Yin, Y., Xu, W., Gupta, J., Guity, A., Marmion, P., Manning, A., & Chen, Q. (2009). Experimental Study on Displacement and Mixing Ventilation Systems for a Patient Ward. *HVAC&R Research, 15*(6), 1175–1191. https://doi.org/10.1080/10789669.2009.10390885

Zhang, C., Nielsen, P. V., Liu, L., Sigmer, E. T., Mikkelsen, S. G., & Jensen, R. L. (2022). The source control effect of personal protection equipment and physical barrier on short-range airborne transmission. *Building and Environment, 211*, Article 108751. https://doi.org/10.1016/j.buildenv.2022.108751

Building and Environment 268 (2025) 112336

Contents lists available at ScienceDirect

Building and Environment

journal homepage: www.elsevier.com/locate/buildenv

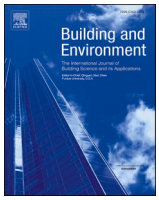

Resource-efficient design of integrated personal exhaust ventilation and physical barriers for airborne transmission mitigation: A numerical and experimental evaluation

Seyedkeivan Nateghi [a,c,*], Shahrzad Marashian [b], Jan Kaczmarczyk [a], Sasan Sadrizadeh [b,c]

[a] Department of Heating, Ventilation and Dust Removal Technology, Faculty of Energy and Environmental Engineering, Silesian University of Technology, 44-100 Gliwice, Poland
[b] School of Business, Society, and Engineering, Mälardalen University, Västerås, Sweden
[c] Department of Civil and Architectural Engineering, KTH Royal Institute of Technology, Stockholm, Sweden

ARTICLE INFO

Keywords:
Airborne transmission
CFD simulation
Physical barrier
Personalized ventilation
Sustainability

ABSTRACT

This study investigates the performance of integrated personal exhaust ventilation and physical barriers in mitigating airborne transmission, addressing the critical need for effective infection control in indoor environments. Using computational fluid dynamics, we modeled aerosol dispersion in a test room and validated these results with experimental data. Experimental validation strengthened the computational findings by providing empirical evidence for system efficacy under varying airflow conditions. We examined various prevention levels, including no prevention measures, only physical barriers, and physical barriers integrated with personal exhaust ventilation. The designed system with a barrier height of 65 cm and a personal exhaust flow rate of 9 L/s per person demonstrated strong efficacy in mitigating airborne transmission. Further numerical analysis was conducted to evaluate the impact of critical parameters, including barrier height and exhaust flow rate, on the aerosol removal efficiency of the integrated system. Results indicate that reducing the barrier height to 45 cm and the exhaust flow rate to 6 L/s per person retains 95% of aerosol removal efficiency, offering the most cost-effective and sustainable design without compromising system's performance in limiting airborne transmission. These findings suggest that moderate adjustments can enhance system sustainability by enabling significant material and energy savings.

1. Introduction

The recent global health crisis (COVID-19) has highlighted the need for effective methods to reduce indoor airborne infection risks [1,2]. The World Health Organization (WHO) has established directives and recommendations to minimize virus spread in public settings [3]. Understanding the transmission routes of these diseases and their characteristics allows for identifying effective prevention and control measures [4–6]. Infected individuals exhale viral particles into the air, posing risks of both short-range and long-range airborne transmission [7–9]. Given the challenges of conducting experiments, Computational Fluid Dynamics (CFD) techniques are widely employed as reliable tools for studying the airborne transmission of pathogens in indoor environments [10–14]. In the past years, numerous studies have examined the flow dynamics of airborne infections. Kotb and Khalil [15] utilized ANSYS-Fluent software to simulate the spread of COVID-19 via sneezing and coughing in a commercial aircraft cabin with a high density of passengers. They found that sneezed droplets could travel farther and affect more seated passengers than droplets from coughing. The speed of movement correlated with increased droplet dispersion. Ren et al. [16] performed numerical simulations on three ventilation strategies in a prefabricated COVID-19 inpatient ward. They discovered that small particles traveled long distances along main airflow streams, with ventilation effectively removing many droplets through exhaust outlets. Larger particles tended to settle on solid surfaces due to gravitational sedimentation in each ventilation strategy across ward regions. Yan et al. [17] used a 3D thermal manikin and a multi-component Eulerian-Lagrangian approach to study the thermal effects of the human body on the dispersion and evaporation of cough droplets. Their findings indicate that human body heat significantly influences droplet mass fraction, and air velocity distributions, and increases the inhalability

* Corresponding author.
E-mail address: seyedkeivan.nateghi@polsl.pl (S. Nateghi).

https://doi.org/10.1016/j.buildenv.2024.112336
Received 11 September 2024; Received in revised form 8 November 2024; Accepted 20 November 2024
Available online 21 November 2024

Nomenclature

F_B	Brownian force
F_D	Drag force
g	Gravitational acceleration
F_e	Additional factors, such as the Thermophoretic force
$D_{i,m}$	Mass diffusion coefficient
$D_{T,i}$	Thermal diffusion coefficient
Sc_t	Turbulent Schmidt number
Y_i	Local mass fraction
U_∞	free-stream air velocity (m/s)
d_c	The characteristic dimension of the obstacle (m).
d	Diameter (m)

Abbreviation

CFD	Computational Fluid Dynamics
WHO	World Health Organization
Covid-19	Corona Virus Disease 2019
LCE	Localized-Chair Exhaust
DPV	Downward Piston Ventilation
PE	Personal Exhaust
PB	Physical Barrier
FCM	Fast Concentration Meters
NDIR	Non-Dispersive Infrared
DRW	Discrete Random Walk
RNG	Re-Normalization Group
EPT	Eulerian Particle Tracking
LPT	Lagrangian Particle Tracking
STK	Stokes number

Greek letters

ρ_p	Particle density (kg/m^3)
μ_g	Molecular dynamic viscosity (kg/m/s)
ρ	Fluid density
υ	Velocity (m^2/s)
ϕ	Solving variables (i.e., velocity, temperature, and concentration)
S_ϕ	Term contributing to sources
μ_t	Turbulent viscosity (kg/m/s)
Γ_ϕ	Effective diffusion coefficient

and infection risks of cough droplets in indoor spaces. Zhang et al. [18] used a Lagrangian model to study the impact of different ventilation systems on the spread of coughed droplets in a conference room. They found that bottom-supply upper-return systems, like Displacement Ventilation, effectively control respiratory disease spread and provide a healthier indoor environment. Yang et al. [19] conducted CFD simulations to examine droplet dispersion carrying viruses or bacteria in a bus. Their research highlighted changes in droplet distribution due to gravity, ventilation, thermal body plumes, and surface deposition mechanisms. Abuhegazy et al. [20] used computational fluid-particle dynamics simulations to study aerosol transport in a classroom, finding that particle size, source location, and mitigation measures like glass barriers and open windows significantly impact aerosol trajectories and deposition. Their results suggest that opening windows can increase particle exit by about 38% and reduce aerosol deposition on people in the room.

Previous research studies, along with the identified concerns and uncertainties regarding infection risks, indicate a necessity for further investigation into virus transmission within indoor environments and the development of strategies to mitigate such transmission. The deployment of physical barriers has emerged as a widely adopted preventive measure, especially in spaces where individuals are in proximity [8,21–25]. These barriers are commonly used to separate workstations, service counters, and communal areas, helping to reduce the risk of direct transmission of airborne particles. However, the effectiveness of these barriers can be influenced by factors such as barrier height and room air distribution [26]. In parallel, personalized exhaust ventilation systems present a targeted approach to mitigating infection transmission [27]. The exhaust vents near the breathing zone of individuals are designed to capture exhaled air directly from the source and significantly decrease the concentration of airborne pathogens in crowded spaces [28,29]. Personal exhaust (PE) ventilation systems, when integrated into educational settings, have showcased efficiency in infection risk reduction while achieving energy savings [30–32]. Numerous studies have used CFD simulations to investigate the physical barriers and personal exhaust ventilation systems, evaluating how various parameters influence their effectiveness in reducing the spread of airborne contaminants. Cheong et al. [33] conducted CFD simulations to investigate the impact of architectural features, such as increased ventilation rates, diffuser positions, and partitions between beds on airborne pathogen dispersion. They showed that increasing the ventilation flow rate is the most effective strategy for reducing pathogen concentration. Mirzaie et al. [23] used CFD to investigate the dispersion of cough droplets containing coronaviruses in a classroom, assessing the impact of ventilation speeds and transparent barriers on droplet concentration. Their results indicated that seat partitions can reduce infection risk, and higher ventilation speeds decrease droplet trapping time by barriers while increasing droplet velocities. Karam et al. [30] proposed integrating a localized-chair exhaust (LCE) device with downward piston ventilation (DPV) to create a safe educational environment while reducing energy consumption. Their CFD model, validated experimentally, demonstrated that this combination, with DPV at 60 l/s per person and LCE at 20 l/s, could maintain high protection levels and thermal comfort with 51% energy savings compared to standalone DPV. The combination of Physical barrier with PE systems, as proposed by Nateghi and Kaczmarczyk [34], has demonstrated promising results in minimizing the intake of contaminated air. They conducted various air distribution systems and demonstrated that the effectiveness of these measures depends on the air distribution type. However, there is still a need to explore how combining physical barriers with personalized exhaust ventilation can control the spread of airborne contaminants in indoor environments. The optimal configuration of these systems, including their aerosol capture efficiency, material usage, visibility, energy consumption, and impact on sustainability and carbon emissions, has not been fully studied due to practical limitations.

This research bridges theoretical concepts with practical applications by combining experimental studies and simulations to offer valuable insights into airborne transmission and infection control. We use CFD simulations to explore the dynamics of airflow and the dispersion of airborne particles in indoor settings. Our experimental studies complement these simulations by measuring air velocity, temperature, and concentrations of airborne particles in a controlled environment. Our main objective is to evaluate how integrated physical barriers and personal exhaust ventilation systems can effectively reduce the risk of airborne transmission by removing airborne particles from indoor spaces. By combining simulation technology with rigorous experimental validation, we provide a detailed analysis of how airflow patterns, physical barriers, and the dispersion of airborne particles interact. Moreover, we focus on CFD modeling, supported by experimental data, to refine and optimize the use of integrated physical barriers and personal exhaust ventilation. Simulations investigate key system parameters, such as barrier height and exhaust flow rate, to determine their

impact on the efficiency of aerosol removal. We aim to find the optimal configuration that maintains aerosol removal efficiency with practical considerations like sustainability, visibility, and energy use. This study employs ANSYS-Fluent software to model the dispersion of aerosols exhaled by an infected person seated in a room with five nearby individuals. The k-ε model is employed to simulate turbulent airflow, solving both the airflow and particle governing equations. The combined use of experimental measurements and simulations provides robust evidence for the efficacy of the proposed integrated system in mitigating airborne transmission risks in indoor environments.

2. Physical model

The selection of the physical model was based on experimental testing conducted in a 9 × 6 × 3.3 m test chamber. Three desks were arranged in a row with a 0.55 m gap between them, positioned centrally in the chamber, as shown in Fig. 1a. The setup included one pollutant source representing an infected person and five measurement points (P1-P5), demonstrating susceptible individuals to capture airborne particles in the vicinity of the breathing zone. Six heated dummies (60 W each), designed to approximate typical high school students engaged in seated activities, were used to simulate occupants. Each dummy was constructed as a cylindrical steel tube, with dimensions of 1.10 m in height and 0.40 m in diameter, resulting in a total surface area of 1.63 m^2. Although cylindrical geometry does not capture all anatomical details of a human body, it was chosen based on its ability to generate accurate enthalpy flux and buoyancy flux, as supported by Zukowska et al. [35]. This approach ensured consistent thermal plume development, which is critical for studying airflow patterns and aerosol dispersion. The test room utilized a mixing air distribution system with four ceiling air diffusers on both sides of the room. These diffusers directed air downward in a swirling motion, while exhaust air was extracted near floor level through grilles. The ventilation system supplied 148 L/s of outdoor air, resulting in an air change rate (ACH) of 3 h^{-1}, with minor fluctuations of ±1.3 L/s. The supply air temperature was maintained at 20.5 ± 0.4 °C, with an average room temperature at 21.5 ± 0.6 °C and relative humidity at 38 ± 8%.

Integrated personal exhaust (PE) ventilation and physical barriers (PB), depicted in Fig. 2, were carefully designed and constructed [36]. These transparent partitions were made to fit on desks. These partitions consisted of a front panel measuring 65 × 138 cm, along with three side panels positioned at the edges of the desk and between occupants. Each partition included a plenum box attached to the front, featuring a narrow 1 cm high slot running across the table's width. This slot functions as an air outlet for personal exhaust ventilation, facilitating air capturing directly from the source infection. Each box is connected to an exhaust duct equipped with an airflow meter and adjustable fan to control the airflow rate. Personal exhaust ventilation was configured to operate at an airflow rate of 9 L/s per person. This rate was carefully balanced with the main exhaust system's ventilation. The main exhaust flow rate was reduced to ensure that the air supply matched the total air removed by both the personal exhaust and the main exhaust systems.

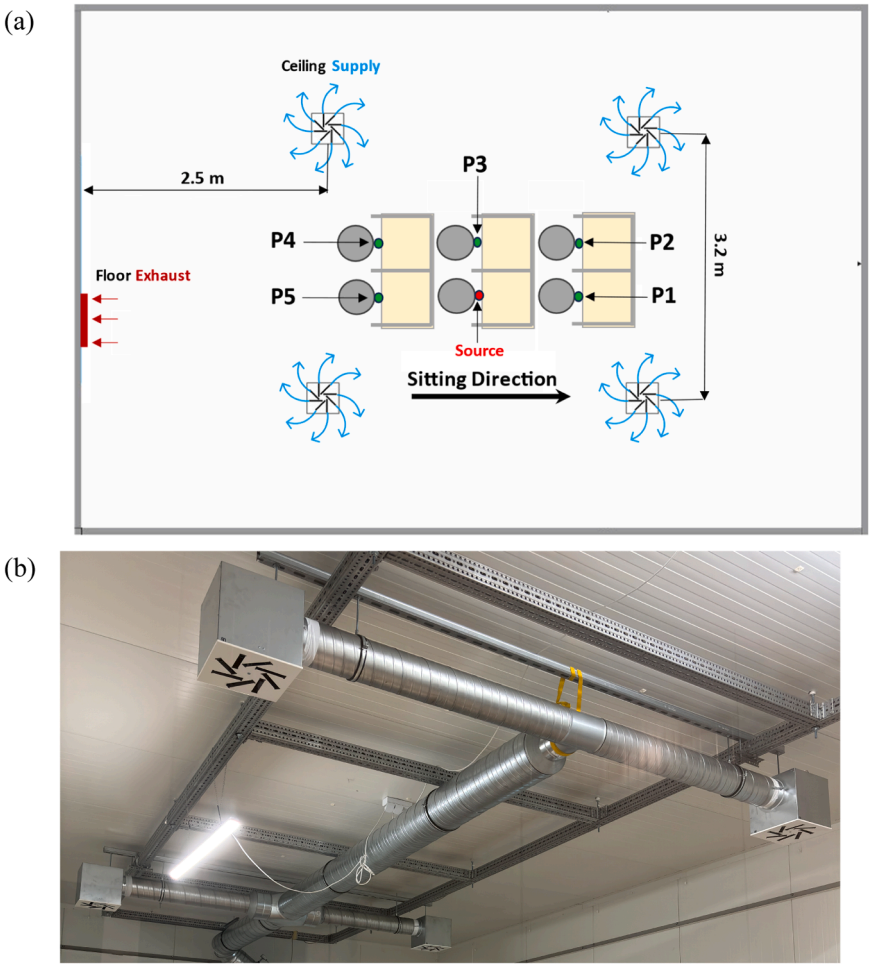

Fig. 1. Test room arrangement. (a) Top-view illustration of the experiment setup (b) The room air supply ventilation system.

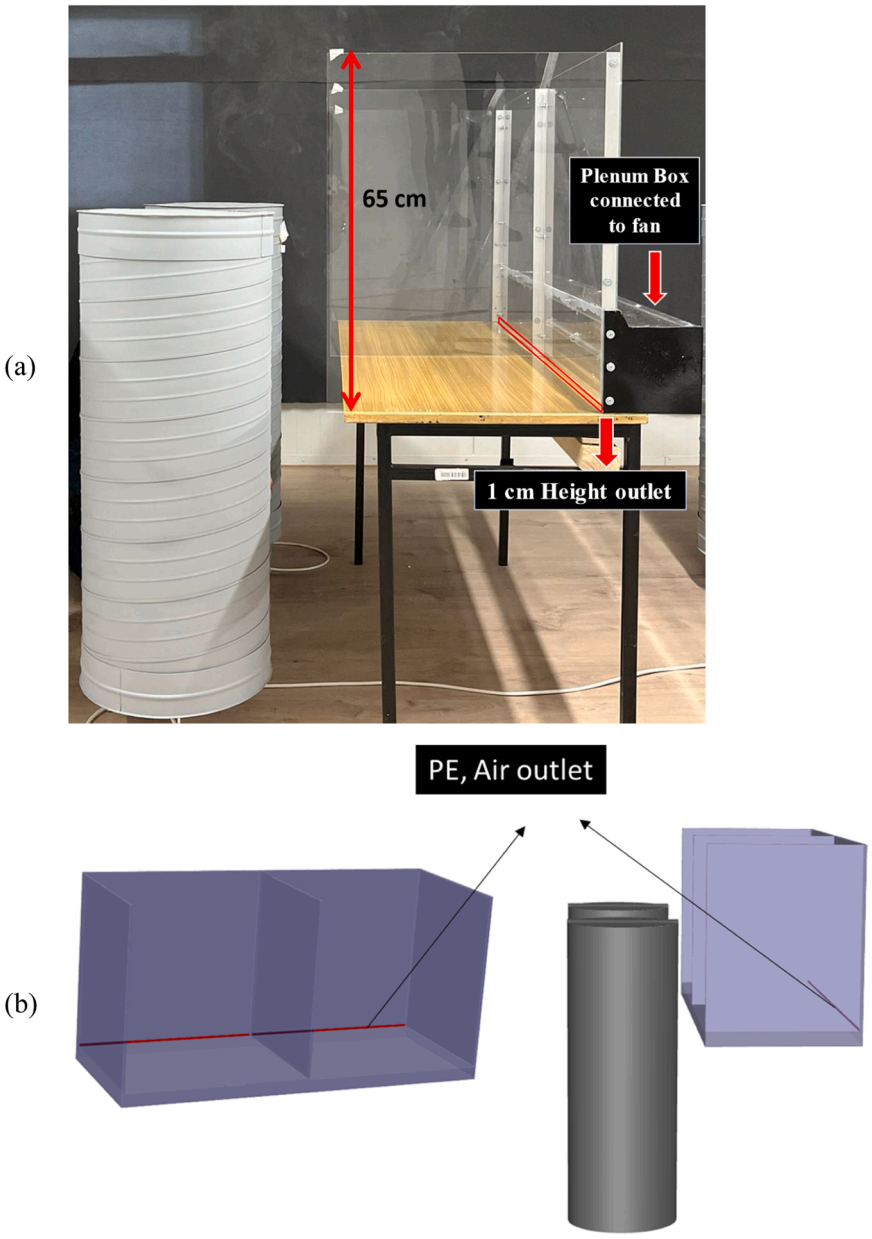

Fig. 2. (a) Experimental setup and (b) 3D geometry model of integrated PE & PB.

3. Methods

3.1. Aerosol generation and measurement

Previous research studies commonly employed the Collison nebulizer for generating aerosols in virus assays [37]. In this study, the 3-jet Collison nebulizer and a sodium chloride (NaCl) solution were utilized to aerosolize human exhaled droplets. According to Nicas et al. [38], respiratory droplets can be simplified as NaCl solution droplets. The solution used in this investigation consisted of 1 gram of NaCl dissolved in a 250 cm^3 solvent mixture comprising 50% distilled water and 50% isopropyl alcohol by volume. Nebulization was conducted at a pressure of 20 pounds per square inch (psi), resulting in 6 L/min flow rate and aerosol droplets with an average diameter of 0.7 micrometers (Geometric Mean) and a geometric standard deviation ranging from 1.22 to 1.35, consistent with the size distribution of human exhaled droplets [39]. The flow rate of nebulization closely matches the airflow of seated individual's exhalation, where the tidal volume is around 500–600 ml per breath with 10–15 breaths per minute [40]. The aerosolized droplets, mixed with clean air, were released from the nebulizer inlet positioned at the mouth level of simulated subjects. Five specific measurement locations (Fig. 1) were chosen at the mouths of the simulated subjects. An aerodynamic particle sizer (PCE-MPC 30 Particle Counter) capable of measuring particles ranging from 0.3 to 10 micrometers in diameter was utilized to determine particle count and aerodynamic diameters, with readings recorded at 1-minute intervals. The particle sizer operated at a flow rate of 2.83 L/min.

3.2. Airflow simulation

The fundamental equations for mass, momentum, and energy conservation in incompressible steady airflow are expressed as follows:

$$\frac{\partial(\rho\phi)}{\partial t} + \nabla.\left(\rho\phi\,\vec{V}\right) = \nabla.\left(\Gamma_\phi \nabla_\phi\right) + S_\phi \tag{1}$$

The RNG k-ε model, known for its robustness in simulating turbulence, has been widely applied in modeling airflow within enclosed

spaces and has demonstrated its suitability in various studies [41]. To enhance the precision of the numerical solution, a second-order upwind discretization scheme was employed for all relevant parameters. Additionally, a coupled algorithm was used to effectively couple pressure and velocity in the steady-state computations, ensuring accurate and stable results.

3.3. Particle movement

Eulerian Particle Tracking (EPT) and Lagrangian Particle Tracking (LPT) are widely used techniques for modeling indoor particle dynamics. EPT models the concentration of particles in a fixed grid, while LPT tracks individual particle trajectories [42]. Recent research suggests that the LPT method may offer greater accuracy than the EPT approach in predicting the distribution and concentration of pollutants, as indicated in studies [43,44]. However, the LPT method often requires substantial memory and computational time to yield statistically significant results. Despite these demands, the Lagrangian method is preferred when detailed particle motion needs to be depicted, as it determines the path of individual particles by integrating force balances on each one. This approach allows for a more precise representation of particle behavior in complex indoor environments. In Fluent, particle motion was simulated using the Discrete Phase Model (DPM) to perform LPT with an automatic time step.

$$\frac{dv_p}{d_t} = F_D(u - u_p) + \frac{g(\rho_p - \rho)}{\rho_p} + F_B + F_e \tag{2}$$

where terms without subscripts refer to the air. The expressions $\frac{dv_p}{d_t}$ and $F_D(u - u_p)$ represent the inertial and drag forces per unit mass of the particle, respectively. Other effects like Basset history, pressure gradient, and virtual mass are considered insignificant compared to the drag force [45]. The Discrete Random Walk (DRW) model is used to simulate the random velocity fluctuations in the fluid phase, assuming these fluctuations follow a Gaussian distribution. Due to high computational demand, particles are injected only after the airflow field is completely resolved, rather than continuously [46]. The effect of these discrete phase trajectories on the continuous phase is ignored. Typically, the interaction between particles and the airflow field in indoor environments is considered a one-way coupling [44,47,48]. Each particle's motion equation was computed until one of the following conditions was met: the particle exited the domain by reaching an escape zone, was deposited in a trap zone, or reached the maximum number of time steps. This study considers Brownian diffusivity to accurately capture the behavior of smaller particles [44]. Generally, particle dispersion is affected by the Stokes number (Stk), the ratio of a particle's aerodynamic response time to the characteristic time. Particles with Stk $<$ 0.1 will follow the airflow streamlines closely [47,49]. The Stokes number is defined as follows:

$$STK = \frac{\rho_p d_p U_\infty}{18\mu_g d_c} \tag{7}$$

By applying the maximum particle diameter of 20 μm and the simulation velocity values we calculated the highest possible Stokes number to be 10^{-3}. Smaller particles would result in an even lower Stk. A Stokes number of this magnitude implies that the particles are highly responsive to the surrounding fluid's movement. Consequently, variations in particle size within the range of 5 to 20 μm have a minimal impact on their trajectories, with only slight differences due to minor variations in drag and gravitational forces. As a result, these small submicron droplets and their residual nuclei remain completely suspended in the air, closely following the flow. Since the Stokes number is significantly less than 1.0, the particles exhibit negligible inertia relative to the fluid, ensuring their motion is dominated by the fluid dynamics.

3.4. Air sampling

In experiments, atmospheric monitoring is conducted using the active air sampling method, which provides data on the concentration of viable air particles. To replicate the active sampling method, sensors were placed near the mouths of dummies to collect airborne particles. In numerical simulation, the active air sampling approach was simulated to examine particle distribution and deposition. Fig. 3 depicts the mouth design that was simulated for this study. It features an 8 mm diameter opening that matches the air inlet nozzle of the sensors. This guarantees that the same measurement location and sampling rate are used in both the experimental and numerical approaches. Particles were considered to have escaped the domain upon reaching the main air exhaust or personal exhaust, and their trajectories were deemed trapped if they hit a rigid surface without considering rebounding [42,50]. The flow rate of sensors for collecting particles was set to match the experiment's active sampling rates. This allows the simulation to mimic active air sampling conditions accurately.

4. Grid independence tests

The computational grid in this study contains approximately 5.6 million cells, as shown in Fig. 4. This grid was generated with ANSYS Fluent's meshing 2022R1 software and employs a poly-hexcore cell type. Five smooth transition boundary layers with a transition ratio of 0.272 and a growth rate 1.2 were applied around the walls to improve solution accuracy in regions with significant gradients. Inflation layers are applied near walls to increase boundary layer resolution and ensure that Y-plus values satisfy the wall function requirements for turbulence simulation. Increase mesh resolution using mesh refinement implemented in critical areas such as dummies' mouths, personalized exhaust vents, and ventilation openings to improve the accuracy of airflow and thermal prediction in regions with complex flow features. To ensure that the computational results are independent of the grid resolution, a grid dependency analysis was conducted using three distinct mesh densities. The simulations were performed with grid counts of approximately 2.4 million, 5.6 million, and 10.8 million cells. Throughout these simulations, the supply air conditions, and ventilation mode were maintained constant, consistent with the experimental setup. The results of the grid independence analysis, as illustrated in Fig. 5, show the impact of

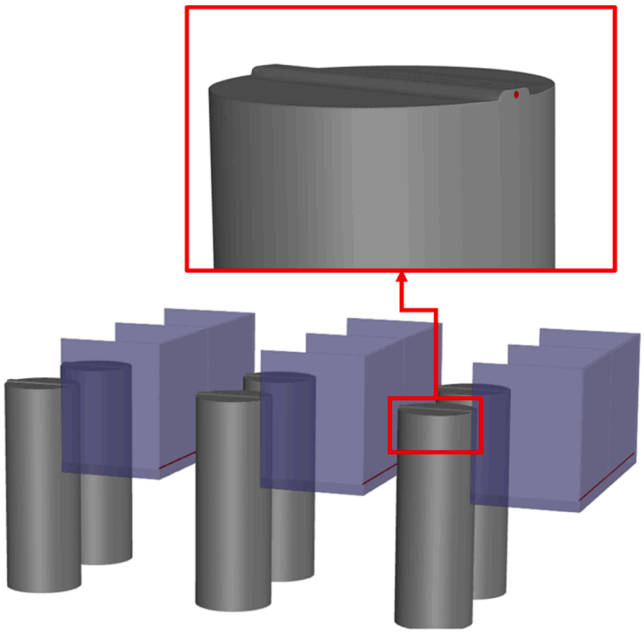

Fig. 3. Simulated Mouth Design for Air Sampling.

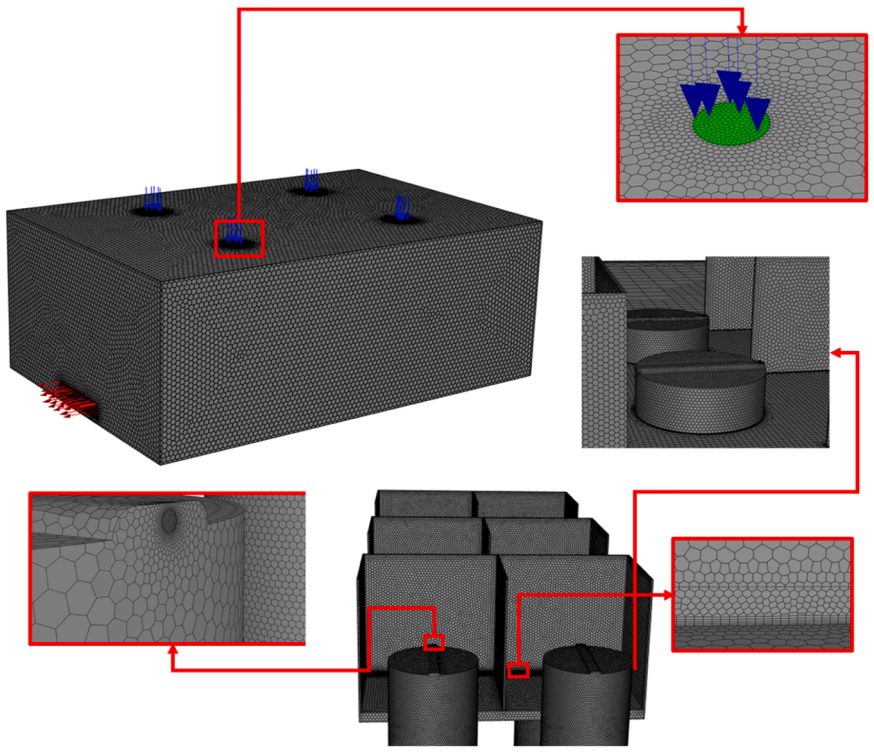

Fig. 4. Computational Mesh Employed in CFD Simulations for the Model.

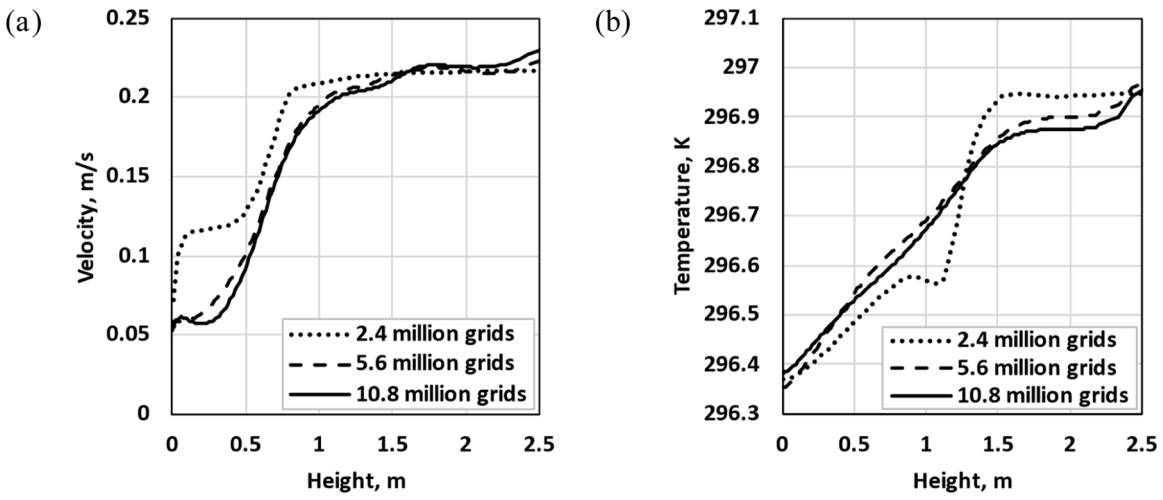

Fig. 5. Grid independence analysis for the grid numbers 2,4, 5,6, and 10,8 million (a) Air velocity (b) Temperature at the center point of the room.

different mesh densities on air velocity and temperature at a central point in the room. The simulations using 5.6 million and 10.8 million grids demonstrated a high degree of consistency, with deviations of less than 7%. Based on these findings, the grid with 5.6 million cells was selected for the final simulations, as it provided a satisfactory balance between computational efficiency and accuracy. This mesh density was deemed sufficient to accurately model pollutant dispersion, thermal behavior, and air movement in the studied environment.

5. Result and discussion

Following the confirmation of grid independence, three distinct simulation scenarios were designed to evaluate particle concentration distributions under various airborne transmission mitigation measures. The reference scenario, which involved no mitigation measures, served as a baseline for comparing the effects of physical barriers and personal exhaust systems on the transmission of airborne infections. The effectiveness of these interventions was assessed by analyzing air distribution patterns, both with partitions alone and in combination with a personal exhaust system. The validation of the numerical results was carried out by comparing air velocity, temperature, and particle concentrations at different points in the room with experimental data. Finally, the study examined how key system parameters, specifically the height of physical barriers and the flow rate of personal exhaust, affect aerosol removal efficiency.

5.1. Air flow distribution and temperature

To ensure the accuracy of the numerical simulation, it is essential to verify the models against experimental data. To verify the outcomes of

computational simulations, practical measurements were carried out within the experimental enclosure. As depicted in Fig. 6, we set up three measurement lines labeled A, B, and C to collect air velocity and temperature data at different heights: 0.1 m, 0.6 m, 1.1 m, and 1.7 m above the floor. The measurement lines are positioned symmetrically in the center of the XZ plane, with the width of the room being 6 m, and the lines placed 3 m from both side walls. Along these lines, physical barriers and personal exhaust systems were strategically placed to assess their impact on airflow and thermal conditions.

Figs. 7-9 juxtapose the experimental airflow and temperature data, recorded by highly accurate AirDistSys 5000 anemometers (±0.02 m/s, ±2% of readings, < ±0.1%/K), with the outcomes derived from computational simulations at three specific locations along the chamber's central plane. Measurements were conducted over a 5-minute duration, with data collected at 1-minute intervals. Error bars representing the standard deviation were included for air velocity to show measurement variability. For temperature, deviations were minimal and ignorable. Fig. 7 illustrates the air velocity and temperature profiles for the case without prevention measures. The figure shows relatively consistent profiles, indicating that natural convection and standard ventilation were adequate for maintaining a stable indoor environment under these conditions. The results demonstrate that in the absence of physical barriers (Without PB &PE), the existing ventilation system was effective in sustaining steady air movement and uniform temperature distribution.

Fig. 8 illustrates the effects of introducing physical barriers without personal exhaust systems (With PB) on airflow patterns and temperature. The presence of physical barriers significantly altered the airflow patterns within space. Physical barriers created localized regions where air velocity was notably reduced. This modification in airflow could restrict the movement and spread of airborne particles.

Fig. 9 depicts the effects of integrating physical barriers with personal exhaust systems (Integrated PE & PB) on airflow patterns and temperature distribution. Compared to the scenario with only physical barriers (With PB), the results demonstrate a more uniform temperature distribution throughout the room and a more controlled airflow profile.

The numerical simulations closely align with the experimental results, showing an average deviation of 16% for air velocity and 5% for indoor temperature, which is acceptable from an engineering perspective. While a slight variance was observed in temperature values on one side of the chamber between the CFD predictions and the experimental data, the computational model accurately predicted the overall airflow patterns. This minor discrepancy could be attributed to nonuniformity and insufficient detail regarding the boundary conditions of the walls, potentially impacting temperature predictions. Fig. 10 presents velocity magnitude contours at the YZ-plane through the centerline of dummies in the presence of physical barriers. The velocity distribution shows a distinct pattern influenced by the air distribution system, physical barriers, and heated dummies. On the top of the dummies, a pronounced thermal plume is observed. This thermal plume is characterized by a vertical column of increased velocity extending upwards, a result of the heat emitted by the dummy that causes the surrounding air to rise due to buoyancy effects. The air distribution system, with supply air descending from the ceiling diffusers and spreading out across the room, contributes to an even distribution of air velocities, effectively maintaining a gentle airflow around the occupants and minimizing drafts. However, the presence of physical barriers also influences the airflow patterns, causing deviations and creating recirculation areas. The middle dummy, which acts as an infection source, generates particles along with the airflow. The resultant distribution of these particles within the airflow pattern provides insights into how airborne contaminants might spread in a controlled environment. The interaction between the thermal plumes generated by the heated dummies and the downward airflow from the ceiling diffusers plays a significant role in the dispersion and dilution of these particles.

Fig. 11 presents temperature contours at the YZ-plane through the centerline of dummies in the presence of physical barriers. The highest temperatures, reaching up to 27 °C, are observed directly above the heated dummies. This temperature distribution results from the heat generated by the dummies, which causes the surrounding air to rise, creating a thermal plume that extends upwards. As this heated air rises, it gradually mixes with the cooler air in the room, leading to a decrease in temperature as it disperses toward the ceiling. The air distribution system, with supply air descending from the ceiling diffusers, aids in mixing the air and helps maintain a more uniform temperature distribution throughout the room. This setup ensures that the thermal comfort of the occupants is maintained, with minimal temperature gradients that could cause discomfort.

5.2. Particle concentration and distribution

Aerosol measurements were conducted at five locations near the infection source to evaluate individuals' exposure risk. The average particle concentration at each location was determined under steady-state conditions over 45 min. Fig. 12 illustrates the normalized particle concentration levels at equilibrium across five locations under various prevention measures. The concentration values varied both between the different scenarios and among the measurement points. To facilitate the comparison between experimental observations and simulation outcomes, we normalized the concentration data using a single reference value, defined mathematically as:

$$C_N = \frac{C_i}{C_{ref}}$$

where C_i is the concentration at a specific location under a given scenario, and C_{ref} represents the reference concentration, calculated as the average concentration across all scenarios and locations. This normalization allows us to compare deviations in particle concentration relative to a reference baseline. The experimental results display standard deviation bars, indicating variability in the measurements. In the scenario

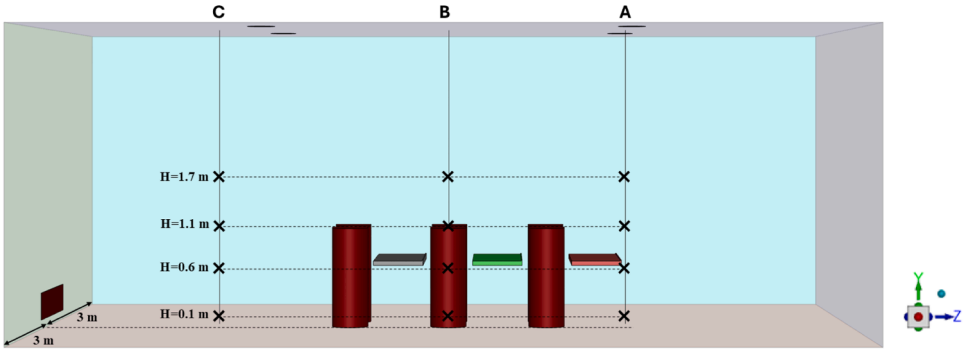

Fig. 6. The configuration of experimental study and sampling points.

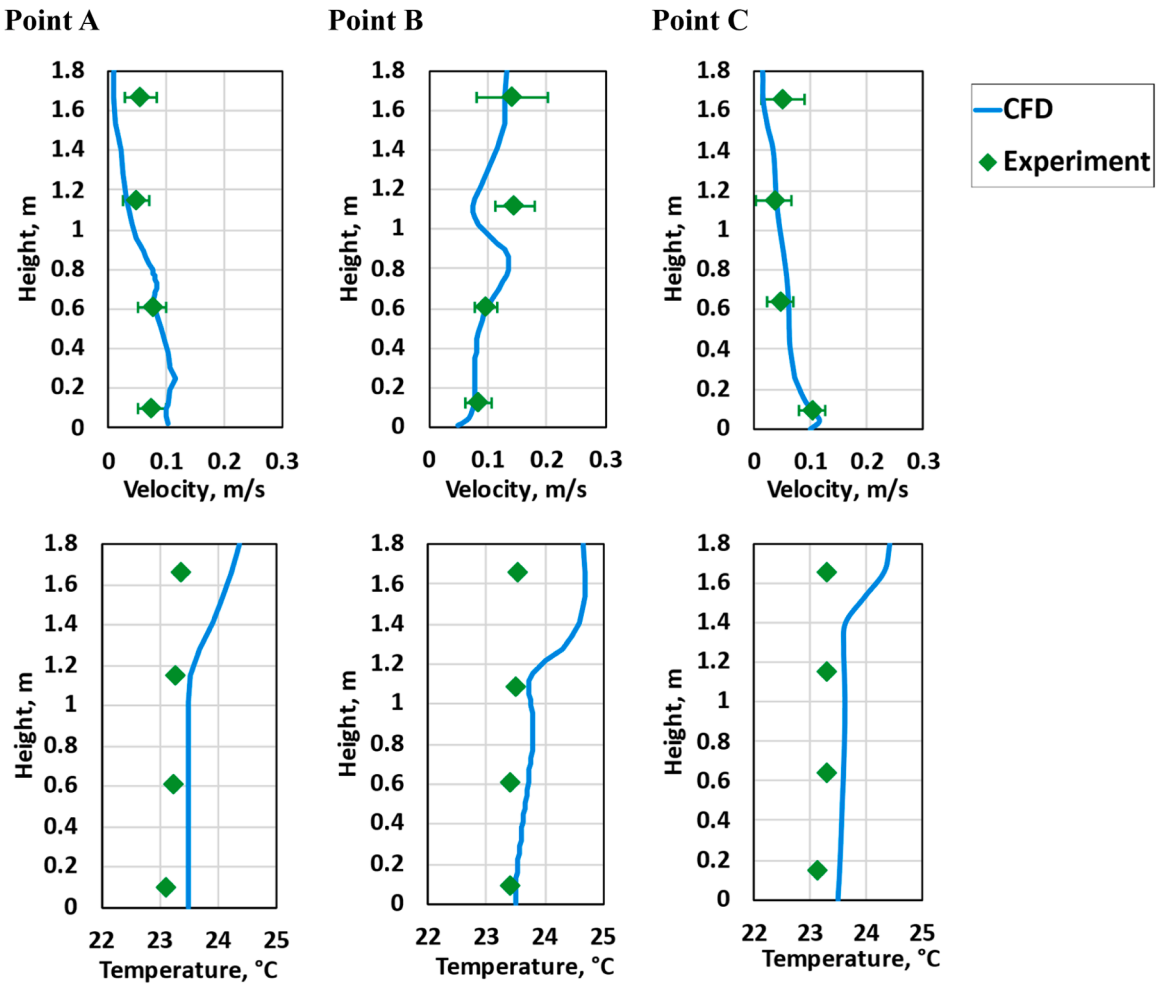

Fig. 7. Comparison of CFD simulations and experimental data for air velocity and temperature—Without PB & PE .

Without PB & PE, the normalized concentration values at all five locations are consistently above 1. This indicates that the particle concentrations at each point in the absence of PB and PE, were higher than the average concentration of all values. The elevated C_N values, particularly at point P3 near the infection source, highlight the significant risk of exposure in the absence of PB and PE. The CFD simulations generally follow this trend but tend to overestimate concentrations at points P4 and P5. The discrepancy between numerical and experimental results may stem from limitations in available data on boundary conditions, such as the lack of wall temperature measurements. Additionally, minor experimental variations such as measurement sensor uncertainty and fluctuations in ventilation rate could further contribute to these differences. In the second scenario, where only physical barriers (With PB) were employed, the C_N was around 0.5 across all points. The concentration reduction by approximately 50% indicates that the barriers effectively minimized particle spread, lowering exposure risk compared to the scenario without prevention measures. The CFD simulations for this scenario closely align with the experimental results. In the third scenario, which integrates both personal exhaust ventilation and physical barriers (Integrated PE & PB), C_N are close to 0 across all points except P3. This near-zero concentration indicates that the combined measures effectively removed airborne particles at the measurement locations. The experimental results demonstrate minimal standard deviations at all measurement points, indicating consistent and reliable performance across all experiments. The CFD simulations corroborate these findings, showing low normalized concentration values. While slightly underestimating concentrations in the last scenario, the CFD model generally aligns well with the experimental results.

The distribution of particles in the room was analyzed by studying how particles emitted by an infected person were dispersed, expelled through personal exhaust systems or the main outlet, and trapped on surfaces. Although the airflow remained steady, the particle distribution varied over time. The study utilized a single-diameter particle for simulation. Fig. 13 illustrates the distribution of aerosol particles in a ventilated room under different scenarios and different times after injection. Three scenarios were analyzed: without preventive measures, with only physical barriers (With PB), and with integrated personal exhaust and physical barriers (Integrated PE & PB). The results presented in the figure clearly demonstrate that preventive measures significantly influence particle dispersion and transport. The scenario without any preventive measures demonstrates a significant and uncontrolled dispersion of particles. Particles begin to disperse upward and outward from the infection source, indicating the rapid spread of aerosols in the absence of physical barriers. At $t = 10$ s, the upward dispersion becomes more pronounced, with particles rising toward the upper part of the room. As time progresses, the spread of particles intensifies. At $t = 20$ s, the particles are widely dispersed and reach near the ceiling level. This trend continues with a wide distribution of particles throughout the room at $t = 50$ s and 100s. The high concentration near the ceiling and around the source highlights the significant risk of airborne transmission. This makes it clear that preventive measures are essential to control aerosol dispersion in indoor environments. However, the presence of physical barriers significantly alters the dispersion patterns. In the presence of physical barriers (With PB), particles initially settle near the source, with barriers providing airborne transmission containment. By $t = 10$ s, the particles start to rise but are confined

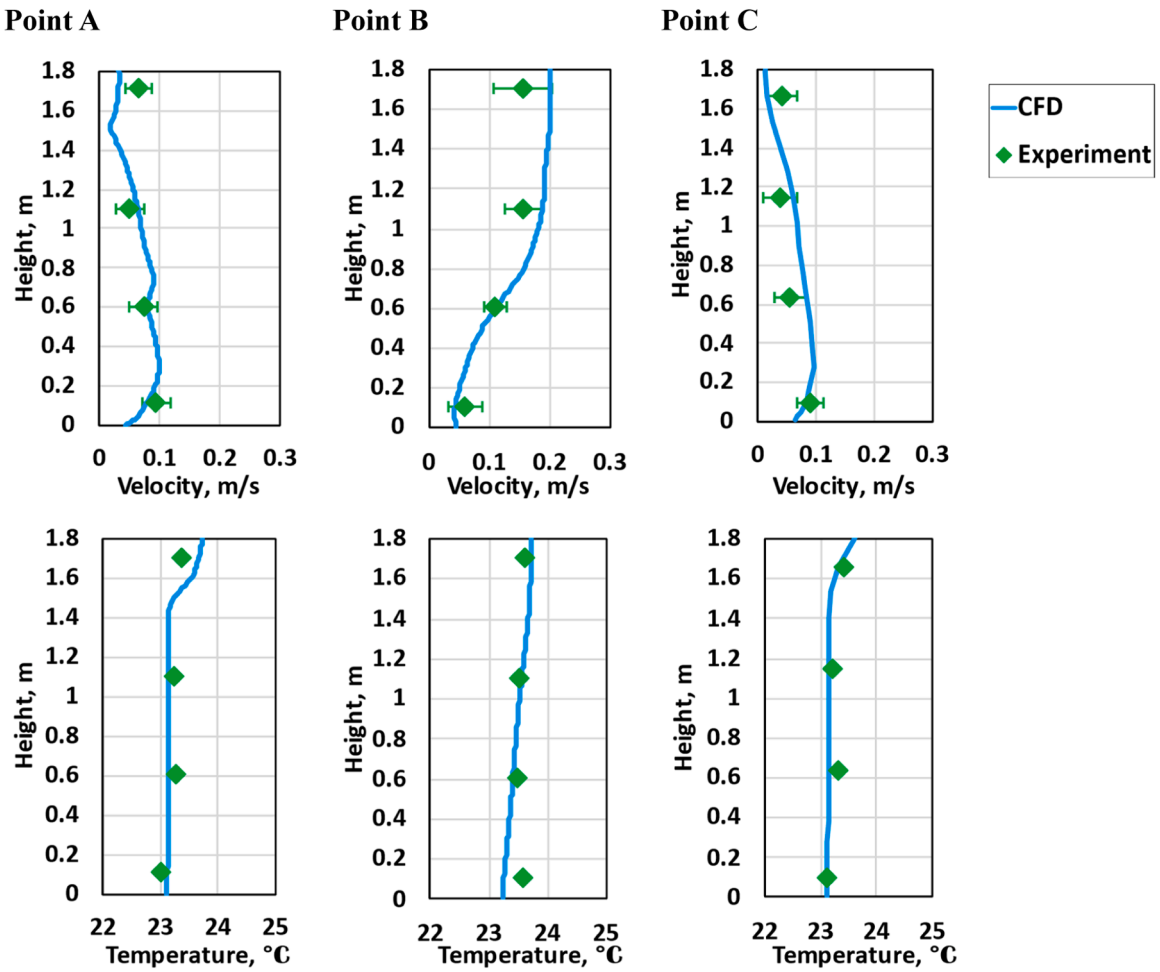

Fig. 8. Comparison of CFD and experimental data for air velocity and temperature—With PB.

within the barriers, indicating a reduction in lateral spread compared to the no-barrier scenario. At $t = 20$ s, the vertical containment becomes more evident, with particles concentrated above the barriers and limited horizontal spread. As observed at $t = 50$ s, the particles remain primarily above the barriers, with the spread controlled. By $t = 100$ s, the particles remain contained around and above the barriers. While physical barriers effectively limit horizontal dispersion, they do not significantly control vertical spread. This indicates that while barriers can somewhat reduce cross-contamination, additional measures are needed to manage vertical aerosol dispersion effectively. In the scenario with integrated PE & PB, particles are initially settled near the source and the exhaust system quickly begins to capture them. By $t = 10$ s, the active removal of particles by the exhaust system is evident. At $t = 20$ s and 50 s, particle dispersion remains upward, leading to limited lateral spread. At $t = 100$ s, the particle concentration and dispersion are evidently lower than the two previous scenarios, demonstrating the effectiveness of the integrated system in removing particles.

5.3. Effect of physical barrier height and exhaust flow rate on aerosol removal efficiency

The height of physical barriers and the personal exhaust flow rate are critical parameters in evaluating the effectiveness of the designed system. While numerous studies have extensively examined the role of personal exhaust ventilation in reducing particle transmission [34] limited research has focused on the influence of barrier height as a key factor in aerosol transmission control. This gap exists primarily due to the practical challenges in experimentally manipulating barrier height in real-world or lab settings, which restricts our understanding of its impact on aerosol containment. Computational Fluid Dynamics (CFD) simulations provide an opportunity to explore critical parameters comprehensively and address the existing in practical experiments. Ren, Chen, et al. [26], suggest that when the position and number of infected individuals are uncertain, it is advisable to use barriers with a height of at least 60 cm above desk level, assuming adequate ventilation is in place. Their investigation demonstrated that higher barriers are more effective in preventing the transmission of airborne particles in ventilated rooms. In our experiments, we used physical barriers with a height of 65 cm, along with additional protection from personal exhaust ventilation systems. Given this combined approach, the minimum effective height for physical barriers may be reduced. The personal exhaust system's ability to capture and remove contaminants directly at their source suggests that shorter barriers may achieve similar levels of protection and potentially lower the requirement for barrier height. Furthermore, the environmental implications of higher plexiglass barriers, including increased material consumption and associated carbon emissions, present additional challenges. Taller barriers can also impede airflow, which may negatively impact both air quality and occupant comfort [26,34]. Thus, a refined approach in designing these systems, balancing barrier height with efficient exhaust flow rates, is essential to achieving sustainable and effective infection control. This study assessed the impact of different barrier heights on aerosol removal efficiency using Relative Aerosol Removal (RAR) as the metric. RAR is defined as:

$$RAR = \frac{N_{removed}(h)}{N_{removed}(65cm)}$$

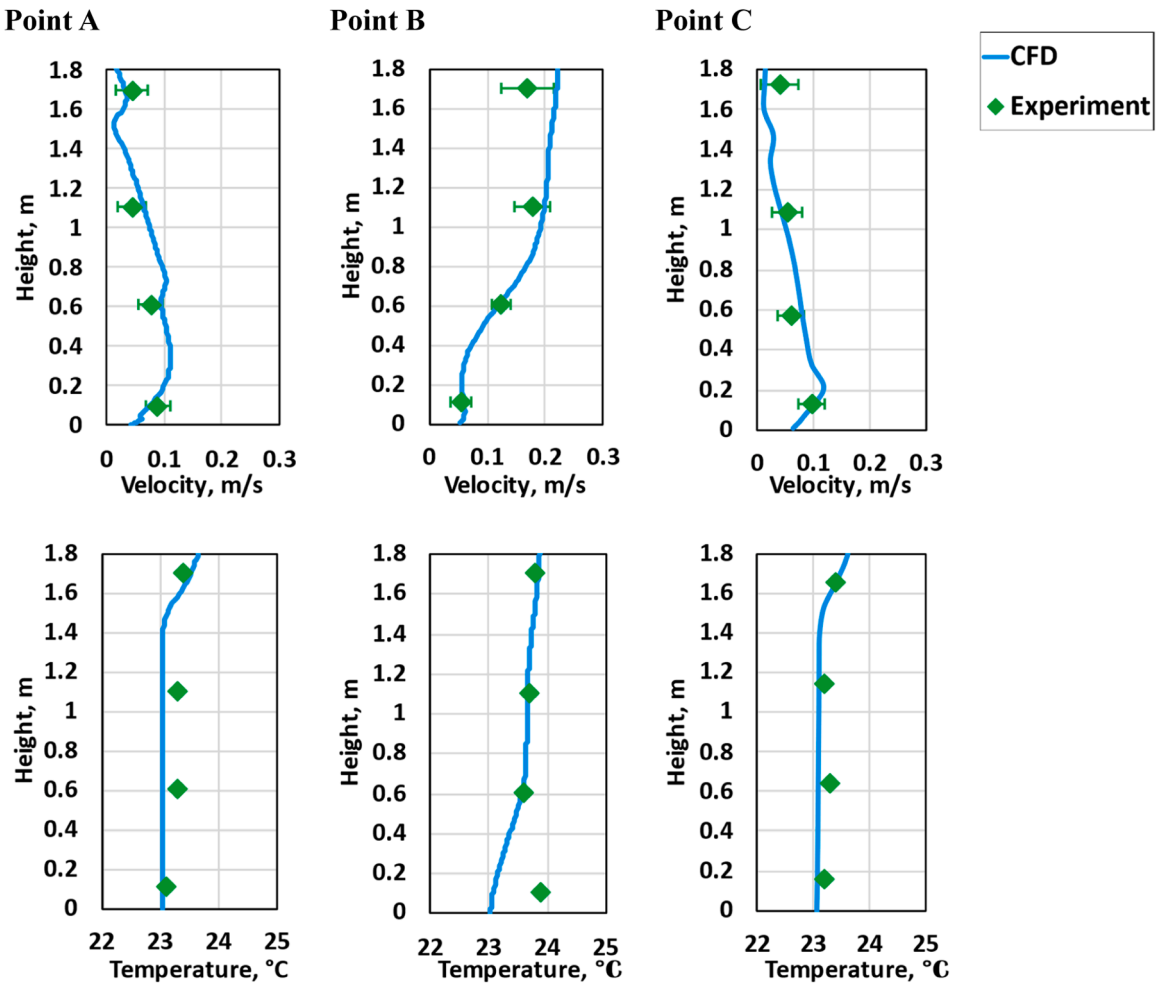

Fig. 9. Comparison of CFD and experimental data for air velocity and temperature— Integrated PE&PB.

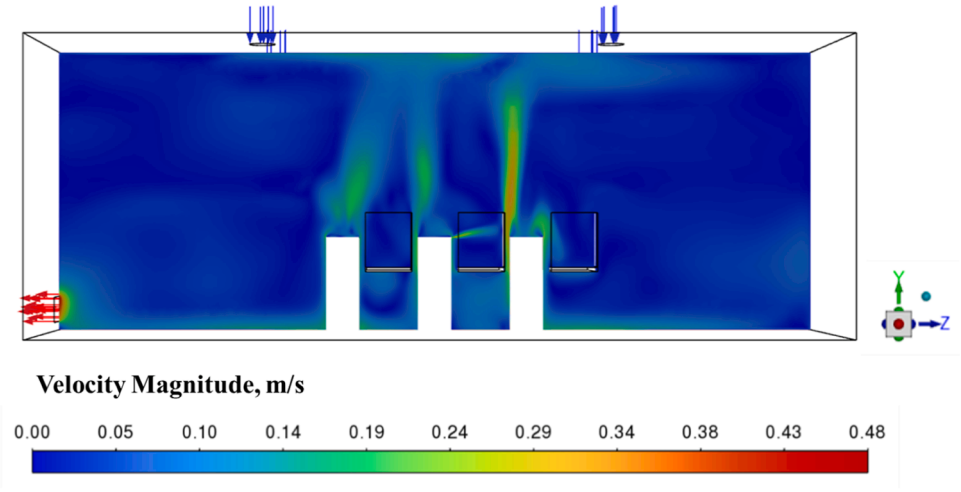

Fig. 10. Velocity magnitude contour at the YZ-plane through the centerline of dummies– With PB.

where $N_{removed}(h)$ is the number of particles removed at a barrier height h, and $N_{removed}(65cm)$ is the number of particles removed by the baseline case with a barrier height of 65 cm. This baseline case served as the reference point for all comparisons. The results, as shown in Fig. 14, indicate that the height of the physical barrier significantly influences the efficiency of the designed system. At the baseline barrier height of 65 cm, the RAR is set at 1. Increasing the barrier height to 85 cm results in a slight increase in RAR. This marginal improvement suggests that while a higher barrier captures slightly more aerosols, the additional material usage, increased carbon emissions, and potential impact on airflow and comfort may not justify the minimal increase in performance. Reducing the barrier height to 45 cm, which matches the height of the aerosol

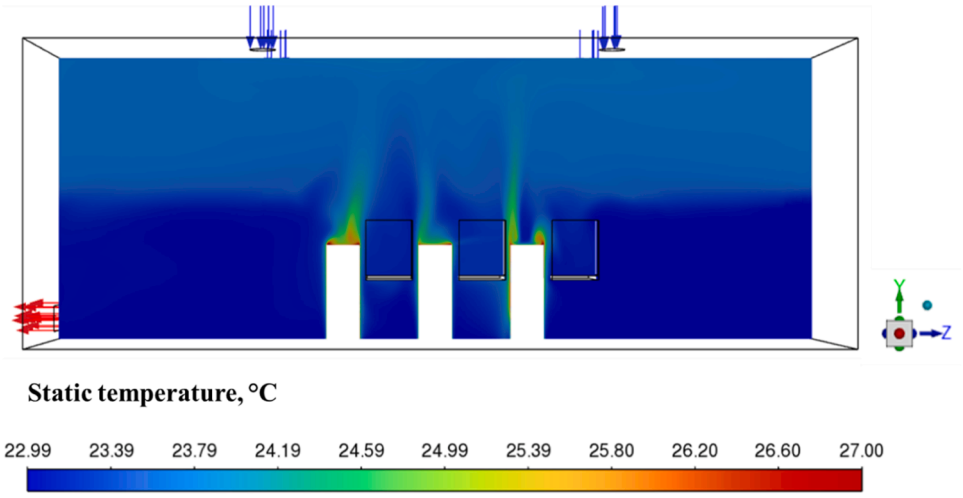

Fig. 11. Temperature contour at the YZ-plane through the centerline of dummies– With PB.

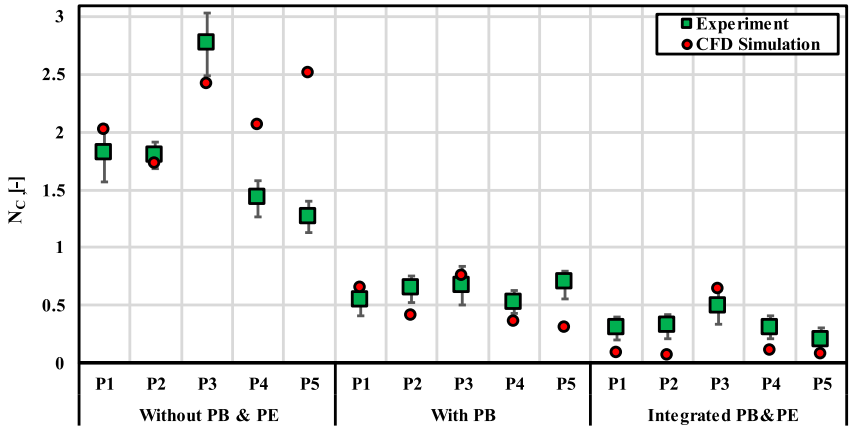

Fig. 12. Comparison of CFD simulation and experimental data: normalized concentration of particles under various preventive measures.

source, results in a slight decrease in RAR to 0.95. A further reduction to a barrier height of 25 cm leads to a drop in RAR to 0.83. The change in RAR from 85 cm to 45 cm was minimal, considering that the 45 cm height of the barrier aligns with the aerosol source generation height. However, the reduction in RAR from 45 cm to 25 cm was more notable as the barrier height dropped below the source level. At 0 cm height, where no barrier is present, the RAR falls sharply to 0.07. This substantial decrease highlights the critical role of the physical barrier in aerosol capture. Therefore, the removal efficiency of the system is severely compromised without a physical barrier. Overall, reducing the barrier height decreases RAR, with the most significant decline occurring when the height is reduced from 25 cm to 0 cm. However, it is noteworthy that reducing the barrier height to as low as 45 cm still maintains 95 % of the aerosol removal efficiency observed with a 65 cm barrier height in the experimental setup.

Different flow rates were investigated to determine the impact of personal exhaust flow rate on aerosol removal efficiency. This investigation is crucial because higher exhaust flow rates typically demand more energy [51,52]. Fig. 15 illustrates Relative Aerosol Removal (RAR) for various personal exhaust flow rates. The RAR values were compared to those observed at a flow rate of 9 L/s per person, which was utilized in experiments. The result reveals a clear trend between exhaust flow rate and aerosol removal efficiency. At the baseline flow rate of 9 L/s per person, the RAR is set at 1 as the baseline. Increasing the flow rate to 12 L/s per person results in a modest increase in RAR to 1.03, while further increasing it to 13.5 L/s per person leads to a slightly higher RAR of 1.05. This suggests that higher flow rates do improve aerosol removal efficiency. However, the improvements become less significant as the flow rate increases, indicating diminishing returns. Considering the additional energy consumption, may not justify the additional increase in flow rate. Conversely, reducing the flow rate below 9 L/s per person results in a noticeable decline in RAR. At 6 L/s per person, the RAR drops to 0.94. A further reduction to 4 L/s per person leads to a more substantial drop in RAR to 0.83, reflecting a significant decline in aerosol removal efficiency. The most dramatic change occurs when the flow rate is reduced to 2 L/s per person, where the RAR decreases to 0.27. With no exhaust flow (0 L/s per person), the RAR is 0, indicating that the exhaust system is inactive. This trend indicates that while increasing the flow rate above 9 L/s per person yields only minor efficiency improvements, reducing the flow rate below this baseline substantially decreases aerosol removal effectiveness. Nonetheless, it is important to note that even with a reduction in flow rate to 6 L/s per person, the system retains 94 % of the aerosol removal efficiency observed at the baseline flow rate in the experimental setup.

Optimizing the exhaust flow rate is crucial to balance efficient aerosol removal with the potential impact on energy consumption, noise, and overall system performance. Future research should further investigate the interactions between the integrated system and factors such as room ventilation rates, the spatial distribution of occupants, and the nature of activities conducted within space. Exploring these variables will help refine system design to enhance both efficiency and occupant comfort.

Fig. 13. Particle dispersion over time for various prevention measures.

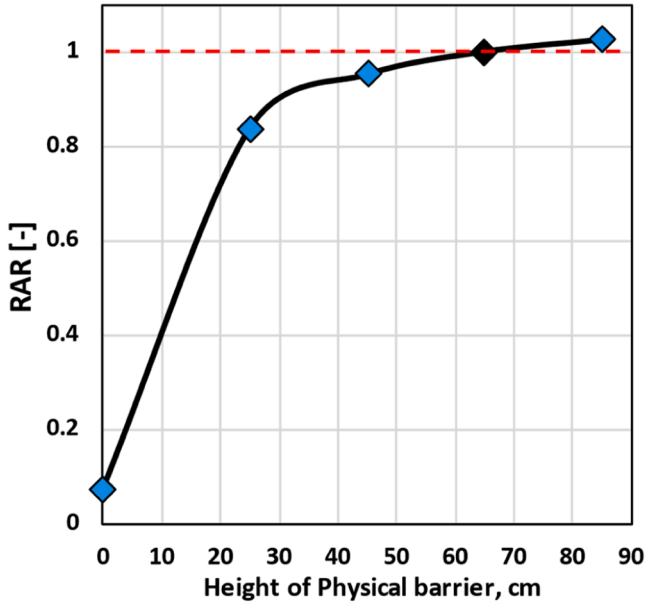

Fig. 14. Relative Aerosol Removal (RAR) for various heights of physical barrier.

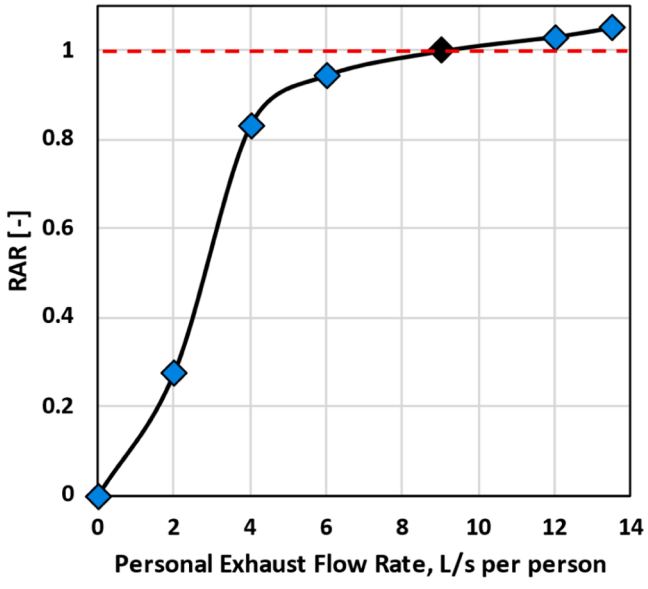

Fig. 15. Relative Aerosol Removal (RAR) for various personal exhaust flow rates.

6. Conclusion

This study confirms that the integration of personal exhaust ventilation and physical barriers significantly enhances airborne particle control, using both experimental and numerical methods. The experimental measurements, which included air velocity, air temperature, and aerosol concentration, validated the result of computational

simulations. Particle concentration measurements revealed that the use of physical barriers alone significantly reduced particle concentrations compared to the scenario without physical barriers. The combination of physical barriers and personal exhaust systems achieved the most significant particle concentration reduction. Therefore, the integration of personal exhaust ventilation and physical barriers proves to be a highly effective approach for minimizing airborne transmission. Further investigations were conducted using CFD simulations to explore the impact of varying physical barrier heights and personal exhaust flow rates. The baseline experimental case utilized a barrier height of 65 cm and a personal exhaust flow rate of 9 L/s per person. Numerical simulations further demonstrated that reducing the barrier height to 45 cm maintained nearly the same level of aerosol removal efficiency. This adjustment not only preserved the system's effectiveness but also improved visibility, minimized potential airflow obstruction, and lowered carbon emissions, thereby enhancing sustainability, air quality, and comfort. Similarly, CFD simulations revealed that lowering the exhaust flow rate down to 6 L/s per person retained almost the same aerosol removal efficiency as the baseline case. This reduction in flow rate not only maintains system effectiveness but also offers significant energy savings, making the system a more practical and sustainable option.

CRediT authorship contribution statement

Seyedkeivan Nateghi: Writing – original draft, Software, Investigation, Funding acquisition, Formal analysis. **Shahrzad Marashian:** Visualization, Validation, Software, Methodology. **Jan Kaczmarczyk:** Writing – review & editing, Supervision, Conceptualization. **Sasan Sadrizadeh:** Writing – review & editing, Supervision, Methodology.

Declaration of competing interest

The authors declare that they have no known competing financial interests or personal relationships that could have appeared to influence the work reported in this paper.

Acknowledgments

This research was supported by the Excellence Initiative - Research University program implemented at the Silesian University of Technology in 2023/24 academic year.

Data availability

No data was used for the research described in the article.

References

[1] R. Khandia, et al., Emergence of SARS-CoV-2 Omicron (B.1.1.529) variant, salient features, high global health concerns and strategies to counter it amid ongoing COVID-19 pandemic, Environ. Res. 209 (2022) 112816, https://doi.org/10.1016/j.envres.2022.112816.
[2] M. Awada, et al., Occupant health in buildings: impact of the COVID-19 pandemic on the opinions of building professionals and implications on research, Build. Environ. 207 (2022) 108440, https://doi.org/10.1016/j.buildenv.2021.108440.
[3] World Health Organization, "Infection prevention and control during health care when COVID-19 is suspected: interim guidance." 2020.
[4] Z. Aghalari, H.-U. Dahms, J.E. Sosa-Hernandez, M.A. Oyervides-Muñoz, R. Parra-Saldívar, Evaluation of SARS-COV-2 transmission through indoor air in hospitals and prevention methods: a systematic review, Environ. Res. 195 (2021) 110841, https://doi.org/10.1016/j.envres.2021.110841.
[5] Z. Zhong, Z. Pan, H. Tang, J. Wang, F. Liu, J. Wang, Camera-based occupant behavior trajectory capture and on-site assessment of spatio-temporal transmission risk of airborne virus in a university office building, Build. Environ. 243 (2023) 110670, https://doi.org/10.1016/j.buildenv.2023.110670.
[6] N. Mao, et al., Transmission risk of infectious droplets in physical spreading process at different times: a review, Build. Environ. 185 (2020) 107307, https://doi.org/10.1016/j.buildenv.2020.107307.
[7] G. Ozler, H. Grosshans, Airborne virus transmission: increased spreading due to formation of hollow particles, Environ. Res. 237 (2023) 116953, https://doi.org/10.1016/j.envres.2023.116953.
[8] C. Zhang, P.V. Nielsen, L. Liu, E.T. Sigmer, S.G. Mikkelsen, R.L. Jensen, The source control effect of personal protection equipment and physical barrier on short-range airborne transmission, Build. Environ. 211 (2022) 108751, https://doi.org/10.1016/j.buildenv.2022.108751.
[9] W. Jia, J. Wei, P. Cheng, Q. Wang, Y. Li, Exposure and respiratory infection risk via the short-range airborne route, Build. Environ. 219 (2022) 109166, https://doi.org/10.1016/j.buildenv.2022.109166.
[10] L. Borro, L. Mazzei, M. Raponi, P. Piscitelli, A. Miani, A. Secinaro, The role of air conditioning in the diffusion of Sars-CoV-2 in indoor environments: a first computational fluid dynamic model, based on investigations performed at the Vatican State Children's hospital, Environ. Res. 193 (2021) 110343, https://doi.org/10.1016/j.envres.2020.110343.
[11] D.E. Faleiros, W. Van Den Bos, L. Botto, F. Scarano, TU Delft COVID-app: a tool to democratize CFD simulations for SARS-CoV-2 infection risk analysis, Sci. Total Environ. 826 (2022) 154143, https://doi.org/10.1016/j.scitotenv.2022.154143.
[12] S. Kumar, M.D. King, Numerical investigation on indoor environment decontamination after sneezing, Environ. Res. 213 (2022) 113665, https://doi.org/10.1016/j.envres.2022.113665.
[13] P.A. Mirzaei, M. Moshfeghi, H. Motamedi, Y. Sheikhnejad, H. Bordbar, A simplified tempo-spatial model to predict airborne pathogen release risk in enclosed spaces: an Eulerian-Lagrangian CFD approach, Build. Environ. 207 (2022) 108428, https://doi.org/10.1016/j.buildenv.2021.108428.
[14] G. Vita, D. Woolf, T. Avery-Hickmott, R. Rowsell, A CFD-based framework to assess airborne infection risk in buildings, Build. Environ. 233 (2023) 110099, https://doi.org/10.1016/j.buildenv.2023.110099.
[15] H. Kotb, E.E. Khalil, Sneeze and cough pathogens migration inside aircraft cabins, Energy 2 (4) (2020).
[16] J. Ren, Y. Wang, Q. Liu, Y. Liu, Numerical study of three ventilation strategies in a prefabricated COVID-19 inpatient ward, Build. Environ. 188 (2021) 107467, https://doi.org/10.1016/j.buildenv.2020.107467.
[17] Y. Yan, X. Li, J. Tu, Thermal effect of human body on cough droplets evaporation and dispersion in an enclosed space, Build. Environ. 148 (2019) 96–106, https://doi.org/10.1016/j.buildenv.2018.10.039.
[18] Y. Zhang, G. Feng, Z. Kang, Y. Bi, Y. Cai, Numerical simulation of coughed droplets in conference room, Procedia Eng. 205 (2017) 302–308, https://doi.org/10.1016/j.proeng.2017.09.981.
[19] X. Yang, et al., Transmission of pathogen-laden expiratory droplets in a coach bus, J. Hazard. Mater. 397 (2020) 122609, https://doi.org/10.1016/j.jhazmat.2020.122609.
[20] M. Abuhegazy, K. Talaat, O. Anderoglu, S.V. Poroseva, Numerical investigation of aerosol transport in a classroom with relevance to COVID-19, Phys. Fluids 32 (10) (2020) 103311, https://doi.org/10.1063/5.0029118.
[21] P. Dacunto, D. Moser, A. Ng, M. Benson, Classroom aerosol dispersion: desk spacing and divider impacts, Int. J. Environ. Sci. Technol. 19 (2) (2022) 1057–1070, https://doi.org/10.1007/s13762-021-03564-z.
[22] J. Bartels, C.F. Estill, I.-C. Chen, D. Neu, Laboratory study of physical barrier efficiency for worker protection against SARS-CoV-2 while standing or sitting, Aerosol Sci. Technol. 56 (3) (2022) 295–303, https://doi.org/10.1080/02786826.2021.2020210.
[23] M. Mirzaie, E. Lakzian, A. Khan, M.E. Warkiani, O. Mahian, G. Ahmadi, COVID-19 spread in a classroom equipped with partition – a CFD approach, J. Hazard. Mater. 420 (2021) 126587, https://doi.org/10.1016/j.jhazmat.2021.126587.
[24] M. Ahmadzadeh, M. Shams, Multi-objective performance assessment of HVAC systems and physical barriers on COVID-19 infection transmission in a high-speed train, J. Build. Eng. 53 (2022) 104544, https://doi.org/10.1016/j.jobe.2022.104544.
[25] W. Guo, et al., Visualization of the infection risk assessment of SARS-CoV-2 through aerosol and surface transmission in a negative-pressure ward, Environ. Int. 162 (2022) 107153, https://doi.org/10.1016/j.envint.2022.107153.
[26] C. Ren, et al., Mitigating COVID-19 infection disease transmission in indoor environment using physical barriers, Sustain. Cities. Soc. 74 (2021) 103175, https://doi.org/10.1016/j.scs.2021.103175.
[27] N. Izadyar, W. Miller, Ventilation strategies and design impacts on indoor airborne transmission: a review, Build. Environ. 218 (2022) 109158, https://doi.org/10.1016/j.buildenv.2022.109158.
[28] J. Yang, S.C. Sekhar, K.W.D. Cheong, B. Raphael, Performance evaluation of a novel personalized ventilation-personalized exhaust system for airborne infection control, Indoor. Air. 25 (2) (2015) 176–187, https://doi.org/10.1111/ina.12127.
[29] Y. Junjing, C. Sekhar, D. Cheong, B. Raphael, Performance evaluation of an integrated Personalized Ventilation–Personalized Exhaust system in conjunction with two background ventilation systems, Build. Environ. 78 (2014) 103–110, https://doi.org/10.1016/j.buildenv.2014.04.015.
[30] J. Karam, E. Katramiz, K. Ghali, N. Ghaddar, Downward piston ventilation assisted with a localized - chair exhaust for mitigation of pathogen transport in educational spaces, J. Build. Eng. 58 (2022) 105066, https://doi.org/10.1016/j.jobe.2022.105066.
[31] S. Schiavon, A.K. Melikov, Energy-saving strategies with personalized ventilation in cold climates, Energy Build. 41 (5) (2009) 543–550, https://doi.org/10.1016/j.enbuild.2008.11.018.
[32] A.Q. Ahmed, S. Gao, Numerical investigation of height impact of local exhaust combined with an office work station on energy saving and indoor environment, Build. Environ. 122 (2017) 194–205, https://doi.org/10.1016/j.buildenv.2017.06.011.
[33] C. Cheong, S. Lee, Case study of airborne pathogen dispersion patterns in emergency departments with different ventilation and partition conditions, IJERPH 15 (3) (2018) 510, https://doi.org/10.3390/ijerph15030510.

[34] S. Nateghi, J. Kaczmarczyk, Compatibility of integrated physical barriers and personal exhaust ventilation with air distribution systems to mitigate airborne infection risk, Sustain. Cities. Soc. 103 (2024) 105282, https://doi.org/10.1016/j.scs.2024.105282.
[35] D. Zukowska, A.K. Melikov, Z.J. Popiolek, Thermal plume above a simulated sitting person with different complexity of body geometry: Roomvent, in: 10th International Conference on Air Distribution in Rooms 3, Roomvent, 2007, pp. 191–198, 2007.
[36] S.K. Nateghi, J. Kaczmarczyk, A. Lipczynska, Potential of physical barriers integrated with personal exhaust ventilation in decreasing airborne infection risk for people, J. Phys.: Conf. Ser. 2600 (10) (2023) 102020, https://doi.org/10.1088/1742-6596/2600/10/102020.
[37] R.H. Alford, J.A. Kasel, P.J. Gerone, V. Knight, Human influenza resulting from aerosol inhalation, in: *Proceedings of the Society for Experimental Biology and Medicine*, 122, 1966, pp. 800–804, https://doi.org/10.3181/00379727-122-31255.
[38] M. Nicas, W.W. Nazaroff, A. Hubbard, Toward understanding the risk of secondary airborne infection: emission of respirable pathogens, J. Occup. Environ. Hyg. 2 (3) (2005) 143–154, https://doi.org/10.1080/15459620590918466.
[39] R.S. Papineni, F.S. Rosenthal, The size distribution of droplets in the exhaled breath of healthy human subjects, J. Aerosol Med. 10 (2) (1997) 105–116, https://doi.org/10.1089/jam.1997.10.105.
[40] "Normal breathing | RESPe." Accessed: Oct. 24, 2024. [Online]. Available: https://respelearning.scot/topic-1-anatomy-and-physiology/normal-breathing.
[41] T.-H. Shih, W.W. Liou, A. Shabbir, Z. Yang, J. Zhu, A new k-ϵ eddy viscosity model for high Reynolds number turbulent flows, Comput. Fluids 24 (3) (1995) 227–238, https://doi.org/10.1016/0045-7930(94)00032-T.
[42] S. Sadrizadeh, A. Tammelin, P. Ekolind, S. Holmberg, Influence of staff number and internal constellation on surgical site infection in an operating room, Particuology 13 (2014) 42–51, https://doi.org/10.1016/j.partic.2013.10.006.
[43] A. Riddle, D. Carruthers, A. Sharpe, C. McHugh, J. Stocker, Comparisons between FLUENT and ADMS for atmospheric dispersion modelling, Atmos. Environ. 38 (7) (2004) 1029–1038, https://doi.org/10.1016/j.atmosenv.2003.10.052.
[44] Z. Zhang, Q. Chen, Experimental measurements and numerical simulations of particle transport and distribution in ventilated rooms, Atmos. Environ. 40 (18) (2006) 3396–3408, https://doi.org/10.1016/j.atmosenv.2006.01.014.
[45] B. Zhao, Y. Zhang, X. Li, X. Yang, D. Huang, Comparison of indoor aerosol particle concentration and deposition in different ventilated rooms by numerical method, Build. Environ. 39 (1) (2004) 1–8, https://doi.org/10.1016/j.buildenv.2003.08.002.
[46] S. Marashian, S. Sadrizadeh, O. Abouali, Modeling particle distribution in a ventilated room with modified discrete random walk methods, Int. J. Ventilation 22 (3) (2023) 289–306, https://doi.org/10.1080/14733315.2022.2143062.
[47] N.P. Gao, J.L. Niu, Modeling particle dispersion and deposition in indoor environments, Atmos. Environ. 41 (18) (2007) 3862–3876, https://doi.org/10.1016/j.atmosenv.2007.01.016.
[48] F. Chen, S.C.M. Yu, A.C.K. Lai, Modeling particle distribution and deposition in indoor environments with a new drift–flux model, Atmos. Environ. 40 (2) (2006) 357–367, https://doi.org/10.1016/j.atmosenv.2005.09.044.
[49] J.E. Martin, E. Meiburg, The accumulation and dispersion of heavy particles in forced two-dimensional mixing layers. I. The fundamental and subharmonic cases, Phys. Fluids 6 (3) (1994) 1116–1132, https://doi.org/10.1063/1.868283.
[50] S. Sadrizadeh, S. Holmberg, Surgical clothing systems in laminar airflow operating room: a numerical assessment, J. Infect. Public Health 7 (6) (2014) 508–516, https://doi.org/10.1016/j.jiph.2014.07.011.
[51] Y. Chen, B. Raphael, S.C. Sekhar, Experimental and simulated energy performance of a personalized ventilation system with individual airflow control in a hot and humid climate, Build. Environ. 96 (2016) 283–292, https://doi.org/10.1016/j.buildenv.2015.11.036.
[52] S. Schiavon, A.K. Melikov, C. Sekhar, Energy analysis of the personalized ventilation system in hot and humid climates, Energy Build. 42 (5) (2010) 699–707, https://doi.org/10.1016/j.enbuild.2009.11.009.